NMR Studies of Polypeptide Structuring and Aggregation

Aimee Byrne

A dissertation submitted in partial fulfillment of the
requirements for the degree of

Doctor of Philosophy

University of Washington

2013

Program Authorized to Offer Degree:
Department of Chemistry

University of Washington

Abstract

NMR Studies of Polypeptide Structuring and Aggregation

Aimee Byrne

Chair of Supervisory Committee:
Professor Niels H. Andersen
Department of Chemistry

The importance of studying polypeptide structuring and folding mechanisms lies in the damage caused by misfolding proteins in the human body. The misfolding of proteins can lead to the off-pathway formation of aggreagates that can prove harmful to living cells. Several disease states result from this aggregation process, *e.g.* Parkinson's disease in which α–synuclein is accumulated into Lewy bodies within the brain. In this work, the aggregation process of α–synuclein is examined through the use of NMR, primarily ^{15}N-NMR. Aromatic-containing, well-folded β-hairpins have been shown to be effective at interfering with the fibril formation pathway. Through NMR, the binding of these hairpins to α–synuclein and the divertion of the fibrils to a non-amyloid precipitate is explored.

The design of stable protein-like structures allows for the study of specific interactions which contribute to folding. The trunctation and mutation of a poorly folded 39-residue peptide has produced 20-residue constructs that are > 95% folded in water. These constructs have been designated as the 'Trp-cage' motif. This construct is characterised by an N-terminal α-helix and hydrophobic collapse centred on a tryptophan indole ring. The majority of this work explores essential features of the Trp-cage that are responsible for its stability. The later part focuses on the circular

permutation of the Trp-cage, followed by the cyclisation of the most stable motif. This results in a hyperstable Trp-cage (T_M >> 100° C at pH 7) which possesses the same diagnostic features as the standard Trp-cage structure.

Table of Contents

List of Figures

List of Tables

List of Abbreviations

CD: Circular Dichroism

CPDB: Circular Permutation Database

CR: Congo Red

CSD: Chemical Shift Deviation

DMF: Dimethyl Formamide

DSS: 2,2-Dimethyl-Silapentane-5-Sulfonic acid

Fmoc: Fluorenylmethyloxycarbonyl

GnHCl: guanidinium hydrochloride

HFIP: Hexafluoroisopropanol

HPLC: High-Performance Liquid Chromatography

MD: Molecular Dynamics

NMP: N-Methyl Pyrrolidine

NMR: Nuclear Magnetic Resonance spectroscopy

NOE: nuclear Overhauser effect

NOESY: Nuclear Overhauser Effect SpectroscopY

ppm: parts per million

RMSD: root mean square deviation

SRE: Self-recognition element

TC: Trp cage

TEM: Transmission Electron Microscopy

TFA: trifluoroacetic acid

TFE: 2, 2, 2-trifluoroethanol

ThT: Thioflavin T

T_M: melting temperature

TOCSY: TOtal Correlation SpectroscopY

TS: transition state

UV-Vis: Ultraviolet-Visible spectroscopy

WT: Wild-type

Acknowledgements

I have been extremely fortunate to have had Prof. Niels H. Andersen as my advisor. He has been both a mentor and inspiration, always willing to answer questions. But it is his enthusiasm for chemistry, along with his drive for scientific simplicity, that made the biggest impression on me.

My fellow scientists from the Andersen group have also been a joy to work with. Vicki Williams and Brandon Kier were instrumental in laying the foundation for much of my research. Lisa Eidenschink Brodersen, James Stewart, Michele Scian, Kelly Huggins and Irene Shu also provided much support. I've also had the pleasure to work with the lab's newest members, Jordan Anderson and Kalkena Sivanesam.

Family and friends, both here and in Ireland, have also played a key role in providing encouragment and support. Finally, I'd like to thank my wife, Robin Taylor, and our son, Darragh, for providing the support necessary to get through graduate school.

Dedication

In loving memory of my father, Anthony Byrne, for pushing me to succeed.

Chapter 1: Introduction

1.1 Protein Structure

The amino acid sequence of a protein encodes the structure and therefore the function of the protein. As proteins are encountered in all living things, their study is an important but complex task. To aid in this, the structuring phenomenon has been broken down into four distinct levels to describe how they influence the determination of shape and function. The four levels are categorised as primary, secondary, tertiary and quaternary structure.

The primary structure is the protein's amino acid sequence, which is encoded in the gene controlling protein synthesis. This results in a chain of amino acids, which contains almost all of the information required to fold and function. Secondary structure motifs result from local interactions between units that are close together in the sequence. The most common secondary structures are α-helices, β-turns and β-strands. These secondary structures, in turn, interact with each other to form tertiary structures. More complex systems may consist of different domains held together, which form quaternary structure.

The importance of studying the protein folding mechanisms lies in the damage caused by misfolding proteins in the human body. β-Hairpins may play a role in the formation of amyloid fibrils, and therefore in a wide range of pathological diseases, e.g. Alzheimer's Disease (Petkova *et al.*, 2002).

1.2 Folding Pathways

In the late 1960's, Levinthal made the argument that finding the native state of a protein through the sampling of all conformational space would take an extraordinarily long period of time. However, proteins reach their native states relatively quickly. This contradiction is known as 'Levinthal's Paradox' (Dill & Chan, 1997; Bai, 2003). The classical view for solving this paradox was the theory that nature had found more efficient ways to fold proteins; by folding pathways (Dill & Chan, 1997). These pathways limit the conformational space that the protein goes through on its path toward its unique folded structure. The elucidation of these pathways is difficult and multifaceted.

Small proteins consisting of less than 100 amino acids are typically limited to two states; the unfolded (or statistical coil state) and the folded state. Larger proteins, however, can have three or more states. The additional states can be various forms of either a molten globule intermediate (Jennings & Wright, 1993), in which the protein collapses into an indefinable but compact state or an intermediate state with some secondary structures (Chowdhury & Raleigh, 2005) that are available to interact and eventually form the fully folded state or both.

Folding analysis is often based on two distinct models. The first is the hydrophobic collapse model; where the bulky hydrophobic sidechains are buried and sequestered from the aqueous solvent before other structural elements appear. Through the formation of the collapsed intermediate, conformational space is reduced which may than allow secondary structural elements to form followed by formation of the final state as native tertiary interactions accumulate. The existence of molten globule states

(Ptitsyn *et al.*, 1990; Jennings & Wright, 1993) potential intermediates in the process can be viewed as evidence for this pathway. The second model is the framework model in which short-range interactions facilitate the formation of secondary structures independent of tertiary interactions (Baldwin & Rose, 1999a, 1999b). Since secondary structures are, to a more significant extent, based on hydrogen bond formation - the primary force that drives this model differs from the hydrophobic collapse model. Baldwin and Rose proposed that protein folding was hierarchical and therefore protein secondary structure should largely be determined by local sequence information.

The reality of protein folding mechanisms probably lies somewhere between these two models; that is secondary and tertiary structure formation tends to be coupled (Daggett & Fersht, 2003a, 2003b). This led to the nucleation-condensation mechanism, which unites features of both the hydrophobic collapse and framework mechanisms. Nucleation-condensation invokes the formation of long range and other native hydrophobic interactions in the transition state to stabilise the otherwise weak secondary structure. This model describes the folding of two-state proteins via concerted and co-operative secondary and tertiary structure formation about the transition state for folding (Daggett & Fersht, 2003b).

A typical energy landscape for protein folding would be funnel shaped, where the native state of the protein is at the bottom of the funnel with the lowest internal energy and entropy. The roughness of the surface of the funnel indicates the presence of energy barriers or kinetic traps (Figure 1.1).

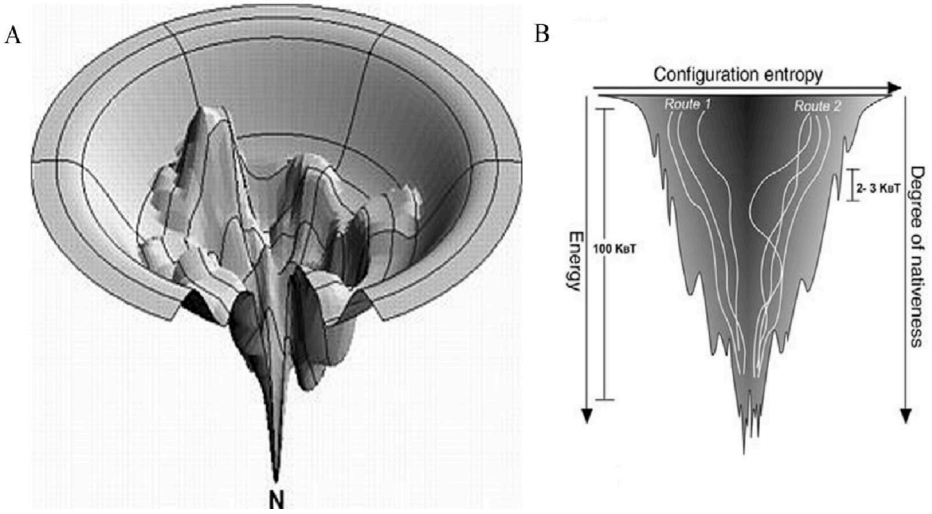

Figure 1.1 Energy landscape and folding funnel models. A. a rugged energy landscape with kinetic traps and energy barriers (Dill & Chan, 1997), and B. a folding funnel (Onuchic & Wolynes, 2004). The paths marked route 1 and route 2 illustrate that two similar sequences can fold to the same structure via different mechanisms.

This energy landscape eliminates the classical folding "pathway" idea, which implied a single (or relatively few) well-defined sequence of events to reach the native structure. Now, folding, the progressive organisation of an ensemble of protein conformations, is believed to proceed down the funnel towards the native state by many different routes (Pande *et al.*, 1998; Dobson & Karplus, 1999).

1.3 Misfolding Diseases

Misfolded or partially folded proteins can result in aggregate deposits, many of which have a common, well-ordered, cross-β-sheet fibrillar geometry. These deposits, referred to as amyloid fibrils or plaques, are associated with more than 40 human diseases or conditions. These disease include type II diabetes (Cooper *et al.*, 1987), Parkinson's disease (α-synuclein aggregates in Lewy bodies) (Goedert, 2001) and other

neurodegenerative conditions (*e.g.* Alzheimer's and Huntington's diseases). In these cases, amyloid fibrils are critical off-path structures formed during protein folding that are the diagnostic hallmark of the diseases.

The fibrils observed by current imaging techniques, *in vitro*, exhibit typical diameters of 5-15 nm and are 0.1-10 μm in length (Luca *et al.*, 2007). A number of models of the amyloid structure of disease-related aggregate deposits have been proposed (Balbach *et al.*, 2002; Kajava *et al.*, 2005; Luca *et al.*, 2007). The structure along the fiber long axis is a twisted intermolecular parallel β-sheet (Benzinger *et al.*, 1998; Antzutkin *et al.*, 2000; Luca *et al.*, 2007) (Figure 1.2). The structure in the cross-fibril direction typically includes the amyloidogenic peptide with chain reversing turns or loops, sometimes as β-hairpins (Hoyer *et al.*, 2008), but more commonly as β-strands. These antiparallel strands, however, are not intra-molecularly H-bonded as observed in typical β-hairpins. Instead, they present the backbone amides for parallel sheet formation along the fibril growth axis (Kajava *et al.*, 2005; Luca *et al.*, 2007).

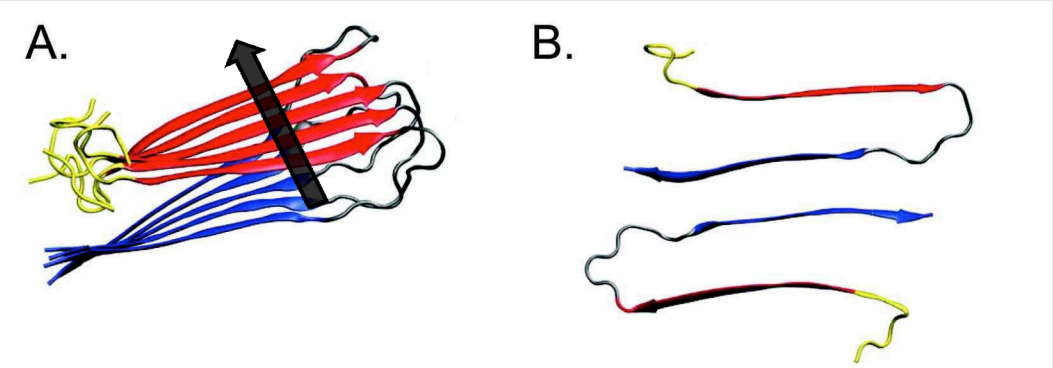

Figure 1.2 Structural models of amyloid fibrils. Structures were derived from solid-state NMR and molecular simulation (Luca *et al.*, 2007). (A) One cross-β molecular layer is shown with N- and C-termini in red and blue respectively. The black arrow represents the fibril axis. (B) Cross-sectional view of 2-amyloid peptide molecules aligned perpendicular to the fibril axis.

The Amyloid Cascade Hypothesis (Hardy & Higgins, 1992) describes the sequence of events leading up to the formation of plaque deposits. Initially it was applied to processes involved in Alzheimer's disease; from the cleavage of Amyloid Precursor Protein (APP) to the eventual formation of the plaques. Fibril formation studies (Rochet & Lansbury, 2000; Padrick & Miranker, 2002; Ruschak & Miranker, 2007) suggest a complex multi-stage, autocatalytic nucleation-dependent polymerisation process. A common feature of the process in *in vitro* assays is the lag-phase followed by rapid, co-operative fibril formation. This appears to be independent of the polypeptides under investigation.

Previously, the fibrils were viewed as causative agents in the disease process (Hardy & Higgins, 1992; Lorenzo & Yankner, 1994; Yang *et al.*, 2002), but the current opinion is that the protofibrils (oligomers or monomeric pre-amyloid conformations) are the toxic species (Meier *et al.*, 2006; Haass & Selkoe, 2007; Haataja *et al.*, 2008). These

intermediate species have proven to be difficult to isolate so their exact structures remain obscure. Before oligomerisation and fibril formation, amyloidogenic proteins can have 'random coil structure', *i.e.* having little or no secondary or tertiary structure (*e.g.* α-synuclein and Aβ) or they can be globular-like proteins with well defined tertiary structure, *e.g.* apolipoprotein A1 which is rich in α-helices. The fibril formation pathway is hypothesized to start when the unfolded protein forms an intermediate structure, or the globular protein partially unfolds exposing patches which encourage self-association. These intermediates may include helical or hairpin-like structures.

Recently, the first atomic-resolution structure of a cross-β amyloid fibril formed by an 11-residue fragment of the protein transthyretin has appeared in the literature (Fitzpatrick *et al.*, 2013). Their results define a parallel, in-register β-sheet geometry within the sheets of the fibrils, which indicates a full complement of nine backbone-backbone hydrogen bonds along the entire length of the molecule; all residues are involved apart from the proline. It's believed that the combination of side chains with identical hydrophobic and hydrophilic character in the ordered self-assembly offsets the more favourable hydrogen-bonding pattern found in antiparallel β-sheets. The in-register alignment of matching residues allows for very tight packing, maximising favourable van der Waals and hydrophobic sidechain contacts along the long axis of the fibril.

Mutations to the amyloidogenic sequence of interest have identified specific residues which are critical for self-association and ensuing fibril formation. These amino acids have provided insight into the features that enhance self-association, namely hydrophobicity, secondary structure propensity and net charge. From this

information, small model peptides have been designed to mimic the pathway allowing further characterization of misfolding and aggregation (Gazit, 2005).

1.4 Are Structuring Propensities of Peptides Relevant to Protein Folding?

Protein study can be complicated due to the size of the macromolecules. Furthermore, the sheer number of interactions involved in protein folding that can occur in a relatively small space making mutational analysis difficult. Decreasing the size of the molecule or excising a subunit of the protein can simplify protein folding analysis. Nonetheless this can also cause problems; often rendering the molecule irrelevant or inactive with respect to its biological function. As mentioned earlier, secondary structure formation may be a required early step in protein folding, hence its structure can be equally as important.

It is more convenient to look at isolated secondary structures for insights into the relationship between primary and secondary structure and folding pathways. Proteins are large, complex molecules, making direct observation of folding pathways problematic. Tertiary interactions can also complicate the study of secondary structure within a protein. Thus, the study of peptides as small models of larger proteins can be advantageous.

Small peptides are easy to synthesise using automated sold-phase synthesis methods. This allows for the easy incorporation of unusual amino acids into the sequence. Purification, using reverse-phase high performance liquid chromatography (RP-HPLC), is generally trivial. Peptides are usually studied using common techniques such as nuclear magnetic resonance (NMR) and circular dichroism (CD). The study of

small (20-40 residues) polypeptide sequences that fold into well-defined native structures can provide an understanding of the principles underlying the folding of larger proteins. Small polypeptide constructs also provide simpler systems that are computationally accessible.

1.5 Protein Design

The protein folding problem consists of two questions – 1) the determination of how a polypeptide chain folds into a native protein within a biologically relevant timescale, and 2) if this native structure can be predicted on the basis of knowledge of its amino acid sequence. The first question is becoming somewhat better understood, it is the second question that is problematic. One approach to this problem is through protein design – is it possible to design amino acid sequences that would adopt a desired three-dimensional structure? The study of small (20-40 residues) constructs that fold into well-defined native structures can provide an understanding of the underlying principles of protein folding. The *a priori* design of sequences and the determination of the requirements for the formation of protein-like structures has been the subject of active research over the past 25 years (Beasley & Hecht, 1997; Plaxco *et al.*, 1998; Head-Gordon, 2003; Dill *et al.*, 2008).

Huge improvement has also been made in the field of theoretical studies of protein folding, leading to more realistic simulations of protein folding interactions (Hellinga, 1997; Nauli *et al.*, 2001; Gnanakaran, 2003; Azia & Levy, 2009; Naganathan, 2012; Tripathi *et al.*, 2013). Computational design is a test of our understanding of the factors that determine the folding of a polypeptide sequence to its

native structure. At the same time, the design of small peptides produces model systems to test molecular dynamics (MD) simulations of folding and folding pathways. This synergy between experiments and theory adds to our knowledge of the protein folding process.

1.6 The Trp-cage

Recently, a 20 residue mini-protein was designed and prepared in the Andersen lab, through the truncation and mutation of a naturally occurring peptide, exendin-4, from the salivary secretion of the Gila monster (Neidigh *et al.*, 2002). This provided the Andersen group with the starting point for the design of a series of miniproteins. The initial NMR structure based on exendin-4 (39 residues) in an artificial media (30 vol-% trifluoroethanol) showed a single helix as the only secondary structure feature; however, tertiary structure was evident with numerous long-range NOE's observed from residues 21 through 38 (Neidigh *et al.*, 2001, 2002). The defining feature of this tertiary structure was the close association of a Gly and three Pro residues with the aromatic residues Trp and Tyr. The fold was designated as the Trp-cage. A series of truncations and mutations of the exendin-4 sequence was carried out to optimise the stability of the Trp-cage and also to impart solubility without the addition of fluoroalcohol co-solvents (exendin-4 aggregated in water in the absence of fluoroalcohol co-solvents).

The original 20-residue Trp-cage, (TC5b - NLYIQ WLKDG GPSSG RPPPS), was > 95%-folded in water with a melting temperature of 42 ºC. An NMR structure ensemble was generated (Figure 1.3) (Neidigh *et al.*, 2002) revealing the stabilising structural features: an N-terminal α-helix, a short 3_{10}-helix, a C-terminal poly-ProII

helix, and a hydrophobic core with a buried Trp indole ring at its centre. As soon as the structure was published, the Trp-cage became a target of molecular dynamics simulated folding studies (Simmerling *et al.*, 2002; Snow *et al.*, 2002). Subsequent computational studies (Chowdhury *et al.*, 2003; Ding *et al.*, 2005; Juraszek & Bolhuis, 2006; Hu *et al.*, 2008) have established it as a valued protein folding model (Searle & Ciani, 2004; Mok *et al.*, 2007). Further stabilising mutations have been implemented, increasing the melting temperature further to > 80 ºC, without making any changes to the backbone structure.

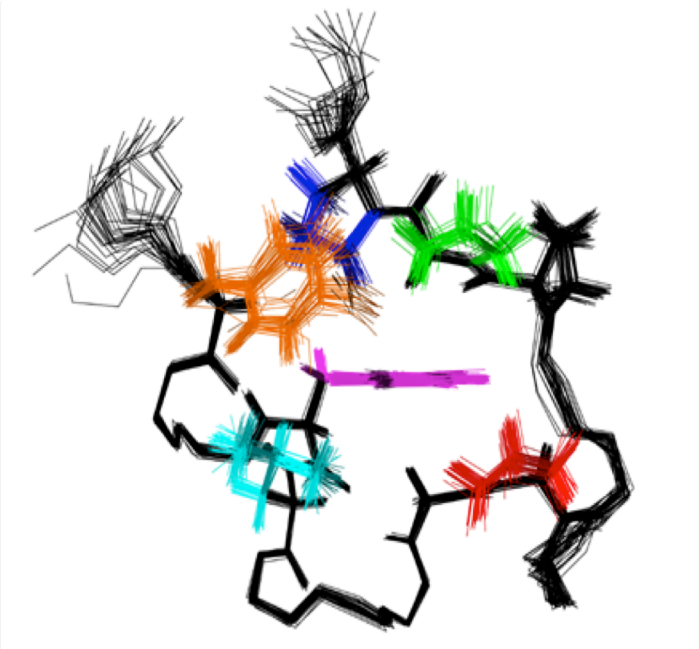

Figure 1.3 NMR generated structure ensemble for TC5b. The hydrophobic core is highlighted: tyrosine 3 (orange), tryptophan 6 (pink), leucine 7 (cyan), proline 12 (red), proline 18 (green), proline 19 (blue).

The Trp-cage represents a simple model for studying peptide folding problems, but its tertiary structure makes it useful in the context of larger proteins. The small size of the Trp-cage makes it easy to study in lab; with only about 20 residues, the Trp-cage

is trivial to synthesise using standard Fmoc solid-phase synthesis. The presence of tryptophan gives rise to a unique ultraviolet absorption (280 nm) and the relatively long α–helix makes it ideal for circular dichroism studies. The folding co-operativity of the Trp-cage allows for remote probes to be examined and global stability characteristics can be inferred throughout the molecule.

1.7 Trp-cage Melting

While the Trp-cage system has been examined extensively through both experimental and theoretical means, its folding mechanism is not yet fully understood. Indeed, some experiments suggest a two-state behaviour (Qiu *et al.*, 2002), whereas others point to the presence of intermediates (Ahmed *et al.*, 2005; Neuweiler *et al.*, 2005; Culik *et al.*, 2011; Hałabis *et al.*, 2012). Its folding behavior has been investigated by various experimental methods. Qui *et al.* (Qiu *et al.*, 2002) suggested a two-state folding mechanism based on laser temperature jump spectroscopy whereas Ahmed *et al*. (Ahmed *et al.*, 2005) using UV-resonance Raman spectroscopy measurements suggested a more complicated folding mechanism through an intermediate molten globule state. The study also provided evidence for α-helical structure even in the denatured state of the Trp-cage protein. Mok *et al*. (Mok *et al.*, 2007) found extensive hydrophobic contacts, even in the unfolded state, employing photochemically induced dynamic nuclear polarization (CINDP)-NMR pulse-labeling experiments.

Computer simulations of the Trp-cage suggest that its folding mechanism is dominated by the formation or initiation of the hydrophobic core (Chowdhury *et al.*, 2003, 2004), and by specific residue-residue contacts (Zhou, 2003b). Some studies

(Chowdhury *et al.*, 2003, 2004) argue for the early formation of the α-helices and the gradual formation of the hydrophobic core. A folding mechanism has also been proposed (Zhou, 2003b) that involves an intermediate state where the structures show two partially prepacked hydrophobic cores separated by a salt bridge. Kannan and Zacharias (Kannan & Zacharias, 2009) found that Trp-cage folding is favored by both van der Waals and to a lesser degree electrostatic contributions. Their simulation also suggest that there is a significant fraction of helical segments even in the absence of a fully folded native structure; this is in agreement with experimental data by Mok *et al*. (Mok *et al.*, 2007).

Both Zhou (Zhou, 2003b) and Ding (Ding *et al.*, 2005) observed folding pathways in which the salt bridge between D9/R16 acts as a kinetic trap. Ding reports that typically the α-helix forms faster than the 3_{10}-helix, the preformed salt bridge then behaves as a trap for the formation of the 3_{10}-helix and needs to break in order for the 3_{10}-helix to form. In Zhou's report, the preformed salt bridge which separates two partially prepacked hydrophobic cores must break in order for the global folding to occur.

Culik (Culik *et al.*, 2013) used D-amino acids to explore the Trp-cage folding mechanism. Three Trp-cage mutants were studied where Gly10 was replaced by a D-amino acid; D-Ala, D-Gln and D-Asn. Their results indicate that the stabilising effect of D-Gln and D-Asn is due almost exclusively to a decrease in the unfolding rate. Whereas, the D-Ala mutation also leads to a similar decrease in the unfolding rate, it also increases the folding rate. These results lead to a folding mechanism in which the α-helix formation in the transition state is nucleated at the N-terminus, whereas the long-

range interactions stabilising the α-helix are developed at the downhill side of the folding free energy barrier.

There is a certain lack of agreement regarding the Trp-cage folding mechanism. To some extent, different spectroscopies have led to differing conclusions. These distinct techniques are carried out by different investigators and are not cross-correlated.

1.8 Spectroscopic Techniques Employed for Studying Polypeptides

1.8.1 Circular Dichroism

Circular dichroism (CD) is a spectroscopic technique that detects the differential absorption of left- and right-handed circularly polarized light. This occurs when a chromophore is chiral due to one of the following: i) its intrinsic structure, ii) being in an asymmetric environment or iii) being covalently linked to a chiral centre. In our case the peptide bonds or interacting aromatic sidechains provide the signal.

CD spectra in the far-UV region (typically 260-180 nm) can be used to quantitatively assess the secondary structure content of a protein or peptide. The primary electronic transitions observed for protein and peptide structure are $n \rightarrow \pi^*$ and $\pi \rightarrow \pi^*$ from the backbone amide and aromatic amino acid sidechains. An advantage of CD is the relatively low concentrations (20-30 μM) required, this can be very useful for peptides that are prone to aggregate.

Certain spectroscopic signatures are observed for different types of secondary structure, arising from the orientation of the interacting transition dipoles. The α-helix is characterised by minima at 208 and 222 nm and a maxima at 190 nm. β-sheets have a minima at 218 nm and a maxima at 195 nm. Random coil structures exhibit a minimum

near 200 nm (Figure 1.4). The spectra observed for an individual peptide is a combination of the spectra of all local conformations in all molecules present, so deconvolution is necessary to determine the relative amounts of different secondary structure components (Johnson, 1990). CD can determine that a protein or peptide contains a certain percentage of each type of secondary structure and how this changes with temperature, pH or other variables. However, it cannot reveal which residues are of which structural type.

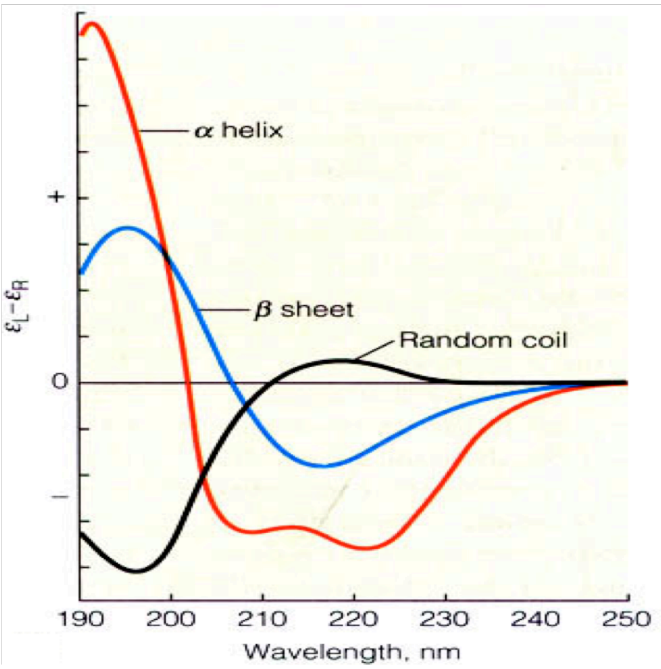

Figure 1.4 Reference CD spectra for secondary structures (Image adapted from Mathews and van Holde, *Biochemistry*, 2nd ed., 1996).

1.8.2 Nuclear Magnetic Resonance

A major disadvantage to CD is the lack of residue-specific information; only a net view of the secondary structure content of a polypeptide is provided by CD. Nuclear magnetic resonance (NMR), however, can provide information about the structure and dynamics on a residue-by-residue basis. The drawback to NMR, in comparison to CD, is the required concentration of the sample (approaching 1 mM for rapid data aquisition). The residue-by-residue information obtained from NMR comes from a number of NMR parameters which are discussed below.

1.8.3 Chemical Shift Deviation

The chemical shift (δ) is the resonant frequency of a nucleus relative to a standard. One of the most commonly used standards for aqueous media is 2,2-dimethyl-2-silapentane-5-sulfonate (DSS). The chemical shift is dependent upon differences in the electron density immediately surrounding the nuclei, and various factors related to the local structure of the molecule about any particular site. The primary effect is the electronic environment around the nuclei. On a simple level, electron donating groups bonded to the nuclei tend to increase local electron density and hence decrease the chemical shift. Other effects that influence chemical shift include Coulombic interactions, hydrogen bonding and diamagnetic anisotropy such as that due to double bonds and aromatic groups. Diamagnetic anisotropy arises from the spatial location of the nucleus relative to near-by non-spherical electron distributions. The most common source of diamagnetic anisotropy in peptides is the ring-current effect due to the π-electron cloud of aromatic residues. Hence, the chemical shift can provide information about the structure of the molecule surrounding the nuclei.

There is a significant difference in the hydrogen bonding and hydrophobic interaction network between α-helices and β-sheets. NMR chemical shifts can used as diagnostic tools to elucidate and identify protein secondary structure; the relationship between protein and peptide structure and the chemical shifts of their nuclei is well established (Wishart *et al.*, 1991).

1.8.4 Fold Population Analysis from Chemical Shifts

For many proteins and peptides, folding occurs sufficiently faster than the "NMR timescale", therefore the chemical shifts are population-weighted averages between all the folded and unfolded states in equilibrium. Since the interconversion between the folded and unfolded states is very fast, the spectrum that is observed is an average of the two states – neither state is resolved. If the interconversion were to be slow then the two conformations would be resolved. The interconversion between the two states is fast on the NMR timescale if it occurs at a rate much faster than the difference in NMR resonance frequencies between the two states. As the difference in frequency between the two states depends on the Larmor frequency of the nucleus being observed and the strength of the magnetic field, the NMR time scale is dependent on the particular probes examined and the field strength.

An unstructured polypeptide is said to be in the random coil state. The chemical shifts for the random coil state have been defined and can be used as a reference. The difference between the observed chemical shift of a peptide and the statistical random coil chemical shift is referred to as the chemical shift deviation (CSD). Site specific proton CSDs are used throughout this work as a measure of fold populations.

1.8.5 Nuclear Overhauser Effects (NOEs)

Nuclear Overhauser effects are due to through-space dipolar interactions between two nuclei. These interactions are proportional to $1/r^6$ with r being the internuclear distance. NOEs between protons are measured as the magnitude of magnetisation transferred between nuclei. The two-dimensional ^{1}H-^{1}H NOESY (**N**uclear **O**verhauser **E**ffect **S**pectroscop**Y**) is the most commonly used experiment to examine through-space interactions. When there is sufficient NOE distance information, an NMR structure can be generated. The generation of an NMR structure, however, requires a well-folded protein (typically $\chi_F > 0.7$ at the temperature observed). Otherwise non-native conformations can provide false distance information which is in conflict with the native state NOEs.

1.8.6 ^{15}N NMR

The 1-dimensional ^{1}H NMR spectra of even small proteins are impossible to interpret in any comprehensive manner. For even moderate sized proteins, addition of a second dimension still does not fully alleviate spectral crowding and overlap in ^{1}H spectra. Modern NMR spectroscopic studies of proteins rely on multidimensional experiments involving ^{1}H, ^{13}C, and ^{15}N nuclei in isotopically labelled proteins. These methods provide for signal selection (selectivity) and a means to reduce signal overlap.

Nitrogen NMR spectroscopy has great importance for structural analysis, since *N*-containing functional groups and N atoms in molecular skeletons are frequently encountered. Nitrogen has two NMR active nuclei; ^{15}N which gives sharp lines but is very insensitive and ^{14}N which is a medium sensitive nucleus but its signals are usually significantly broadened by quadrupolar interactions sometimes to the extent that they

are unobservable on a high resolution NMR spectrometer. The 1-D ^{15}N NMR experiment is much less sensitive than ^{1}H and ^{13}C NMR experiments, it yields narrow lines and has a large chemical shift range. Its low natural abundance (0.37%) makes its low sensitivity even worse so it is often enriched for NMR studies.

The use of hetero nuclei allow for some new features in NMR which facilitate the structure determination of larger proteins (> 100 AA).The natural abundance of ^{15}N is very low so isotopic enrichment of these nuclei in proteins is one of the strategies used to increase the low sensitivity. Enhancement of the signal to noise ratio through the use of inverse NMR experiments in which the magnetisation is transferred from protons to the hetero nucleus. The most important inverse NMR experiment is the HSQC (heteronuclear single quantum correlation), it correlates the nitrogen atom of an NH_x group with the directly attached proton. Each signal in a HSQC spectrum represents a proton that is bound to a nitrogen atom.

1.9 Overview of Research

The research presented in this account has two distinct parts. The first focuses on the binding studies performed on α–synuclein, whereas the second explores the features that are responsible for the stability of the Trp-cage fold.

The α–synuclein aggregation process was examined through the use of ^{15}N-NMR. This data indicated that residues that are located in the amyloidogenic patches are among those which can be viewed as indicators of pre-amyloid oligomer formation. Aromatic-containing, well-folded β-hairpins have been shown to be effective at

interfering with the fibril formation pathway. This work explores the how these hairpins bind to and divert the fibrils formed to a non-amyloid precipitate. When this precipitate is formed, the inhibitor itself appears to be incorporated into the aggregate that forms.

The other, larger, focus of my research was on the Trp-cage miniprotein. Here numerous mutations were explored, both stabilising and destabilising, with the goal of gaining more insight into specific interactions within the structure. Mutations to the salt bridge lead to the realisation that a Trp-cage could be designed that would be more stable at pH 2.5 versus pH 7 (until then all Trp-cages have been vastly more stable at the neutral pH).

Circular permutation of the Trp-cage, first realised by Dr. Brandon Kier, was optimised to the extent that T_M = 63 °C was achieved. The first Trp-cage circular permutant had a T_M ~1 °C. Mutations in the Trp-cage circular permutant were primarily based in the loop region connecting the N- and C-termini of the original Trp-cage construct. Finally, the synthesis of the cyclic form of the circular permutant of the Trp-cage has been successfully performed to yield a hyperstable miniprotein with the same structure as its linear counterparts.

Chapter 2: Materials and Methods

2.1 Peptide Synthesis and Purification

Peptides were synthesised using either an Applied Biosystems 433A or an Advanced Chemtech 496 peptide synthesiser employing Fmoc chemistry. Peptides requiring a free C-terminal were synthesised on Wang resin preloaded with the requisite C-terminal residue. For those in which an amidated C-terminal was necessary, the peptide was constructed on Rink amide resin. Peptides requiring acetylation were shaken for one hour in a mixture of 3mL dimethylformamide (DMF), 140μL triethylamine and 95μL acetic anhydride, while still attached to the Rink resin. Peptides were cleaved from the resin with 1.5 hours of shaking using 95% trifluoroacetic acid (TFA), with 2.5% triisopropylsilane (TIPS) and 2.5% nanopure water acting as scavengers. A vacuum equipped with a dry ice cold finger was used to reduce the volume to about 2 mL, the peptide was then precipitated and washed with cold diethyl ether using centrifugation at 3000 rpm for 5 minutes between washings. The ether was decanted and the pellet allowed to dry overnight.

The peptides were then dissolved in a minimal amount of nanopure water followed by purification using reverse-phase HPLC on either a Duragel or Agilent C18 column with a water (0.1% TFA)/acetonitrile (0.085% TFA) gradient. UV detection was utilized during the process; the amide backbone and tryptophan absorbs light at 215 and 280 nm, respectively. The identities of the collected fractions were confirmed on a Bruker Esquire ion-trap mass spectrometer, and the fraction containing the required peptide was rotavaped down and lyophilised.

2.1.1 Trp-cage Cyclisation

Trp-cage cyclisation was achieved through the folding-mediated cyclisation of fully deprotected AYAQWLADaGWASaRPPPSDUA. 100 μM of the peptide was dissolved in 25 mM MOPS buffer, pH 6.5. The reaction was set up in an ice bath, 150 μM of sulfo-NHS sodium salt was added followed by 1 mM EDC·HCl. The ice was allowed to melt and the reaction come up to room temperature. The reaction was monitored by HPLC. Over the course of the cyclisation, sulfo-NHS and EDC·HCl were added to the reaction mixture daily. In order to quench the reaction, preventing Trp-cage oligomerisation, 10 mM 2-mercaptoethanol and 300 μM hydroxylamine.HCL was added. The reaction solution was rotavaped down and lyophilised. Purification by HPLC followed by lyophilisation gave the final product. The cyclic product was obtained in low yield and unreacted acyclic material could be recovered via HPLC and recycled to increase the net conversion.

2.1.2 Hairpin Cyclisation

The cyclisation of hairpin cp-WW2, (GKWITVSIpPKKLTVWIp) was achieved by following the work of Robinson *et al*. (Robinson *et al.*, 2005). D-Proline-2-chlorotrityl resin was suspended in dichloromethane (DCM) to swell the resin. The synthesis of the linear peptide followed standard Fmoc procedures; some residues required double couplings. After completion of the synthesis, the resin was stirred in the presence of 10% glacial acetic acid, 10% trifluoroethanol and 80% dichloromethane for 30 minutes to remove the chlorotrityl resin, while leaving the sidechain protecting groups attached. The resin was then washed with the same cleavage cocktail again. A vacuum equipped with a dry ice cold finger was used to reduce the volume to about 2

mL; the peptide was then precipitated and washed with cold diethyl ether. The product was then cyclised overnight with stirring in DMF (9 mL) with HOAt and HATU (each 3 equivalents) and 1% v/v DIEA. After evaporation of the DMF, the product was dissolved in DCM, washed with water and dried. The cyclic protected peptide was treated with 95% trifluoroacetic acid (TFA), with 2.5% triisopropylsilane (TIPS) and 2.5% nanopure water at room temperature for 2.5 hours. After evaporation to about 2 mL, the peptide was precipitated and then washed with cold diethyl ether. This produced the desired product, which was purified by reverse-phase HPLC.

2.2 Aggregation Assays

Studies of α-synuclein have been shown to be sensitive to buffer salt and concentration, temperature, agitation and vol-% hexafluoroisoproponal (HFIP) (Huggins, 2010). Aggregation studies followed procedures already established in the lab by Dr. Kelly Huggins. Most aggregation assays report long lag times (from days to many weeks) even at high protein concentration (150-250 μM) with warming and vigorous agitation (Conway *et al.*, 1998; Narhi *et al.*, 1999; Hoyer *et al.*, 2002; Fink, 2006). Dr. Huggins designed an assay with a shorter lag time allowing for the ready monitoring of the course of amyloid formation by utilising 1.5-2 vol-% HFIP. Munishkina (Munishkina *et al.*, 2003) has reported shorter lag times for α-synuclein in buffers with added HFIP; the fibrils formed were indistinguishable from those observed under more physiological conditions. This report also proposed that HFIP addition could serve as a model for the effects of membranes on fibril formation.

2.2.1 α-Synuclein Assay Sample Preparation

The α-synuclein utilised in this study was provided by M. Bisaglia and L. Bubacco at the University of Padova, Italy. Human α-synuclein cDNA was subcloned into the NcoI and XhoI restriction sites of the pET28a plasmid (Novagen). Because ≈ 20% of the expression product from *Escherichia coli* represents mistranslation such that a cysteine residue is incorporated at position 136 instead of a tyrosine, site-directed mutagenesis of codon 136 (TAC to TAT) was employed. This results in the 100% expression of α-synuclein with the correct sequence. The protein was expressed in *E. coli* BL21(DE3) growing in Luria-Bertani medium. The overexpression product was recovered from the periplasm by osmotic shock as previously described (Huang *et al.*, 2005). The cell homogenate was boiled for 15 min, and the soluble fraction was treated with a two-step (35 and 55%) ammonium sulfate precipitation. The pellet was resuspended, dialyzed against 20 mM Tris-HCl (pH 8.0), loaded into a 6 mL Resource Q column, and eluted with a 0 to 500 mM NaCl gradient. After dialysis against Milli-Q water, the protein was lyophilized and stored at −20 °C.

100 μM α-synuclein was placed in a vial, containing a small Teflon stir bar, to which was added either 200 μL of 20 mM Tris-HCl buffer, pH 7.5 (to act as the control) or 150 μL of buffer and 50 μL of peptide inhibitor stock. Peptide inhibitor stocks were readied as 1 mM in 20 mM Tris-HCl buffer, pH 7.5. 50 μL of a prepared HFIP stock (7.5 vol-% HFIP in 20 mM Tris-HCl buffer, pH 7.5) was added to initiate aggregation. The assay was carried out with continuous vigorous stirring while in a 37 °C waterbath. Aliquots were periodically removed over a number of hours.

2.3 Nuclear Magnetic Resonance (NMR) Spectroscopy

Nuclear magnetic spectroscopy, unless otherwise specified, was performed on Bruker spectrometers that ranged from 500 to 800 MHz, with peptide samples of 1-1.5 mM concentration in 50mM phosphate buffer at pH 7 and 2.5 with 10% D_2O for locking purposed. Much lower concentrations of α-synuclein were used, 30-400 μM depending on the experiment. In addition, a small amount of 2,2-dimethyl-2-silapentane-5-sulfonate (DSS) was added as a chemical shift reference; all spectra were calibrated such that the DSS proton signal was 0 ppm. Since these experiments are all carried out in aqueous media, the water signal predominates and thus interferes with the peptide proton signals. Water suppression is hence required. To achieve this, two methods can be used. The majority of my proton NMR work employed the WATERGATE suppression technique (Piotto *et al.*, 1992). The remainder of these experiments used excitation sculpting (Hwang & Shaka, 1995). This technique essentially consists of two pulsed field gradients spin echo units; the second unit cancelling out any remaining phase errors.

A combination of TOCSY and NOESY 2D NMR spectra recorded at temperatures ranging from 280-320 K were used to assign all resonances. TOCSY spectra yield crosspeaks that correlate all of the protons within one spin system. This through-bond technique helps to identify individual amino acids as, in most cases, the backbone and sidechain protons are in one spin system. An MLEV-17 spinlock (Bax & Davis, 1985) with a 60 ms spinlock was employed for the TOCSY spectra. NOESY spectra have crosspeaks that relate two signals that experience NOEs to each other. Mixing times of 150 ms were normally used, although shorter mixing times were

sometimes used to reduce secondary NOEs. The information from the through-space effect is extremely useful in elucidating the structure of the peptide.

2.3.1 Chemical Shifts

As chemical shifts are dependent upon the local electronic environment, they are usually different between a peptide's folded and unfolded state. With rapid equilibrium between the folded and unfolded state, chemical shifts are population-weighted averages.

2.3.2 Chemical Shift Deviation

Chemical shift deviations (CSDs) are defined as the difference between the observed chemical shift and the statistical random coil chemical shift.

Equation 2.1. Calculation of chemical shift deviations:

$$CSD = \delta_{observed} - \delta_{random\ coil}$$

Factors which influence CSD values include hydrogen bond participation, specific dihedral angles and ring current effects. In a well-folded Trp-cage motif (Figure 1.3), the protons above and below the indole ring of Trp^{6} experience large CSDs due to shielding ring-current effects (Gly^{11} Hα2: -3.45 ppm, Pro^{18} Hα: -1.96 ppm, Pro^{18} Hβ3: -1.95 ppm) (Neidigh *et al.*, 2002). The resulting CSDs melt out in concert upon warming and are reduced by the same extent upon introduction of destabilising single site mutations. The large CSDs of Gly^{11} Hα2, Pro^{18} Hα and Hβ3, and the presence of characteristic long-range nuclear Overhauser effects (nOe's), *e.g.* Y^{3}α to P^{19} δ2, W^{6}ε1 to P^{18}α, are diagnostic of the structure of the Trp-cage.

2.3.3 Calculating Fold Populations from CSDs

CSD values are not only useful in the identification of secondary structure, but can also be helpful in determining accurate fold populations. The conversion of CSDs to %-fold is linear as the exchange rate between the folded and unfolded states of the Trp-cage is fast on the NMR timescale. The conversion to %-fold is relatively straightforward if given the chemical shift values of the two states (folded and unfolded). The statistical coil values represent the 0%-fold chemical shift, obtaining the 100%-fold chemical shift is more complicated. One method is to use a mutant with a higher fold population but the same structure. Another is the use of hydrogen/deuterium exchange studies; TC16b has been established to be 99.5+%-folded at 280K by Vicki Williams based on exchange protection (Williams *et al.*, 2008). A structured reference peptide of known χ_F can be used to calculate the %-fold (Equation 2.2).

Equation 2.2. Calculation of %-fold from CSD values using a reference value at 98%-folded.

$$\chi_F = \frac{CSD_{experimental}}{CSD_{98\%}} \times 0.98; \%\text{-Fold} = 100 \cdot \chi_F$$

The CSD values and the %-fold values can be used to determine the melting temperature (T_M); the temperature at which the peptide is 50%-folded. Each probe representing the fold population is site-specific. Fold populations and T_M values can be obtained for each probe and their comparison can illustrate the extent of co-operativity of the peptide. In the case of the Trp-cage, the diagnostic values can be divided into two groups representing the two sections of structure: the α-helix (Y3 Hα, Q5 Hα, W6

Hα, K/A8 Hα) and the cage (L7 Hα, G11 Hα2, P18 Hα, P18 Hβ3, P19 Hδ2/δ3). The L7 Hα proton also has significant helix values. Both groups have similar melting temperatures, though the helix is always slightly higher arising from the slight residual helicity independent of the C-terminal cage portion. As all the CSD values have similar melting profiles (Neidigh *et al.*, 2002), each group is represented by the sum of all its diagnostic CSDs which can then be used in the calculation of the folded state population. Data reported herein will predominantly utilise the G11 Hα2, P18 Hα, P18 Hβ3, P19 Hδ2/δ3 protons. The G11 protons can however be absent especially at higher temperatures due to broadening, which may occur at lower %-fold populations for peaks with a large Δδ between the folded and unfolded state.

2.3.4 ^{15}N NMR

The ^{15}N labelled α-synuclein sample was prepared at the University of Padova. The sample preparation for ^{15}N labelled samples is the same as their non-labelled counterparts. No internal standard was used; indirect referencing was employed instead. Internal standards are appealing due to their convenience, but they are not without problems. Sensitivity to salt, pH and temperature variations (De Marco, 1977), nonspecific interactions with the biomolecule of interest (Lam & Kotowycz, 1977; Shimizu *et al.*, 1994), solvent effects and limited solubility or stability can all affect the chemical shift of an internal standard. Indirect referencing for multidimensional heteronuclear NMR is a way to tackle this problem. Frequency ratios (Ξ) can be used to calculate chemical shifts when two or more nuclei are being measure simultaneously (Live *et al.*, 1984; Edison *et al.*, 1994). This requires the measure of just a single reference compound (DSS) for a single nucleus type (^{1}H) to indirectly determine the

zero-point reference for another nucleus (^{13}C or ^{15}N) (Wishart *et al.*, 1995). A temperature dependence correction was also taken into account.

^{1}H-^{15}N **H**eteronuclear **S**ingle **Q**uantum **C**oherence (HSQC) spectra were used to examine α-synuclein binding sites and their effects on aggregation. ^{15}N-HSQC spectra were consistent with the assignments reported by Bax (Bodner *et al.*, 2010).

2.4. NMR Structure Ensemble Generation

Structure ensemble generation is performed by a modified version of a program called *CNS* (Crystallography and NMR System) (Brünger *et al.*, 1998; Brünger, 2007) which utilizes distance constraints and converts them into a structure using energy algorithms. The distance constraints are derived from NOE data, NOESY experiments at 280K are repeated with varying mixing times to distinguish primary versus secondary through space magnitisation transfer components. All peaks in the NOESY spectra are assigned using *SPARKY* (Goddard & Kneller, 2006), which is used to generate a peak height list. NOE peak intensities were converted to distance constraints using an in-house program, *DistInt v0.8 (Fesinmeyer 2005)*. *DistInt v0.8* corrects for the greater intensity of sharp aromatic peaks as well as contributions from multiple chemically equivalent protons e.g. methyls. *DistInt* also allows for the calculation of the upper and lower distance bounds of each NOE peak, these are designated as d+ and d- for the long and short bounds, respectively.

In our CNS protocol, high temperature torsion angle dynamics create a host of random structures which are then subjected to simulated annealing with Cartesian dynamics. A final minimisation step, using a Lennard-Jones potential to calculate the van der Waals interaction energies, was added to the original CNS annealing script. The

final step is an acceptance protocol that is based on both atomic and bond geometry along with constraint list agreement. The acceptance criteria were no NOE violation > 0.25 Å and agreement with idealized covalent geometry (the mean of the bond, angle and improper torsion violations could not exceed 0.01 Å, 0.55° and 0.25° in any structure with no individual values exceeding 0.02 Å, 3° and 2°, respectively).

A structure ensemble was generated using the accepted structures. The backbone and heavy atom root mean squared deviations (RMSD) were measured for residues 2-19 for pairwise comparisons over the accepted ensemble. The RMSD calculations and figures depicting structure ensembles were generated using both MolMol (Koradi et al. 1996) and PyMol (DeLano, 2002).

2.5 Circular Dichroism Spectroscopy

Circular dichroism (CD) measures the difference in absorptivity by a chiral molecule of left- and right-handed circularly polarised light. Since the CD spectrum of folded structures differs from unfolded random coil, as the temperature increases the folded structure starts to melt. From this melting profile, melting temperatures can be calculated. The specific application in the present work focused on measuring thermal stability. CD allows for a greater temperature range than NMR, therefore a more complete melting profile can be determined.

Circular dichroism (CD) stock solutions were prepared by dissolving weighed amounts of peptide in 20 mM aqueous pH 7 or pH 2.5 potassium phosphate buffer to make a solution with an approximate concentration of 200 μM. The concentration of the stock solution was measured using UV absorption at 280 nm (based on $\varepsilon = 5690\ M^{-1}$

cm^{-1} for tryptophan and 1200 M^{-1} cm^{-1} for tyrosine). CD solutions were then diluted appropriately to make 30μM solutions of the peptide in buffer.

Spectra were recorded on a Jasco J-720 spectropolarimeter with a Peltier temperature controller and calibrated to d-10-camphorsulfonic acid $[\theta]_{192.5} = 15{,}600$ (Yang *et al.*, 1986). The CD spectra were measured using 0.10 cm path length quartz cells, with low birefringence. Samples were scanned at 10 temperatures in 10° C increments, ranging from 5° C to 95° C. There was a five minute equilibration period prior to data collection at each temperature. The typical spectral accumulation was a scan rate of 100 nm/min with a 0.2 step resolution over a range of 190-270 nm, with eight scans averaged for each spectrum.

The average spectra were trimmed at a dynode voltage of 600 V prior to blank subtraction and smoothing via a reverse Fourier transform procedure. All the data processing was done using Jasco spectra analysis software. The raw ellipticity data for Trp-cages was converted into mean residue molar ellipticity units $(deg.cm^2)/(residue.dmol)$. Units for α-synuclein and β-hairpins are displayed in molar ellipticity.

2.5.1 Analysis of Melting Data

CD melts were analysed as plots of mean residue molar ellipticity at 222 nm ($[\theta]_{222}$) versus temperature. The $[\theta]_{222}$ were converted into fraction-unfolded values and the Tm's were obtained from the plots of fraction-unfolded versus temperature. The 100% unfolded CD spectrum (Barua, 2005) and its temperature dependence were previously determined in the Andersen lab by analysis of the thermal melting data of several Trp-cages in 7 M GdmCl resulting in Equation 2.3:

Equation 2.3. Temperature dependence of the unfolded state of the Trp-cage.

$$[\theta]_U = -900 - 29 \bullet T\ (°C) \text{ for TC10b and}$$

$$[\theta]_U = -720 - 29 \bullet T\ (°C) \text{ for TC16b}$$

The 100% folded baseline was calculated by assuming a temperature gradient that was 0.32% of the 100%-folded ellipticity at 0 °C and an intercept equal to the 100%-folded ellipticity at 0 °C:

Equation 2.4. Calculation of 100%-folded ellipticity at a given temperature, T (°C).

$$[\theta]_F = (-0.32/100 \bullet [\theta]_{100\%,\ 0\ ^\circ C}) \bullet T + [\theta]_{100\%,\ 0\ ^\circ C}$$

For determining the melting point for more stable peptides (the cyclised circular permutant, Chapter 7), the CD melts were performed without added denaturant and with 1–7 M guanidinium chloride (GdmCl) present.

2.5.2 α–Synuclein Aggregation Assays

Stock α–synuclein-peptide solutions for CD experiments were prepared in either buffer alone or in buffer-HFIP mixtures. The same parameters were used as described previously, but with 12 scans performed. To perform the CD experiment, 5 μl aliquots were removed from the assay sample and diluted with 195 μl of 1.5% HFIP Tris-HCl

buffer, resulting in a 2.5 μM final α-synuclein concentration. This was carried out every 2 hours to monitor the α-synuclein transition from random coil to β-sheet.

Chapter 3: α-Synuclein Binding Studies

3.1 Introduction

Protein folding studies not only explore how a protein folds or unfolds, but also examine protein misfolding. The misfolding of proteins can lead to the formation of off-path intermediates that can be detrimental to living cells. Protein aggregation can result from protein misfolding, and is known to be involved in more than 40 disease states in humans (Chiti & Dobson, 2006, 2009). These disease states, otherwise known as amyloid diseases, such as Alzheimer's, Parkinson's and Huntington's are associated with and derive their class name from the ordered aggregate structures (amyloid fibrils) that accumulate as plaques in vital organs.

The currently held view is that β-oligomers (or pre-amyloid conformations) are the toxic species of the disease rather than the mature fibrils. Hence, developing therapeutic strategies that can target the early steps along the protein misfolding (fibril forming) pathway has become a more prominent feature in the field of amyloid disease research. There are three major therapeutic strategies (Lansbury, 1997; Stains *et al.*, 2007; Roberts & Shorter, 2008; Takahashi & Mihara, 2008; Chang *et al.*, 2009; Nerelius *et al.*, 2009) for amyloid associated diseases that are discussed in the literature: 1) interfering with protein processing that results in the amyloidogenic peptides, 2) diverting pre-amyloid intermediates to non-toxic aggregates, and 3) reducing the steady-state concentration of toxic intermediates in the amyloidogenic pathway by altering the relative rates of reactions within the aggregation pathway. The second and

third strategy requires a greater understanding of the amyloidogenesis mechanism. Selective inhibitors of the processes should prove to be useful for this.

3.2 Pre-amyloid Processing

Several disease-related amyloidogenic peptides are produced from pro-proteins by enzymatic cleavage. With Alzheimer related Aβ species, the amyloidogenicity of different cleavage products of amyloid β-protein precursor (AβPP) varies significantly, *e.g.* Aβ (1–42) aggregates more aggressively than Aβ (1-40). Two of the key enzymes involved in AβPP processing are β-secretase and γ-secretase, as a result the inhibition of either of these two enzymes is seen as a therapeutic target for Alzheimer's disease. Non-steroidal anti-inflammatory drugs (NSAIDs) appear to bind to AβPP and reduce the rate of γ-secretase processing (Eriksen *et al.*, 2003; Kukar *et al.*, 2008).

3.3 α–Synuclein

The α-synuclein used in these studies is the full length 140-residue species. The α-synuclein was provided by M. Bisaglia and L. Bubacco, produced by over expression in *E. coli* BLD1 (DE3). This protein is implicated in Parkinson's disease and is the primary component of Lewy bodies found in patients. The exact function of α-synuclein is unknown, but it is found in predominantly in neural tissue possibly functioning as molecular chaperones and/or as a microtubule associated protein (Alim *et al.*, 2004).

The primary structure of α-synuclein is divided into three distinct domains: 1) residues 1-60 is an amphipathic, N-terminal region made up of 11-residue repeats with a

highly conserved hexamer (KTKEGV) motif, 2) residues 61-95 is the central hydrophobic region including the *non-Aβ component* (NAC) region which is involved in protein aggregation, and 3) residues 96-140 is a highly acidic and proline-rich section with no distinct structural propensity. The *non-Aβ component* (NAC) was originally observed in amyloid plaques associated with Alzheimer's disease (Uéda *et al.*, 1993). The full sequence is shown in Figure 3.1.

1 MDVFMKGLSK AKEGVVAAAE KTKQGVAEAA GKTKEGVLYV GSKTKEGVVH
51 -GVATVAEKTK **EQVTNVGGAV VTGVTAVAQK TVEGAGSIAA ATGF**VKKDQL
101 -GKNEEGAPQE GILEDMPVDP DNEAYEMPSE EGYQDYEPEA

Figure 3.1. Full sequence of α-synuclein, with the NAC region in bold.

Monomeric α-synuclein is a random coil structure in aqueous media, but there are helical conformations at the lipid binding N-terminal region. This can be mimicked *in vitro* in the presence of membranes and membrane-like environments (Eliezer *et al.*, 2001; Jao *et al.*, 2004; Bisaglia *et al.*, 2005, 2006; Ulmer & Bax, 2005). Solid-state NMR studies of fibrils (Vilar *et al.*, 2008) have given hints to the optimal sites that can be targeted to prevent fibril assembly.

3.4 Small Molecule Inhibitors

(-)-Epi-gallocatechin-3-gallate (EGCG) (structure shown in Figure 3.2) is a green tea polyphenol component that has been shown to improve age-related cognitive decline and protect against cerebral ischemia (Lee *et al.*, 2000) and brain inflammation and neuronal damage in experimental autoimmune encephalomyelitis (Aktas *et al.*, 2004). Low neuroprotective concentrations of EGCG decreased the expression of pro-apoptotic genes, while high concentrations increased apoptosis (Levites *et al.*, 2002).

EGCG has also been reported to exert a neurorescue activity and to promote neurite outgrowth of PC12 cells (Reznichenko *et al.*, 2005). Its proposed mechanism of action is through acting as a radical scavenger (Nanjo *et al.*, 1996) and possibly through the regulation of antioxidant protective enzymes (Levites *et al.*, 2001).

EGCG possesses 'inhibitory potency' against at least five amyloidogenic systems (Ehrnhoefer *et al.*, 2008; Hudson *et al.*, 2009). It has been proposed that this polyphenol compound acts by diverting poorly folded species to non-amyloidogenic oligomers and eventually to non-toxic aggregates. This diversion is instead of to toxic pre-amyloid species, along the path to amyloid fibrils.

Resveratrol, a polyphenol (structure shown in Figure 3.2) found in grapes and red wine, possesses a range of biological effects including potential neuroprotective activities. Studies have shown that moderate consumption of wine is associated with a lower incidence of Alzheimer's disease (Marambaud *et al.*, 2005). The exact molecular mechanisms involved in the beneficial effects of wine intake on the neurodegenerative process in Alzheimer's remain to be clearly understood. One study (Marambaud *et al.*, 2005) shows the resveratrol lowers the levels of secreted and intracellular amyloid-β (Aβ) peptides from different cell lines. Resveratrol does not inhibit Aβ production (there is no effect on β- and γ-secretases), rather promotes intracellular degradation of Aβ via a mechanism that involves the proteasome.

The bioavailability of resveratrol in the brain is unclear. The studies by Karuppagounder (Karuppagounder *et al.*, 2009) were unable to detect resveratrol or its conjugated metabolites in the mouse brain. On the other hand, Vingtdeux (Vingtdeux *et al.*, 2010) was able to detect orally administered resveratrol in the mouse brain where it

activated AMP-activated protein kinase (AMPK) and reduce cerebral Aβ levels and deposition in the cortex. Resveratrol also inhibited the AMPK target mTOR (the mammalian target of rapamycin) to trigger autophagy and lyosomal degradation of Aβ.

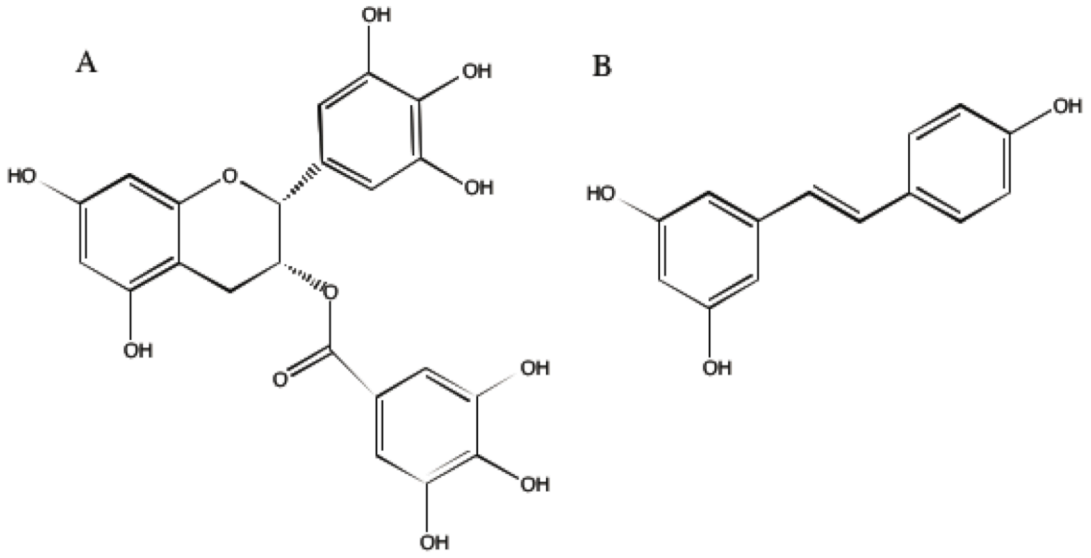

Figure 3.2 Structure of (-)-Epi-gallocatechin-3-gallate (EGCG) (A), structure of *trans*-resveratrol (B).

3.5 Protein and Peptide Inhibitors

The majority of the protein and peptide amyloidogenesis inhibitors are solubilised (El-Agnaf *et al.*, 2004; Austen *et al.*, 2008) and/or mutated versions of the most amyloidogenic sequence fragments (Figure 3.3). A popular approach to creating an agent which could interfere with the fibril growth process is to synthesise short peptides that correspond to a self-recognition element (SRE) of the native amyloid sequence but contain modifications so that the peptides bind to the parent protein at this element and prevent further aggregation (Sciarretta *et al.*, 2006). The common strategy for inhibition is β-assembly disruption through the introduction of mutations that discourage β-strand formation and/or association such as proline, N-methylation or α-

disubstituted amino acid residues (Gilead & Gazit, 2004; Etienne *et al.*, 2006). N-methylation has other benefits besides acting as an aggregation inhibitor: the modifications provide greater solubility in both aqueous and organic media, resistance to proteolytic degradation and aid in the diffusion across membranes (Gordon *et al.*, 2002; Adessi *et al.*, 2003; Kokkoni *et al.*, 2006).

Studies indicate that the NAC (Figure 3.3) is the main region linked with protein aggregation (Bisaglia *et al.*, 2006; Du *et al.*, 2006). Consequently, peptide based inhibitors were designed based on this region, primarily residues 68-72 (GAVVT) and 77-82 (VAQKTV) (El-Agnaf *et al.*, 2004). Peptide inhibitor strategies include the design of methylated peptide inhibitors analogous to α-synuclein residues 68-72 and solubilising peptide fragment of the NAC region. Both strategies were effective against fibril formation and protein toxicity (Bodles *et al.*, 2004; Madine *et al.*, 2008). Current design inhibitors of α-synuclein target the critical binding domain responsible for self-association. Small molecule inhibitors include L-DOPA (Amer *et al.*, 2006) and EGCG (Ehrnhoefer *et al.*, 2008), the latter of which has been the subject of much attention due to its effect on different amyloid systems.

α-Synuclein 61-EQVTNVGGAVVTGVTAVAQKTVEGAGSIAAATGFV-95
Inhibitors RGAVVTGR-NH_2 (El-Agnaf *et al.*, 2004) // VAQKT-(N-Me)V (Madine *et al.*, 2008)

Figure 3.3. β-Assembly disruption strategy for α-synuclein.

Madine (Madine *et al.*, 2008) utilised N-methylation of a 12-residue region (residues 71-82) of α-synuclein to develop a peptide inhibitor of α-synuclein aggregation. This region was chosen as their starting point as its residues constitute a critical SRE of α-synuclein and are absent in β-synuclein, a non-aggregating

homologue which has been reported to protect α-synuclein from aggregating (Fan *et al.*, 2006), the peptide alone readily aggregates to form insoluble amyloid fibrils (Madine *et al.*, 2008) with a similar morphology to the parent protein, and in the presence of full length α-synuclein, the peptide binds to and co-fibrillises with the aggregating α-synuclein (Giasson *et al.*, 2001). It was established that the C-terminal residues of the 12-mer (VAQKTV) accelerated the aggregation into amyloid species, indicating that this region represents the critical region for forming ordered fibrils. N-methyl derivatives of this 6-mer were prepared to test their effectiveness as inhibitors of α-synuclein aggregation. It was found that VAQKT-(N-Me)V had a significant inhibitory effect on the aggregation of α-synuclein.

El-Agnaf (El-Agnaf *et al.*, 2004) synthesised an overlapping library of synthetic 7-mer peptides, each of which was tagged with a biotin group. The biotin tag allowed for binding detection of the peptide to full-length α-synuclein. Peptides covering the hydrophobic region located in the central part of α-synuclein (residues 64-100) produced the highest binding levels. Peptides from the N-terminal region (1-60) had low binding, while peptides from the C-terminal region (101-140) showed no binding at all. The peptides that gave the highest level of binding covered the N-terminal half of the NAC region (64-86). From this data, the GAVVT region was chosen to explore further. Following optimisation, the peptide RGAVVTGR-NH_2 showed complete inhibition of amyloid fibril formation at a 2:1, 1:1 and 1:2 (α-Synuclein: peptide molar ratio) when incubated with 50 μM α-synuclein.

3.6 Aromatic Residues in Peptide Amyloid Inhibitors

Over the course of the last decade, the Andersen lab (Fesinmeyer *et al.*, 2005; Andersen *et al.*, 2006; Kier & Andersen, 2008; Eidenschink *et al.*, 2009) and other groups (Espinosa & Gellman, 2000; Cochran *et al.*, 2001; Hughes & Waters, 2006a, 2006b; Riemen & Waters, 2009) have improved the *a priori* design of β-hairpins to the extent where 10 – 16 residue constructs that are >85% folded in water can be routinely designed and prepared. Consequently, it became of great interest as to whether or not these β-hairpins could serve as pharmacophore display scaffolds for drug lead discovery.

Specific literature reports drew the Andersen group's attention towards the possibility of Trp/Tyr-containing β-hairpins acting as potential amyloidogenesis inhibitors. The key report was published by Ghosh and co-workers (Smith *et al.*, 2006), who revealed that a hyperstable mutant of the B1 domain of protein G could be mutated into a potent inhibitor of Aβ40 aggregation. The mutations used to form the inhibitory protein included K → W, G → W, K → Y and E → Y. Seven of the eight mutations occurred on the exposed face of a single hairpin of the B1 domain. Sato *et al*. (Sato *et al.*, 2006) showed that for inhibitors of the sequence type RGT**X**EGK**X**-NH_2, the potency of the inhibitor increases as X changes from Phe to Tyr to Trp. Tryptophan rich peptides also reportedly inhibit the aggregation of poly-Q segments in for example Hungington's disease (Nagai, 2000; Nagai *et al.*, 2007). A F23Y mutation in an 8-residue variant of the amyloidogenic patch of hAM produces inhibitory activity (Porat *et al.*, 2004).

For the Andersen group's research into the aggregation of α-synuclein, Dr. Kelly Huggins (Huggins, 2010) chose to examine designed hairpins containing multiple Trp and Tyr residues. These hairpins had no structural resemblance to the amyloidogenic peptide. In continuing on this research, I have only focused on a small selection of these hairpins (Table 3.1), those that Dr. Huggins showed to be the most promising as inhibitors. These hairpins, the majority of which contain aryl-turn-aryl motifs, have all been previously characterised by NMR and CD and are, with the exception of ssW which serves as a control, at least 50% folded under the assay conditions (Huggins *et al.*, 2011)

Name	Sequence
ssW	KKLTV**W**I
WW2	KKLTV**W**-IpGK-**W**ITVSA
Cyclo WW2	pPKKLTV**W**-IpGK-**W**ITVSI
cp-WW2	GK**W**ITVSIpPKKLTV**W**Ip
μPro1	C_2H_5-**W**-IpGK-**W**TG-NH_2

Table 3.1. Hairpins used for amyloid inhibition studies.

The basis of this amyloid study relies on the hypothesis that with well designed β-hairpins, the β strands will facilitate intermolecular sheet formation with a pre-amyloid state and hence prevent the self-self recognition associated with fibril growth and as a result inhibit amyloid formation. To allow for the initial association of the hairpin inhibitor with the pre-amyloid state, Trp residues are included in the strands. Trp and Tyr residues are often observed at peptide/protein interfaces (Ma *et al.*, 2003), they form favourable cross-strand interactions in β sheet systems, and occur quite frequently in prior peptide modulators of amyloidogenesis.

cp-WW2 is the acyclic version of cyclo WW2, the cyclisation method is discussed in Chapter 2. This hairpin was characterised by both NMR and CD. CD displays the expected exciton couplet at ~228 nm (Figure 3.4).

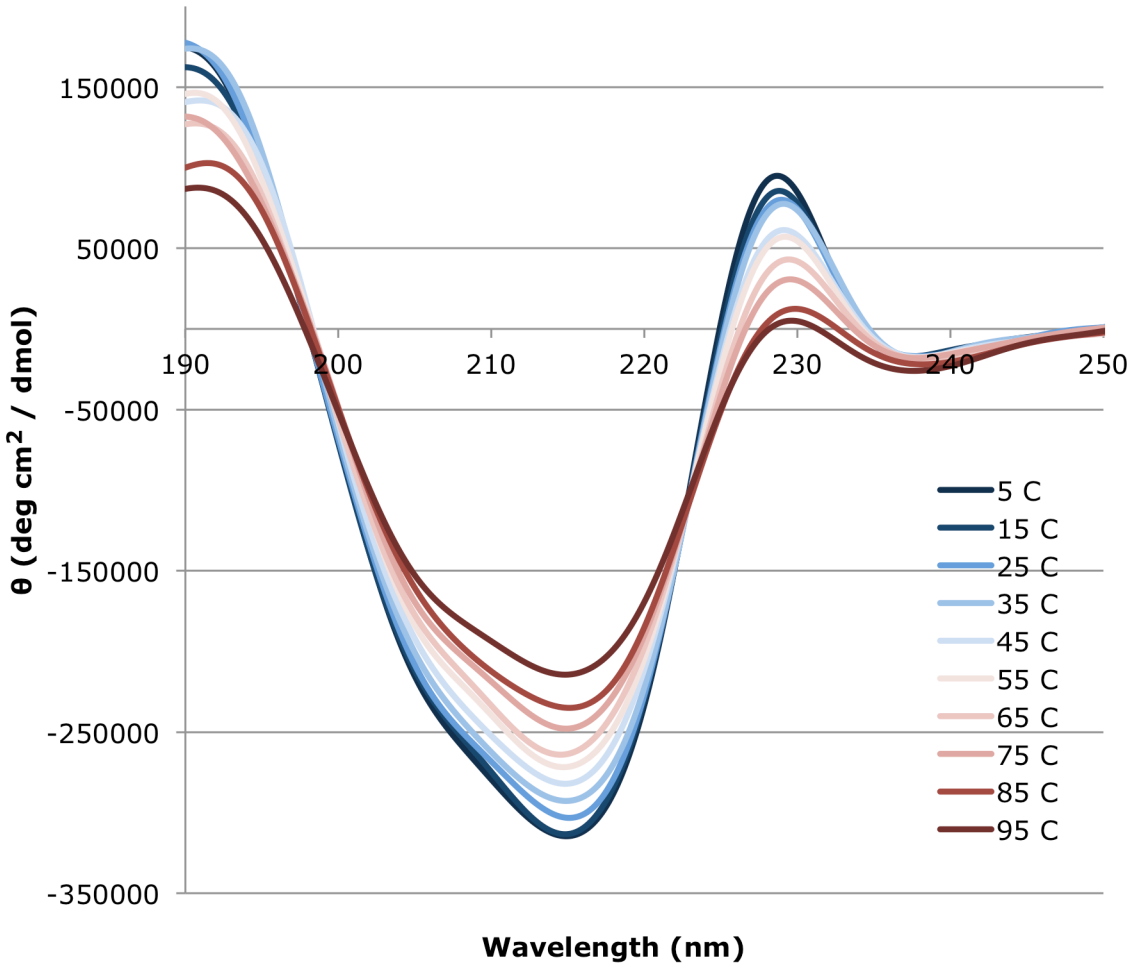

Figure 3.4. CD melt for cp-WW2.

The 2D NMR indicated that this hairpin had some interesting characteristics. The Trp pair, located near the termini, is acting like a β-cap with the C-termini Trp being the edge in the EtF (edge-to-face) interaction. This is indicated by the large upfield shift of the C-termini's Trp Hε3. The shift at this probe site is even more upfield that what is observed for WW2 and for cyclo WW2 (Figure 3.5).

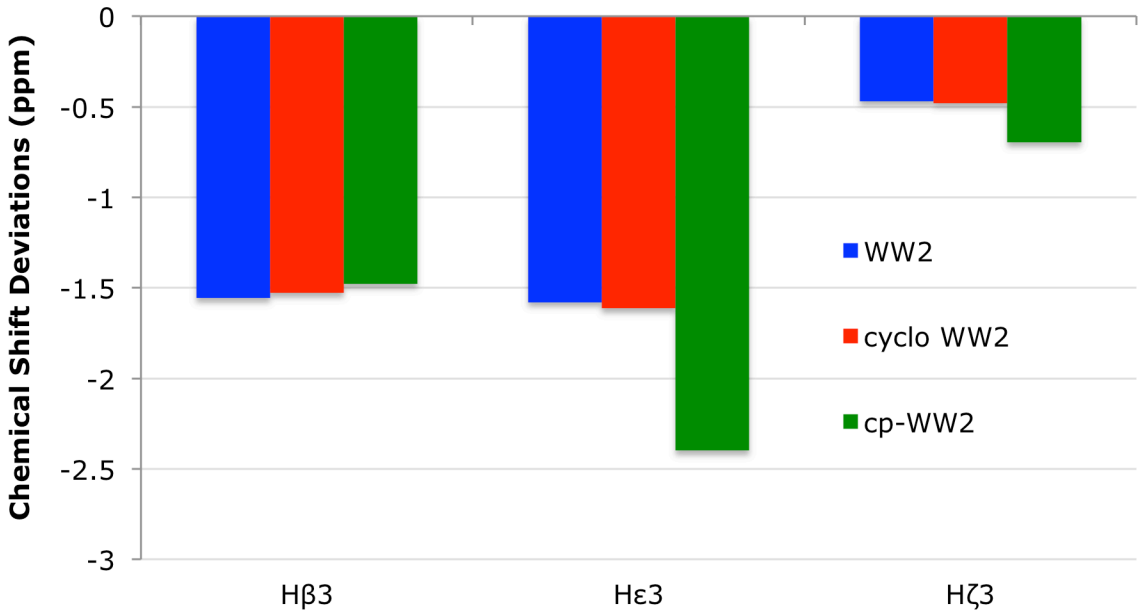

Figure 3.5. Diagnostic shifts for the edge Trp in the WW2 series.

The larger upfield shift for the Hε3 proton in cp-WW2 in comparison to cyclo WW2 may be a reflection of the cyclised hairpin being in a very rigid conformation. In cp-WW2, the Trp/Trp pair has some room to 'wiggle', finding the optimal position for the Trp/Trp interaction to occur.

3.7 Previous Hairpin Work

The Andersen lab has previously established that designed hairpin peptides, with no sequence similarity to the amyloid-producing polypeptides, interfere with the amyloidogenesis of α-synuclein (Huggins *et al.*, 2011). The most potent 'amyloid inhibitors' appear to function by diverting α-synuclein to non-amyloid aggregates. Dr. Hugggins showed that certain hairpins, those from the MrH class with stable folds ($\chi_F \geq$ 0.70 at 280 K) bearing two aromatic sidechains, produced immediate cloudiness upon

initiating amyloidogenesis. This precipitation occurred on addition of 0.5 to 2 molar equivalents of the aromatic hairpins to the assay mixture. Among this class of hairpins is WW2 (sequence shown in Table 3.1). Through a control experiment, it was shown that HFIP appears to enhance, rather than cause, the observed precipitation of α-synuclein in the presence of certain hairpins. The fibril morphology was also examined through the use of TEM imaging and congo red (CR) staining. Fibrils of normal morphology were *not* observed for the WW2 hairpin; CR staining was less extensive and intense, with no green birefringence observed. Shorter thicker fibrils were also produced for WW2.

A single strand control for WW2, designated ssW, was examined to aid in the isolation of structural or sequence determinants for the precipitation occurrences observed for WW2. In the presence of this peptide a helical CD spectrum appeared at the 4-6 hour points in the α-synuclein aggregation assay. As a helical CD signature had not been observed for non-inhibited α-synuclein controls, the helical CD signals observed when ssW is present is attributed to oligomerisation inhibition which allows the observation of a pre-amyloid state.

For my studies, I examined the early stages of α-synuclein aggregation by NMR spectroscopy, both with and without added peptide 'inhibitors'. The inhibitors used are shown in Table 3.1. Both ^{1}H and ^{15}N NMR experiments were used. Known inhibitors of α-synuclein were also examined by CD; EGCG and resveratrol were both examined.

3.8 Circular Dichroism Studies

EGCG was examined at three different concentrations in relation to 100 μM α-synuclein; at a 1:1 (α-synuclein:EGCG), 1:5 and 1:10 ratio. HFIP was added to the assay mixture to initialise aggregation; the final HFIP concentration was 1.5 vol-%. The 1:1 sample showed a random coil signature for the first 8 hours of observation, upon performing a CD scan at 24 hours, the signature had changed to β-sheet. The 1:5 sample began the transition to β-sheet around the 6 hour mark, though the CD signal was somewhat noisier than the 1:1 sample. This could be due to the formation of invisible aggregates. In the 1:10 sample, no random coil signal was observed even at the time zero time point, though there was no helical signature seen either. Yet again, this is presumably due to the presence of invisible non-amyloid aggregates.

The CD studies for resveratrol had to be carried out with DMSO present; resveratrol dissolves only in the presence of DMSO. I had hoped to examine at both a 1:1 (α-synuclein:resveratrol) and a 1:5 ratio, the α-synuclein concentration was 100 μM. However the final DMSO concentration (6%) in the 1:5 sample was prohibitive to performing CD. The 1:1 sample (final HFIP concentration of 1.5-vol-%) showed a random coil signature for the first 4 hours of observation, with a β-sheet signal transitioning in at the 6 hour time point.

The results for both the EGCG and resveratrol assays replicate prior published results (Ahn *et al.*, 2007; Bieschke *et al.*, 2010).

3.9 Proton NMR Studies

The first experiments were set up to look for exchanging broadening of peptide 'inhibitor' signals upon addition of increasing amounts of α-synuclein. The experiments started with 300 μM inhibitor and no α-synuclein present, followed by 0.1 molar equivalents α-synuclein, 0.2 molar equivalents α-synuclein and 0.5 molar equivalents α-synuclein. After the final titration was examined by ^{1}H NMR, the sample was adjusted to 2 vol-% HFIP content to examine the effects of either β oligomerisation or non-amyloid aggregate formation. Of the inhibitors studied, only the single strand hairpin (ssW) showed any broadening of signals. Significant broadening was observed only for the Trp resonances of peptide ssW (Figure 3.6).

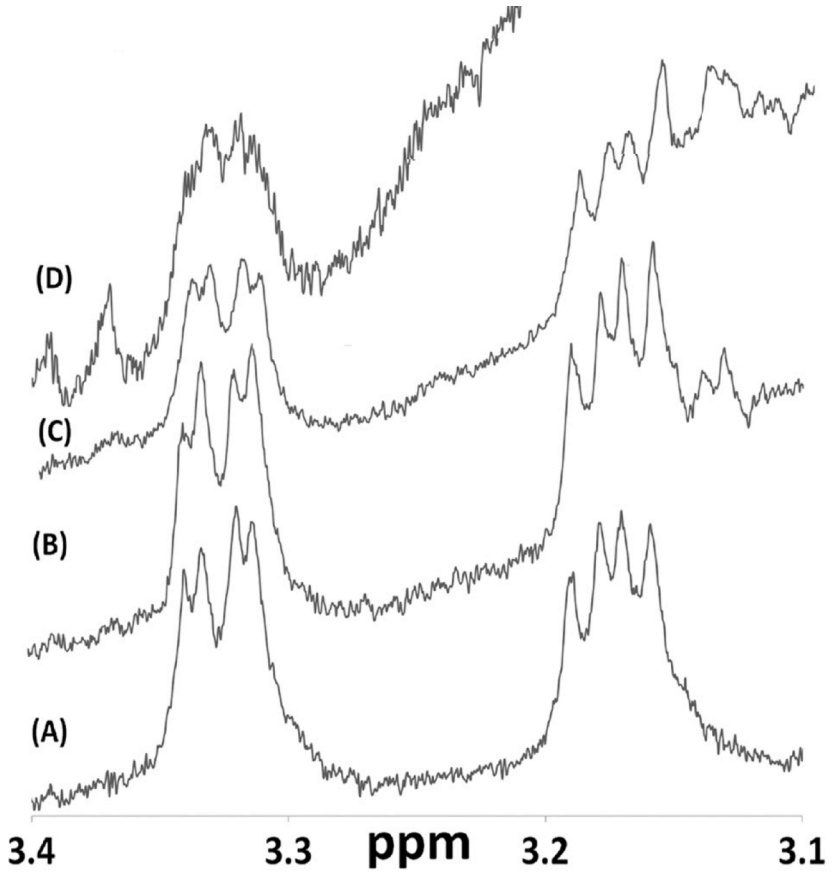

Figure 3.6. Broadening observed at the Trp Hβ signal of ssW upon α-synuclein addition: A) no α-synuclein, B) 0.1 equiv, C) 0.2 equiv, D) 0.5 equiv.

None of the other inhibitors displayed any signal broadening. In fact the μPro1 sample remained transparent for a fortnight after the HFIP addition and failed to produce either amyloid or non-amyloid precipitate even when the HFIP content was increased to as much as 3 and 4 vol-%. Warming the sample up along with intensive agitation failed to promote the formation of fibrils either. In the absence of μPro1, 150 μM α-synuclein forms amyloid fibrils under the latter conditions. The μPro1 peptide appears to greatly prolong the lag time for α-synuclein amyloidogenesis. Mirroring Dr. Huggins published observations (Huggins *et al.*, 2011); WW2/α-synuclein samples exhibited a non-amyloid precipitate in 6 hours at a 2:1 peptide/α-synuclein ratio in the

absence of HFIP. Additional precipitation occurred immediately upon HFIP addition. The WW2/α-synuclein titration experiment also provided some insight into the nature of the non-amyloid aggregate formed. As the precipitate forms the signals due to WW2 disappear (Figure 3.7). No WW2 signals appear in the filtrate after aggregation is complete; aggregation was considered complete when no more visible precipitate formed. This is highly indicative of the inhibitor becoming incorporated into the non-amyloid aggregate that forms.

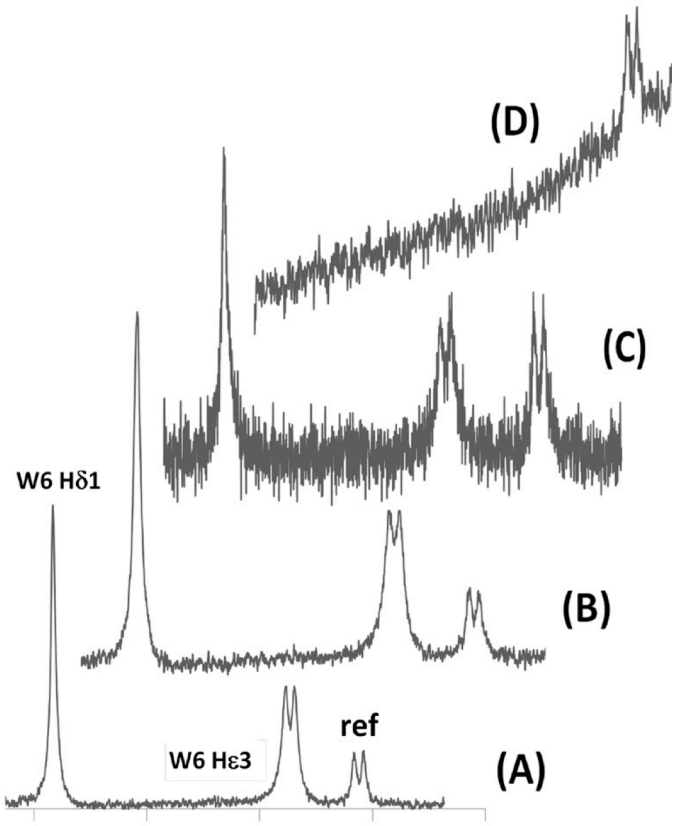

Figure 3.7. Following two signals of the edge-Trp of WW2 through a titration/HFIP addition experiment: A) no α-synuclein, B) 0.5 equiv, prior to precipitation, C) upon HFIP addition, D) filtrate after aggregation.

Based on the data presented so far, along with Dr. Huggins observations (Huggins, 2010) it would appear that a hairpin is required to generate non-amyloid precipitates. While μPro1 is also a hairpin it possesses shorter β strands than WW2. A less stable hairpin and a single strand control confirmed the importance of hairpins with cross-strand aromatics and β-strand propensity for off-path aggregate formation. In order to validate the hairpin hypothesis, as prior hairpins were just suggestive, Dr. Irene Shu was the first to synthesise a cyclic version of WW2 (sequence given in Table 3.1).

Cyclo WW2/α-synuclein samples showed a non-amyloid precipitate within 30 minutes at a 2:1 peptide/α-synuclein ratio in the absence of HFIP. As observed with WW2, the formation of the precipitate led to the disappearance of signals associated with cyclo WW2. No cyclo WW2 signals appear in the filtrate after aggregation is complete.

The circularly permuted version of cyclo WW2 was also examined. As seen with WW2 and cyclo WW2; cp-WW2 also precipitated out quickly – within 4-6 hours at a 2:1 peptide/α-synuclein ratio in the absence of HFIP. The addition of HFIP caused immediate precipitation, with protein/peptide aggregate forming at the meniscus and drifting down through the solution. Once the 1-D experiment was complete, a solid clump of precipitation had formed near the bottom of the NMR tube. No cp-WW2 signals appear in the filtrate once aggregation is complete.

The peptide inhibitor developed by El-Agnaf (El-Agnaf *et al.*, 2004) was also examined utilising the same conditions as a control. However, the relatively few proton signals from the peptide were overwhelmed once α-synuclein was present.

3.10 ^{15}N-HSQC Spectral Studies

After the 1D NMR studies, I turned to exploring the changes that result during the early stages of uninhibited amyloid formation and modifications to those that occur in the presence of added peptide inhibitor by 2D experiments with ^{15}N-labelled α-synuclein. In a variety of buffers, both with and without the addition of 1.5% vol-% HFIP, the initial ^{15}N-HSQC spectra of 400 μM α-synuclein alone reproduced the results reported by Bax (Bodner *et al.*, 2010). Fully 75% of the signals produced were sufficiently resolved for assignment by analogy.

The first experiments run were to follow the time course of α-synuclein aggregation; these experiments were to explore whether there were specific areas of α-synuclein that would disappear from the spectra or if the disappearing peaks were 'randomly' spread throughout the sequence. The spectral changes for an uninhibited 100 μM α-synuclein sample with 1.5 vol-% HFIP present throughout were followed over a 12 hour period (Figure 3.8). The solution was still transparent at the 12 hour time point, this implied the absence of mature fibrils; these precipitate from the sample at longer times (several days).

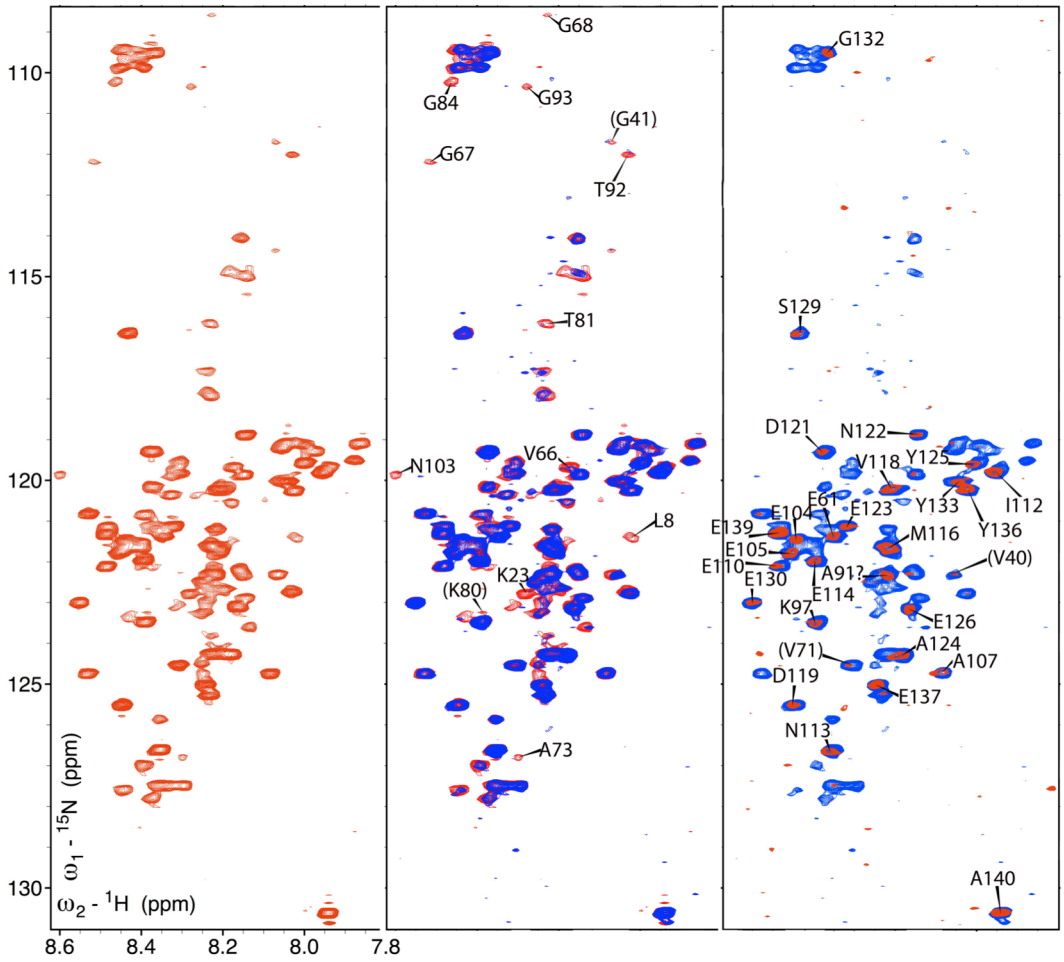

Figure 3.8. Time course of α-synuclein aggregation. The panel on the left shows α-synuclein at Time 0. The central panel shows α-synuclein at 6 hours (**blue**) overlaid with Time 0 (**red**). Labels indicate residues which have disappeared by 6 hours. The panel on the right shows α-synuclein at 12 hours (**red**) superimposed on 6 hours (**blue**). Labels show residues that are still present at 12 hours.

In Figure 3.8, the peaks that disappeared rapidly, by 6 hours, were mainly those within the "amyloidogenic patches" ($V^{66}GGAVVTA^{73}$ or $V^{77}AQKTV^{82}$). These patches have been the basis of previous sequence-related inhibitor designs. The disappearance of these peaks and the L8, K23, T92 and N103 peaks are viewed as indicators of pre-amyloid oligomer formation. By the 12 hour time point, the remaining peaks that could be definitively assigned were those in the C-terminus: E105-A140. No peaks more N-

terminal to E105 could be unequivocally assigned. This region appears to retain random coil flexibility in the pre-amyloid oligomeric state.

The single strand hairpin, ssW, when added as an inhibitor also failed to produce any significant shifts. The inhibitor was added at a 200 μM concentration in the presence of 100 μM α-synuclein with 1.5 vol-% used to start the reaction. Rather than producing any chemical shifts, the presence of ssW showed a delay in the formation of the pre-amyloid state mentioned earlier. The delay indicated that there was notable protection at L8, V37, V40 and V48 sites (Figure 3.9). L8 is still present at 6 hours, though has broadened out by the 8 hour time point. The peaks associated with V37, V40 and V48 are all still visible at 8 hours.

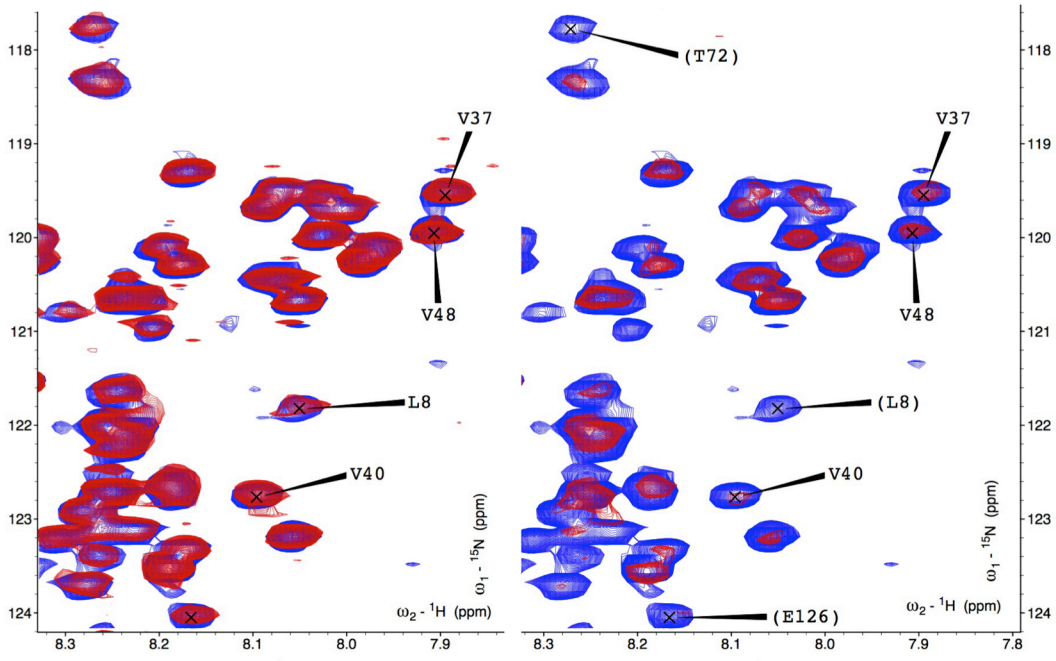

Figure 3.9. Time course of α-synuclein aggregation with ssW present. The panel on the left shows α-synuclein at time 0 (**blue)** in the presence of ssW at 6 hours (**red**). The panel on the right shows α-synuclein at time 0 (**blue**) overlaid with ssW at 8 hours (**red**). Labels show the residues indicative of a delay in the formation of the pre-amyloid state. (Labels) indicate those peaks which have disappeared at 8 hours.

The hairpin WW2 was examined in the same experiments, both before and after HFIP addition. Large, presumably binding-associated shifts were observed at N122 and S129, and K97 was added to the list of rapidly broadened to non-observable group.

3.11 Determining Binding Shifts

However, the shifts due to peptide binding to monomeric α-synuclein were more easily observed at higher concentrations α-synuclein (400 μM) at 293 K. ^{15}N-HSQC spectra were recorded as the inhibitor (WW2, μPro1 or ssW) concentration was serially increased to 120, 240 600 μM. Following the final addition of inhibitor, 1.5 vol-% HFIP was added. The purpose of μPro1 was to serve as an inactive control; the addition of this hairpin failed to have any effect on the α-synuclein HSQC peaks.

In contrast to both ssW and μPro1, substantial titration shifts were observed for WW2 (Figure 3.10).

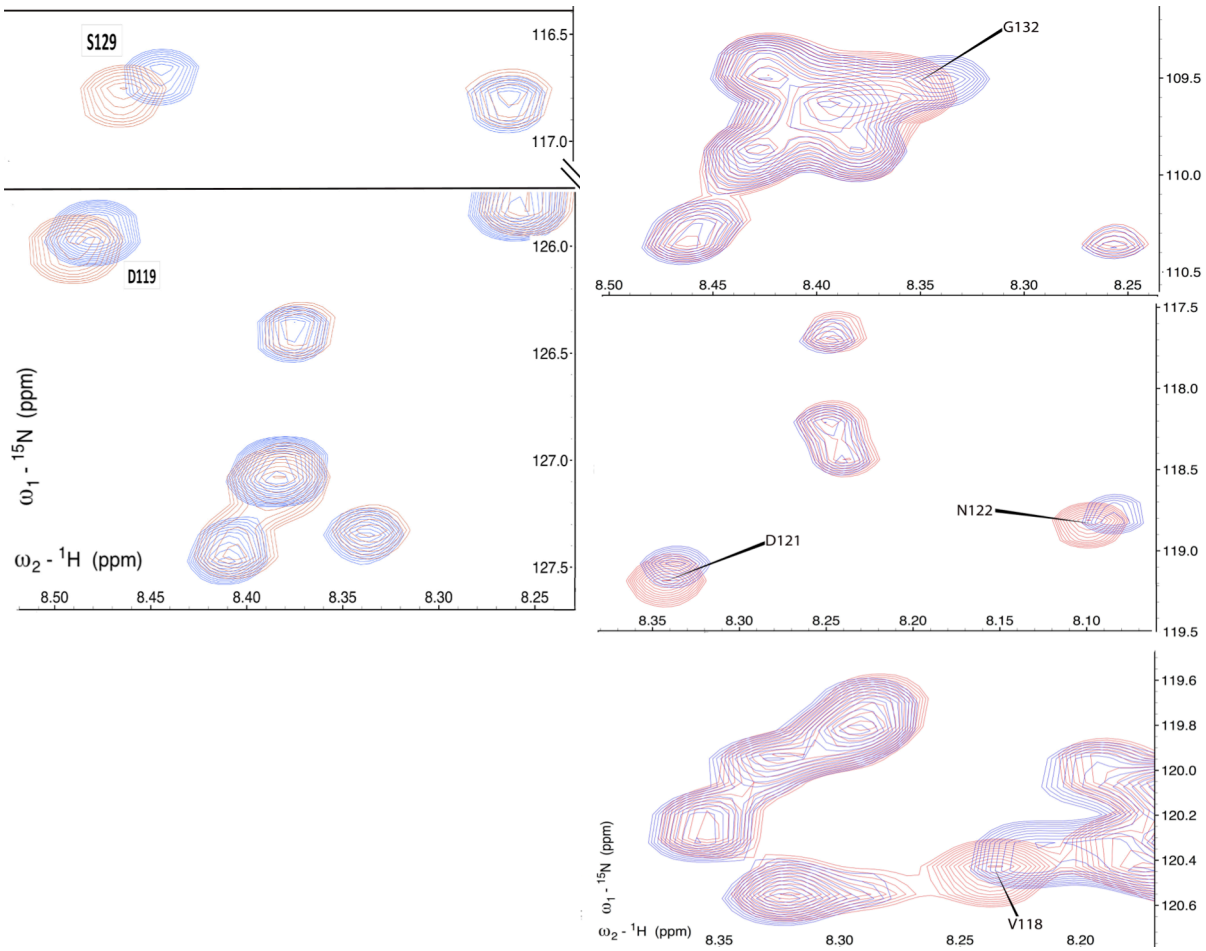

Figure 3.10. Titration shifts in segments of the HSQC spectrum of 400 μM α-synuclein upon increasing the WW2 concentration from 240 (**red**) to 600 μM (**blue**).

The largest shifts were observed at V118, D119, D121, N122, S129 and G132. No comparable shifts were detected N-terminal to these. This leads to the suggestion that the formation of the non-amyloid aggregates observed with WW2 results from a binding-induced structuring transition in the random coil C-terminus of α-synuclein. This C-terminal binding event may also result in conformational changes in the amyloidogenic N-terminal region that impedes the formation of pre-amyloid oligomers.

This same mechanism of α-synuclein amyloid inhibition has been suggested for EGCG (Ehrnhoefer *et al.*, 2008).

Considerable titration shifts were also observed for cp-WW2; D121, S129 and Y136 all shift in the presence of 240 μM peptide inhibitor. When the cp-WW2 concentration is increased to 600 μM, the S129 broadens and disappears completely. The peaks associated with D119 and E137 also shift when the cp-WW2 concentration is 600 μM. The CSDs associated with cp-WW2 are similar to those of WW2; the hairpin strands form the same structure even though the residues comprising the turn are different.

NMR binding studies for EGCG/α-synuclein were reported (Ehrnhoefer *et al.*, 2008), stating that 'progressive broadening of resonances were most evident at five-fold and ten-fold excess of EGCG. Resonances concentrated at the C-terminus of α–synuclein (D119, S129, E130, D135) disappeared already at equimolar compound concentration, indicating that the compound binds preferentially to a highly flexible region of the protein'. Based on my α-synuclein HSQC assignments, derived from those of Bax (Bodner *et al.*, 2010), the published ^{15}N-HSQC spectra of Ehrnhoefer for their titration does not support the statement concerning the disappearance of the D119, S129, E130, D135 signals. These peaks are all clearly visible in their published spectra.

While EGCG has 'inhibitory potency' against at least five diverse amyloidogenic systems; in the case of α-synuclein the non-amyloid aggregates do not form until a five-fold excess of EGCG is present. The WW2 peptide inhibitor is more potent, precipitation of aggregates incorporating WW2 is observed with as little as 0.5 equivalents of added peptide (Huggins *et al.*, 2011).

3.12 Conclusions

NMR methods provided some insights into the process of α-synuclein aggregation. Residues within the amyloidogenic patches (V^{66}GGAVVTA^{73} or V^{77}AQKTV^{82}) of α-synuclein along with L8, K23, T92 and N103 are viewed as indicators of pre-amyloid oligomer formation. The single strand hairpin control, ssW, delays the formation of this pre-amyloid state, with visible protection seen at L8, V37, V40 and V48 sites.

The WW2 hairpin, along with its cyclic and circularly permuted variants, provided some of the most interesting data. Replicating prior published results (Huggins *et al.*, 2011), a non-amyloid precipitate was formed in WW2/α-synuclein samples. The use of proton NMR in the form of a WW2/α-synuclein titration experiment provided some understanding of the precipitate; the inhibitor becomes incorporated into the aggregate that forms. Under the same experimental conditions, cyclo and cp-WW2 are also incorporated into the aggregate formed.

Binding studies of α-synuclein in the presence of WW2 gave more insights into the nature of the non-amyloid precipitate formed. Non-amyloid aggregate formation results from a binding-induced structuring transition in the random coil C-terminus of α-synuclein. This C-terminal binding event may also result in conformational changes in the amyloidogenic N-terminal region that impede the formation of pre-amyloid oligomers.

Chapter 4: Exploring Stabilising Interactions in the Trp-cage

4.1 Introduction

The Trp-cage has proven to be useful in quantitating fold stabilising effects of both sidechain interactions and mutations that influence the intrinsic stability of secondary structure features (Lin *et al.*, 2004; Naduthambi & Zondlo, 2006; Barua *et al.*, 2008). The basic features of the Trp-cage consist of an N-terminal α-helix, a short 3_{10}-helix, a C-terminal poly-ProII helix, and a hydrophobic core with a buried Trp indole ring at its centre. The key stabilising features of the Trp-cage motif have been determined by experimental studies within the Andersen group. In order of contribution these features are: 1) the burial of the Trp side chain as part of the hydrophobic core with the Arg side chain also playing a key role in burial (Barua & Andersen, 2002), 2) the Try3/Pro19 interaction which serves as a hydrophobic staple holding the structure together near its extreme termini (Barua *et al.*, 2008), 3) a buried H-bonded Ser14 hydroxyl (Barua *et al.*, 2008), 4) intrinsic stabilisation of the N-terminal α-helical domain (Lin *et al.*, 2004), and 5) an Asp9/Arg16 salt bridge interaction (Neidigh *et al.*, 2002).

Replacing glycine or residues with long side chains with alanine is a known strategy for increasing protein fold stability (α-helix stability specifically) by decreasing the entropic advantage of unfolding (Matthews *et al.*, 1987; Nicholson *et al.*, 1989; Neidigh *et al.*, 2002; Williams *et al.*, 2008). The fold stabilising effect of a Gly → Ala mutation at a site with no conformational strain has been measured at 2.6 kJ/mol (Barua

et al. 2008). That there are conformational strain effects is suggested by the observation of fold stabilisation of L-amino acids to Gly mutations. This has been observed for some examples (Matthews *et al.*, 1987; Karplus, 1996; Kim *et al.*, 2003) of the introduction of Gly in place of L-residues that have a positive ϕ angle. As glycines in native protein folds commonly occur in turn or loop sites where a positive ϕ torsion angle is required (Nicholson *et al.*, 1989; Hovmoller *et al.*, 2002; Kim *et al.*, 2003), it is necessary to consider the use of D-alanine mutations for protein fold stabilisation. Due to the difficulty of incorporation unnatural D-amino acids into proteins, there are very few examples of Gly → D-Ala mutations. Bang and co-workers (Bang *et al.*, 2006) prepared Gly35 → D-amino acid ubiquitin mutations by chemical ligation of synthetic fragments. No net stabilisation was observed, however the D-Ala mutation was more stable that the corresponding L-Ala mutations at the helix C-capping site with ϕ/ψ = +82/+10°. The Raleigh group (Anil *et al.*, 2004, 2006) have provided three examples of this stabilising Gly → D-Ala mutation in small protein domains that could be prepared by automated peptide synthesis, two of which were at helix C-capping sites.

4.2 Exploring Trp^2 Cages

While several stabilising interactions are known in the Trp-cage and these have been well studied, there is still scope for further explorations. In 2006, Gai and co-workers (Bunagan *et al.*, 2006) reported computational design studies that a P12W mutation would stabilise the Trp-cage. They performed experimental studies that confirmed the stabilisation effect of P12W on TC5b. An unfavourable R16W mutant was also briefly examined. Since their computational design work focused primarily on

the 9 and 12 positions (sites viewed as having the most potential for stabilising interactions), leaving the rest of the peptide 'fixed' at their original amino acids, would a second Trp work at a different site in the construct?

Dr. Brandon Kier confirmed the stabilising effect a P12W mutation has in TC13b and Vicki Williams also utilised this mutation in creating a hyperstable cage in TC16b. Dr. Kier also examined [Y3W]-TC13b as a potential stabilising Trp/Trp interaction. A Trp/Trp exciton couplet was observed in circular dichroism for this mutant, signifying the existence of a geometrically specific Trp/Trp interaction. However, upon examination of the CSD melts for the mutant, it was obvious that the Y3W mutant did not have the same stabilising effect as the P12W mutant. In fact, Y3W was actually slightly destabilising when compared to the WT TC13b.

I examined several other Trp^2-cage possibilities (Table 4.1). These site mutations were chosen from close examination of Trp-cage NMR structures; these sites appeared to be the most promising for stabilising Trp/Trp or Trp/Tyr interactions.

	Sequence
TC13b	DAYAQWLADGGPASGRPPPS
TC13b P12W	DAYAQWLADGG**W**ASGRPPPS
TC13b L7W	DAYAQW**W**ADGGPASGRPPPS
TC13b P18W	DAYAQWLADGGPASGRP**W**PS
TC13b P19W	DAYAQWLADGGPASGRPP**W**S

Table 4.1: Trp^2-cage mutations in the TC13b Trp-cage series.

Fold populations for these mutations could not be calculated based on reference shifts for other Trp-cages since the Trp mutation likely changes the 100%-folded

chemical shifts for each mutation. The near neighbour effects associated with the ring-current effects of tryptophan make it difficult to ascertain accurate fold populations. CD spectra were also very different from one another (Figure 4.1).

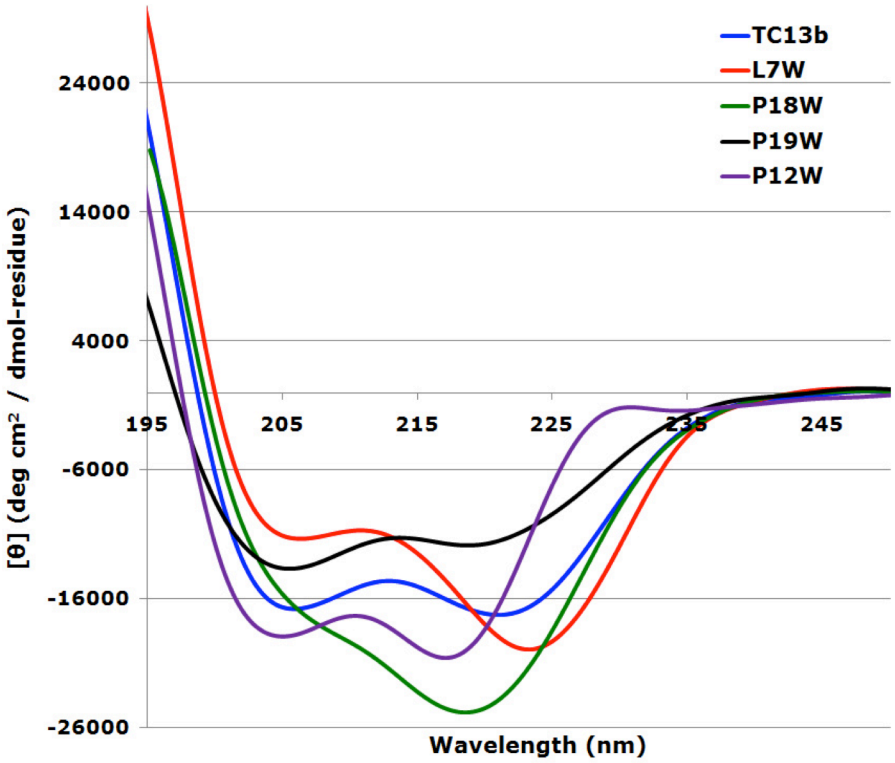

Figure 4.1. The per-residue CD spectra of the Trp^2-cages.

Thus, the usual folded and unfolded baselines (given in Chapter 2) could not be employed to provide T_Ms in the usual manner. Because of this, 1st derivative melting temperatures from the CD spectra (Figure 4.2) (given in Table 4.2) were used for an initial determination of whether a mutation in this series is stabilising or destabilising; all three new Trp^2-cage mutations are destabilising in relation to the WT TC13b.

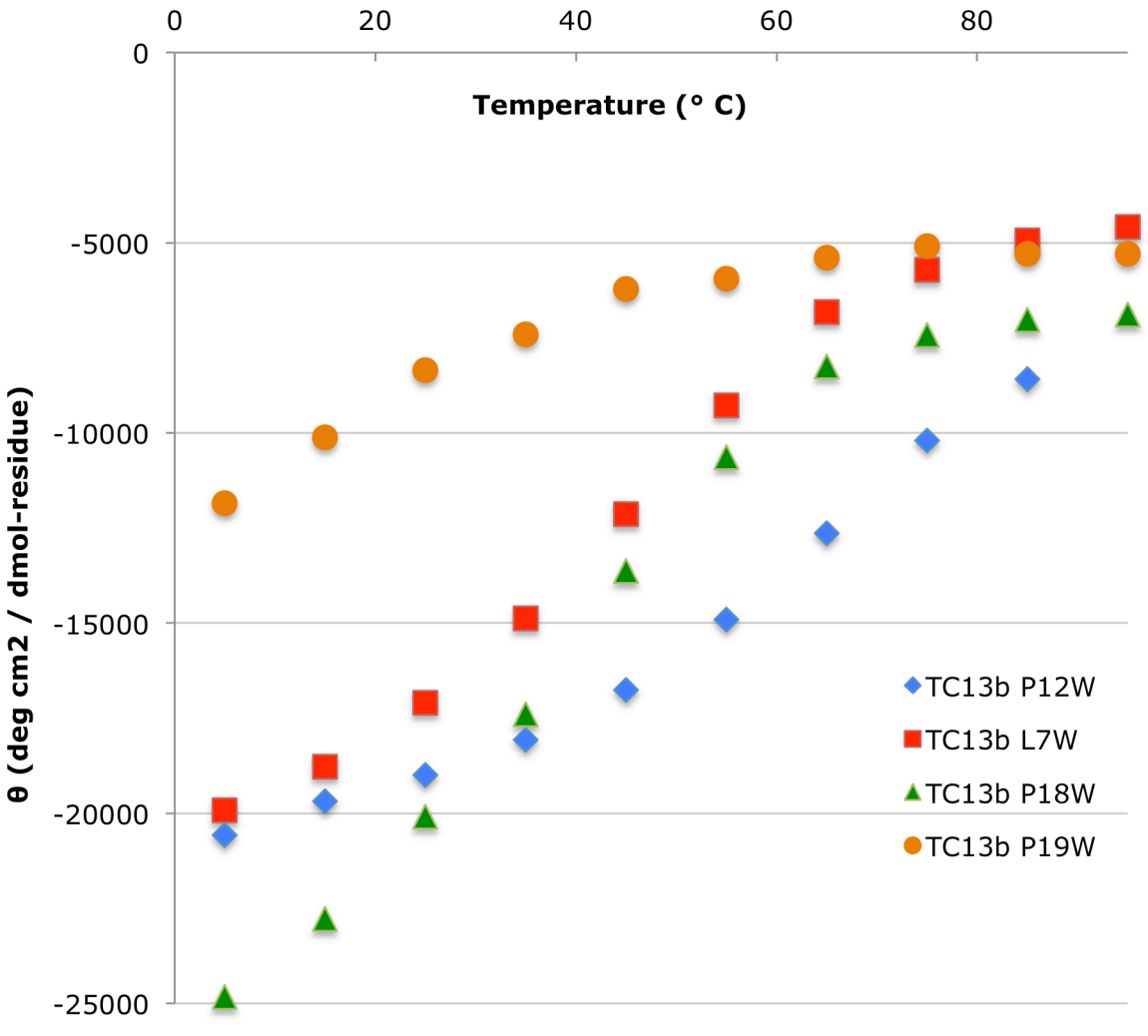

Figure 4.2. CD melts (raw ellipticity values vs *T*) of the TC13b Trp^2-cages.

Name	T_M (° C)
TC13b	68
TC13b P12W	77
TC13b L7W	~45
pH 2.5	~40
TC13b P18W	~40
pH 2.5	~25
TC13b P19W	~25
pH 2.5	~20

Table 4.2: Melting Temperatures at pH 7 for Trp^2-cage mutations in the TC13b Trp-cage series, derived from circular dichroism melts.

With a melting temperature of ~45 °C, [L7W]-TC13b is roughly 95%-folded at 280K. The W7 NH proton experiences a large chemical shift deviation; downfield with respect to where L7 would typically appear. This proton could be located closer to the deshielding, nodal plane of the indole ring than the L7 NH or it could be involved in a better H-bond to the Tyr3 C=O. The G11 Hα2 has an even larger upfield shift than that of the WT, while this might indicate that [L7W]-TC13b is more stable the TC13b itself, the T_M's in Table 4.2 reveal that this is not the case. This misleading piece of data is caused by extra ring current effects for the Trp7 leading to a greater downfield shift than would otherwise be expected.

The [P19W]-TC13b mutant is the most destabilising of the three and displays no evidence of a significant Trp/Trp or Trp/Tyr interaction in the CD spectra. There is, however, a large CSD increase for the Trp19 NH proton. Based on the known orientation of Pro19, this Trp NH should be pointing towards Tyr3. This lone piece of evidence for a Trp/Tyr interaction was somewhat surprising given the close nature of Tyr3/Pro19 in a typical Trp-cage construct. This indicates that at this site in the Trp-cage a Trp/Tyr interaction is not as stabilising as a Pro/Tyr hydrophobic interaction.

The P18W mutation is also destabilising, though not to the same extent as P19W. This mutation displays some interesting characteristics. Both the Hε1 and Hδ1 protons of Trp6 are not as shifted downfield as in the WT, this could be due to the Hε1 proton not being H-bonded to Arg16 or additional ring current effects. Having a tryptophan inserted into the polyPro helix may destabilise this substructure; resulting in a different docking of the C-terminal portion of the cage. This slight change in structure,

along with the new aromatic residue, could change the ring current effects felt by Trp6 – cancelling out the downfield shift observed in the WT.

Curiously, [P18W]-TC13b at pH 2.5 has two sets of peaks in the NMR spectra, the second set of peaks can be also be assigned all the way through the sequence at 280K with only a handful of protons missing. This is presumably associated with the presence of cis/trans proline isomers. Aromatic-proline CH/π interactions between the proline Hα and the negatively charged π face lead to an increased preference for the cis amide bond in aromatic-proline sequences (Pandey *et al.*, 2013). Based on CSDs, one of the isomers possesses a larger helical content than the other isomer, even though they both show similar peak intensities in the NMR spectra. At pH 7, the P18W mutant also exhibits signs of a cis/trans proline isomer, though this pH proved to be more difficult to assign even for the dominant isomer. Large CSDs for both pH 2.5 isomers and pH 7 are observed at the tyrosine position (Figure 4.3), although the different pHs exhibit distinctive effects on the tyrosine protons.

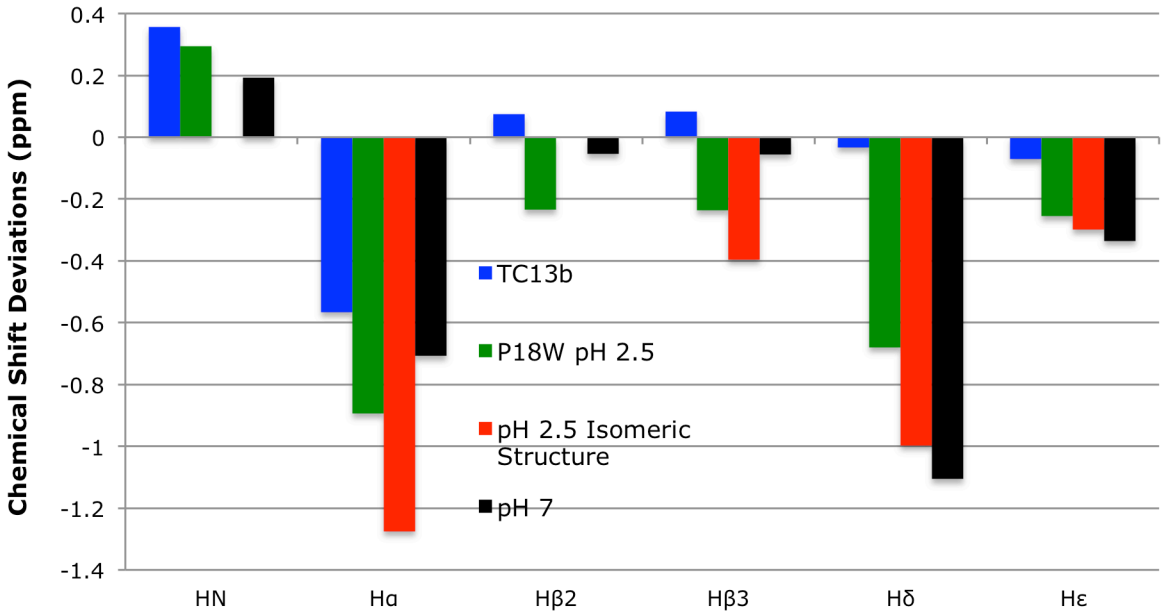

Figure 4.3. Chemical Shift Deviations for Tyr3 of the P18W mutant.

For both pHs, the greater CSDs when compared to WT TC13b itself are observed at the Hα, Hδ and Hε protons. The pH 2.5 isomers also display a greater change in the CSDs for the Hβ protons. This change in normal CSD pattern could be explained by a Trp18/Tyr3 interaction, caused by ring current shifts associated with Trp18. The difference between the CSDs for P18W isomers could be due to the tyrosine having a slightly different dihedral angle in each. The circular dichroism data corroborates the idea of a Trp18/Try3 interaction (Figure 4.4).

Figure 4.2 shows both the raw CD data for the Trp^2-cages as well as a difference spectra resulting from subtracting the raw WT data from the mutant data, with P19W excluded from the difference spectra. As seen in the raw CD data for P19W, this mutant displays a weak helical signal, upon subtraction a reverse helical signal is observed indicating its relative lack of stability. These difference spectra should remove helical contributions to the spectra leaving only possible aromatic/aromatic interactions. The

data for [P12W]-TC13b (Figure 4.4) shows the positive exciton couplet that has been observed for all Trp/Trp or Trp/Tyr interactions in both hairpins and the Trp-cage in the Andersen lab. Both the L7W and P18W mutants actually show a negative exciton couplet. Theoretically, the negative exciton couplet should be observed as frequently as a positive exciton couplet. The L7W exciton couplet has its minima at ~ 227 nm, which is where the Trp/Trp exciton couplet is typically observed. The P18W mutant, on the other hand, has its minima at ~ 217 nm. This blueshift is presumably due to the exciton couplet being from a Trp/Tyr interaction rather than Trp/Trp.

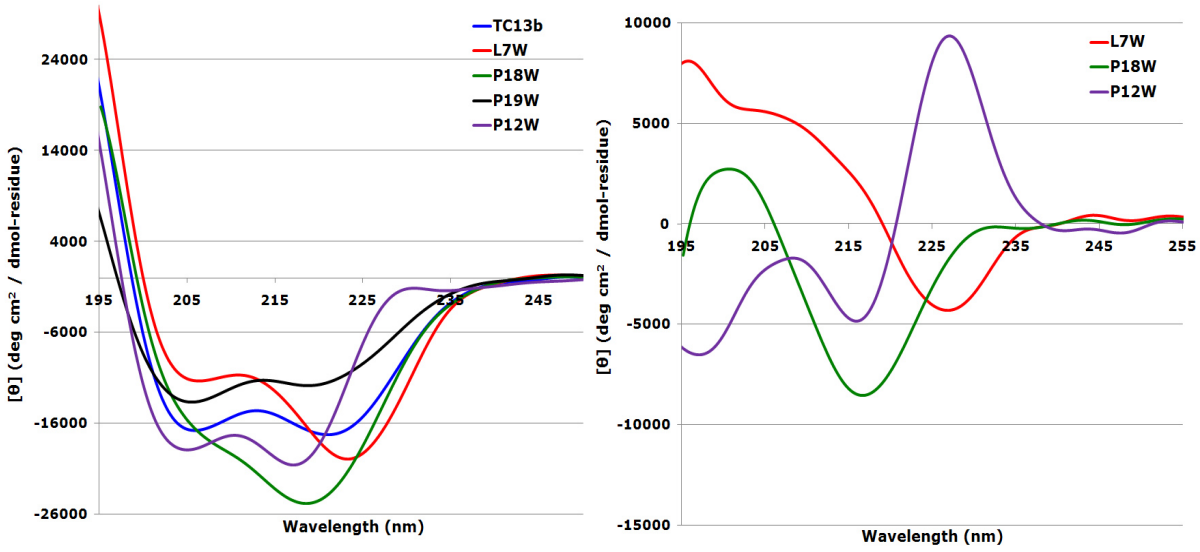

Figure 4.4. Trp[2]-cage CD comparisons. The left panel shows the per-residue CD spectra, while the right panel shows the difference spectra of the CD spectrum of TC13b subtracted from the mutants.

The P18W and P19W mutations are assumed to be destabilising due to a disruption of the polyPro helix; this would likely result in an incorrect docking (or packing) of that segment of the Trp-cage.

Along that line, I also explored P12W P17A and P12W P18A mutants (sequences given in Table 4.3). The proline at the 17 position is solvent exposed;

although this proline itself is important in the formation of the polyPro helix, it is not involved in any other stabilising interactions in the Trp-cage.

	Sequence
TC13b	DAYAQWLADGGPASGRPPPS
TC13b P12W	DAYAQWLADGG**W**ASGRPPPS
TC13b P12W P17A	DAYAQWLADGG**W**ASGR**A**PPS
TC13b P12W P18A	DAYAQWLADGG**W**ASGRP**A**PS
TC13b P12W P17A P18A	DAYAQWLADGG**W**ASGR**AA**PS

Table 4.3: Mutations in the polyPro helix in the TC13b P12W Trp-cage series.

The P12W P17A mutation was surprisingly stable, with T_M = 64 °C from the CD melt and χ_F = 0.980 at 280 K. The CSDs observed for P12W P17A are very similar to P12W at 280 K, although P12W P17A melts out faster as indicated by the lower T_M (Figure 4.5). The proline to alanine mutation does result in the breaking of the polyPro helix (a polyPro helix needs a minimum of three prolines to form a helical structure). A possible rationale for this stability is that A17 may be able to pack closer against the tryptophan at the 12 position than the proline would be.

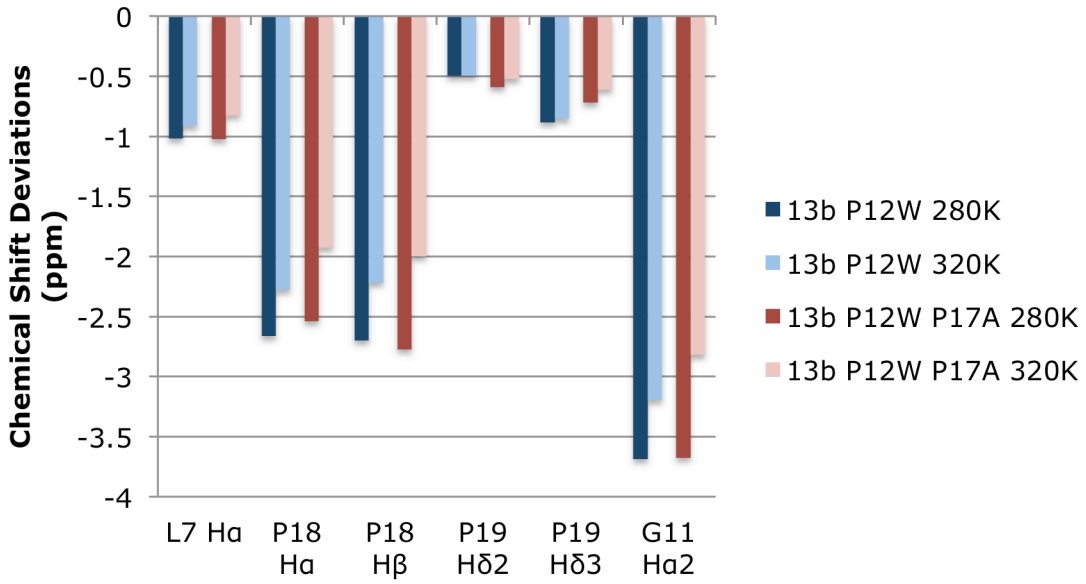

Figure 4.5. Melting profile of the key CSDs for TC13b P12W and TC13b P12W P17A and 280 K and 300 K.

The P12W P18A mutant was also well tolerated, with T_M = 61 °C from the CD melt and χ_F = 0.866 at 280 K. This mutation was also explored for dynamic lineshape analysis of the Trp-cage and this will be discussed further in Chapter 6. The P18A mutant was not as well accepted as the P17A mutant. The insertion of an alanine into the middle of a polyPro helix would cause a greater disruption to the overall docking as opposed to a P17A mutation.

Since the P12W P17A mutation was unexpectedly stable, how would the combination of P17A P18A be tolerated? This could be of interest to dynamics studies. While the helix part of the Trp-cage forms as normal with this extra mutation, the overall cage structure does not appear to be as well formed. The insertion of two alanines into the polyPro helix should effectively change the docking conformation, though the upfield CSDs for Ala18 do indicate that it is still located above the Trp6 ring (Figure 4.6). The smaller CSD seen at the 18 Hβ site is a reflection of the alanine Hβ signals being averaged out to create a single peak.

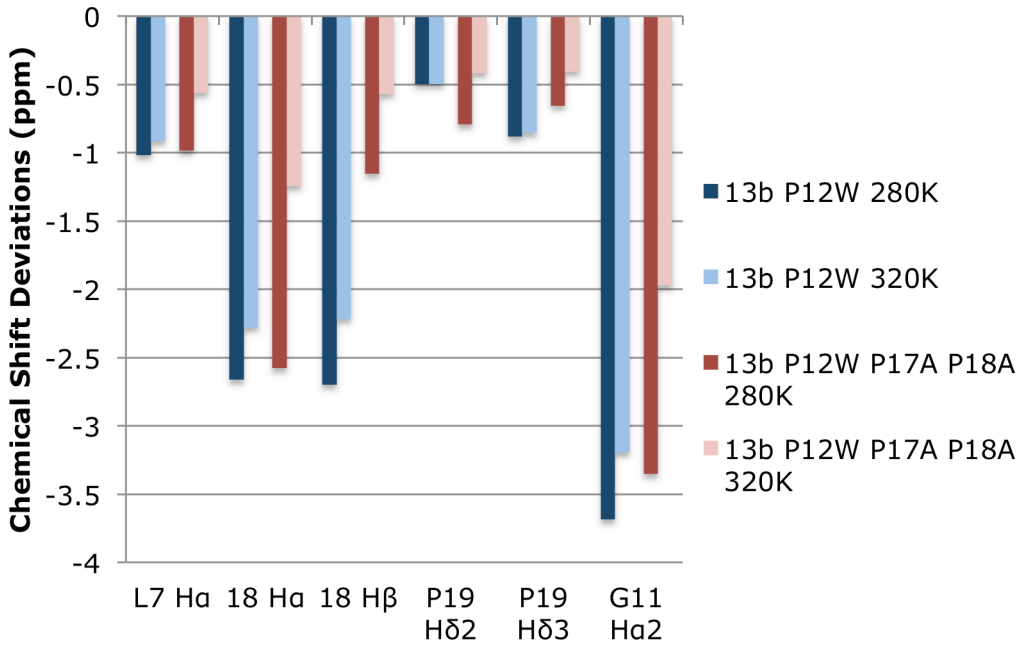

Figure 4.6. Melting profile of the key CSDs for TC13b P12W and TC13b P12W P17A P18A at 280 K and 300 K.

While none of these new Trp^2 cages are stabilising over the WT, they do provide some new and interesting data particularly the negative exciton couplet.

4.3 Glycine Mutations in the α-Helix

An α-helix is stabilised primarily by a favourable enthalpic contribution of ~ 1 kcal/mol per residue from the formation of the backbone hydrogen bonds, and from van der Waals interactions that are more favourable in the helix than the random coil state (Scholtz *et al.*, 1991; Yang & Honig, 1995). The random coil state is favoured by conformational entropy (Aurora *et al.*, 1997). In forming an α-helix, the entropic cost for fixing the backbone dihedral angles is 1.5 – 2 kcal/mol at 25 °C (Yang & Honig, 1995; Wang & Purisima, 1996). Glycines are known to be 'helix-breakers'. If an α-helix is composed of alanine, the favourable interactions will win out, but if the an α-helix were to be made up of glycine, the unfavourable interactions will win and the coil will be more stable than the helix. The 1 kcal/mol difference in helix propensity between Gly and Ala is due largely to the large reduction in Φ/Ψ space available to residues when the Gly H has been replaced by a CH_3 in Ala (Pace & Scholtz, 1998); additionally an enthalpic interaction between the alanine Cβ and the α-helix backbone favours the helix and is missing in glycine.

The α-helix in the Trp-cage has been improved through alanine mutations. The TC5b construct, (NLYIQ WLKDG GPSSG RPPPS), had a series of alanine mutations explored (Barua *et al.*, 2008). The L2A, I4A and K8A mutations each individually increased fold stability, whereas the Q5A and L7A mutations resulted in decreased fold stability. Dr. Jasper Lin explored the extension of the Trp-cage N-terminus through alanine insertion (Lin *et al.*, 2004). Residues inserted between the N-cap and Ala2 are too far away from the remainder of the Trp-cage structure to have any tertiary interactions, so any stability increase would solely reflect intrinsic helix propensities.

The serial addition of alanines (1, 3, 4, 5 and 7) led to a steady increase in both the magnitude of the 222 nm minimum in CD and the apparent melting temperature.

While glycines are known to disrupt α-helices, molecular dynamic simulations have indicated that a glycine would be a more co-operative folder (more two-state folder despite a lower T_M) at the 4-position of the Trp-cage rather than the Ile that was present in TC5b, despite the greater α-helix propensity of Ile (Neuweiler *et al.*, 2005) (though Ile is also somewhat poor). This computational outcome appeared contrary to expected and warranted further testing. As a consequence of this finding, the primary goal of this series of Trp-cage mutations was to examine the helix propensity of glycine (expected to be poor) at different helical positions, rather than to improve the Trp-cage. But the Gly mutants should be excellent probes for dynamic NMR, which could confirm folding co-operativity. It was decided to explore this mutation both in TC13b and in TC16b (Table 4.4). We viewed A → G mutations in the N-terminal helix of TC16b as a means to destabilise it sufficiently to allow NMR relaxation easurement.

Name	Sequence
13b	DAYAQWLADGGPASGRPPPS
13b A4G	DAY**G**QWLADGGPASGRPPPS
16b	DAYAQWLADaGPASaRPPPS
16b A4G	DAY**G**QWLADaGPASaRPPPS
16b A8G	DAYAQWL**G**DaGPASaRPPPS

Table 4.4: Glycine mutations in the α–helix.

Name	%-Fold 300K	T_M CD (°C)	ΔG_U (kJ/mol) Σ CSDs	mut$\Delta\Delta G_F$ (kJ/mol)	$\Delta\Delta G$(pH) (kJ/mol)
13b	0.914	68	5.43		
13b A4G	0.845	50	3.99	1.43	
16b	0.971	83	8.79		
pH 2.5	0.907	74	5.69		3.10
16b A4G	0.953	68.2	7.49	1.29	
pH 2.5	0.872	59.2	4.80		2.70
16b A8G	0.902	55.1	5.53	3.27	
pH 2.5	0.770	46.5	3.02		2.50

Table 4.5: Mutational and pH-induced Fold Stability Changes for the Glycine Helical Mutations [a,b]

[a] mut$\Delta\Delta G$ is the $\Delta\Delta G_F$ associated with each mutation, +ve values indicate fold destabilisation. $\Delta\Delta G$(pH) is the effect of ionization. +ve values indicate fold stabilisation on deprotonation.

[b] The ΔG_U values are based on the Σ CSD measure for the following shifted sites: L7Hα, G11α2, P18Hα/Hβ3 and P19Hδ2/δ3.

Barua (Barua *et al.*, 2008) tested main side chain entropy effects in the Trp-cage at the Pro17 site; this site has its side chain solvent exposed and is not a part of the hydrophobic cluster. The sequential substitution of P17 with Ala and Gly led to increasingly less stable constructs; there was a decrease in T_M in the order P17 (56 °C) > A17 (42 °C) > G17 (32 °). This decrease in melting temperature corresponds to a $\Delta\Delta G_F$ of 2.6 kJ/mol for A17 and 4.5 kJ/mol for Gl7 at 300 K. This indicates that the fold destabilising effect of an Ala → Gly mutation at a site with no conformation strain is 1.9 kJ/mol.

The insertion of a glycine at the 4-position causes a T_M decrease of ~15°C (Table 4.5), regardless of whether it is inserted into TC16b or TC13b. Graphs of the CSDs of [A4G]-TC16b for the diagnostic probe sites show only small changes (Figure

4.7), when the temperature is increased from 280K to 320K. Both NMR melts and CD measurements indicate that this A4G construct is still ~80%-folded at 320K in both the TC13b and TC16b motifs. This glycine mutation was found to be only slightly less favoured than the WT at 300K. While it was expected that the glycine mutation would be less stable, it was somewhat surprising that the effect was smaller than expected. The $\Delta\Delta G_F$ for the A4G mutations is slightly smaller than the number arrived at by Barua (Barua *et al.*, 2008).As a result, it was decided to look at a similar mutation at the eight position of the peptide. This would hopefully provide a value for the insertion of a glycine close to the end of an α-helix, compared to the beginning of said helix.

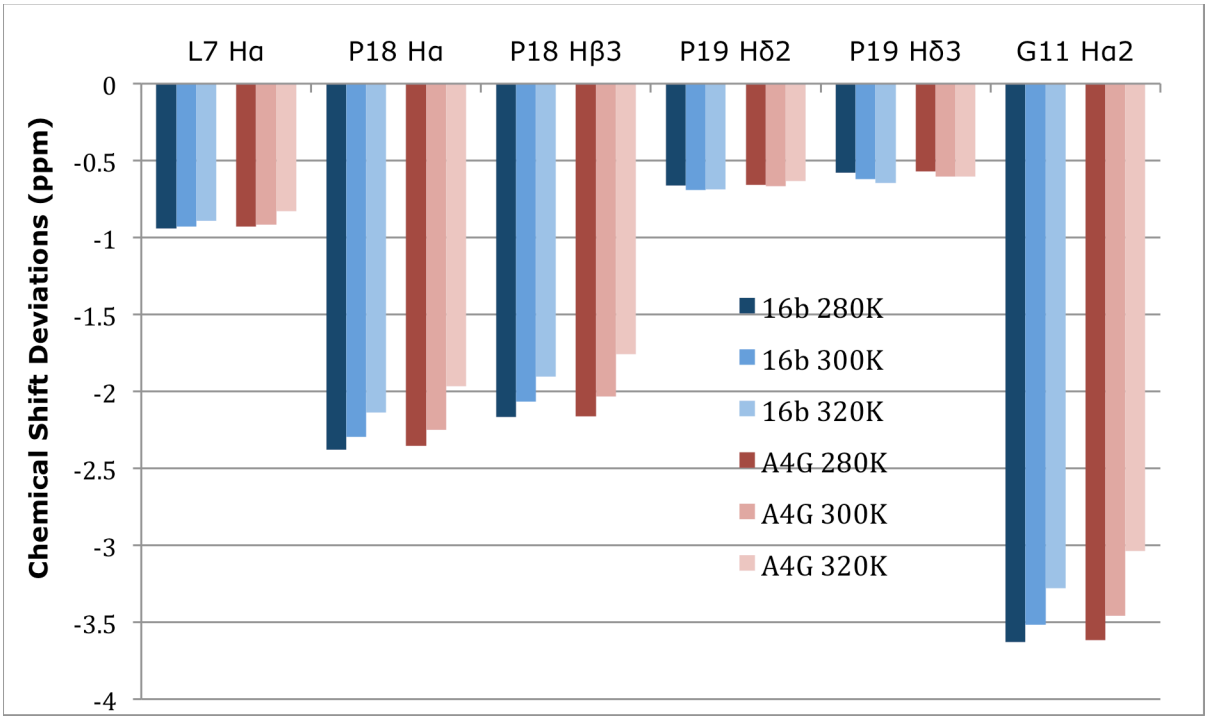

Figure 4.7: Thermal melts for TC16b and [A4G]-TC16b shown as CSDs for L7Hα, G11α2, P18Hα/Hβ3 and P19Hδ2/δ3.

Placing a glycine at the end of an α-helix proves to be not as well tolerated as the A4G mutation. An A8G mutation in TC16b is destabilising by 3.27 kJ/mol at 300K.

This number is much larger than the 1.9 kJ/mol calculated by Barua, this indicates that the 8 position in the helix has significant conformational strain. Glycine is a 'floppy' residue and has a high entropic cost of folding; a glycine mutation in the helix would favour the unfolded state.

With χ_u = 10-20% for the [A8G]-TC16b mutant, NMR dynamics for G11, along with a P18A mutant, should afford folding rates for this construct. This, along with other Trp-cage kinetics data, will be discussed in a later chapter (Chapter 6).

4.4 Mutations at the Serine 14 Position

A buried H-bonded Ser14 hydroxyl in the Trp-cage is known to be a key stabilising feature, being worth ≈ 10 kJ/mol of fold stabilisation (Barua *et al.*, 2008). One of the first hints that a hydrogen bond was occurring was the presence of a threonine hydroxyl proton resonance in the TOCSY and NOESY spectra of an [S14T]-TC5b mutant in aqueous buffer with 30% TFE added (Neidigh, 1999). This indicated that the proton was protected from exchanging with the solvent. The Ser14 hydroxyl can also be detected in the TOCSY and NOESY spectra of more stable Trp-cages. To investigate the interactions of the S14 side chain (Barua *et al.*, 2008), several mutants were prepared: [S14A]-TC10b, [S14T]-TC9b and [S14alloT]-TC9b. Both of the threonine mutants were fairly well tolerated, the allo-Thr mutant had a $\Delta\Delta G_F^{280} \leq 0.7$ kJ/mol with the threonine mutation being slightly more destabilizing at 2 kJ/mol. The S14A mutant on the other hand was extremely destabilizing at 8.4 kJ/mol. Furthermore, the diastereomeric S14T mutants both display a side chain hydroxyl proton in the NMR spectra. A point to note is that Ser-OH groups are observed in only ~2% of proteins and

only in systems with large hydrophobic cores, while Thr-OH groups are observable slightly more often (~4%). The Thr mutants appear to form the same H-bond in both diastereomers, with the Cβ diastereotopic change only altering the methyl group location. The Thr and allo-Thr side chain CSDs provided further insights into the S14 side chain positioning in the Trp-cage. The S14 Hβ's have distinct CSD values, CSDs as large as -0.45 have been observed for S14Hβ3 in more stable Trp-cage analogues. Using the IUPAC naming convention, Thr Hβ corresponds to Ser Hβ2, and Hβ3 in the case of allo-Thr. The S14 CSD values mirror the similar magnetic environments experienced by the corresponding nuclei in allo-Thr Hβ (-0.49 p.p.m.) and Thr Hβ (-0.005 p.p.m.). The estimate for the stabilising effect of the S14 hydroxyl also takes into account the expected fold improvement for a S → A mutation with the 3_{10} helix (1.8 kJ/mol for S13A). As a result, the buried H-bond effect is ≈ 10 kJ/mol.

Does the alanine, due to its small size, create a hole in the core leading to fold destabilisation or is the serine hydroxyl group required to satisfy other buried sites needing a H-bonding partner? Could a larger nonpolar group fill in some of the space in the core resulting in less destabilisation than observed with the alanine mutation? To explore this in further detail, I examined two mutations; a S → V and a S → Abu mutant (sequences given in Table 4.6, amino acid sidechains shown in Figure 4.8). Abu is the 3-letter code for 2-aminobutyric acid; this residue is also known as ethylglycine.

	Sequence
16b Y3F	DA**F**AQWLADaGPASaRPPPS
16b Y3F S14V	DA**F**AQWLADaGPA**V**aRPPPS
16b Y3F S14Abu	DA**F**AQWLADaGPA **Abu** aRPPPS

Table 4.6. Serine 14 mutations in the TC16b Y3F series.

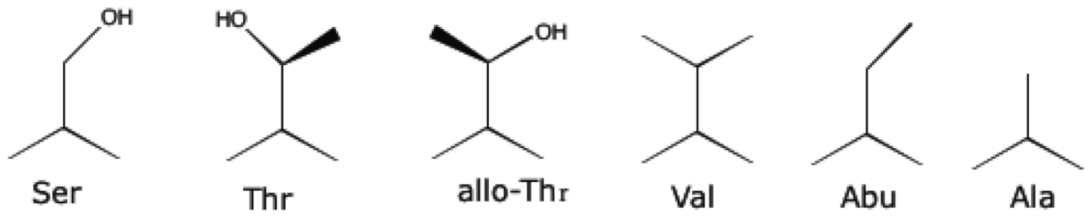

Figure 4.8. Amino acid mutations carried out at the serine14 position.

As part of a collaboration project with Dr. William Parson, a series of Trp-cages were synthesised with a Y3 → F mutation. Andy McMillan in Dr. Parson's lab was performing fluorescence studies on the Trp-cage (McMillan *et al.*, 2013), a tyrosine mutation to phenylalanine was necessary to simplify the fluorescence. Simplification would occur by eliminating the conflicting Tyr absorbance (small but potentially significant at 280 nm) and allowing excitation at the stronger 280 nm band instead of the Trp absorbance shoulder at 295 nm. A Y3F mutation is known to be only slightly destabilising (Barua *et al.*, 2008; McMillan *et al.*, 2013) and has no impact upon the Trp-cage fold geometry. These mutations were carried out in concert with Andy's project; Andy wished to rule out any possibility of the serine hydroxyl being H-bonded to the Trp indole nitrogen.

Name	%-Fold 300K	ΔG_U (kJ/mol) Σ CSDs	mut$\Delta\Delta G$ (kJ/mol)	$\Delta\Delta G$(pH) (kJ/mol)
Y3F	0.959	7.88		
pH 2.5	n.d.			
Y3F S14V	0.426	-0.74	8.61	
pH 2.5	0.314	-1.94		1.20
Y3F S14Abu	0.622	1.24	6.64	
pH 2.5	0.458	-0.41		1.65

Table 4.7: Mutational and pH-induced Fold Stability Changes for the Serine 14 Mutations. [a,b]

[a] mut$\Delta\Delta G$ is the $\Delta\Delta G_F$ associated with each mutation, +ve values indicate fold destabilisation. $\Delta\Delta G$(pH) is the effect of ionization. +ve values indicate fold stabilisation on deprotonation.

[b] The ΔG_U values are based on the Σ CSD measure for the following shifted sites: G11α2, P18Hα/Hβ3 and P19Hδ2/δ3.

Both the S14V and S14Abu mutants are extremely destabilising (Table 4.7). The mutational $\Delta\Delta G_F$'s calculated for both these mutations indicate that these mutations are roughly as destabilising as an alanine was. As both Ser and Thr are able to fit into that space in the hydrophobic core, neither valine or the ethylglycine residues should be a problem in that regard. These mutations clearly indicate that the serine hydroxyl being H-bonded is the basis for the mutational effects and results in the folded structure.

A recent crystal structure (Scian *et al.*, 2012) actually confirms this hydrogen bond. Even though in the crystal structures there is a great deal of variability for the Gly10 to Arg16 loop region (high B values), the Ser14 side chain conformation is nearly constant ($\chi1 = 72 \pm 3°$). Two hydrogen bonding interactions are likely given then heavy atom locations: Ser14 Hγ → O=C Gly11 and Ser14 Oγ ← H_N Arg16.

4.5 Salt Bridge Background

Evaluating the effects Coulombic interactions have on protein folding is problematic. Introducing favourable Coulombic interactions between the termini has been shown to stabilise hairpins, however the net effect is small, only a few kJ/mol at the most (Ramirez-Alvarado *et al.*, 2001; Fesinmeyer *et al.*, 2004; Huyghues-Despointes *et al.*, 2006). Hydrogen bonding between charged sites in proteins has long been shown to have a more favourable stabilising effect on protein folding than any other H-bonding interactions. A combination of site mutations and acid-base titration studies have discovered 12 – 20 kJ/mol stabilisations associated with buried H-bonded salt bridges involving Asp/His (Anderson *et al.*, 1990), Asp/Arg (Tissot *et al.*, 1996) and Glu/Arg (Waldburger *et al.*, 1995) sidechains.

Solvent exposed Coulombic interactions (Dong & Zhou, 2002) and salt bridges (Horovitz *et al.*, 1990; Sali *et al.*, 1991) typically contribute smaller contributions to fold stability. Desolvation issues allow buried salt bridges to be replaced with hydrophobic pairings, typically leading to an increase in fold stability (Waldburger *et al.*, 1995). Favourable surface charge/charge interactions contribute *circa* 4 kJ/mol of stabilisation with a further 4 kJ/mol of stabilisation suggested in one instance for a carboxylate/arginine H-bonding interaction (Makhatadze *et al.*, 2003). In ubiquitin (Loladze *et al.*, 1999), for example, a charge reversal on the surface leads to a 4-7 kJ/mol increase on fold stability. Favourable carboxylate/Lys interactions have been associated with the stability of a 39-residue minimized fold motif; a peptide fragment derived from the N-terminal domain of the ribosomal protein L9 (NTL9) (Horng *et al.*, 2002). The potential energies of unfolded states can even be altered by charged

sidechain interactions; Cho and Raleigh (Cho & Raleigh, 2005) have reported a case of an 8 kJ/mol stability increase in a truncated protein as a result of removing a favorable Coulombic effect in the unfolded state. The C-terminal domain of fibritin can be used as an artificial trimerisation domain; this 27 residue trimer is superstable except below pH 2 when its essential salt bridge between E5-R15 is destroyed and the trimer falls apart entirely to the monomer. Nonetheless numerous questions remain concerning the effects of charge-pairing and salt bridging sites upon protein fold stability.

A solvent exposed salt bridge between residues 9 and 16, aspartic acid and arginine respectively, has been reported to provide 4.7±1.3 kJ/mol of fold stabilisation in Trp-cage species (Barua *et al.*, 2008). In folding simulations of the Trp-cage, the formation of the Asp/Arg salt bridge is seen as important interaction, typically by acting as a fold facilitating interaction (Snow *et al.*, 2002; Chowdhury *et al.*, 2003), however some folding simulations report the salt bridge as a stabilising feature in kinetic traps (Zhou, 2003b; Ding *et al.*, 2005; Linhananta *et al.*, 2005; Hu *et al.*, 2008).

4.6 The D9E Controversy

The original Trp-cage construct (TC5b, NLYIQ WLKDG GPSSG RPPPS) (Neidigh *et al.*, 2002) is only marginally stable, with a melting temperature, T_m, of 42 °C (ΔG_U^{280} = 9 kJ/mol). Even though more stable constructs with Asp and the helix N-cap and L-Ala (Andersen *et al.*, 2002; Lin *et al.*, 2004; Barua *et al.*, 2008) and D-Ala mutations (Williams *et al.*, 2008) substitutions have been reported, TC5b continues to the subject of both experimental studies (Bunagan *et al.*, 2006; Chatterjee & Gerig, 2006, 2007; Mok *et al.*, 2007; Neuman & Gerig, 2008; Wafer *et al.*, 2010; Culik *et al.*,

2011; Rovo *et al.*, 2011; Rovó *et al.*, 2013) and molecular dynamics folding simulations (Juraszek & Bolhuis, 2008; Xu & Mu, 2008; Cerny *et al.*, 2009; Marinelli *et al.*, 2009).

In 2006, Gai (Bunagan *et al.*, 2006) reported computational design studies suggesting that D9E and P12W mutations would stabilise the Trp-cage. They performed experimental studies confirming the stabilising effect of the P12W mutation on TC5b. In 2008, a publication (Hudaky *et al.*, 2008) appeared indicating that the D9E mutation was also stabilising. The rationale for this conclusion was the retention, in the [D9E] mutant of TC5b, of more long-range NOEs and a more helical CD spectrum at higher temperatures. Perczel and co-workers suggested that [D9E]-TC5b represents a more compact, and melting resistant structure due to the "optimal distance between the two sides of the molecule". Even with this conclusion, the authors still reported essentially the same CD melting temperature, 38±0.3 °C, for TC5b and its [D9E] mutant at pH ~6.6, implying that their higher temperature NMR ensembles are based on constraints obtained for a *circa* 60:40 mixture of the folded and unfolded species. The CD melt reported for the [D9E] mutant was also more gradual, which is usually equated with less co-operative folding.

Based on the claims of Hudaky et al., it was clear that the optimisation of the Trp-cage salt bridge needed to be re-examined. Rather than repeat Hudaky's experiments in the TC5b construct, the Andersen group turned to the TC10b Trp-cage (DAYAQ WLKDG GPSSG RPPPS, T_m, = 56 °C, ΔG_U^{280} = 12 kJ/mol) (Lin *et al.*, 2004; Barua *et al.*, 2008) to perform mutational studies. Mutants of TC10b were examined to probe the chain length dependence and directionality of the Coulombic effect of the salt bridge interaction.

4.7 Salt Bridge Mutations

My research on the salt bridge mutations focused on three mutations of TC10b; [D9R,R16E], [D9R,R16D] and [K8A,D9R,R16D] (Table 4.8). For completeness, TC10b and its D9E mutant (characterised by Bipasha Barua and Vicki Williams, respectively) will also be discussed.

	Sequence
10b	DAYAQWLKDGPSSGRPPPS
10b D9E	DAYAQWLK**E**GPSSGRPPPS
10b D9R,R16E	DAYAQWLK**R**GPSSG**E**PPPS
10b D9R,R16D	DAYAQWLK**R**GPSSG**D**PPPS
10b K8A,D9R,R16D	DAYAQWL**AR**GPSSG**D**PPPS

Table 4.8: TC10b and salt bridge mutations.

Concerns with the conclusions reached by Hudaky et al. prompted an examination of additional mutations of TC10b to probe the chain length dependence and directionality of the salt bridge Coulombic effect. Based on α–helix studies by Jack Stewart, a former Andersen group member, (Stewart, 2009) glutamate should provide less helix destabilisation than aspartate at the C-terminus of the α helix. Asp^- has a larger N-capping constant than Asp^0, therefore protonation of the N-terminal Asp destabilises the N-terminal helix and as a result the Trp-cage fold. This effect is expected to be a constant context effect throughout the entire mutational series.

Since residue 9 is the C-terminus of this α–helix, both substitutions and ionisation state changes at the D9 site could also influence fold stability through affecting the intrinsic stability of the helix, an essential element of this folding motif. Indeed, the increased fold stability for TC10b versus TC5b is attributed to helix stability

effects: N → D1 and X → A. Previous work by J. Stewart (Stewart, 2009) shows that an Asp → Glu mutation at the C-terminus of a peptide helix results in a significant increase in helicity at pH 7. This effect should apply to both the folded *and unfolded* state of Trp-cage sequences with this mutation. Based on this work, protonation of D9 is predicted to be significantly fold-destabilising since it removes an unfavourable Coulombic interaction between the D sidechain and the helix macrodipole. A D9E mutation is, hence, expected to be both fold stabilising and to impart increased helicity in the unfolded state. Protonation effects for the D9E mutations would be expected to be smaller since the charge is further away from the helix macrodipole when the sidechain is longer.

A number of examples have appeared in the literature in which salt bridge stabilisation remains following residue swaps, for both D/R and E/R interactions, examples appear in protein kinase activation studies (Dey et al. 2007). These reports led to the exploration of both a [D9R,R16D] and [D9R,R16E] mutation. These swaps would also serve as an additional probe of potential helix C-termination effects. An Arg+ sidechain should be helix-stabilising at all pH's examined.

The CD melts for the newly synthesised species at pH 7 are compare to the 'wild-type' TC10b in Figure 4.9.

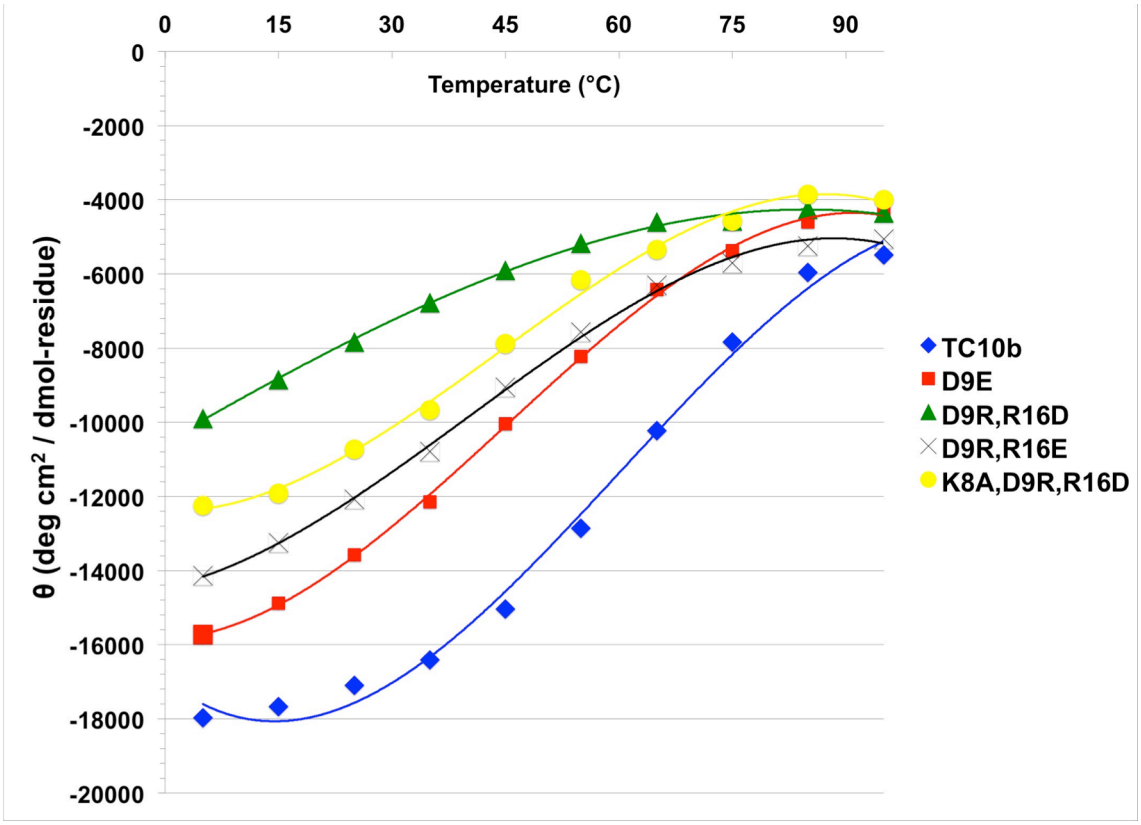

Figure 4.9: CD melts (raw ellipticity values versus T) of TC10b and its [D9E], [D9R,R16D], [D9R,R16E], [K8A,D9R,R16D]-mutants at pH 7. The points for TC10b are fitted to a 3rd order polynomial to provide line to guide the eye.

It was apparent that WT TC10b displayed the largest $[\theta]_{222}$-values and the sharpest unfolding transition in the CD melt. All of the mutants displayed smaller ellipticites at the temperature limit but the [D9E] mutant had the largest negative ellipticities at the higher temperatures. All of the mutants displayed less co-operative melts and less evidence of approaching a 100% folded plateau at the low temperature.

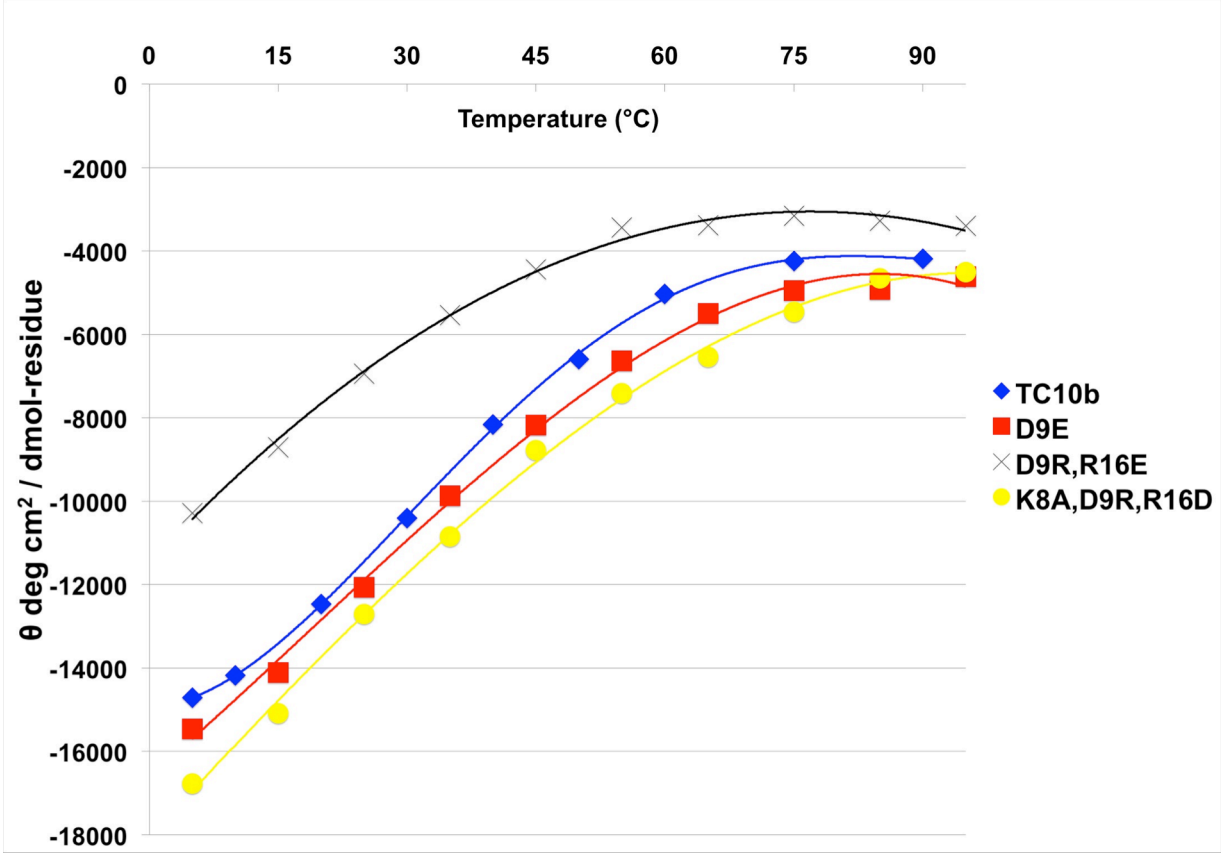

Figure 4.10: CD melts (raw ellipticity values versus T) of TC10b and its [D9E], [D9R,R16E], [K8A,D9R,R16D]-mutants at pH 2.5.

Similar to the data shown at pH 7 (Figure 4.9), WT TC10b again displayed the sharpest unfolding transition in the CD melt at pH 2.5 (Figure 4.10). All of the mutants showed less co-operative melting behaviour at this acidic pH. Peptide helices generally display less co-operative CD melting 'curves' than helical proteins, with a more

gradual, nearly linear, loss in fractional helicity opon warming. At pH 2.5, the species examined (Figure 4.10) displayed evidence of fold destabilisation as a result of carboxylate protonation, with the most affected being [D9R,R16E]-TC10b; the [D9E] mutant had the smallest acidification-induced change in the apparent T_M. But these changes cannot be assigned solely to a disruption of the D/R or E/R sidechain interactions, protonation of the N-capping Asp^- clearly has a role. For an initial estimate of T_M values (Table 4.9), it was assumed that the CD specturm for the fully-folded Trp-cage state at the two pH values is not changed by the mutations.

Peptide	T_M CD (°C)
TC10b	56
pH 2.5	40
D9E	57
pH 2.5	41
D9R,R16E	57
pH 2.5	25
K8A,D9R,R16D	51
pH 2.5	35
K8A,D9R	34
pH 2.5	n.d.

Table 4.9: CD measures of fold stability for TC10b and its mutants.

Since this assumption concerning CD parameters is not necessarily valid, chemical shift measures of folding were also examined. The Trp-cage fold displays consistent dramatic upfield shifts due to ring current effects. The sum of the L7α, P18α,β3 and P19δ2,δ3 CSDs has been established as a measure of the extent of cage formation (Barua *et al.*, 2008); when available, the CSD of the upfield G11Hα is also included in this measure of the extent of folding. The diastereotopic chemical shift difference observed for the Gly11 CH_2 (ΔδG11) is another useful diagnostic. In

previous studies (Neidigh *et al.*, 2002; Naduthambi & Zondlo, 2006; Barua *et al.*, 2008), partial melting as well as all destabilising mutations decreased ΔδG11, reflecting increases in the contribution of the unfolded state. However, it should be noted that changes in ΔδG11 could also reflect changes in geometry of the loop connecting the helix to the docked triproline unit or the fluxionality of the fold.

Peptide	Σ CSD's (+ 11α2)	ΔδG11
TC10b	6.534 (10.028)	2.486
pH 2.5	5.80 (8.67)	1.700
D9E	6.436 (9.725)	2.203
pH 2.5	5.61	n.d.
D9R,R16E	6.204 (9.095)	1.648
pH 2.5	4.81 (7.33)	1.623
K8A,D9R,R16D	5.957 (9.061)	1.951
pH 2.5	5.05 (7.696)	1.616
D9R,R16D	4.905 (7.806)	1.857
pH 2.5	4.113	n.d.

Table 4.10: NMR measures of fold stability for TC10b and its mutants at 280K.

The entries in Table 4.10 are shown in order of decreasing values for the chemical shift changes that are diagnostic of cage formation. This also corresponds to the ordering based upon the melting temperatures. The ranking based on ΔδG11 has one notable outlier, the [D9R,R16E] double mutant, which reverses the directionality of the potential salt bridge. It has the smallest ΔδG11 value at pH 7 and this value does not decrease upon acidification, although other measures of folding indicate decreased fold stability at pH 2.5.

The key chemical shift deviation comparisons between TC10b and the current set of analogues appear in Figure 4.11. While the structuring chemical shifts at essentially all proton sites of the new TC10b mutants were uniformly concordant with those of the WT, indicating the formation of essentially the same fold geometry; the [D9R,R16E]-mutant presented a number of changes.

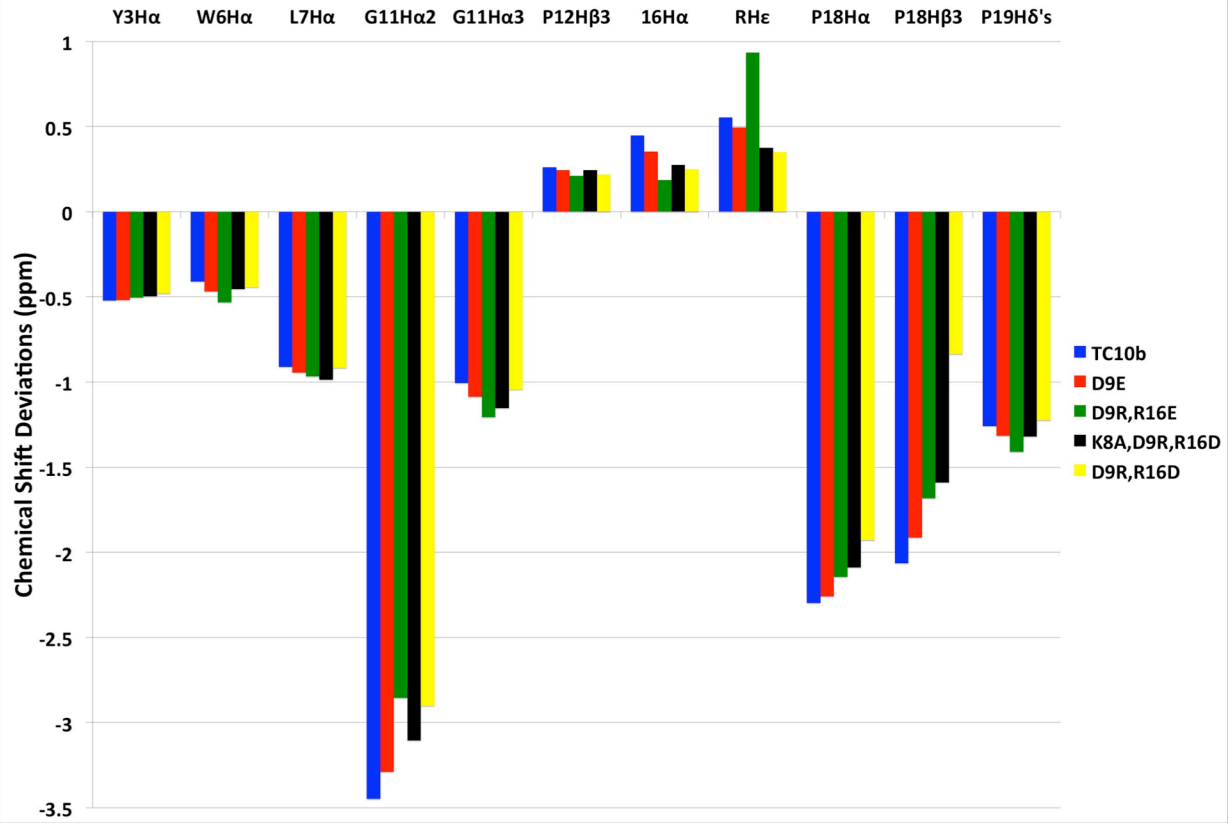

Figure 4.11: Chemical shift deviations comparisons for TC10b and mutants with mutations at D9 and/or R16. All CSDs were measured at pH 7 and 280K. The P19Hδ entry is the sum of the CSDs for the two Hδ resonances.

The downfield shifts at P12Hβ3 and 16Hα are of particular interest, these indicate that these two protons are quite close to the indole ring plane independent of amino acid substitutions at residues 9 and 16. This leads to the conclusion that the geometry of the loop and 3_{10} helix connecting the α helix to the tri-Pro unit appears to be retained. These positive CSDs seem to reflect the same order of fold stability as the

negative ring current shifts at G11Hα2, P18α,β3. The most significant changes associated with reversing the positions of the Glu and Arg units are: a further downfield shift for RHε, increased negative CSDs at W6Hα as well as P19 $C\delta H_2$ and, as previously shown, a distinctly different CSD ratio for G11Hα2 and Hα3. While the change in G11-CH_2 shifts could represent either a repositioning of the indole ring, or a change in backbone geometry in the G10-P12 loop region, these seemed to be ruled out by the typical P12Hβ3 and 16Hα CSDs. Since both the [D9E] and [D9R,R16E] mutants were greater than 93% folded at 280K, higher precision NOESY data was collected for the calculation of NMR structure ensembles.

4.8 Do Salt Bridge Mutations Change the Trp-cage Structure?

Perczel and co-workers (Hudaky *et al.*, 2008) reported that a [D9E] mutant in the marginally stable TC5b Trp-cage results in a "more compact and more thermoresistant" structure and presented NMR structure ensembles for TC5b and its [D9E] mutant at both 282 and 300K. Even in the low temperature generated NMR ensembles, TC5b and [D9E]-TC5b did not display backbone overlap over the residue 10 – 19 span. Although the key CSDs associated with ring current effects were very similar, there were some differences noted for the NOEs; *e.g.* Hudáky *et al.* reported that the [D9E] mutant lacked NOE connectivities between the Y3 sidechain and P19 sites. These through-space interactions were, however, observed for the D9E mutant of TC10b; in fact, they were observed for all of the new analogues prepared in this study.

Ring current calculations on structures generated during MD runs (Fesinmeyer, 2005) starting from the our published TC5b structure have revealed that residue 3 – 19

backbone RMSDs within 0.9Å of the starting structure are required to rationalize the ring-current CSDs observed for Trp-cage species (Barua *et al.*, 2008). The observation that all of the mutants examined in this study reproduce (Figure 4.7) the key CSDs of the Trp-cage, including the upfield shifts at 12β3 and 16α, thus implies structures within a 1Å backbone RMSD of the standard Trp-cage conformation. In Barua et al., it was also indicated, without presenting the details, that as few as 52 medium- and long-range constraints are sufficient to generate an ensemble within a 0.63±0.17Å backbone RMSD of the published TC5b structure.

Here, I was able to demonstrate that a limited set of NOEs (Williams *et al.*, 2011) would generate TC10b structures that would predict all of the ring current shifts. While high precision NOESYs for a structure elucidation were not obtained for all of the new analogues, a survey of the NOESY data collected during the course of spectral assignment revealed that all of the new species (along with other TC10b salt bridge mutations) displayed a common set of 77 NOEs of which 35 provided long-range constraints (residue i to i + n sites, n > 3). This set of NOEs generated an NMR ensemble with an intra-ensemble 0.82±0.33Å residue 3-19 backbone RMSD, and within 0.90±0.39Å of a typical member of the published TC10b ensemble generated with the full set (186) of NOE constraints (of which 32 were long-range). The inclusion of one additional NOE constraint, between methylene hydrogens of residues 9 and 14, which was present for TC10b and its [D9E] and [D9R,R16E] mutants, greatly improved convergence (intra-ensemble RMSD 0.58±0.19Å, nearly comparable to the value obtained with the full set of TC10b constraints, 0.41±0.14Å) and provides full agreement with the literature structure of TC10b. The distance constraints used appear

in Appendix C. Hence, it can be concluded that salt bridge mutations of TC10b do not alter the cage conformation in an appreciable way. The ensembles are shown in Figure 4.12.

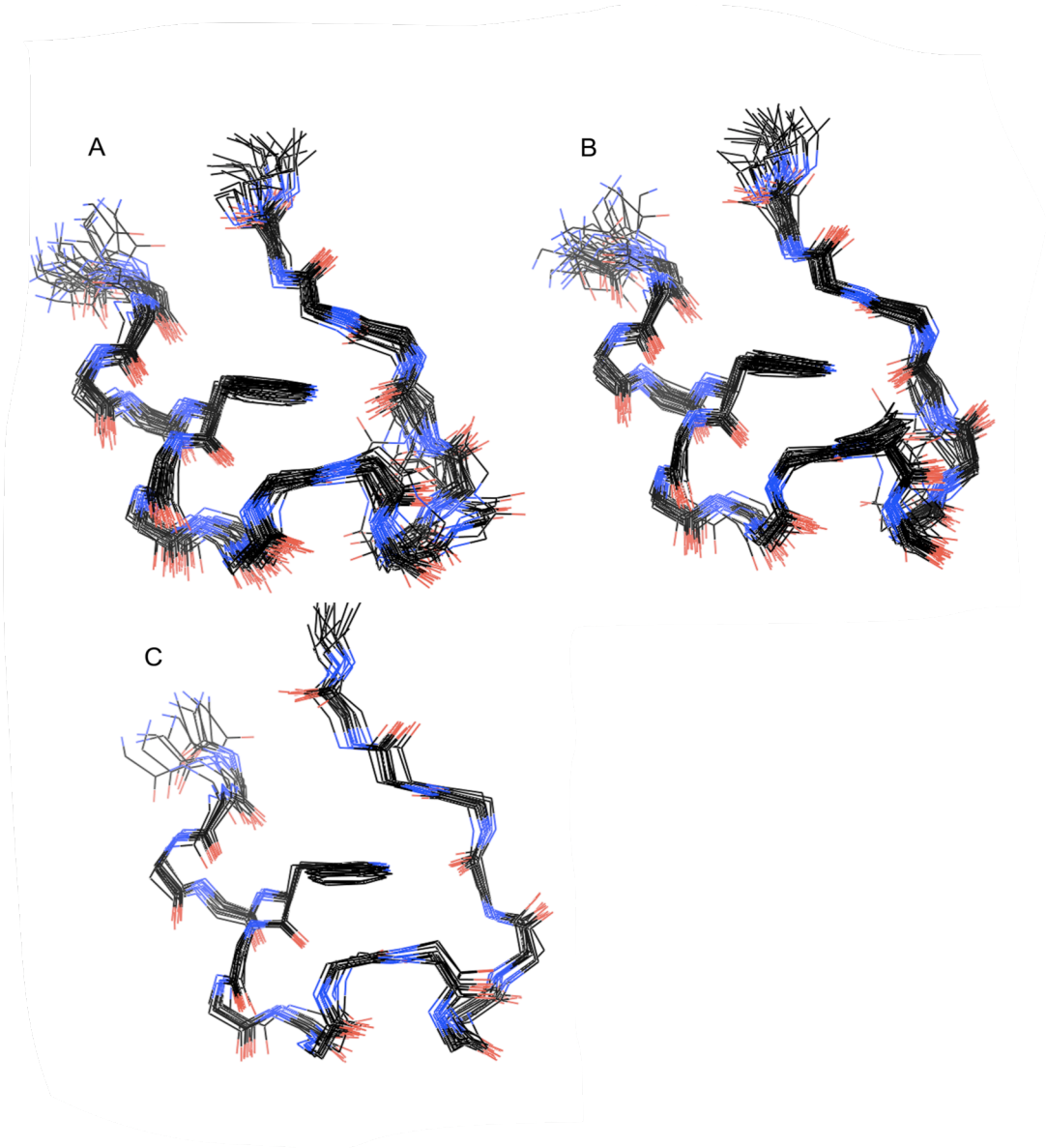

Figure 4.12: A comparison of Trp-cage NMR structure ensembles for TC10b generated from limited set of NOEs and the consensus ensemble previously published (Barua *et al.*, 2008) which employed 186 constraints (panel C): (A) The structure generated from 77 constraints appearing in all TC10b analogues examined; (B) the structure generated with the addition of one additional constraint between residues 9 and 14.

These structures illustrate the extent to which a high resolution structure can be generated from a relatively small number of long and medium range constraints. The 108 additional constraints employed in the original TC10b structure generation provide very little additional structural definition.

NMR structures were derived for the [D9E] and [D9R,R16E]-mutants in an attempt to determine how these sidechains and P19 orient themselves relative to the indole ring (Williams *et al.*, 2011). The structure generation for the [D9E] mutant was performed by Vicki Williams.

4.9 Trp-cage NMR Structure Comparisons

The NOESY data obtained for both [D9E]- and [D9R,R16E]-TC10b provided a sufficiently rich web of NOE constraints to define their Trp-cage residue 3 – 19 backbone conformations. The intra-ensemble 3-19 backbone RMSD for [D9E]-TC10b was calculated as 0.28 ± 0.11 Å; when compared to a representative TC10b structure it was 0.49 ± 0. 11 Å. The 3-19 backbone RMSD for the intra-ensemble of [D9R,R16E]-TC10b was 0.17 ± 0.09 Å. The statistics for [D9R,R16E]-TC10b are given below (Table 4.11), and the distance constraints used appear in Appendix C.

Type of constraint	Number	r.m.s deviation
Intraresidue	91	0.027 ± 0.011
Sequential	72	0.047 ± 0.025
i/i+n, n = 2-4	46	0.018 ± 0.008
i/i+n, n ≥ 5	60	0.13 ± 0.17
Structure statistics[a]:		
E_{TOTAL} (kcal/mol)		-50.4 ± 2.6
E_{NOE} (kcal/mol)		5.05 ± 0.4
E_{vdW} (kcal/mol)		-79.8 ± 2.7
Bond violations (Å)		0.0037 + 0.0002
Angle violations (°)		0.196 ± 0.004
Improper torsion violations (°)		1.06 ± 0.1
Convergence within final ensemble, atomic r.m.s deviations (Å)[b]:		
Pairwise over the ensemble (±s.e.)		
Backbone		0.17 ± 0.09
Heavy atom		0.65 ± 0.2

Table 4.11: NMR structure statistics for the [D9R,R16E]-TC10b ensemble (34 accepted structures from 50 starts). [a.] Values are mean ± standard deviation. [b.] All convergence measures are over residues 3-19.

As each ensemble has intra-residue RMSDs less that 0.3 Å, a representative structure close to each mean can be chosen to represent these structures. These representative structures are superimposed on the TC10b structure in Figure 4.13.

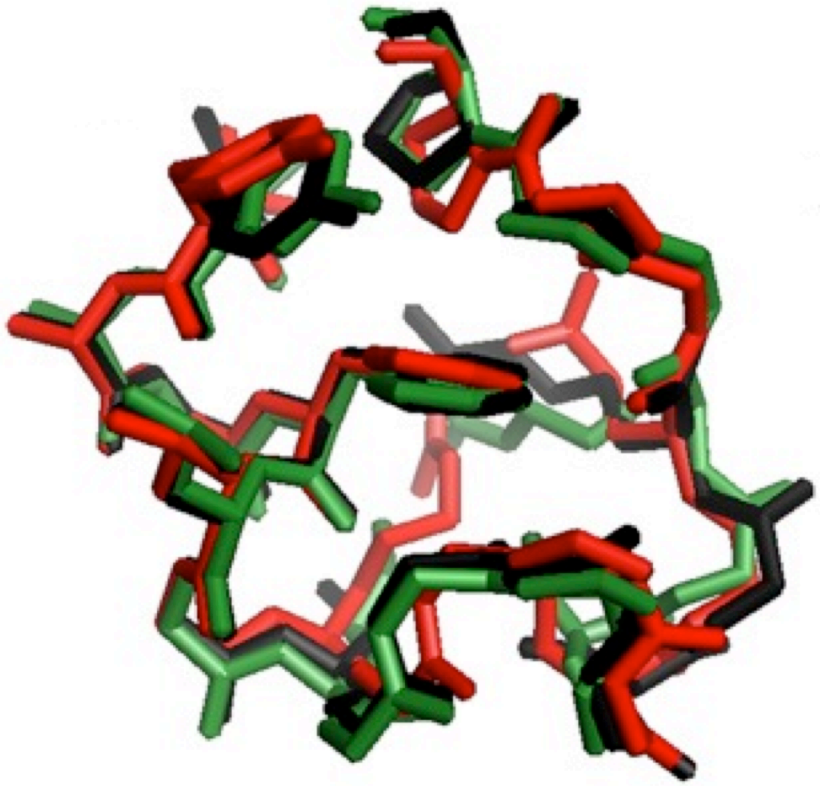

Figure 4.13: A comparison of the salt bridge mutant structures to the prior TC10b NMR ensemble. Representative structures from each ensemble are shown with the residue 2 – 19 backbone and the heavy atoms of residues 3, 6, 12, 16, 18 and 19: TC10b (black), [D9E] (green) and [D9R,R16E] (red).

The [D9E]-mutant structure lies within the TC10b ensemble and, like the TC10b structure, the R16 sidechain wraps around the backside of the Trp indole ring. This function, providing burial of the Trp residue, cannot be filled by the shorter E16 sidechain. This would be expected to be a fold stabilising effect of R16 that is unrelated to salt bridge effects. Pi-cation effects, an alternative source of stabilisation that might be associated with R16, appear highly unlikely since a Arg/Trp π-cation would require placing the planar guanidinium unit (as a π-cation) over the electron-rich face of the

indole ring: the TC10b and [D9E]-TC10b structures place the guanidino-group of Arg in the electron-poor nodal plane rather than over the π-cloud of the indole.

Neither the TC10b or [D9E]-TC10b structures provide evidence of an H-bonded D9/R16 salt bridge. This could reflect the lack of definable sidechain/sidechain NOEs; but in the case of [D9E]-TC10b, the addition of distance constraints that would enforce a tighter salt bridge interaction introduces greater violations for NOE-based distance constraints. The Andersen group has previously reported (Barua *et al.*, 2008) that TC10b structures can be generated with an H-bonded salt bridge.

In the case of the [D9R,R16E]-mutant, there appear to be some structural differences: 1) even though the 3-19 backbone RMSD is more converged (0.17±0.09Å) in the NMR ensemble, it lies outside of the limits for the TC10b ensemble (RMSD = 0.63Å versus the TC10b representative), 2) a significant cluster of structures display a tighter salt bridge geometry (Fig. 3.6) and 3) P19 and the indole ring are in closer contact. The displacement of the P19 unit towards the indole ring is consistent with the observation of slightly larger upfield ring current shifts for 19Hδδ' and also alters the G11Hα2,3 ring current prediction toward the ΔδG11 observed for the [D9R,R16E] analogue. The [D9R,R16E] analogue ensemble also provides an explanation for the downfield shift of R9Hε (Figure 4.14). This proton appears nearly in the deshielding, nodal plane of the indole ring. An H-bond to the E16 carboxylate (Figure 4.14) would also result in deshielding.

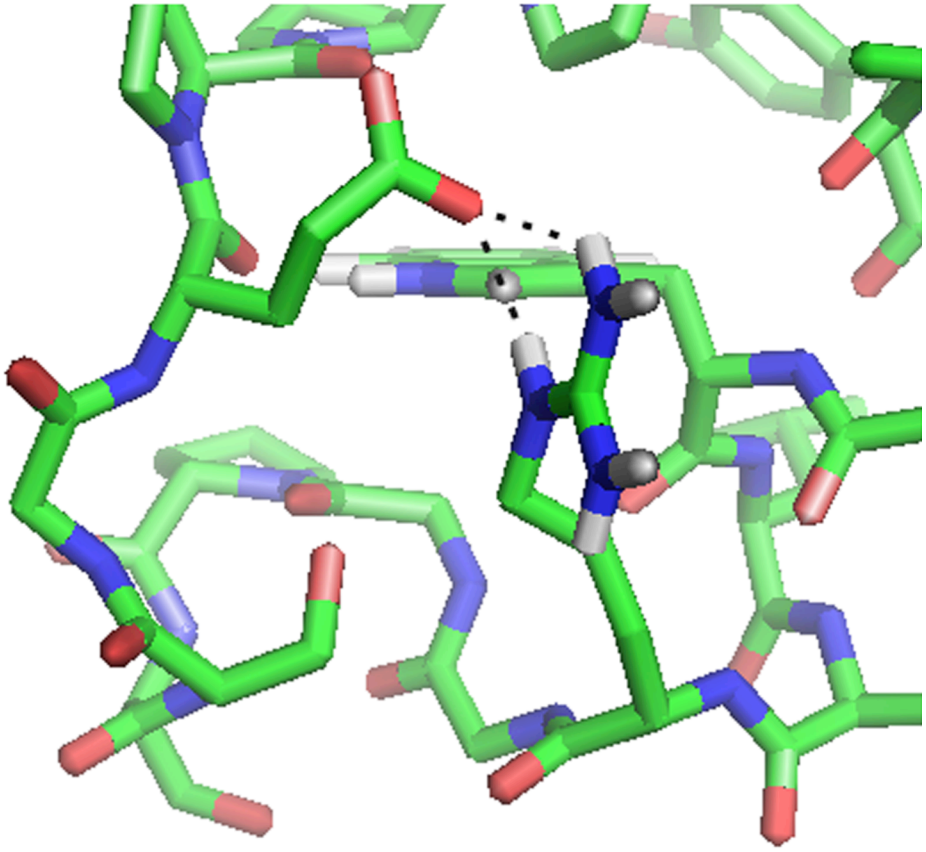

Figure 4.14: An R9/E16 geometry that is frequently observed in the ensemble, showing the R9Hε proton in the plane of the ring and also illustrating a potential H-bond to the E16 carboxylate.

All of the TC10b mutants examined in the present study displayed additional TOCSY and NOESY peaks due to species with *cis* Xaa-Pro linkages that are not in rapid equilibrium with the all-*trans* species that folds to the Trp-cage conformation (Figure 4.15); these increase in intensity on warming and acidification. Minor isomer peaks were totally absent in the spectra recorded for TC10b. This observation stands as irrefutable evidence that the Trp-cage fold is significantly destabilised for all of the mutations examined.

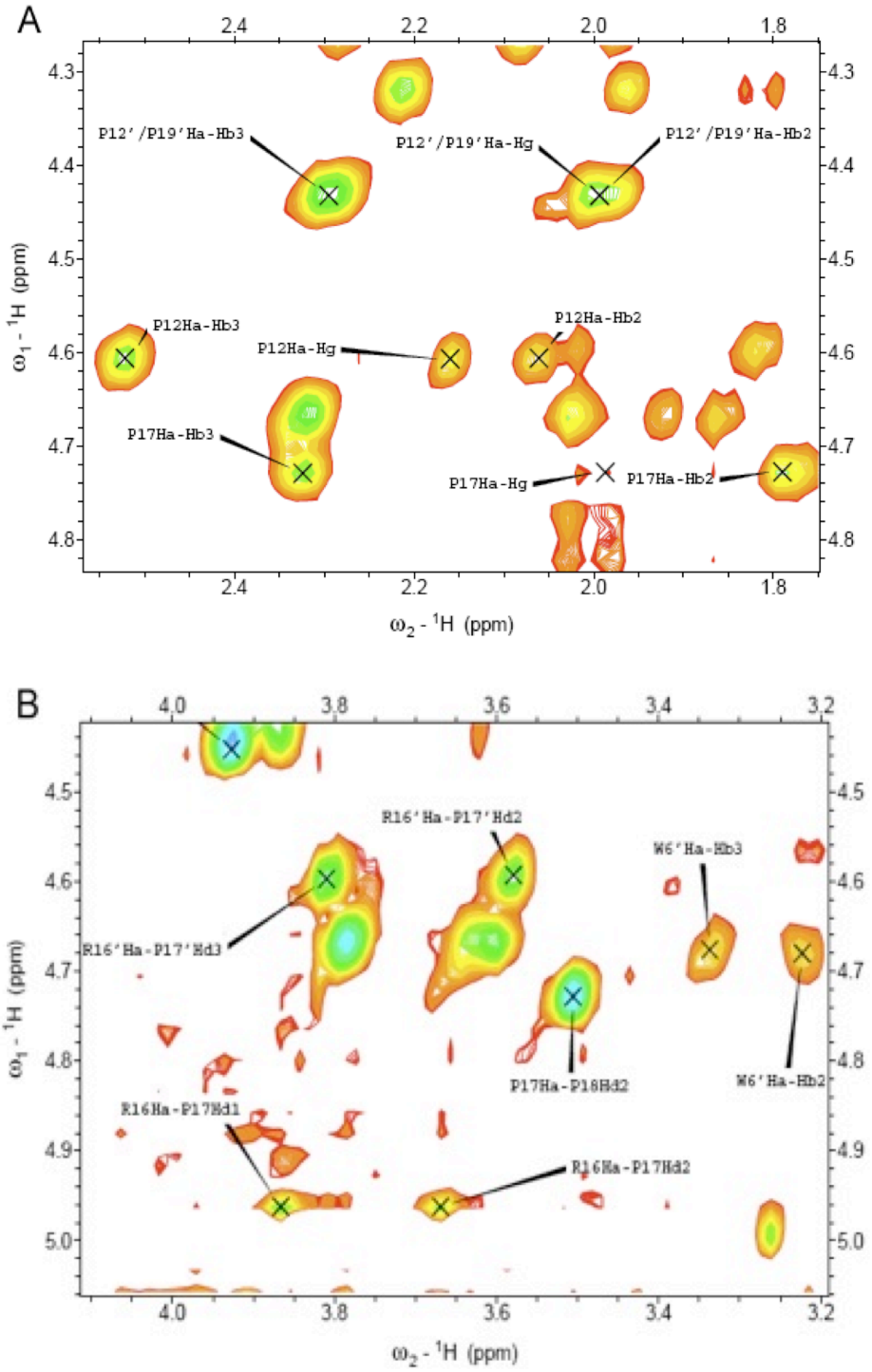

Figure 4.15: Illustration of NOESY spectral features of [D9E]-TC10b that can only be explained as peaks due to *cis*-Xaa-Pro isomers that are not in rapid equilibrium with the all-*trans*-Xaa-Pro isomer that forms the Trp-cage fold: (a) shows an additional Pro, either residue 12 or 19; (b) illustrates R16Hα (at an unshifted δ, 4.6 rather than downfield at 4.95 ppm due to being in the plane of the indole ring) connection to P17δδ' sites that are not coincident with the P17 resonances of the fully folded state. The smaller intensity of the folded R16Hα peaks is not a reflection of fold population; a problem with water suppression is that it may also attenuate the resonances of interest close to the water.

4.10 Evaluating the ΔG_U Contributions of Alternate 'Salt Bridge' Pairings to Cage Formation.

For salt bridged systems there are two potential sources of ΔΔG information, changes in fold population associated with each mutation, ($m\Delta\Delta G_U$), and the effect of acidification, $\Delta\Delta G_U(pH)$. Though there are complicating factors in the analysis of each in the present case. Acidification alters a number of features that could affect structure stability. As previously noted, the effects of protonation of the helix-N-capping Asp (and the C-terminal Ser-CO_2^-) are constant throughout the series, but the effects of protonating the Glu or Asp at the C-terminus of the α helix are not. Protonation of Asp1 decreases the Trp-cage fold population by affecting the intrinsic helicity of the N-terminal helix. This effect could be greater for CD measures of folding since removal of the N-cap would increase terminal fraying and decrease $[\theta]_{222}$ to a greater extent than it would decrease the cage fold population. For species with an Asp at residue 9, the C-terminus of the helix, the opposing helix stability effects associated with the C-terminal Coulombic effect on the helix should largely offset the helix destabilisation associated with D1 protonation. A larger effect would be expected for any mutated sequence with Glu or Arg at residue 9. Significant fold stabilisation upon deprotonation for TC10b and any mutant retaining D9 implies that the Coulombic interaction between D9 and the residue-16 sidechain function is highly stabilising; it offsets the unfavourable helix C-terminus effect of aspartate.

Table 4.12 shows the ΔG_U measures derived from chemical shifts and includes the $m\Delta\Delta G_U$ values for each mutation and $\Delta\Delta G_U(pH)$ values for those mutants examined at both pHs.

Name	ΔG_U (kJ/mol)			mut$\Delta\Delta$G (kJ/mol)			$\Delta\Delta$G(pH) (kJ/mol)		
	Σ CSDs		ΔG_U^{CD}	NMR		CD	NMR		CD
	280K	300K		280K	300K		280K	300K	
TC10b	11.5	5.28	5.86						
pH 2.5	4.64	1.93	1.89				(> 6)	3.35	3.97
D9E	8.62	4.55	4.64	2.9	0.73	1.22			
pH 2.5	4.04	0.22	1.71				4.58	4.33	2.93
D9R R16E	6.41	3.58	3.47	5.1	1.70	2.40			
pH 2.5	2.32	-0.22	-0.23				4.10	3.80	3.7
K8A D9R R16D	5.28	3.38	3.67	6.26	2.15	-2.19			
pH 2.5	2.79	0.52	0.83				2.49	2.86	-2.85
D9R R16D	2.51	1.02	0.70	9.03	4.50	-5.16			
pH 2.5	1.20	-1.49					1.31	2.51	

Table 4.12: Mutational and pH-induced Fold Stability Changes for salt bridge mutants. [a,b]

[a] mut$\Delta\Delta$G is the $\Delta\Delta G_F$ associated with each mutation, +ve values indicate fold destabilisation. $\Delta\Delta$G(pH) is the effect of ionization. +ve values indicate fold stabilisation on deprotonation.

[b] Unless otherwise indicated, the ΔG_U values are based on the Σ CSD measure for the following shifted sites: L7α, P18Hα/Hβ3 and P19Hδ2/δ3. With the exception of the D9R,R16E mutant, when G11Hα2 shifts are available including these larger structuring shifts in the sum does not change the ΔG_U values (±0.3 kJ/mol).

Considering the $\Delta\Delta G_U(pH)$ measures at 300K first; the fold stabilising contribution of the favourable Coulombic interactions between the residue 9 and 16 sidechains have the following ranking: D9/R16 > E9/R16 > R9/E16 > R9/D16. However, it is difficult to determine when (if at all) this interaction shifts from being only a Coulombic effect to an H-bonded salt bridge. At 280K, all of the D9/R16,

E9/R16, R9/E16 and R9/D16 effects are significantly larger; with the 'native salt bridge' contribution exceeding 5 kJ/mol.

Turning to the $m\Delta\Delta G_U$ effects of a D9E mutation upon TC10b, this mutation is destabilising by about 1 kJ/mol at 300K, and by a significantly larger ($\geq$ 3 kJ), but less well determined, amount at lower temperatures. As all prior mutations (N1D, L2A, I4A and K8A) that stabilise the N-terminal helix have resulted in comparable increases in the cage fold population (Barua et al. 2008; Lin et al. 2004), stabilisation of the Trp-cage fold by a D9E mutation would be expected in the absence of a salt bridge; reflecting the enhancement of the intrinsic helix formation propensity. At pH 7, there is lesser helix destabilisation by C-terminal glutamate than aspartate. Specific cage-stabilizing interactions, other than salt bridging, associated with R16 are suggested by the observation that all analogues with a substitution at Arg16 are significantly destabilized: $\geq$2 kJ/mol at 300K (> 5 kJ at 280K). The NMR structure ensemble suggests that this reflects burial of the indole ring by the (CH_2CH_2) unit of R16.

4.11 Replacing the Salt Bridge with a Hydrophobic Pair

The swapping of the salt bridge (D/R $\rightarrow$ R/E or R/D) produced a somewhat disappointing result. This swap should have worked better; the positioning of an Arg at the helix C-terminus instead of the incumbent Asp should have better satisfied the helix macrodipole over the Asp. This led to the idea of replacing the salt bridge residues with hydrophobic replacements.

Hydrophobic interactions play a key role in protein folding. Hydrophobic residue side chains are 'oily' in character and prefer to be segregated in contact with

each other, and out of contact with water. The folding of a protein results in the majority of the hydrophobic side chains clustering together within the core of the protein. Removal of the hydrophobic side chains from water is highly favourable. As these hydrophobic residues tend to stick together, could this type of interaction be used in place of the salt bridge interaction in the Trp-cage?

	Sequence
16b Y3F	DA**F**AQWLADaGPASaRPPPS
16b Y3F D9L	DA**F**AQWLA**L**aGPASaRPPPS
16b Y3F D9L R16I	DA**F**AQWLA**L**aGPASa**I**PPPS

Table 4.13: Hydrophobic Mutations to the Salt Bridge in the TC16b Y3F series.

Two of the more hydrophobic residues, leucine and isoleucine, were chosen for this mutational series. The aromatic residues were not chosen as they would have added further complication to Andy McMillan's fluorescence studies, and as discussed in Section 4.1 earlier, tryptophan at the 16 position was established as being unfavourable (Bunagan *et al.*, 2006). The Φ/Ψ backbone angles of Arg16 were taken into account when choosing which of the two hydrophobic residues to mutate in at that position. The Φ/Ψ angles indicate a β-sheet conformation so isoleucine would be the better mutation over leucine at that site.

Name	%-Fold 300K	ΔG_U (kJ/mol) Σ CSDs	mut$\Delta\Delta G$ (kJ/mol)	$\Delta\Delta G$(pH) (kJ/mol)
Y3F	0.959	7.87		
pH 2.5	n.d.			
Y3F D9L	0.907	5.68	2.19	
pH 2.5	0.857	4.46		1.22
Y3F D9L R16I	0.936	6.69	1.18	
pH 2.5	0.904	5.58		1.11

Table 4.14: Mutational and pH-induced Fold Stability Changes for the Hydrophobic Mutations in the TC16b Y3F series. [a,b]

[a] mut$\Delta\Delta G$ is the $\Delta\Delta G_F$ associated with each mutation, +ve values indicate fold destabilisation. $\Delta\Delta G$(pH) is the effect of ionization. +ve values indicate fold stabilisation on deprotonation.

[b] The ΔG_U values are based on the Σ CSD measure for the following shifted sites: G11Hα2, P18Hα/Hβ3 and P19Hδ2/δ3.

Both the [Y3F,D9L] and [Y3F,D9L,R16I] mutants are somewhat destabilising when compared to the [Y3F]-TC16b parent construct (Table 4.14). The [Y3F,D9L]-TC16b mutant being more destabilising than the [Y3F,D9L,R16I] mutant is indicative of a Leu9/Ile16 hydrophobic interaction taking place; a Leu9/Arg16 interaction would have no stabilising contacts. Unfortunately, no NOEs were visible in the NOESY between Leu9/Ile16 to verify that these residues were close in space. Both of these mutants remove the potentially helix stabilising QXXXD interaction, which could also be a factor in a lower fold population. The presence of a pH effect should be due to the change in charge state at the aspartic acid at the N-terminus and the Coulombics between the termini.

4.12 Conclusions

The NMR and CD studies reported here for salt bridge mutations of TC10b do not support the assertion (Hudaky et al. 2008) that an E9/R16 salt bridge provides superior stabilisation of the Trp-cage than the D9/R16 unit that had been used in the

prior cage constructs. Cage-stabilising effects, if any, of [D9E] substitutions are due to contributions from an intrinsic helicity increase not improvements in salt bridging. The helix disfavouring effect (~2 kJ/mol) of an Asp^- at the C-terminus of a helix has been recognized previously (Doig et al. 1995; Huyghues-Despointes et al. 1993) but the present study demonstrates that it has consequences in protein folding thermodynamics.

The absence of NMR peaks for *cis*-Xaa-Pro isomers for WT TC10b, while such peaks are observed for all of the salt bridge mutants, along with the enhancement of folding co-operativity is considered the most compelling evidence for the greater fold stability of TC10b and salt bridge optimisation with the D9/R16 unit. The greater ΔG_U for the D9E mutant at pH 2.5 (as shown in Table 3.5) as measured by CD rather than NMR (which follows only the cage measures) suggests contributions from unfolded states which retain helicity (and which would include the *cis*-Xaa-Pro species). The presence of aspart**ate** at the C-terminal of a helix is known to be destabilising, this then raises an interesting question concerning the salt bridge. Can a Trp-cage species be designed that would be more stable at pH 2.5 than pH 7?

Chapter 5: Reversing pH Stability

5.1 Introduction

All Trp-cage species synthesised previously have been significantly less stable at lower pH, as CO_2^- functional groups are protonated. To successfully create a Trp-cage construct that would be more stable at pH 2.5, side chain- CO_2^- units could not be involved in helix or fold stabilising interactions. That means there could be no salt bridge interaction and no other pH dependent effects. In a typical Trp-cage construct, there are a number of favourable interactions for $-CO_2^-$ functions: 1) the greater N-capping effect of Asp^- versus Asp^0, 2) the D9/R16 salt bridge, 3) the C-terminus macrodipole.

The quantitative measure of these effects has been of interest for some time but much remained to be determined. The more complete previous effort was by Bipasha Barua (Barua *et al.*, 2008).

Dr. Barua's study used the TC9b Trp-cage series (NAYAQ WLKDG GPSSG RPPPS) for her analysis. Asn^1 was utilised as the N-cap; to reduce the pH dependence of the N-capping effect. For constructs with an Asn N-cap, a number of pH effects can be suggested: 1) the D9/R16 salt bridge, 2) the N-capping proficiency of Asp is highly pH dependent ($N_{Asp0} = 2.8$ *versus* $N_{Asp-} = 6.5$) (Andersen et al.g 1997; Doig et al. 1995), 3) the helix-stabilising QXXXD interaction is pH dependent, it gets weaker upon Asp protonation, 4) an effect related to C-terminus protonation.

The helix-stabilising QXXXD interaction is believed to be important as hydrogen bonds between these side chains have been shown to be energetically favourable in peptide helices (Huyghues-Despointes, 1995). The hydrogen bond studied, Gln-Asp (i to i +4), was found to have a ΔG of *ca.* 4 kJ/mol at pH 7 and 1.5 kJ/mol at pH 2. However, it was earlier noted (Huyghues-Despointes, 1993) that the interaction of the charged Asp with the helix macrodipole effects helix stability throughout the helix; it is notably destabilising at the C-terminus.

Barua (Barua et al. 2008) examined Q5A, D9N and R16Nva mutations in TC9b. In the Q5A and D9N mutants, pH 7 was found to be more stable than pH 2.5. While R16Nva had a very similar fold population and melting temperature at both pHs. This data seemed counter-intuitive, for the R16Nva mutant an increase in stability (melting behavior really) at pH 2.5 would be expected. With no salt bridge present, the Asp would only partake in the QXXXD interaction. C-terminal Asp^0 has less of a destabilising effect than Asp^-; this can be traced to the side chain charge interacting with a C-terminal charge of the helix macrodipole.

5.2 α-Helix C-Terminus Substitutions

With residue 9 of the Trp-cage being the C-terminus of the α-helix, substitutions at this position could also influence fold stability by affecting intrinsic helix stability. Ionisation state changes at this site could also play a role in affecting intrinsic helix stability. The effects of substitutions at the C-terminal helix site were modelled (Stewart Thesis; Williams 2011) in a peptide helix, Ac-KAAAAKAAAAKAAAAXGY-NH_2, where X is the residue varied and "AA" is a pair of labelled alanines. The CSDs of the

^{13}C=O units (Song 2008; Stewart 2008) of the AA pair were used to monitor helicity changes; labels were located in the central section of the helix, as 100% CSDs at the C-terminus are not clearly defined. A favourable C-capping interaction should propagate within the helix and lead to enhanced helicity in the central portion. Stewart designed his helix system to explore a series of positive, neutral and negative amino acids at the X site; amino acids examined include A, D, E, N and R among others.

Figure 5.1 shows the CSDs seen at different positions according to varying C-caps. The order of helicity at Ala 8 is: X = R > A > N > E >> D. Positively charged Arg provides the best possible single residue interaction at the C-terminus. The likely explanation for this is the positively charged side chain interacts with the negative macrodipole at the α-helix C-terminus. Alanine is the next best in the series examined; probably through its high propagation co-efficient. Ala increases the length of the helix and thus its overall helicity. Asparagine is only slightly less helix-favouring than Ala at the C-terminus. Asn provides as much destabilisation to the C-terminal macrodipole with the carboxyl unit as it provides stabilisation with its amide group. Asn can also be used as a surrogate for Asp^0. As would be expected, negatively charged side chains interact unfavourably with the negative end of the helix macrodipole. Glu is presumably better than Asp because of its longer side chain. The shorter side chain of Asp places the negative charge closer to the macrodipole; increasing the chances of fraying and decreasing the likelihood for helix extension towards the C-terminus.

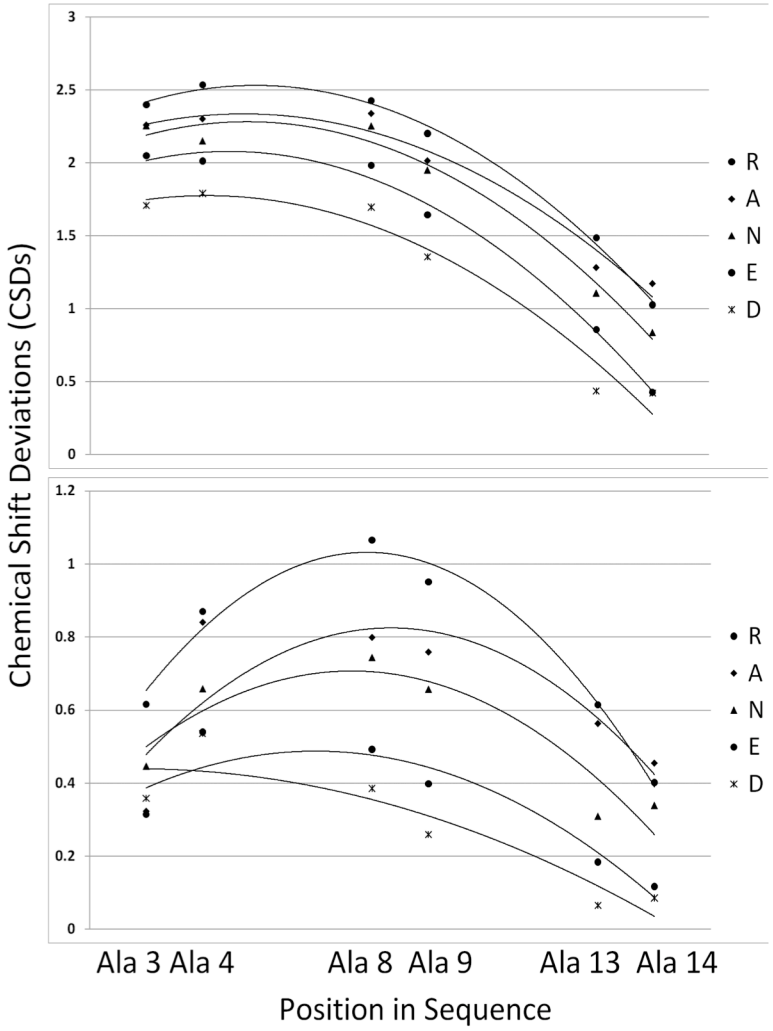

Figure 5.1. Sequence plot of the Ala $^{13}C=O$ CSDs along the sequence of Ac-KAAAAKAAAAKAAAAXGY-NH_2 (top panel) and the desacetyl species (bottom panel) at pH 7. In the central repeat, a CSD of 3.5 ppm corresponds to 100%helicity.

Relating this set of results to the Trp-cage; the data shows that an Asp → Glu mutation at the C-terminus of a peptide helix should result in a significant increase in helicity at pH 7. This helicity increase should apply to both the folded and unfolded state of Trp-cages with this mutation. Helicity $\Delta\Delta G_F$ values, derived from the CSDs observed for the central repeat (Song 2008), were -0.40 for R^+, 0.0 for Ala (the reference), 0.20 for N (or Asp^0), 0.97 for E^-, and 1.73 kJ/mol for D^-. Based on these

numbers, protonation of D9 (modelled as the D → N change at pH 7) is projected to be significantly fold-destabilising. Dr. Stewart also explored this system as the desacetyl species. This less stable system shows fractional helicities similar to those seen for Trp-cage sequences which have been truncated to prevent cage formation. In this desacetyl system, $\Delta\Delta G_F$ (D → N) = 1.8 kJ/mol, effectively the same value as in the acetylated helices. A D9E mutation is therefore expected to be fold stabilising and to effect increased helicity in the unfolded state. Protonation effects for the [D9E] mutants would be anticipated to be smaller because the charge change is further from the helix macrodipole when the side chain is longer.

5.3 Design of the Mutational Series

I decided to investigate a series of mutations (Table 5.1) in the more stable TC16b series (DAYAQ WLADa GPASa RPPPS).

Peptide	Sequence
16b tr	**Ac**-AYAQWLADaGPASaRPPPS-**NH_2**
16b tr Q5A	**Ac**-AYA**A**WLADaGPASaRPPPS-**NH_2**
16b tr D9N	**Ac**-AYAQWLA**N**aGPASaRPPPS-**NH_2**
16b tr Q5A D9N	**Ac**-AYA**A**WLA**N**aGPASaRPPPS-**NH_2**
16b tr Q5A R16Nva	**Ac**-AYA**A**WLADaGPASa**Nva**PPPS-**NH_2**
16b tr Q5A D9N R16Nva	**Ac**-AYA**A**WLA**N**aGPASa**Nva**PPPS-**NH_2**
16b tr R16Nva	**Ac**-AYAQWLADaGPASa**Nva**PPPS-**NH_2**
16b tr R16Cit	**Ac**-AYAQWLADaGPASa**Cit**PPPS-**NH_2**

Table 5.1. Peptides examined for a pH 2.5 stable construct.

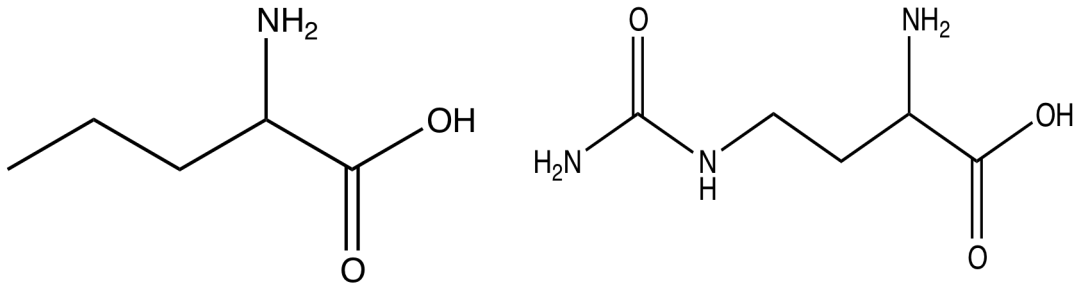

Figure 5.2. Structure of norvaline (left) and citrulline (right).

This set of mutations was designed to focus on Asp9's interactions with other residues within the Trp-cage. This meant looking at the aspartic acid in two ways: i) with and without the presence of a salt bridge and ii) with and without the potentially helix-stabilising QXXXD interaction. The QXXXD interaction should be a pH-dependent helix-favouring interaction.

In all cases, the constructs are lacking D1 and are both acetylated and amidated. The N-terminal aspartic acid was removed to eliminate the pH-dependent helix N-capping effect. Acetyl is almost as good an N-cap as aspartate and is significantly better than aspartic acid. The presence of the acetyl and amide at their respective termini eliminates any Coulombic effects between the termini. An alanine inserted at the 5 position removes the potential helix stabilising QXXXD interaction but still allow for salt bridge formation. The mutation of D9 to asparagine would reduce the H-bonding interaction action in the helix and also eliminates the salt bridge. Whereas the mutation of arginine at the 16 position to a norvaline (Nva) (an analogue of arginine minus the guanidino group – structure shown in Figure 5.2) also effectively removes the salt

bridge interaction, but allows the QXXXD interaction. The norvaline should provide enough length at that position to potentially perform a similar action to that of the arginine, enabling the side chain to wrap around the central Trp; facilitating in its burial. The mutation of arginine to citrulline should allow for H-bonding between it and the glutamine, but obviously there wouldn't be any electrostatic interactions. Citrulline contains a urea group rather than the guanidino group in arginine – structure shown in Figure 5.2. Citrulline would also allow the QXXXD interaction to occur.

5.4 Mutational Effect on Stability

The calculated fold populations for all mutations at both 280 K and 300 K along with the T_Ms from CD melts are given in Table 5.2. The parent peptide, TC16b tr, is well folded at 280 K; its stability at pH 7 is extremely similar to that of TC16b itself based on the CD melt but a stability difference is apparent based on NMR measures of folding at lower temperatures. This is presumably due to the N- and C-termini of TC16b not having as much of an effect as in earlier constructs. The lack of change seen in the T_Ms between pH 7 and pH 2.5 can only be explained by the lack of a salt bridge at pH 7, the reasoning as to why the salt bridge didn't form is unclear.

Peptide		% Fold 280K	% Fold 300K	CD T_M (°C)	% Fold 280K	% Fold 300K	CD T_M (°C)	pH Effect
Residues	5 9 16	pH 7			pH 2.5			
tr-16b	Q D R	0.995	0.958	66.7	0.959	0.909	67.9	Y
Q5A	A D R	0.990	0.946	63.7	0.965	0.916	64.4	Y
D9N	Q N R	0.911	0.841	57.9	0.910	0.840	59.1	N
Q5A,D9N	A N R	0.913	0.845	62.7	0.913	0.843	59.9	N
Q5A,R16Nva	A D Nva	0.874	0.756	41.9	0.907	0.854	63.3	Rev[a]
Q5A,D9N,R16Nva	A N Nva	0.906	0.845	61.9	0.903	0.845	60.4	N
R16Nva	Q D Nva	0.888	0.784	49.5	0.903	0.847	65.2	Rev
R16Cit	Q D Cit	0.928	0.841	49.7	0.945	0.888	67.4	Rev

Table 5.2. Fold populations at 280 K and 300 K and T_M's of the constructs at both pH 7 Hα/Hα3 and P19 Hδ2/δ3. [a] Rev indicates that the pH stability has been reversed.

The larger stability difference observed in the Q5A mutation is due to the larger effect upon helical stability rather than an effect on the salt bridge. This is due to alanine having the largest intrinsic helix propensity of the 20 amino acids, whereas glutamine is 0.39 kcal/mol less favourable in a helix (Pace, 1998). The loss in stability (but different melting prolife) in the Q5A mutant could indicate that the Q5 side chain is involved in a fold stabilizing interaction. This stabilization could be due to a QXXXD hydrogen-bonding interaction between the Q5 and D9 side chains. Gln - Asp/Asn (i, i+4) hydrogen-bonding interactions have been reported to occur in helices (Huyghues-Despointes, 1993; Huyghues-Despointes, 1995; Stapley, 1997). It has also been reported that this interaction is more stabilizing when the Gln is N-terminal to the Asp/Asn, and particularly when the Asp is ionized. Therefore the destabilization due to

the Q5A mutation can be attributed to the loss of this helix-stabilizing Gln5-Asp9 side chain-side chain H-bonding interaction.

The melting temperatures obtained from CD do not seem to line up with the fold populations resulting from NMR melts, as a result NMR measures of cage fold population were relied upon. Since %-fold estimates, and ΔG values derived from them, are in the absence of confirmation by amide exchange protection factors subject to larger error when > 0.95, the remaining discussion focuses on ΔG values NMR measures of fold populations at 300 K (Table 5.3).

The difference in free energy (Table 5.3) for the Q5A mutant between pH 7 and pH 2.5 should correspond to the free energy contribution of the salt bridge (assuming no fold stability effect of C-terminal protonation), whereas the difference in free energy between TC16b tr and the Q5A mutant corresponds to the free energy contribution of the QXXXD H-bond (assuming no other Q5 side chain interactions that affect fold stability).

Residues 5 9 16	ΔG_U (kJ/mol) Σ CSDs 300K	$\Delta\Delta G_F$ (mut) (kJ/mol) 300K	$\Delta\Delta G_F$ (pH) (kJ/mol) 300K
tr-16b Q D R	7.77		
pH 2.5	5.75		2.02
Q5A A D R	7.14	0.63	
pH 2.5	5.85		1.31
D9N Q N R	4.16	3.62	
pH 2.5	4.14		0.02
Q5A,D9N A N R	4.23	3.54	
pH 2.5	4.20		0.03
Q5A,R16Nva A D Nva	2.82	4.95	
pH 2.5	4.21		-1.58
Q5A,D9N,R16Nva A N Nva	4.24	3.54	
pH 2.5	4.23		0.01
R16Nva Q D Nva	3.22	4.56	
pH 2.5	4.26		-1.04
R16Cit Q D Cit	4.16	3.62	
pH 2.5	5.17		-1.01

Table 5.3. Mutational and pH-induced changes in fold stability. The ΔG_U values are based on the Σ CSD measures at the following sites: G11 Hα2, P18 Hα/Hα3 and P19 Hδ2/δ3. ΔΔG(pH) is the effect of ionisation; positive values indicate fold destabilisation.

The free energy change corresponding to the D9N mutation can be attributed to the loss of the salt bridge as well a weakening of the helical H-bonding interaction. There is no pH dependence observed for this mutant (Figure 5.3). For all probes, shown at 280 K and 300 K, the chemical shift deviations are basically identical. As it should, a D9N mutation always possesses $\Delta\Delta G_F(pH) = 0$.

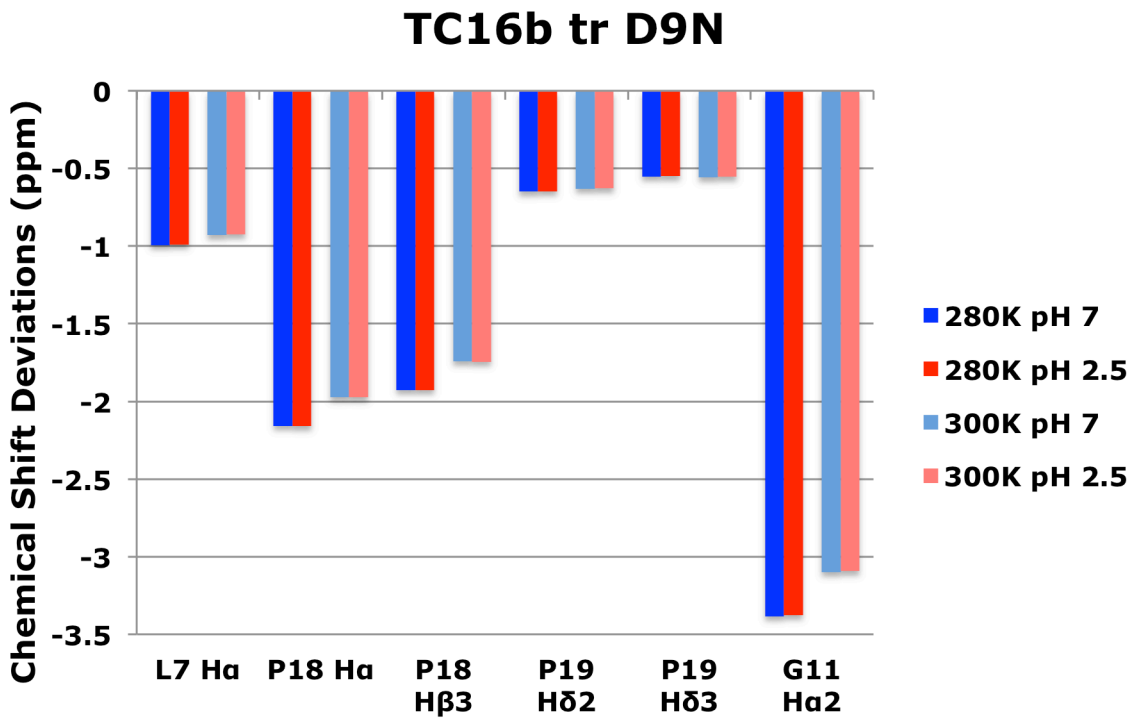

Figure 5.3: Chemical shifts deviations for the key measures of fold populations for the D9N mutant at 280 K and 300 K.

As expected for both the Q5A,R16Nva, R16Nva and R16Cit motifs, there was a significant increase in stability observed at pH 2.5 (Table 5.3). The increase observed for the R16Nva motif is shown in Figure 5.4 in the form of CSDs. The R16Nva mutant destroys the salt bridge completely, while the R16Cit mutant removes the electrostatic interaction associated with the salt bridge; it could still have H-bonding interactions.

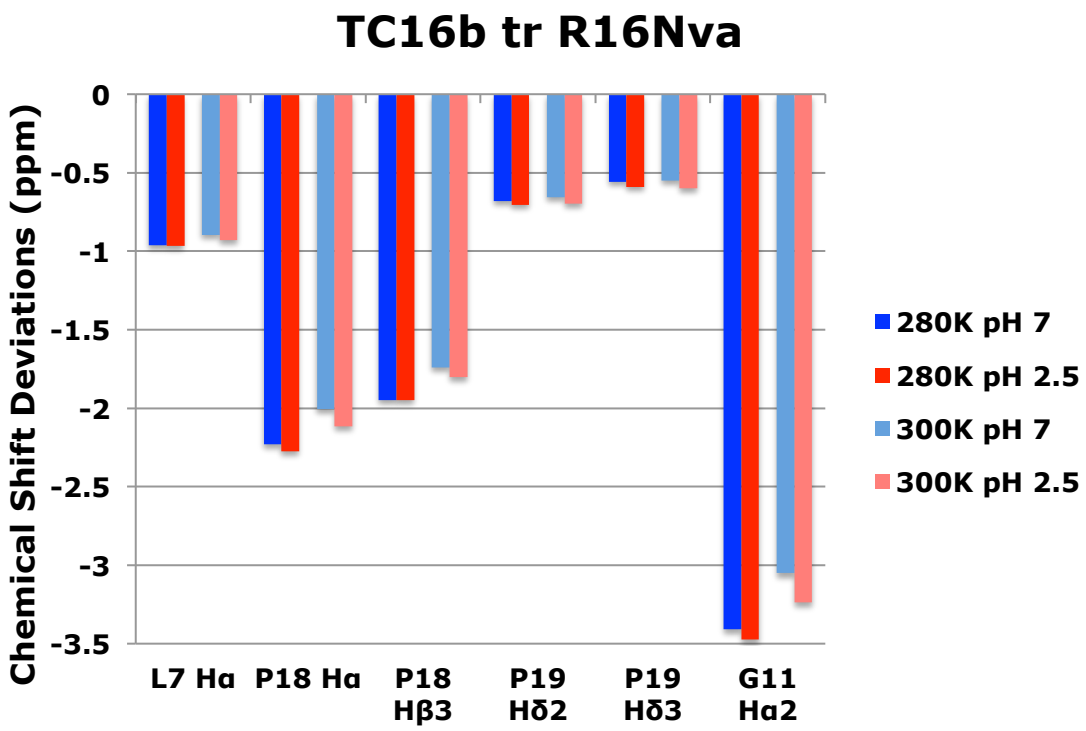

Figure 5.4. Chemical shifts deviations for the key measures of fold populations for the R16Nva mutant at 280 K and 300 K.

As before, the difference in free energy (Table 5.x) between the R16Nva mutant and the parent TC16b tr corresponds to the contribution of the salt bridge, whereas the difference in free energy between pH 7 and 2.5 for the R16Nva mutant corresponds to the contribution of the QXXXD H-bonding interaction.

From Table 5.3, a number of conclusions can be reached. The salt bridge itself is worth close to 3 kJ/mol of fold stability. The effect Asp9 has varies with and without the presence of Q5; when Q5 is present the pH effect is 1 kJ/mol. When Q5 is mutated to alanine, this pH effect is now 1.6 kJ/mol. The difference between these two pH effects corresponds to the QXXXD interaction, this interaction is worth 0.6 kJ/mol in this Trp-cage system. This 0.6 kJ/mol is also observed in a Q5A mutation.

The observed increase in stability at pH 2.5 is, presumably, due almost exclusively to aspartic acid being ionised to its carboxylate base at pH 7. The carboxylate base of aspartic acid at pH 7 interacts with the C-terminal negative charge of the helix macrodipole in an unfavourable manner; thus at pH 2.5 the protonation of the Asp side chain carboxylate has a stabilising effect. The salt bridge has been removed (to some extent) in all three mutations, but the aspartic acid is still present; so the only effect remaining is Asp9's effect on intrinsic helicity. As expected there is now a huge pH change in T_Ms with the aspartic acid being stabilising upon protonation. This justified the original hypothesis: using Asp protonation to improve the N-terminal helix.

5.5 NMR Structure Generation for TC16b tr R16Nva

An NMR structure elucidation was undertaken to establish that the same Trp-cage structure would be formed at pH 2.5, as is observed at pH 7 (Neidigh *et al.*, 2002; Barua *et al.*, 2008; Williams *et al.*, 2011). As the R16Nva mutant is more stable at pH 2.5, being 89% folded at 280K (vide infra), higher precision NOESY data was collected for the calculation of an NMR structure ensemble. Over the accepted structures (31 structures from 40 random starting points) in the ensemble, the pairwise RMSD for residues 3–19 was 0.13 ± 0.05 Å for the backbone atoms and 0.54 ± 0.14 Å for all heavy atoms. The remainder of the statistics are given below (Table 5.4) A representative member of the ensemble appears in Figure 5.5 with the ensemble in Figure 5.6. The complete set of constraints appears in Appendix C.

Type of constraint	Number	r.m.s deviation
Intraresidue	71	0.014 ± 0.007
Sequential	79	0.056 ± 0.12
i/i+n, n = 2-4	42	0.031 ± 0.014
i/i+n, n ≥ 5	58	0.015 ± 0.008
Structure statistics[a.].		
E_{TOTAL} (kcal/mol)		-61.21 ± 2.14
E_{NOE} (kcal/mol)		1.11 ± 0.14
E_{vdW} (kcal/mol)		-72.54 ± 1.92
Bond violations (Å)		2.56 ± 0.12
Angle violations (°)		6.97 ± 0.27
Improper torsion violations (°)		0.69 ± 0.18
Convergence within final ensemble, atomic r.m.s deviations (Å)[b.]:		
Pairwise over the ensemble ((±s.e.)		
Backbone		0.13 ± 0.05
Heavy atom		0.54 ± 0.14

Table 5.4: NMR structure statistics for the TC16b tr R16Nva ensemble (31 accepted structures from 40 starts). [a.] Values are mean ± standard deviation. [b.] All convergence measures are over residues 3-19.

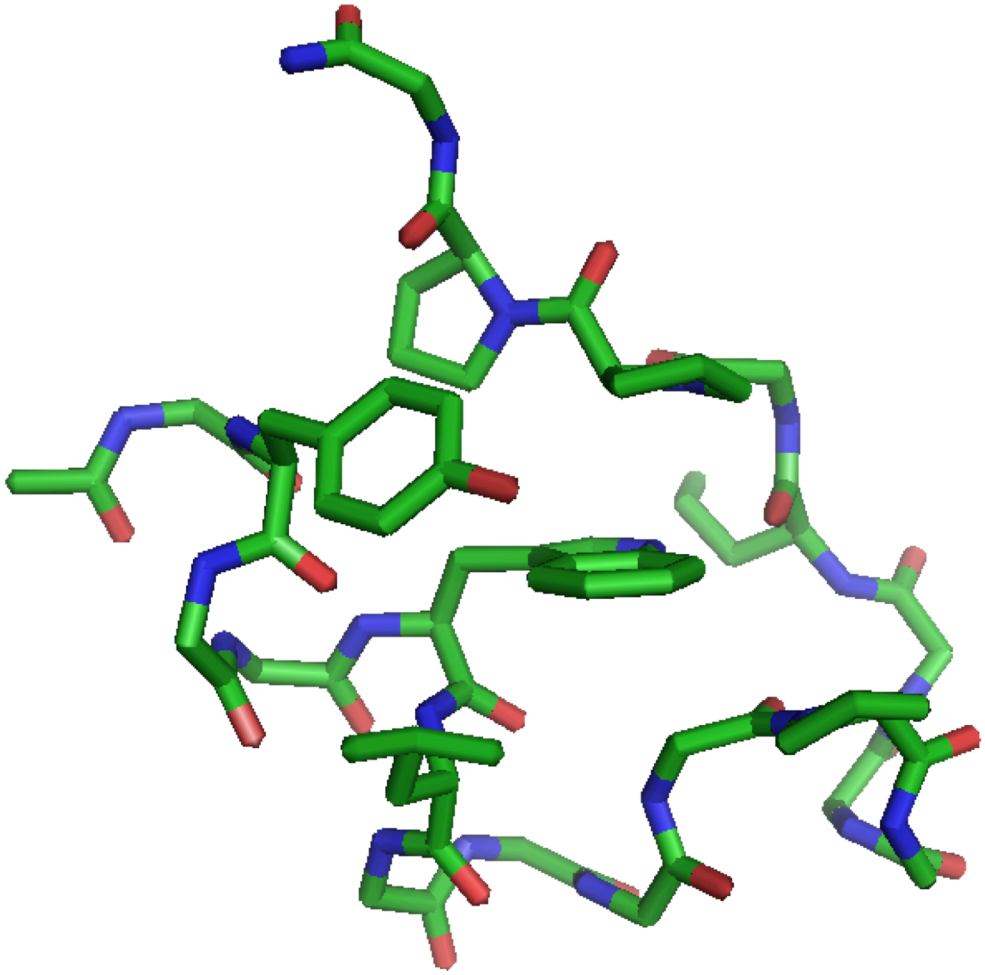

Figure 5.5: Representative structure of TC16b tr R16Nva.

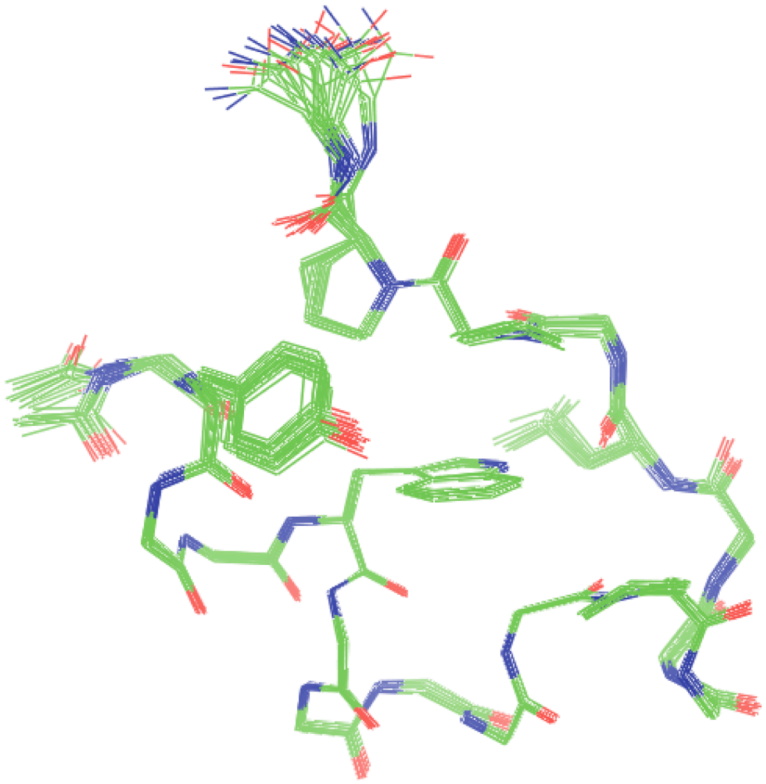

Figure 5.6: NMR ensemble structure of TC16b tr R16Nva generated from 31/40 lowest energy structures.

As evidenced in the overlay (Figure 5.7) of a representative structure of TC16b tr R16Nva with a representative structure of TC16b the pairwise RMSD for residues 3–19 was 0.904 Å for the backbone atoms. This indicates that the same overall structure is being formed. The major deviation between the two structures takes place in the 3_{10} helix region of the structure. The serine 14 sidechain in TC16b tr R16Nva is not placed as high up in the core as in TC16b. This could reflect an H-bonding interaction between the Ser-OH and the ε-NH of the Arg in the unmutated sequence.

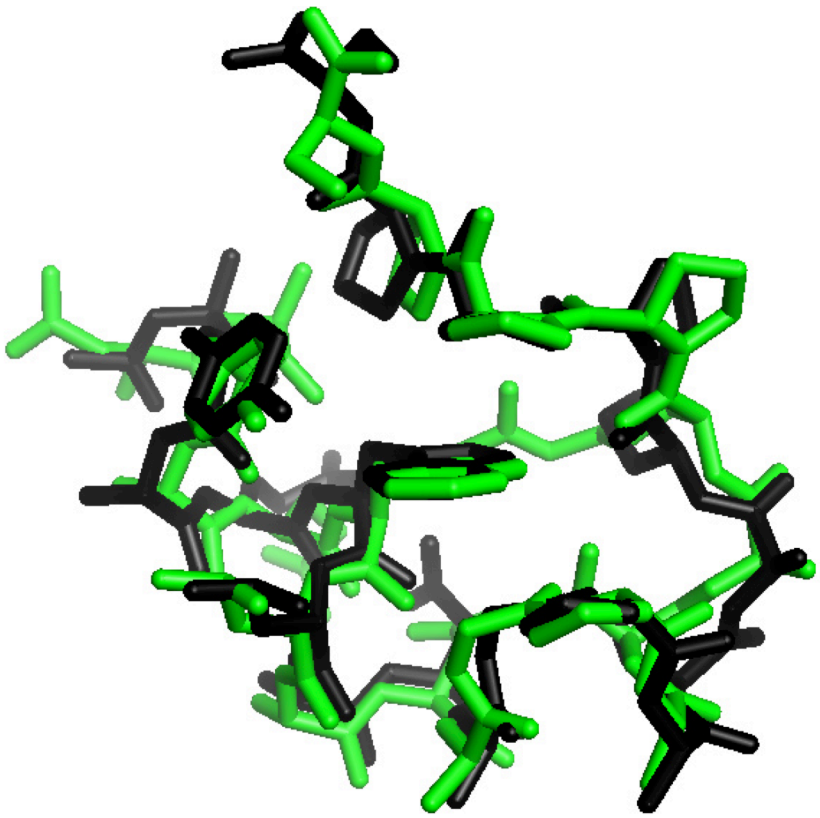

Figure 5.7 Overlay of TC16b tr R16Nva (black) with TC16b (green).

TC16b, along with other Trp-cage structures, places the Arg16 side chain wrapping around the back-side of the Trp indole ring. This provides burial of the Trp residue and cannot be performed to the same extent by the shorter norvaline side chain. Thus, the norvaline mutation would also be expected to have a fold destabilising effect that is unrelated to salt bridge effects.

5.6 Conclusions

A Trp-cage can be successfully designed to be more stable at pH 2.5. This can be achieved through using Asp protonation to improve the N-terminal helix, as aspartic acid at the C-terminal of an α-helix is less destabilising upon protonation. In all cases, the removal of the salt bridge through a mutation at the 16 position, while leaving Asp9 in place, results in a Trp-cage which is more stable at the more acidic pH. An NMR structure ensemble confirms that the Trp-cage structure is retained at pH 2.5, this can be seen clearly in Figure 5.7.

Chapter 6: Kinetic Studies of the Trp-cage

6.1 Introduction

The protein folding problem entails understanding the mechanism by which proteins fold into their native structure and identifying the sequential and structural features of the protein that determine these mechanisms. Studying the kinetics of protein folding can provide a wealth of information regarding protein folding mechanisms. Proteins fold and unfold over a vast range of time frames, from microseconds to minutes. A number of processes, however, related to protein folding, for example the formation of the basic structural elements such as α-helices, β-hairpins and loops, occur in the microsecond or less timescale (Eaton *et al.*, 1997, 1998). These fast-folding secondary structure fragments can provide model systems to test molecular dynamic simulations of folding. Methods used to examine fast-folding proteins include continuous flow methods, temperature-jump (T-jump) methods and the dynamic nuclear magnetic resonance (NMR) method (Eaton *et al.*, 2000; Myers & Oas, 2002; Olsen *et al.*, 2005).

The use of one or more of the above methods resulted in determining the rates of formation of the basic elements of protein structure. The time scales for the formation of secondary structure elements were found to be approximately 0.5 μs for α-helices (Werner *et al.*, 2002) and 1-10 μs for β-hairpins (Muñoz *et al.*, 1997; Ferguson & Fersht, 2003; Kubelka *et al.*, 2004). The 20-residue Trp-cage miniprotein (TC5b) is amongst the fastest folding proteins with a folding time ($1/k_F$) of approximately 4 μs

(Qiu *et al.*, 2002; Culik *et al.*, 2011). Other fast folding proteins are the 35-residue villin subdomain with a fold lifetime of 4-10 μs (Wang *et al.*, 2003; Kubelka *et al.*, 2004), and the 23-residue miniprotein BBA5 (7.5 μs) (Kubelka *et al.*, 2004). Some examples of proteins where the NMR lineshape analysis method was used to determine the folding kinetics are, the 79-residue λ-repressor (20 μs) (Huang & Oas, 1995; Yang & Gruebele, 2003), the 56-residue N-terminal domain of the ribosomal protein L9 (50 ms) (Kuhlman *et al.*, 1998), the 36-residue villin headpiece subdomain, HP36 (10 μs) (Wang *et al.*, 2003), the 58-residue B-domain of staphylococcal protein A (3-10 μs) (Myers & Oas, 2001; Arora *et al.*, 2004), and the peripheral subunit-binding domain (43 μs) (Spector & Raleigh, 1999).

This chapter will describe the folding kinetic studies performed on Trp-cage mutants using the dynamic NMR method of rate determination.

6.2 Dynamic Nuclear Magnetic Resonance

The lineshapes of nuclear magnetic resonance (NMR) spectra can provide kinetic information for motions on the timescales of NMR methods. For a protein undergoing two-state transition, if the resonance frequency differences for the folded and unfolded state resonances are large compared to the folding and unfolding rates, two peaks are observed. The ratio of the integrals of these peaks is determined by the ratio of the folded and unfolded population in the sample. At the other extreme, when the difference between the resonance frequency between the folded and unfolded state is small compared to the folding and unfolding rates, the peaks are averaged and only a single sharp resonance is observed. The frequency of this resonance is determined by the

relative populations of folded and unfolded states. The lineshape of the resonance frequencies are determined by the rate of exchange between the two populations. Hence, if the folded and unfolded state frequencies are known, the lineshape can provide an accurate estimate of the rate constants of folding and unfolding. This method is generally useful in determining folding rates in the 1 μs – 1 ms time scale where there is a significant population of both folded and unfolded states under the conditions examined.

6.3 NMR Lineshape Analysis

The two-state folding equilibrium can be described using the following simple kinetic model:

$$F \underset{k_F}{\overset{k_U}{\rightleftharpoons}} U$$

where U and F represent the unfolded and folded states, respectively, and k_F and k_U are the rate constants for folding and unfolding, respectively. In the case of Trp-cages, this is a fast exchange process, where the rates of folding and unfolding are faster than the difference in resonance frequencies between the folded and unfolded state NMR signals. This fast exchange results in averaging of the resonance peaks, this is reflected in the population-weighted averaging of the chemical shifts observed for the Trp-cages.

Proton resonances that have large chemical shift differences between the folded and unfolded states undergo additional broadening of the line widths of their NMR peaks, this is known as ‘exchange broadening’. These exchange-broadened line widths

can provide information about the exchange rates (k_F and k_U) associated with the folding-unfolding equilibrium.

According to the Heisenberg uncertainty principle, to observe folded and unfolded signals in an NMR spectrum, the lifetime of each nucleus τ in each of the two states must be no longer than:

$$\tau \geq \frac{1}{2\pi\,\delta\nu}$$

where $\delta\upsilon$ is the frequency difference ($\nu_F - \nu_U$). The rate constants of chemical exchange determine τ of each species. Figure 6.1 shows the lineshape effects in three exchange systems. When the exchange rate becomes faster than the coalescence rate, the single peak observed as the population-weighted average chemical shift and the resonance gets sharper as k_{ex} increases. This is the exchange timescale for peptide folding motifs and some small proteins.

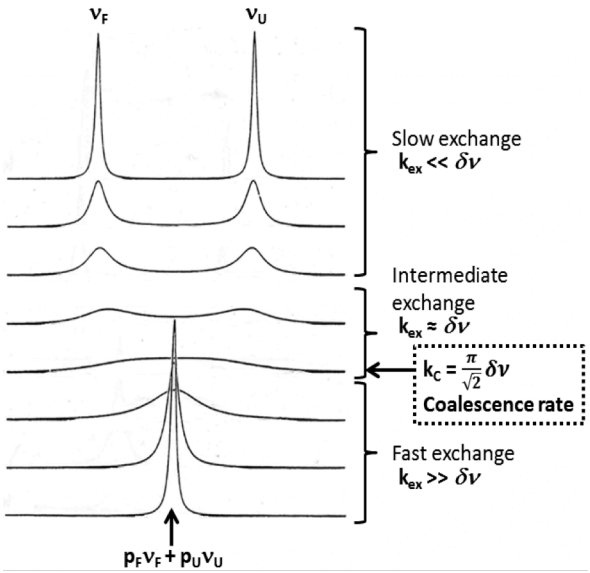

Figure 6.1. The lineshape effects in three exchange regimes, k_{ex} values relative to δν: slow exchange ($k_{ex} << \delta\nu$), intermediate exchange ($k_{ex} \approx \delta\nu$) and fast exchange ($k_{ex} >> \delta\nu$). Figure taken from Dr. Irene Shu's thesis (Shu, 2011).

The equation (6.1) for the lineshape g (ν) of a resonance signal is (Gunther, 1992):

$$g(\nu) = [(1 + \tau\pi\Delta)P + QR]/ (4\pi^2P^2 + R)$$

where $P = (0.25\Delta^2 - \nu^2 + 0.25\ \delta\nu^2)\tau + \Delta/ 4\pi$

$Q = [-\nu - 0.5\ (\chi_F - \chi_U)\ \delta\nu]\tau$

$R = 0.5\ (\chi_F - \chi_U)\ \delta\nu - \nu\ (1 + 2\pi\tau\Delta)$

The symbols in the above equation have the following meanings:

$\tau = \tau_F\tau_U/(\tau_F + \tau_U)$, where τ_F and τ_U are the average life times of the nuclei in the folded and unfolded states.

χ_F, χ_U are the populations of the folded and unfolded states.

$\delta\nu = \nu_F - \nu_U$, where ν_F and ν_U are the resonance frequencies of the nuclei in the folded and unfolded states (Hz).

Δ is the width at half-height (Hz) of the signal in the absence of exchange ($\tau \rightarrow \infty$) in which case Δ_F would be set equal to Δ_U for simplicity.

ν is a variable frequency (Hz).

This complex equation (6.1) has been simplified to give approximate rate constant values. The equation (6.2) derived for fast-exchange processes is (Sandstrom, 1982; Gunther, 1992):

$$k_U = 4\pi \chi_F(\chi_U)^2\delta\nu^2 / \Delta_{ex}$$

where k_U is the rate constant for unfolding and Δ_{ex} is the exchange broadening in Hz.

The exchange broadening can be obtained (Equation 6.3) from the observed line width, Δ_{obs}, by subtracting the intrinsic line width, Δ_o, and the broadening due to inhomogeneity, Δ_I:

$$\Delta_{ex} = \Delta_{obs} - \Delta_o - \Delta_I$$

This method can be applied to proton resonances that display large ring current shifts due to their orientation around aromatic rings, and their chemical shift melting curves provide an accurate measure of δ_F. Thus $\delta\nu$ is known and the chemical shifts observed at each temperature can provide χ_U. A reference signal with the same spin multiplicity (and coupling constant) that shows little or no structuring shift can be used to provide a measure of $(\Delta_o + \Delta_I)$. As this reference signal is from the same peptide, its line width will include the same state population averaging and magnetic inhomogeneity as the observed signal. Therefore, the exchange-broadening component can be acquired from equation 6.3 as:

$$\Delta_{ex} = \Delta_{obs} - \Delta_{ref}$$

The assumption used here is that the reference signal has no exchange-broadening component in its line width.

The Δ_{ex} values were based on line shape differences between the reference peak and the broaden peak, each expressed in terms of a broadening parameter Δ_{total}. These were calculated from three different doublet line features: half-height line width, %-dip of the doublet peak with respect to the total height of the peak and the ratio of the heights of the broadened and reference peaks.

6.4 Trp-cage Dynamics

The fast folding of the Trp-cage (5b, in this case) was noted in the very first report on the fold (Andersen *et al.*, 2000), given as $1/k_F = 7 \pm 2$ μs. Measures were G11α line width and IR monitored T-jump. The upper temperature was 40 °C for the latter and the measurement used the exponential decrease in the 'solvated' helical amide I' band (1628 cm^{-1}).

With the 2002 publication of the details regarding the characterization of TC5b (Neidigh *et al.*, 2002) the system attracted the attention of other biophysicists. Due to the extreme quenching of Trp fluorescence associated with the folded state (McMillan *et al.*, 2013), fluorescence-monitored T-jump experiments were another possibility. Hagen (Qiu *et al.*, 2002) reported $1/k_F = 4.1$ μs at 23.5 °C. Data presented in the Hagen paper indicates that $1/k_F = 3.56$ μs at 300 K. In 2011, the Gai lab (Culik *et al.*, 2011), reported essentially the same value in T-jump experiments monitoring the helical amide band (1630cm^{-1}), $1/k_F = 3.7$ μs at 25 °C.

The original hallmark for folding dynamics in the Andersen lab, the broadening of the far upfield G11α signal, which in some analogues leads to the disappearance of this signal as the unfolded population increases on warming, was employed for additional dynamics measures by B. Barua (Barua, 2005). The quantitative use of this probe has a number of problems, the signal is a doublet of doublets or doublets in H_2O, and the coupling constants likely change as the cage unfolds. In addition, the 'unfolded' reference shift value cannot be equated with the random coil shift for Gly-α due to half-cage contributions in the 'unfolded' state. To allow for the observations of both the extremely shifted and less shifted Gly-Hα throughout a melt in ^{13}C-edited 1D spectra, a series of ^{13}Cα-Gly-11 labelled peptides were prepared: ***X***-YAQWLKDG-G*-PSSGRPPPS (***X*** = DA-, GA-, and N-) were prepared, CD T_M = 56, 39, and 35 °C, respectively. The ***X*** = DA species is TC10b. With the expectation 'unfolded state' shifts modelled as the temperature dependent shifts for the Gly-CH_2 of NAUYUQWLKDG-Gly-PSSGRPAA which does not form the complete cage structure (it lacks the terminal hydrophobic staple), the folding rate of TC10b from line broadening was $1/k_F$ = 1.5 μs at 298K. The Hagen lab performed a fluorescence-monitored T-jump experiment on unlabelled TC10b. The results are compared in figure 6.2 (Barua, 2005). Our best estimate for $1/k_F$ at 298K is 1.4 μs from this comparison.

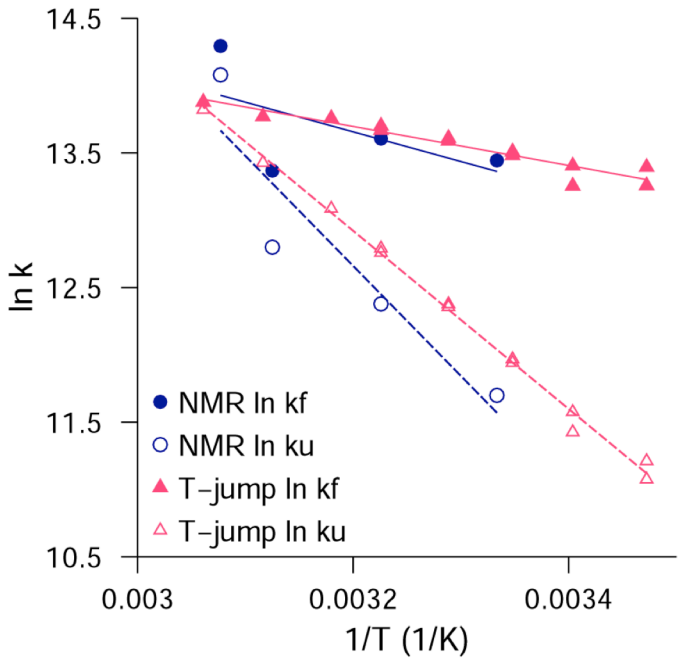

Figure 6.2. Comparison of the rates obtained from NMR lineshape analysis and fluorescence-detected T-jump experiments for TC10b.

Culik et al. (Culik *et al.*, 2011) have also reported dynamics data for TC10b. They employed the DA*YA*QWLADGGPSSGRPPPS sequence with A* = ^{13}C=O-labelled Ala and observed peaks at 1586, 1615, and 1646 (all with decreasing absorbance on warming) and 1664/72 cm^{-1} (increasing absorbance on warming) in the temperature difference FT-IR spectrum. There was a distinct maximum at 1630 cm^{-1} separating the 1615 and 1646 minima. These were attributed to: 1586 (the Asp-CO_2^- signal in the salt bridge), 1615 (helical A*), 1646 (a shifted unlabeled helical amide band, shifted due to overlapping non-helical A*), and 1664 cm^{-1} (3_{10} helical signal and increasing random coil signal). However, the effect of ^{13}C=O labeling is expected to be a 36 cm^{-1} shift, and has been measured (Werner *et al.*, 2002) at 39 cm^{-1} in model helices. Thus we would attribute the 1630 cm^{-1} maximum to random coil A* and would expect

the negative peak at 1586 to contain a significant component of helical-A* melting. Gai and co-workers monitored relaxation after the T-jumps at 1580, 1612, and 1664 cm^{-1}. At 1664 cm^{-1} the data was bi-exponential, τ = 300 ns (attributed to local unfolding of the 3_{10} helix) and τ = 2.5 μs (growth of random coil $^{13}C{=}O$) at 292 K. The slow phase was attributed to global unfolding and gave the same time constants observed as when monitoring at 1580 or 1612 cm^{-1}: $1/k_F$ = 1.6 μs at 25 °C.

Of interest in the present discussion, the Feng Gai group has also measured the effects of a number of mutations upon folding dynamics: a G10**a** mutation in TC5b (ΔTm = +21 °C) increased the folding rate by a factor of 2 (Culik *et al.*, 2013); in the case of TC10b R16K and P19A, the latter a particularly destabilizing mutation (ΔTm = -44 °C), mutations did not alter the folding rate appreciably (Culik *et al.*, 2011). As a result, Feng Gai and coworkers have proposed that hydrophobic staple and salt bridge formation occur on the downhill side of the folding transition and only stabilize the final state; that helix formation is rate determining and sets the stage for downhill folding events thereafter. However, throughout the dynamics probes have been the disappearance of helical amide I' bands, either monitored directly or as the appearance of random coil amide absorbance.

My studies focus on TC16b and other more stable constructs, allowing for the examination of some strongly destabilising mutations. The TC16b system, however, with D-Ala's replacing G10 and G15 is too stable for NMR lineshape analysis below 325 K. Based on Gai's results (Culik *et al.*, 2013), a 2x increase for a G10**a** mutation and a somewhat muted 1.3x increase for G15**a** (this mutation is known to be less stabilising that G10a) would put the rate for TC16b at 0.5 – 0.7 μs at 25 °C.

Dr. Barua also initiated studies using a probe that should reflect only the final formation of the complete cage structure. A P18A mutation, although somewhat destabilizing (ΔTm = - 9 °C, for TC10b), still allows formation of the full cage structure with the Ala18 Hα and Hβ now appearing far upfield; any less-folded state would show random coil values for these sites. The Hβ signal appears as a first-order doublet in the 0.2 – 0.8 ppm span where there are no generally confusing overlapping peaks: an ideal situation for applying the linewidth difference methods developed by Olsen et al. (Olsen *et al.*, 2005). The [P18A]-TC10b species was also examined by fluorescence-monitored T-jumps (Hagen and co-workers, unpublished). The results are compared in figure 6.3.

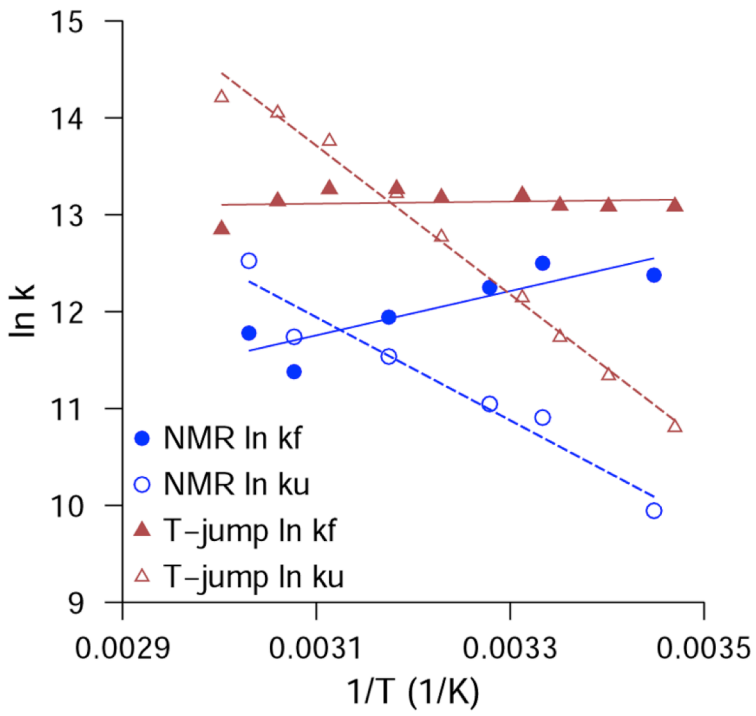

Figure 6.3. Comparison of the rates obtained from NMR lineshape analysis and fluorescence-detected T-jump experiments for TC10b P18A.

The P18A mutation significantly reduces the slope of the folding Arrhenius plot. In the case of the NMR dynamics data based on A18β linewidths, with other methyl

doublets providing the measure of intrinsic broadening for the system, a positive Arrhenius slope, faster folding upon cooling is evident. The 2 to 3-fold slower folding and unfolding rates obtained from the NMR relaxation method were not fully rationalized. One possible rationale is that partially folded states, in which complete cage formation has not developed, are both fully helical and place the Trp indole in an environment which quenches the fluorescence. The prior dynamics measures may not be probes of complete cage formation.

Vicki Williams continued the work on dynamics employing the P18A probe. A repeat for [P18A]-TC10b yielded the same positive slopes with $1/k_F$ = 3 μs at 300 K. [P18A]-TC16b gave data for pH 2.5, again a positive slope with $1/k_F$ = 1.2 μs at 310 K. Data at pH 7, could only be analyzed at higher temperatures and suggested a point lying nearly on the same line, $1/k_F$ = 2 μs at 325 K. The [R16Nva,P18A] analogue gave excellent data with the expected curved Arrhenius plot for ln k_F. The maximum rate, $1/k_F$ = 0.95 ± 0.10 μs, was observed between 290 – 305K. This data appeared to imply that salt bridge formation was not important for folding rate acceleration.

In contrast, the Arrhenius plots for Trp-cage folding in the literature to this point indicated faster folding on warming. The slopes for folding were always less than for unfolding but positive Ea (folding) values were observed throughout. Bunagan et al. (2006) reported dynamics data for [P12W]-TC5b, T_M = 57 °C, which were considerably more protein-like. A curved plot for log k_F versus 1/T with an increasingly negative Ea as the melting temperature was approached. Positive Arrhenius slopes for folding usually indicate a compact transition state with hydrophobic surface burial. This mutation also provided a notable acceleration of folding, $1/k_F$ = ~1 μs at 300K.

6.5 P18A Mutants

In this account, the A18 Hβ resonance was used for lineshape analysis of the P18A mutants with the other alanine Hβs in the sequence acting as the reference peak. Where possible multiple alanine Hβs were used and averaged to provide reference numbers. The values of χ_F and χ_U were calculated using the CSDs for A18 Hβ: $\chi_F = CSD_{obs} / CSD_{100\%\text{-folded}}$, where $CSD_{obs} = \delta_{obs} - \delta_{rc}$. The random coil chemical shift used (δ_{rc}) was 1.37 ppm and $CSD_{100\%\text{-folded}}$ was calculated by assuming the CSD at 280 K for TC16b P18A to be 99.4%-folded. δν was calculated from the $CSD_{100\%\text{-folded}}$ values and took into account ring current changes with temperature.

The Δ_{ex} values were based on line shape differences between the reference peak and the broadened probe peak, each expressed in terms of a broadening parameter Δ_{total}. These values were calculated from three different doublet line features: half-height line width, %-dip of the doublet peak in relation to the total height of the peak and the ratio of the heights of the broadened and reference peaks.

The kinetic studies of four Trp-cages each containing a P18A mutant (Table 6.1) were carried out by the dynamic NMR method using lineshape analysis. The rates of folding and unfolding and their Arrhenius plots were calculated for these Trp-cages.

TC16b A8G P18A	DAYAQWL**G**DaGPASaRP**A**PS
TC16b S14A P18A	DAYAQWLADaGPA**A**aRP**A**PS
TC16b P12W S14A P18A	DAYAQWLADaG**W**A**A**aRP**A**PS
TC13b P12W P18A	DAYAQWLADGG**W**ASGRP**A**PS

Table 6.1. Trp-cage sequences used for NMR lineshape analysis.

6.6 TC16b A8G P18A

As stated earlier, TC16b P18A was examined by Vicki Williams. Data at pH 7 could only be analysed at higher temperatures and suggested $1/k_F$ = 2 μs at 325 K. Data at pH 2.5 gave a positive slope with $1/k_F$ = 1.2 μs at 310 K.

The TC16b A8G mutant was discussed earlier in section 4.3. The insertion of a glycine into the α-helix is known to lead to an intrinsic destabilisation of the helix. This mutation causes the Trp-cage to fold slower than normal, folding in 6.7 ± 1.6 μs at 300 K (Table 6.2). For this P18A mutant, a negative slope is observed for the folding rates at both pH 7 and pH 2.5.

	χ_F 300 K	ln k_F 300 K	ln k_U 300 K	$1/k_F$ 300 K (μs)	$1/k_U$ 300 K (μs)
pH 7	0.933	11.9 ± 0.3	9.3 ± 0.3	6.7 ± 1.6	92.4 ± 22.5
pH 2.5	0.828	11.8 ± 0.3	10.2 ± 0.3	7.9 ± 2.3	37.8 ± 11.3

Table 6.2. Rate constants for TC16b A8G P18A in pH 7 and pH 2.5 buffer.

An interesting point to note with this mutation is the almost identical Arrhenius plot of the folding rates (Figure 6.4) for the two different pHs. While the change in pH from 7 to 2.5 has an effect on fold stability (Table 6.2), the pH change has no effect on the folding rate. The change in pH essentially just removes the salt bridge at the lower pH. So since the folding rate does not change, it indicates that the salt bridge is late forming; it forms post transition state.

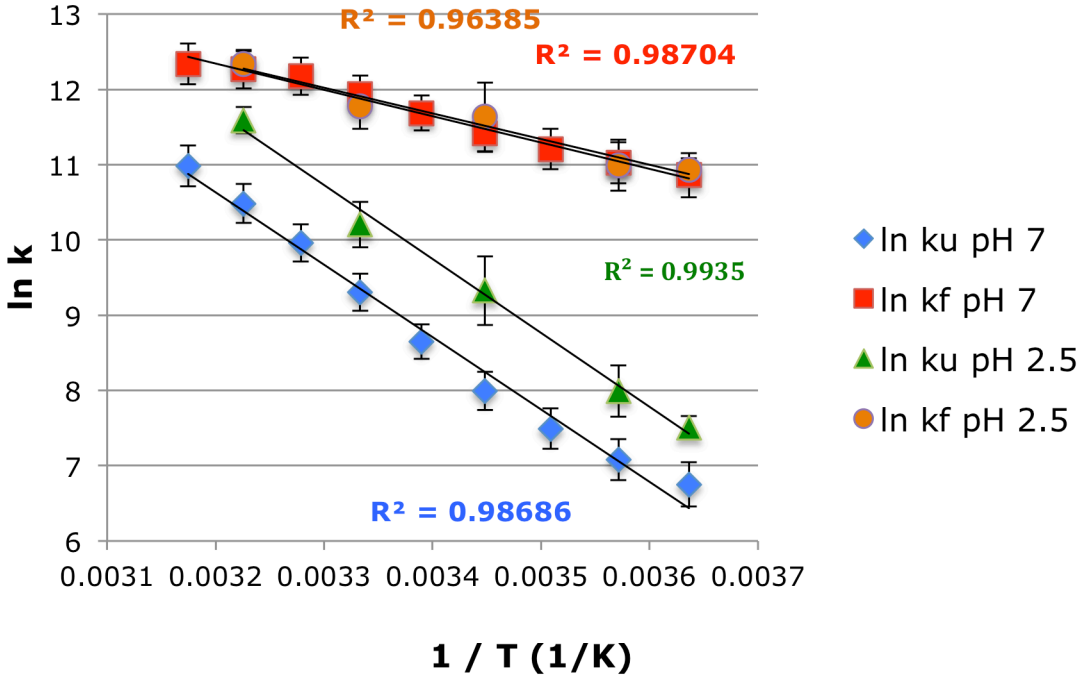

Figure 6.4. Folding and unfolding rates at pH 7 and pH 2.5 for TC16b A8G P18A.

6.7 TC16b S14A P18A

A S14A mutation removes the buried H-bond, the H-bonding network associated with the hydroxyl group of S14 in the complete Trp-cage fold (Scian *et al.*, 2012) is not just a requirement for burial but also enhances fold stabilisation. An S14A mutation is known to be destabilising in less folded systems. While fraction folds make

it appear that this mutation is not as fold destabilising in the TC16b construct as in less stable Trp-cage series (Table 6.3), χ_F = 0.886 at 300 K versus 0.444 for the TC10b S14A motif, upon converting the fraction folds to ΔΔG's the mutation is comparably destabilising in both parent constructs.

The folding rates for pH 7for the S14A mutant show that it is a very fast folder; much faster than expected (Table 6.3). There is only pH 7 lineshape data for this mutant, the probe Hβ resonance for pH 2.5 was overlapped with other proton signals in the temperature range from 275 K – 330 K.

	χ_F 300 K	ln k_F 300 K	ln k_U 300 K	$1/k_F$ 300 K (μs)	$1/k_U$ 300 K (μs)
pH 7	0.886	13.2 ± 0.2	11.1 ± 0.2	1.9 ± 0.3	15.0 ± 2.6

Table 6.3. Rate constants for TC16b S14A P18A in pH 7 buffer.

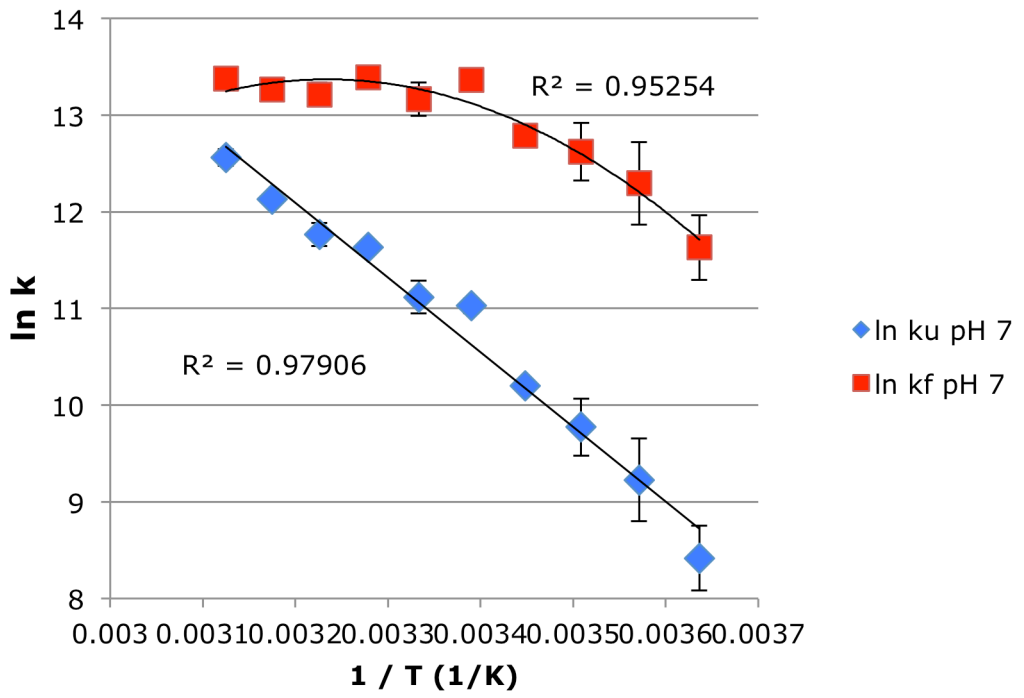

Figure 6.5. Folding and unfolding rates at pH 7 for TC16b S14A P18A. A second-order polynomial was used to fit the ln k_F data points.

It would appear that neither Ser14 hydroxyl burial nor 3_{10}-helix formation are complete at the transition state for folding. The mutation of an alanine into the 3_{10}-helix in place of the serine leads to a more stable helix. The helical propensity of alanine means that in isolation this 3_{10}-helix would be more stable than one containing serine. If this initial 3_{10}-helix is more stable, then it would be formed more often. As a 3_{10}-helix is shorter in length that random coil segment, this 3_{10}-helix would make it easier for the hydrophobic staple between Tyr3 and Pro19 to be formed. The fast rate of folding also indicates that the serine is not buried by the transition.

6.8 TC16b P12W S14A P18A

A TC16b P12W P18A mutant was initially synthesised and characterised by Vicki Williams, T_M = 97 °C. However, this proved to be too stable for NMR lineshape analysis; there was no discernable line broadening prior to 330 K. In an attempt to obtain rates data for a P12W mutant in the TC16b series, an S14A mutantion was introduced to this construct. As is shown in Table 6.4, the unfavourable S14A mutant has a greater effect on fold populations when combined with P12W. While the Trp/Trp pair provides stability, it may lack the enforced rigidity at the position provided by the proline. This in combination with the S14A mutation would give rise to a less stable 3_{10}-helix.

	χ_F 300 K	ln k_F 300 K	ln k_U 300 K	$1/k_F$ 300 K (μs)	$1/k_U$ 300 K (μs)
S14A, P18A	0.886	13.2 ± 0.2	11.1 ± 0.2	1.9 ± 0.3	15.0 ± 2.6
pH 7	0.724	13.3 ± 0.3	12.4 ± 0.3	1.7 ± 0.5	4.3 ± 1.3

Table 6.4. Rate constants for TC16b P12W S14A P18A in pH 7 buffer.

The insertion of P12W into TC16b S14A P18A led to an increase in the folding rate (Table 6.4). A P12W mutant in the TC5b series has been shown to fold at 1μs at room temperature (Bunagan *et al.*, 2006), so observing an increase in the folding rate when P12W is added to a TC16b construct would be expected. The unfolding rate is also faster than its TC16b S14A P18A counterpart; it unfolds 3.5 times faster indicating it has lower fold stability.

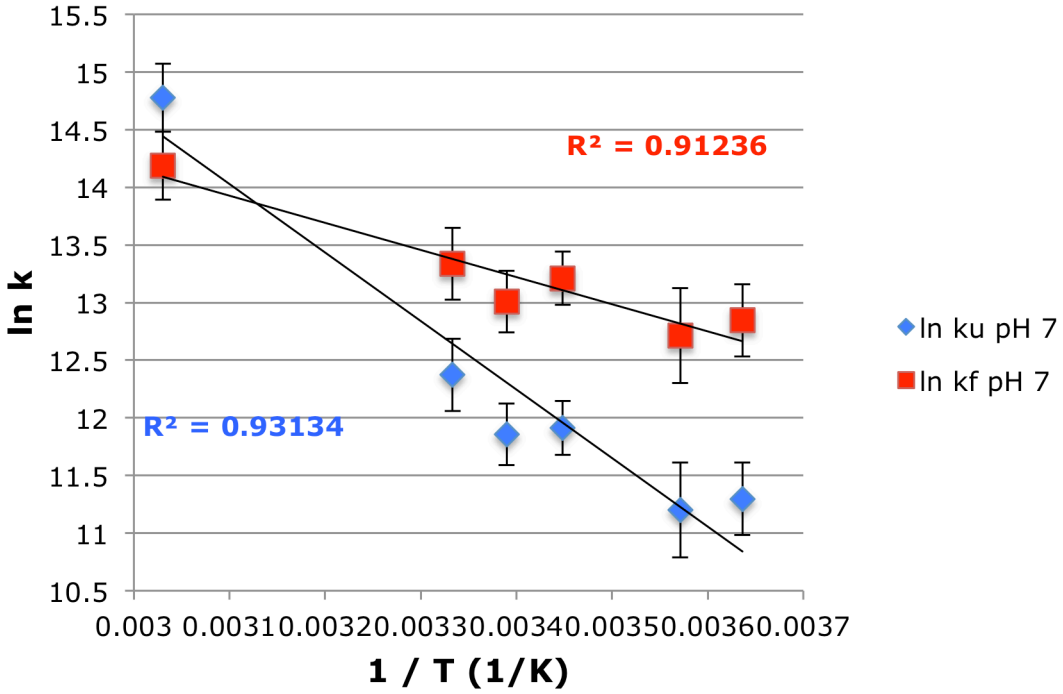

Figure 6.6. Folding and unfolding rates at pH 7 for TC16b P12W S14A P18A.

6.9 TC13b P12W P18A

As the TC16b construct is too stable to obtain folding rates of a P12W P18A mutant, the use of a less stable parent motif may allow for this. The TC13b series was chosen for this. Yet again, the P12W mutant creates a very stable structure. Even though data was collected from 275 K to 315 K at pH 7, the lowest temperatures are unusable due to no apparent line broadening. As a result, only data from 290 K onwards can be used.

The folding rate for this mutant at both pH 7 and pH 2.5 is very fast, ~ 1.5 μs at 300 K (Table 6.5). The unfolding rates, however, are different; pH 2.5 unfolds faster than pH 7. This is due to the salt bridge not being in place at the lower pH, pH 2.5 does not have this unfavourable transition that has to be broken.

	χ_F 300 K	ln k_F 300 K	ln k_U 300 K	$1/k_F$ 300 K (μs)	$1/k_U$ 300 K (μs)
pH 7	0.889	13.6 ± 0.6	11.5 ± 0.6	1.4 ± 0.8	11.1 ± 6.4
pH 2.5	0.70	13.3 ± 0.4	12.4 ± 0.4	1.8 ± 0.7	4.2 ± 1.6

Table 6.5. Rate constants for TC13b P12W P18A in pH 7 and pH 2.5 buffer.

As with other constructs for which I have pH 2.5 data, yet again upon the pH effect is only observed in the k_U data. This is strong evidence for the salt bridge being form post transition state.

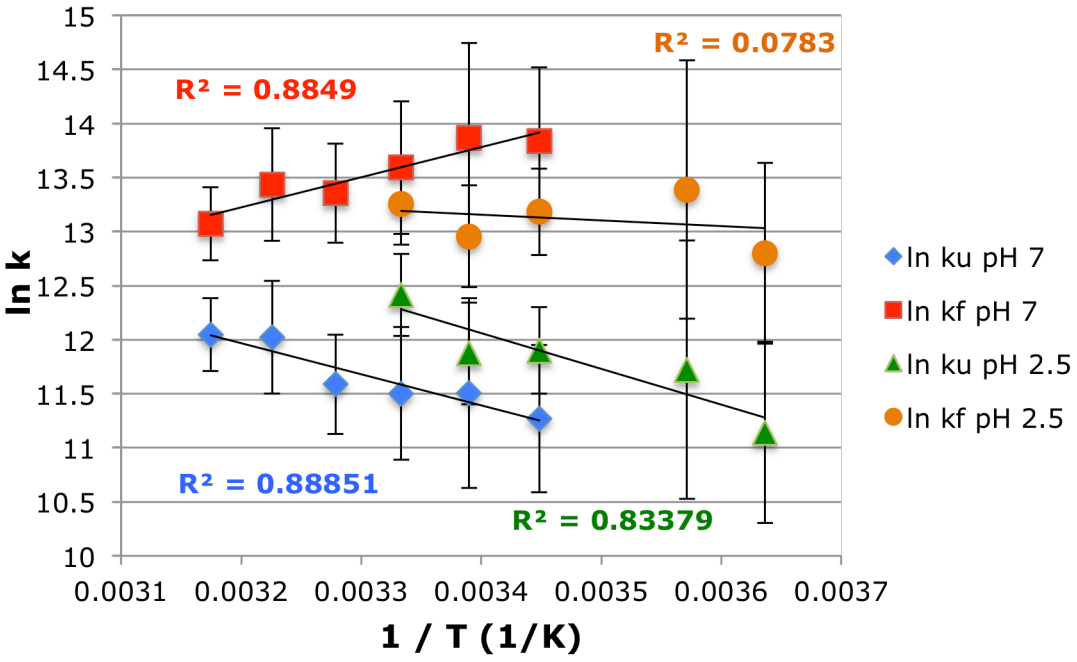

Figure 6.7. Folding and unfolding rates at pH 7 and pH 2.5 for TC13b P12W P18A.

The positive slope seen for the folding rate at pH 7 is indicative a more protein-like fold.

6.10 Conclusions

The lineshape analysis of these four Trp-cages provides some interesting data, as well as valuable information. The, in general, slightly slower folding rates observed from this method in relation to other published data (Bunagan *et al.*, 2006; Culik *et al.*, 2011) can be attributed to the use of P18A as a probe of full cage formation rather than helix measures.

From the data presented here, both the formation of the salt bridge and the burial of the serine 14 hydroxyl happen post transition state. The change in pH only having an effect on the k_U is strong evidence for the formation of the salt bridge occurring after the transition state. The burial of the serine 14 hydroxyl is in conjunction with the formation of the 3_{10}-helix; burial will not take place with the helix being formed. The fast folding rate for an S14A mutation indicates that helix does form until after the transition state.

The insertion of a P12W mutation results in a fast folding rate whether it is a fold stabilising mutation (as is the usual observation) or fold destabilising (in an S14A, P18A- mutant).

Chapter 7: Circular Permutation of the Trp-cage

7.1 Introduction

Circular permutation of protein structures is defined as the linking of N- and C-termini by an amide bond or a short peptide linker and cutting elsewhere in the sequence. Both natural and designed examples of circular permutation are common for larger proteins, there appear to be no examples of smaller (<50 residue) protein folds per the CPDB database (Lo *et al.*, 2009). There are examples of protein cyclisations in the 30 – 40 residue size range (Camarero *et al.*, 1998, 2001; Zhou, 2003a), but these do not appear to have been circularly permutated (*i.e.* there is no new N- and C-termini). Protein cyclisation has often been cited as a protein stabilisation strategy (Iwai & Plückthun, 1999; Trabi & Craik, 2002), but there are several cases in which circularised proteins do not gain significant fold stability. Circular permutation can serve to separate topology from sequence and provide new understanding into what drives protein folding pathways. Decoupling structure and folding pathways is extremely useful in studying contact order effects. The circular permutation of smaller domains should be particularly useful, as more synthesis options and experimental techniques are available in comparison to larger protein domains. This includes the simple incorporation of labelled residues and non-natural amino acids. The Trp-cage appears to be the smallest fully protein-like fold and accordingly a suitable test system for the effects of cyclisation and circular permutation at the extreme lower limit of fold size.

Like many other small proteins (Thornton & Sibanda, 1983; Iwai & Plückthun, 1999; Camarero *et al.*, 2001; Kier & Andersen, 2008), the N- and C- termini of the Trp-

cage are in close spatial proximity. As a result, cyclisation was proposed as an alternative fold stabilisation strategy and from this utilising circular permutation as a probe of the key interactions that are responsible for the significant fold stability and rapid folding of this system.

The cyclisation of the Trp-cage was recently reported (Scian *et al.*, 2012). This new construct linked the N- and C-termini together using a Gly-Gly linker (GDAYAQWLADGGPSSGRPPPSG), resulting in the creation of a hyperstable Trpcage, with a T_m = 95 °C. High resolution structural information was obtained from X-ray diffraction crystal structures. The structures were fundamentally identical to the solution-state NMR structure and were also within a 0.45 Å backbone RMSD over residues 3 – 19 of prior NMR structures for acyclic Trp-cage species. The success of the cyclo Trp-cage (cyclo-TC1) led to the hypothesis that it should be possible to create a circular permutation of the Trp-cage with a 2-residue linker.

The first decision that had to be made was where to cut the sequence; therefore creating new termini. There are really only two options; you can either cut between the α-helix and the 3_{10} or between the 3_{10} helix and the polyPro unit. But it's been shown through previous work in the Andersen lab that mutating the glycine at position 10 to D-Ala is stabilising, more so than mutating G15 to D-Ala (Williams *et al.*, 2008). So the decision was made to cut at and excise G15. This cut site has an added advantage in that it allows for potential interaction between the cationic N-terminus and/or the sidechain of R1 with the negatively charged carboxylate of the C-terminus.

7.2 Why Explore Circular Permutation?

Circular permutation causes a dramatic shift in the contact order of the key interactions that stabilise the Trp-cage. Some of the long-range key interactions for the Trp-cage are shown in Figure 7.1.

Figure 7.1. Illustrating changes in contact order between the native Trp-cage and a circularly permutated construct.

A potential benefit for rapid folding results; the formation of the Tyr^{3}/Pro^{19} interaction which serves as a hydrophobic staple providing in excess of 13 kJ/mol of fold stabilisation (Barua et al. 2008). This would present a smaller entropic penalty to folding in the circular permutant. Based on this, Dr. Brandon Kier synthesised the first circular permutant of the Trp-cage, RPPPSGGDAYAQWLADGGPSS, using the Gly-Gly linker. A significant decrease was expected in fold stability as the Arg/Asp salt bridge (Williams *et al.*, 2011) would now include the more mobile sidechain of an N-terminal residue. It was also anticipated the 3_{10} helix (GPSS) might be less well formed due to C-terminal fraying. With the chemical shifts of the cyclo Trp-cage serving as the 100%-folded reference values, all the diagnostic ring current shifts of the permutated construct have significantly reduced values. The structuring shifts within the helical

segment and at the P^{19}δ-CH_2 report a higher fold population than the P18 sites, which suggests that the Y3/P19 hydrophobic staple may be present in a partially folded state of the circular permutant.

7.3 Optimising the Linker

I performed an extensive series of alterations to the SGGDA loop of the RPPPSGGDAYAQWLADaGPAS construct. This series included longer loops along with specific residues which were chosen to reflect the backbone angles observed in this region in the cyclised Trp-cage crystal structures (Table 7.1). Removing the aspartic acid at position 1 was also explored, as the Asp was no longer the N-cap of the longer helix observed in the crystal structures of cyclo-TC1.

Residue	Φ (±s.d)	Ψ (±s.d)
S20	-86 (7)	-31 (6)
G21	-74 (8)	147 (4)
G(-1)	-67 (4)	-40 (6)
D1	-70 (4)	-43 (3)

Table 7.1. Dihedral angles statistics (±s.d.) for the loop residues of the crystal structures of cyclo Trp-cage.

The first mutations I examined were changes to the loop linker length (Table 7.2). These included switching out the Asp at the helix N-cap for an asparagine, this would remove some pH dependency, and adding extra alanines to increase the helix length. The added helix length would hopefully allow the asparagine to act as a helix N-cap, providing a stabilising element to the construct.

Sequence	Name	% Fold (280K)	%Fold (320K)	T_M (° C)	ΔG_U (kJ/mol) (280K)
RPPPS**GGDA**YAQWLADaGPSS	GGDA	59	20	17	0.86
RPPPS**GNAA**YAQWLADaGPSS	GNAA	57	18	15	0.78
RPPPS**GGNAA**YAQWLADaGPSS	GGNAA	49	14	6	-0.04
RPPPS**GGGGNAA**YAQWLADaGPSS	G4NAA	59	12	13	0.86

Table 7.2. Stability measures in the loop lengthening mutational series.

From this set of data, it was concluded that the original GG loop provided the optimal length, any residues more than two destabilised or maintained the fraction fold of the motif. As in prior Trp-cage studies, NMR structuring shifts, as chemical shift deviations, are used to determine whether the same fold forms and to determine the extent of folding. The chemical shifts the cyclo Trp-cage served as the 100%-folded reference values. In comparing the folding probes (Figure 7.2), the G4NAA displays greater fold populations at the proline sites measuring cage formation at 280K; this is a reflection of greater flexibility in the loop region lending itself to better proline docking over the Trp middle ring.

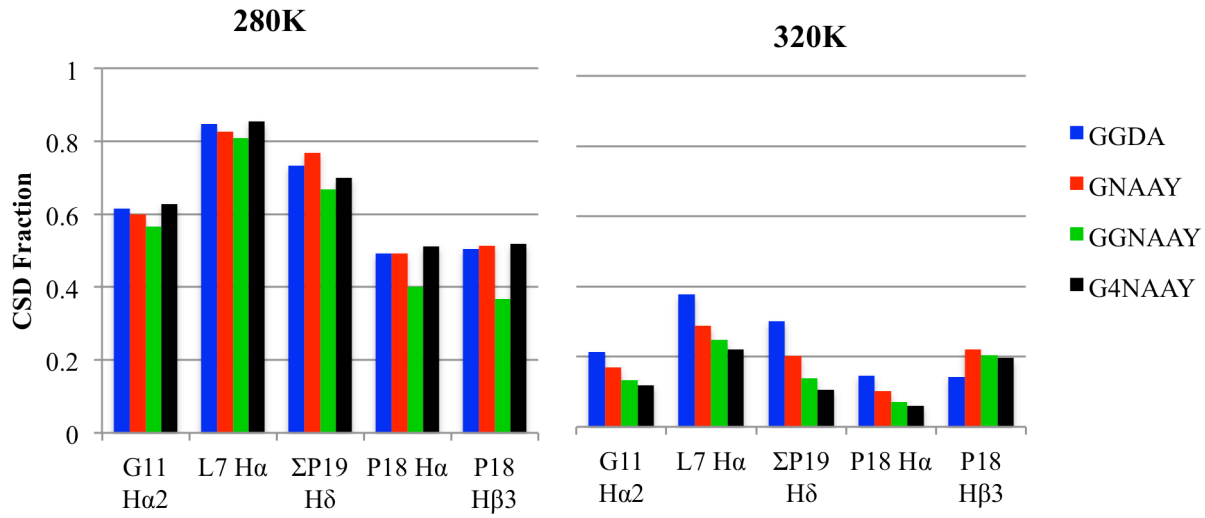

Figure 7.2. Local χ_F measures at of the NMR probe sites of the long loop series of Trp-cage circular permutants.

Next I turned to the Φ/Ψ angles shown in Table 7.1. Using a Ramachandran Plot, the Gly at -1, Asp and Ser all have helical Φ/Ψ values, whereas the Gly at 21 is either located in PolyPro or in the β area of the plot. Also of note from the Φ/Ψ numbers is the small standard deviation; the area is well defined indicating that it is not an area of segmental motion within the cyclic structure. Knowing the Φ/Ψ values, I attempted to take advantage of this to improve the fold stability of the circular permutant. This involved utilising a proline and then a threonine as a β residue (Table 7.3).

Name	% Fold (280K)	%Fold (320K)	T_M (° C) NMR **(CD)**	ΔG_U (kJ/mol) (280K)
GGDA	59	20	17	0.86
PADA	25	13	<0	-1.49
TADA	64	28	22.5 (**19**)	1.29

Table 7.3. Stability measures in the PADA and TADA loop series.

The proline mutant was a complete failure, being only 25% folded at 280K. This is presumably a result of the proline being too rigid for the loop due to its constrained Φ/Ψ values. On the other hand threonine did result in a slight increase in the fold populations at all temperatures, and hence a marginally higher melting temperature.

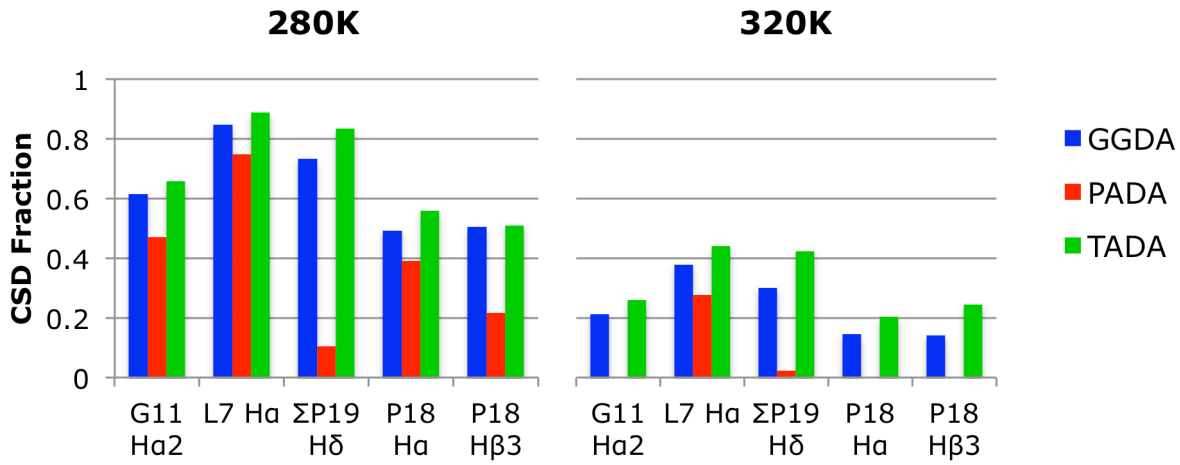

Figure 7.3. Local χ_F measures at the NMR probe sites of the PADA and TADA circular permutants.

In Figure 7.3 there are some discrepancies; this indicates that not all the structure is forming, or docking correctly or that some sections of the folded structure

are present in the unfolded state. Ideally when you look at fold populations, there should be a similar population across all probes.

From here, I decided to explore the use of aminoisobutyric acid (Aib) (Table 7.4). Aib prefers to adopt the conformations in which its Φ/Ψ angles are -60/-30 or 60/30 (Millhauser, 1995; Andersen *et al.*, 1996; Ro *et al.*, 2001; Toniolo *et al.*, 2001). It is restricted to (and has equal propensity for) left and right handed helices.

Name	% Fold (280K)	%Fold (320K)	T_M (° C) NMR	ΔG_U (kJ/mol) (280K)
GGDA	59	20	17	0.86
TUDA[a]	62	37	26.5	1.14
GUDA	76	36	36	2.63

Table 7.4. Stability measures in the TUDA and GUDA loop series. [a]U is the one letter code for aminoisobutyric acid.

The replacement of the loop Ala with an Aib proved to be beneficial in the TUDA linker series. The Aib residue provides an additional increment of thermal robustness versus an alanine. The fold stabilising effect of Aib insertion is presumably associated with its strong preference for helical Φ/Ψ values. Also changing the GGDA to a GUDA link was shown to be advantageous. As expected, replacing a glycine residue with a less flexible residue increases the fold stability, especially at higher temperatures.

7.4 Is the Serine Necessary?

All of the mutations presented to this point have retained the original C-terminal serine. Based on the Φ/Ψ values given in Table 7.1, this serine is in a 3_{10} helix conformation. Could this site be mutated to a residue that would function better there? This led me to explore two additional mutations where the serine has been mutated out (Table 7.5).

Name	% Fold (280K)	%Fold (320K)	T_M (° C) NMR	ΔG_U (kJ/mol) (280K)
SGGDA	59	20	17	0.86
SGUDA	76	36	36	2.63
DGUDA	78	37	36.5	2.95
GAUDA	51	24	8	0.056

Table 7.5. Stability measures in the DGUDA and GAUDA loop series.

The mutation of Ser to Asp made very little difference to the fold populations or overall thermal stability when compared to the DGUDA linker shown above in Table 7.4. The mutation of serine to glycine, however, showed a significant decrease in the stability of the construct. This is due to the inclusion of a residue with greater flexibility in place of one that is more constrained in the Φ/Ψ angles it is allowed to adopt. I made the decision to continue with the serine at that position for all further mutational studies into the Trp-cage circular permutation. In retrospect, a serine to alanine mutation should have been attempted, although it might have led to decreased solubility.

7.5 Further Aib Explorations

The cyclised crystal structure confirmed that the Asp in in the original Trp-cage series is not involved in H-bonding with the helix. Would it be possible to lengthen the helix through the use of alanines; allowing the Asp to become involved in a helix capping interaction? I used a simple loop linker, DAAA, to explore this (Table 7.6).

Name	% Fold (280K)	%Fold (320K)	T_M (° C) NMR **(CD)**	ΔG_U (kJ/mol) (280K)
GGDA	59	20	17	0.86
DAAA	65	42	36.5	2.63
DAUA	57	34	14 (**18**)	0.68
DUAA	73	50	48 (**48.5**)	2.36
DAAU	18	9	<<0	-3.53
DAAL	79	46	43.5	3.10

Table 7.6. Stability measures in the SDAAA loop series, with Aib mutations at each of the Ala sites.

Of the linkers presented to this point, the DAAA linker was the best linker with no Aib residues. Though its T_M was pretty much identical to the GUDA linker listed in Table 7.4, the DAAA linker did not improve on anything that had been previously examined. The NMR data for DAAA did show, however, that the alanine just prior to the tyrosine wasn't very helical. In hopes of improving the motif, I decided to insert an Aib at the second helical position following the aspartic acid; attempting to force the alanine next to the tyrosine to a better helical position. Though this construct displays a

lower %-fold at 280K, it melts out pretty slowly; indicating it possesses greater thermal stability. Placing Aib at the position just after Asp greatly improved the melting behaviour of the circular permutant. However, Aib is notably destabilising as the third helical residue (ΔΔG *circa* 6 kJ/mol versus the optimal first position). Studies in designed helices indicate that this is a general feature of Aib insertions into helices (Stewart 2009).

Yet the destabilising nature of Aib as the third helical residue was somewhat puzzling. A previous construct of the Trp-cage (NLYIQWLKDGGPSSGRPPPS) has a leucine at this same site that was not significantly destabilising (98%-folded at 280K, $T_M = 42\ ^\circ$ C). So obviously the length of the sidechain shouldn't be an issue, was it the presence of the geminal carbons on the Aib? To ensure the circular permutant wasn't adopting a somewhat different conformation with the Aib here, I mutated in a leucine at this site. This mutation actually proved to be the most fold-stabilising substitution for the original GGDA motif, but the DUAA loop provided the more stable fold at temperatures greater than 310 K.

A former Andersen group member, Dr. Jack Stewart, observed that at low temperatures Ala was better in a helix than Aib (Stewart, 2009). Whereas at higher temperatures, that order switches with Aib now being the better helix stabiliser. At higher temperatures, the preference for alanine to remain in a helix is outweighed by entropic considerations. At the same temperatures, Aib is locked into an α configuration. As a result entropic considerations become more important than helix propensity.

7.6 Adding Stabilising Mutations Together

A further study of structural similarity despite differing contact order was carried out. I, along with Dr. Kier, examined how established Trp-cage fold stabilisation strategies (and destabilising mutations) affect the circular permutant. Dr. Kier performed 2 mutations, a G10→D-Ala (Williams, et al. 2008) and P12→W (Bunagan *et al.*, 2006); mutations which are known to be favourable in the original Trp-cage. The D-Ala mutation had been demonstrated to increase ΔG_U by 4 kJ/mol, but there was only a ΔG_U = 0.8 kJ/mol increase in the permutant based on NMR shift measures of the fold population. However, the ΔTm effect (ΔTm = 16 °C) was identical for both. The Pro to Trp mutation provided greater fold stabilisation to the circular permutants, ΔTm = 18 °C. I explored the S13 (S20 in the circular permutant) and S14 (S21) positions, both of which have been examined in the original Trp-cage topology. As was the case in the original Trp-cage, replacing the buried S14 with an alanine was fold destabilising while the S13 mutation was fold stabilising (Table 7.7).

Name	% Fold (280K)	%Fold (320K)	T_M (° C) NMR	ΔG_U (kJ/mol) (280K)
GGDA	44	10	1	-0.61
GGDA G10a	59	20	17	0.86
P19W	79	34	35	3.03
S20A	62	25	20	1.09
S21A	43	20	4	-0.62

Table 7.7. Stability measures in the GGDA loop with a P19W mutation and serine to alanine mutations in the 3_{10} helix.

The majority of these mutations displayed fold-stabilising increments that are similar to those of the non-permutated species. However, the destabilising S14A mutant proved to be an outlier. This mutation caused a decrease in the melting temperature of 13 °C in the circular permutant, but a decrease of 35 °C in a non-permuted construct (Barua *et al.*, 2008). This is attributed to the greater burial of the serine side chain in the non-permutated constructs; when the S14 side chain is buried it has two hydrogen bonding interactions: Ser14 Hγ → O=C Gly11 and Ser14 Oγ ← H_N Arg16 (Scian *et al.*, 2012). The equivalent position in the permuted series is S20, the C-terminal residue; this would be a frayed site in the construct resulting in less opportunities for the H-bonding to form. This implies that the H-bonding network associated with the hydroxyl group of S14 in the complete Trp-cage fold (Scian *et al.*, 2012) is not just a requirement for burial but also enhances fold stabilisation.

One of the goals of this project was to elucidate an NMR structure for a circular permutant. However, none of the single mutations (including loop optimisation) gave a %-fold at 280K which was high enough to support a meaningful NMR structure derivation. I examined combining the best mutations together (Table 7.8). I chose to combine the stabilising mutations in the DUAA loop instead of the DAAL loop due to the greater thermal stability of DUAA.

Name	% Fold (280K)	%Fold (320K)	T_M (° C) NMR **(CD)**	ΔG_U (kJ/mol) (280K)
DUAA	73	50	48 (**48.5**)	2.36
DUAA S20A	73	53	(**50.4**)	2.33
DUAA P19W S20A	93	69	63 (**67**)	6.24

Table 7.8. Stability measures in the stabilising mutations to the DUAA loop.

As expected the S20A mutation with the DUAA loop linker provided only a modest additional increase in T_M. However, adding the P19W mutation to this (RPPPSDUAAYAQWLADaGWAS) greatly increased the %-fold and the melting temperature. With a fold population of 93% at 280K, this was enough to derive an NMR structure. Due to problems with how Pymol and MolMol handled Aib, I replaced the Aib with a glycine for the restrained dynamics runs (and deleted the NOE constraints for the Aib methyl groups); the resulting structure does predict the observed NOE contacts when the methyl groups are reinserted. The intra-ensemble 3-19 backbone RMSD was calculated as 0.014 ± 0.003 Å (See Table 7.9 for all statistics).

Type of constraint	Number	r.m.s deviation
Intraresidue	132	0.014 ± 0.003
Sequential	73	0.051 ± 0.043
i/i+n, n = 2-4	49	0.018 ± 0.015
i/i+n, n ≥ 5	47	0.04 ± 0.064
Structure statistics[a.].		
E_{TOTAL} (kcal/mol)		-64.9 ± 4.3
E_{NOE} (kcal/mol)		4.18 ± 0.20
E_{vdW} (kcal/mol)		-90.7 ± 4.0
Bond violations (Å)		3.10 ± 0.19
Angle violations (°)		17.4 ± 0.87
Improper torsion violations (°)		1.15 ± 0.10
Convergence within final ensemble, atomic r.m.s deviations (Å)[b.]:		
Pairwise over the ensemble ((±s.e.)		
Backbone		0.19 ± 0.06
Heavy atom		0.65 ± 0.16

Table 7.9. NMR structure statistics for the DUAA P19W S20A ensemble (32 accepted structures from 40 starts). [a.] Values are mean ± standard deviation. [b.] All convergence measures are over residues 3-19.

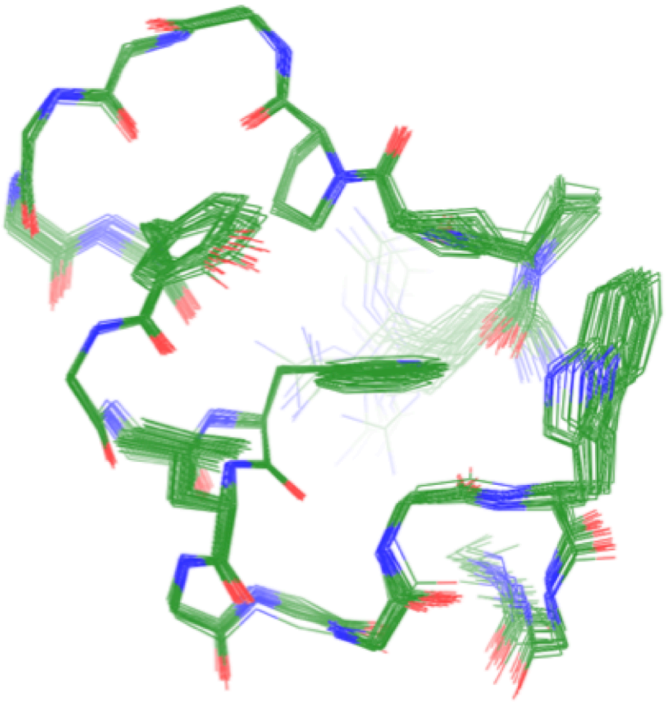

Figure 7.4. DUAA P19W S20A ensemble generated from 32/40 lowest energy structures.

Vicki Williams had previously determined the NMR structure for [P12W]-TC16b (DAYAQWLADAGWASaRPPPS). This, along with the crystal structure, was used for structural comparisons. The circular permutant and [P12W]-TC16b structures are almost identical, with RMSDs of 0.49 and 0.75 Å for the backbone and heavy atoms, respectively, over the shared residues and backbone (Figure 7.5).

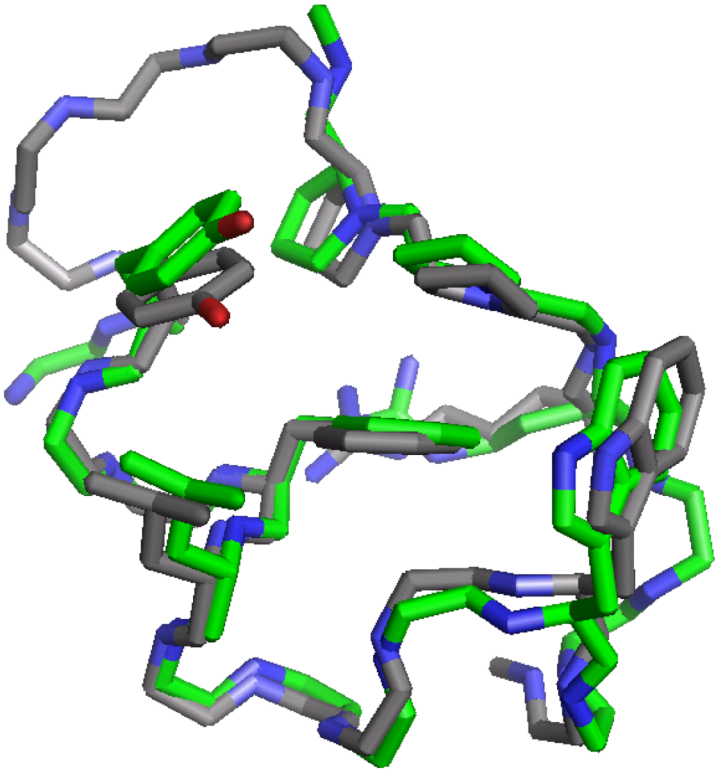

Figure 7.5. A comparison of representative structures from the NMR ensembles of [P12W]-TC16b (green) and DUAA P19W S20A (grey).

A comparison of the dihedral angles, ϕ, ψ and χ^1 between [P12W]-TC16b and DUAA P19W S20A (Table 7.10) shows that significant differences occur only in the dihedral angle values of the 3_{10}-helix. This is understandable given that 3_{10}-helix will be more frayed in the permutant versus the normal Trp-cage motif. Comparing the angles for the loop linker region with the cyclised Trp-cage values shows that the loops are virtually identical, both being well ordered.

(P12W)-TC16b				DUAA P19W S20A			
Residue	Φ	Ψ	χ^1	Residue	Φ	Ψ	χ^1
D1		112.6(105.2)	-118.8(76.7)				
A2	-117.0(75)	-45.1(31.2)		A9	-68.9(2.0)	-29.9(0.7)	
Y3	-66.4(3)	-50.1(2.4)	-151.5(0.6)	Y10	-61.2(0.6)	-35.2(0.2)	-168.7(2.0)
A4	-65.6(1.5)	-34.2(1.3)		A11	-69.7(1.5)	-53.2(0.3)	
Q5	-69.0(1.2)	-38.4(0.6)	178.1(2.8)	Q12	-60.3(0.7)	-35.5(1.0)	-152.3(1.1)
W6	-60.7(0.6)	-48.9(0.2)	179.2(0.4)	W13	-56.4(0.9)	-46.8(1.2)	179.7(0.9)
L7	-64.4(0.4)	-36.4(0.3)	-62.4(1.1)	L14	-62.4(1.1)	-42.9(1.4)	-68.0(0.3)
A8	-75.4(0.7)	-18.3(1.0)		A15	-59.7(1.4)	-31.8(2.1)	
D9	-88.8(1.0)	15.7(0.6)	-117.9(9.6)	D16	-87.3(3.7)	10.9(8.6)	-129.4(12.3)
a10	103.3(0.8)	-3.4(0.4)		a17	90.3(10.6)	7.4(9.1)	
G11	67.3(0.2)	-96.9(0.4)		G18	61.7(3.4)	-105.6(3.4)	
W12	-97.3(0.4)	10.8(1.6)	-82.0(0.3)	W19	-68.2(2.7)	-30.0(1.8)	-74.4(4.1)
A13	-85.5(1.6)	-31.8(0.4)		A20	-90.4(8.0)	36.8(17.4)	
S14	-62.9(0.7)	-29.6(0.7)	32.7(0.9)	S21	-93.4(12.5)	178.8(30.2)	
a15	100.1(0.7)	-24.3(0.5)	89.3(86.5)				
R16	-86.0(0.4)	153.6(0.3)	80.1(1.1)	R1	133.6(8.6)	57.9(6.9)	
P17	-83.5(0.4)	166.1(0.5)	5.0(0.4)	P2	-73.9(10.3)	164.0(5.4)	8.0(23.1)
P18	-62.8(0.8)	145.9(0.9)	17.8(0.5)	P3	-53.4(3.9)	117.3(3.7)	1.4(17.3)
P19	-80.8(0.4)	142.2(12)	22.7(0.4)	P4	-81.5(1.4)	142.4(6.6)	30.7(0.6)
S20	-129.9(30)	57.2(80.2)					
	cyclo-TC1						
S20	-86(7)	-31(6)		S5	-57.7(4.9)	-44.9(2.8)	52.8(1.1)
G21	-74(8)	147(4)		D6	-57(6)	142(7)	-55(78)
G(-1)	-67(4)	-40(6)		U7	-70(7)	-38.3(1.5)	
D1	-70.0(4.0)	-43.0(3.0)		A8	-56.4(2.8)	-56.9(1.1)	

Table 7.10. Dihedral angles statistics (±s.d.) for the NMR ensembles of (P12W)-TC16b (30 structures) and DUAA P19W S20A (32 structures), as well as cyclic loop.

Additional dihedral angle comparisons for Trp-cages are given in M. Scian *et al.* (Scian *et al.*, 2012); these include the averages for all Trp-cages prior to the two additions shown above.

The formation, upon circular permutation, of the same hydrophobic core, substantiated by the usual set of long-range NOEs that define the Trp-cage motif (Neidigh *et al.*, 2002; Williams *et al.*, 2011) is clearly demonstrated. This was fully validated by a direct NMR structure comparison (Figure 7.4). The distance constraints used for the generation of the structure ensemble are provided in Appendix C.

7.7 Alternative cps: Can cyclo-TC1 be cut at another site?

I mentioned earlier in this chapter that there were two possible cut sites in the Trp-cage: between the α-helix and the 3_{10} helix or between the 3_{10} helix and the polyPro unit. All the work previously described employed the cut between the 3_{10} helix and the polyPro unit. Would a cut between the α-helix and the 3_{10} helix provide sequences that would fold?

Sequence	Name	% Fold (280K)	%Fold (320K)	T_M (° C)
GPSSaRPPPSGGDAYAQWLADG-NH2	Cut 1	12	5	<< 0
PSSaRPPPSGGDAYAQWLANGG-NH2	Cut 2	24	10	< 0
PSSaRPPPSGGDAYAQWLANGG-NH2 *w/ TFE*	Cut 2	33	n.d.	< 0
WSSaRPPPSGGDAYAQWLANGG-NH2	Cut 2 P1W	17 at 300 K		< 0

Table 7.11. Trp-cage circular permutant through the 'other' cut.

Two slightly different scission sites were attempted - between what would be G10 and G11 in standard Trp-cage numbering and between G11 and P12. The scission between G11 and P12 (Cut 2) proved to be slightly more effective than the scission between G10 and G11. Examining Cut 2 in the presence of TFE, known to help stabilise helical structure (Myers *et al.*, 1998), resulted in the measures of helical folding being slightly elevated. The fold populations at 280 K were so low for both new scission sites that T_Ms could not be calculated. Inserting a stabilising mutation, P12W (P1W in the circular permutant), did little to improve the fold stability. There was no evidence from the NMR data that a Trp/Trp interaction was occurring.

Folding was unable to be rescued for any scission within the loop between the α and 3_{10} helix, this indicated that the initial scission point (between the 3_{10} helix and the polyPro helix) was the correct choice.

7.8 Additional Mutations

The initial circular permutant of the Trp-cage had a glycine at the 10 position with $\phi/\psi = +100/+10$. This was successfully mutated to a D-Ala in the standard Trp-cage construct (Williams *et al.*, 2008) and also by Brandon Kier in the permutant series. But would other D-amino acids work?

It was hypothesised that polar D-amino acids could stabilise the carboxy termini of α-helices through sidechain to backbone hydrogen bonds (Rodriguez-Granillo *et al.*, 2011). They explored the use of D-Gln at the 10 position in the TC5b variant of the Trp-cage. Their NMR structure showed the presence of capping interactions in the form of a D-Gln hydrogen bond with the backbone carbonyl of Lys8, leading to a more stable structure. Rodriguez-Granillo observed a $\Delta Tm = +23$ °C with D-Gln present, compared to their observed $\Delta Tm = +20$ °C with D-Ala. Culik (Culik *et al.*, 2013) presents results that show the stabilising effect of D-Gln originates almost entirely from a decrease in the unfolding rate, while the D-Ala mutation results in a similar decrease in the unfolding rate, but it also increases the folding rate.

Would this mutation provide a small, but important, amount of added stability to the circular permutant? The D-Ala to D-Gln mutation was explored in the TADA loop series (Table 7.12).

Name	% Fold (280K)	%Fold (320K)	T_M (° C) NMR **(CD)**	ΔG_U (kJ/mol) (280K)
TADA	64	28	22.5 (**19**)	1.29
TADA G10q	65	30	23	1.44

Table 7.12. Stability measures in the mutations to the TADA loop series.

The D-Gln mutation provided a very small increase in fold stability, with an even smaller change in temperature than observed by Rodriguez-Granillo (Rodriguez-Granillo *et al.*, 2011). The replacement of Gly with D-Ala allows the helix capping structure to form without the entropic cost of fixing the conformation of glycine (Bang *et al.*, 2006). Molecular dynamics simulations of TC5b G10q (Rodriguez-Granillo *et al.*, 2011) show that D-Gln can hydrogen bond with the backbone carbonyl of Leu7, Lys8 and Asp9. These interactions, however, were not present in the average structure; strong hydrogen bonding to the backbone carbonyls only showed up in ~10% of structures. The slight increase in stability for D-Gln versus D-Ala is presumably due to transient H-bonding in the D-Gln mutation.

Since D-Gln did not introduce significant stability to the circular permutant, a D-Arg mutation at the same site was also explored. A DeGrado study (Schneider & DeGrado, 1998) showed that a D-Arg at the C-capping site of a helix stabilised the helix by ~1 kcal/mol. The D-Arg mutation was carried out in the GUDA linker series (Table 7.13).

Name	% Fold (280K)	%Fold (320K)	T_M (° C) NMR **(CD)**	ΔG_U (kJ/mol) (280K)
GUDA	76	36	36	2.63
GUDA G10r	77	41	39	2.86

Table 7.13. Stability measures in the mutations to the GUDA loop series.

The presence of D-Arg at the 10 position in the Trp-cage increases the fold stability at 280 K as well as the overall thermal stability. There is a more pronounced difference in the fold stability at 320 K versus 280 K; the D-Arg mutation causes the melting out of the Trp-cage structure to be slower than with D-Ala. The positive charge of arginine helps to stabilise the helix macrodipole over a D-Ala. There may also be some hydrogen bonding with backbone carbonyls similar to D-Gln.

The decision was made to stick with the original D-Ala at the 10 position. There was a concern that D-Arg would introduce repulsion with the Arg at the 1 position; though the CSDs give no indication of this. I wished to keep the overall structure as close to the non-permutated constructs.

7.9 Cyclising the Circular Permutant

The loop optimisation studies in the circular permutant along with the large fold stability increase observed for 'P12W' generated a circular permutant with χ_F = 93% at 280 K. Could these improvements be incorporated into a hyperstable cyclic construct? This new cyclic Trp-cage would have its starting point in my most stable permutant construct; RPPPSDUAAYAQWLADaGWAS.

In order to create a cyclic structure, a different N- and C-termini would have to be created; an attempted cyclisation between the arginine and serine termini in the circular permutation would be difficult. A new linear Trp-cage sequence was synthesised (AYAQWLADaGWASaRPPPSDUA), the new termini would allow for the easiest possible cyclisation. The G15 excised from the original Trp-cage was reinserted, but mutated to a D-Ala. This mutation is known to provide additional stability (Williams *et al.*, 2008).

Cyclisation of the circular permutant would only work if the permutant was very well folded and the N- and C- termini were close in space. To ascertain this, the acyclic construct was first examined (Table 7.14) (Sequence = AYAQWLADaGWASaRPPPSDUA).

Name	% Fold (280K)	%Fold (320K)	T_M (° C) NMR **(CD)**	ΔG_U (kJ/mol) (280K)
DUAA P19W S20A	93	67	63 (**67**)	6.24
Acyclic	94	74	(~ **55**)	6.52

Table 7.14. Fold stability measures for the acyclic circular permutant.

The acyclic variant proved to be well-folded, χ_F = 0.941 at 280 K. In CD analysis, however, the use of standard Trp-cage folding and unfolding baselines results in a $T_M \approx 85$ °C. Closer inspection of the data indicates that the T_M is in fact closer to 55 °C (Figure 7.6), a 1st derivative melting temperature from the CD spectra was used to obtain this number.

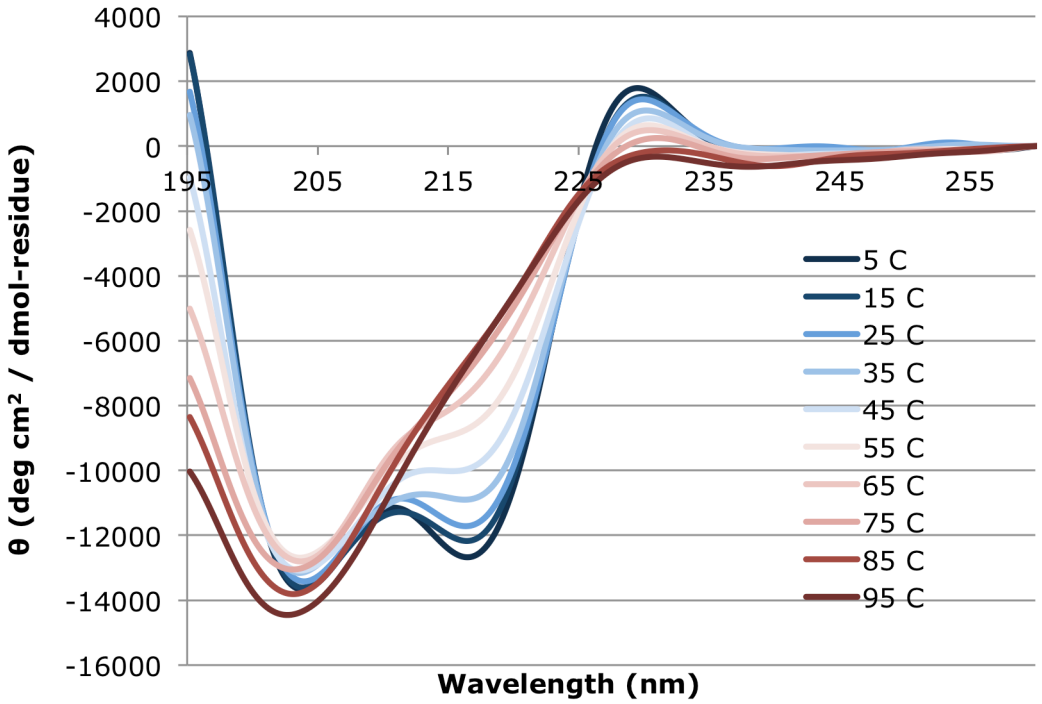

Figure 7.6. CD melting profile for the acyclic circular permutant.

The indications that the acyclic circular permutant was well folded led me to pursue the creation of its cyclic counterpart. Due to poor yields from cyclisation, the peptide was first examined via circular dichroism (Figure 7.6).

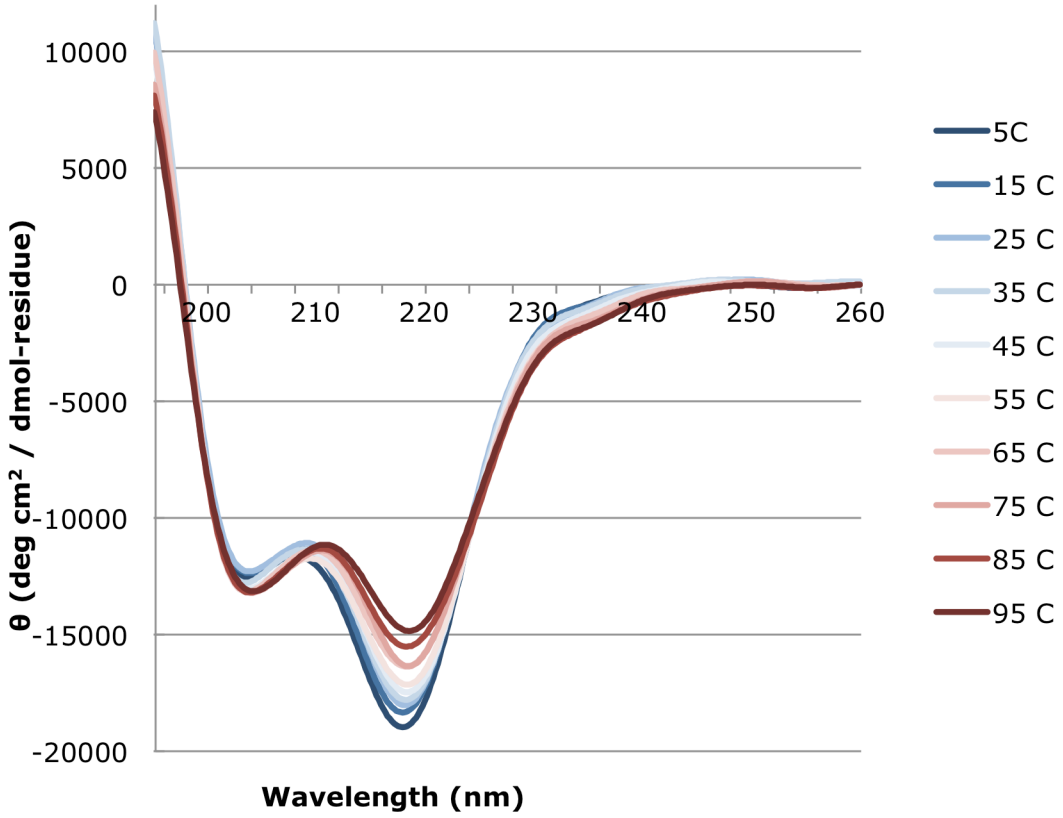

Figure 7.6. The CD melt of the cyclo circular permutant.

As can be seen in the above figure, there is little to no melting out of the structure. The redshift observed as the temperature increases is a result of segmental motion in the α-helix along with motion between the two Trps. The lack of melting indicates that the T_M would be in excess of 100 °C. As a result, a denaturant guanidinium chloride (GdmCl) was added to determine a melting point (Table 7.15). A number of hyperstable Trp-cages have been examined at 5M GdmCl; this was the logical GdmCl concentration to start with.

	T_M (° C) Water	T_M (° C) 5 M GdmCl
TC16b	83	22
TC16b P12W	97	52
cyclo-TC1	95	48
cyclo 2 $_D$-Ala's	> 100	69
cyclo CircMut	>> 100	> 95

Table 7.15. CD melting temperatures for hyperstable Trp-cages in water and 5 M GdmCl.

As can be seen the T_M for the cyclo CircMut in 5 M GdmCl is still > 95° C. The concentration of GdmCl was then increased to 7M, this indicated that the T_M > 90° C. Some CD difference spectra were examined, to observe whether Trp/Trp exciton couplet melting or α-helix melting was occurring (Figure 7.8). Regardless of the GdmCl molarity, all of the difference spectra examined appear to indicate that the Trp/Trp exciton couplet is disappearing from the spectra faster. The exciton couplet possesses a high temperature dependence.

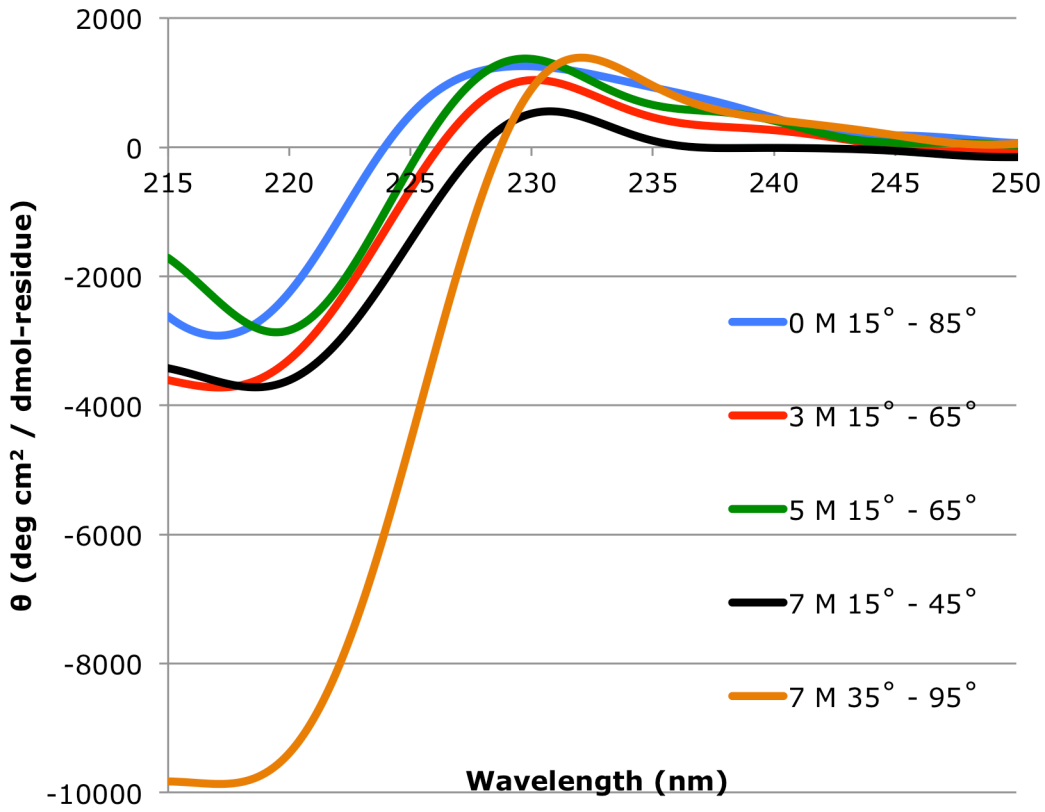

Figure 7.8. CD difference spectra for the cyclo CircMut.

7.x Conclusions

A stable circular permutant was achieved through loop optimisation and the addition of known stabilising mutations. The Pro to Trp mutation (P12W in non-permutant topology) provides greater fold stabilisation to the permutant series. This stable construct then allowed for cyclic circular permutant to be synthesised, thus creating a truly hyperstable Trp-cage. The cyclo CircMut is the most stable Trp-cage prepared to date, proving to be significantly more stable than even other cyclised Trp cages.

Bibliography

Adessi, C., Frossard, M.-J., Boissard, C., Fraga, S., Bieler, S., Ruckle, T., Vilbois, F., Robinson, S.M., Mutter, M., Banks, W. a, & Soto, C. (2003) Pharmacological profiles of peptide drug candidates for the treatment of Alzheimer's disease. *J. Biol. Chem.*, **278**, 13905–13911.

Ahmed, Z., Beta, I.A., Mikhonin, A. V, & Asher, S.A. (2005) UV-resonance raman thermal unfolding study of Trp-cage shows that it is not a simple two-state miniprotein. *J. Am. Chem. Soc.*, **127**, 10943–10950.

Ahn, J.S., Lee, J.-H., Kim, J.-H., & Paik, S.R. (2007) Novel method for quantitative determination of amyloid fibrils of alpha-synuclein and amyloid beta/A4 protein by using resveratrol. *Anal. Biochem.*, **367**, 259–265.

Aktas, O., Prozorovski, T., Smorodchenko, A., Savaskan, N.E., Lauster, R., Infante-duarte, C., Brocke, S., & Kloetzel, P. (2004) Green Tea Epigallocatechin-3-Gallate Mediates T Cellular NF- κ B Inhibition and Exerts Neuroprotection in Autoimmune Encephalomyelitis. *J. Immunol.*, **173**, 5794–5800.

Alim, M.A., Ma, Q.-L., Takeda, K., Aizawa, T., Matsubara, M., Nakamura, M., Asada, A., Saito, T., Kaji, H., Yoshii, M., Hisanaga, S., & Uéda, K. (2004) Demonstration of a role for α-synuclein as a functional microtubule-associated protein. *J. Alzheimers Dis.*, **6**, 435–442.

Amer, D.A., Irvine, G.B., & El-Agnaf, O.M. (2006) Inhibitors of alpha-synuclein oligomerization and toxicity: a future therapeutic strategy for Parkinson's disease and related disorders. *Exp. Brain Res.*, **173**, 223–233.

Andersen, N.H., Brodsky, Y., Neidigh, J.W., & Prickett, K.S. (2002) Medium-dependence of the secondary structure of exendin-4 and glucagon-like-peptide-1. *Bioorg. Med. Chem.*, **10**, 79–85.

Andersen, N.H., Fesinmeyer, R.M., Neidigh, J.W., & Barua, B. (2000) The Trp-Cage: A Notably Stable Mini-Protein Fold. *Peptides*, 45–46.

Andersen, N.H., Liu, Z., & Prickett, K.S. (1996) Efforts toward deriving the CD spectrum of a 3(10) helix in aqueous medium. *FEBS Lett.*, **399**, 47–52.

Andersen, N.H., Olsen, K.A., Fesinmeyer, R.M., Tan, X., Hudson, F.M., Eidenschink, L.A., & Farazi, S.R. (2006) Minimization and optimization of designed beta-hairpin folds. *J. Am. Chem. Soc.*, **128**, 6101–6110.

Anderson, D.E., Becktel, W.J., & Dahlquist, F.W. (1990) pH-Induced denaturation of proteins: a single salt bridge contributes 3-5 kcal/mol to the free energy of folding of T4 lysozyme. *Biochemistry*, **29**, 2403–2408.

Anil, B., Craig-Schapiro, R., & Raleigh, D.P. (2006) Design of a hyperstable protein by rational consideration of unfolded state interactions. *J. Am. Chem. Soc.*, **128**, 3144–3145.

Anil, B., Song, B., Tang, Y., & Raleigh, D.P. (2004) Exploiting the right side of the Ramachandran plot: substitution of glycines by D-alanine can significantly increase protein stability. *J. Am. Chem. Soc.*, **126**, 13194–13195.

Antzutkin, O.N., Balbach, J.J., Leapman, R.D., Rizzo, N.W., Reed, J., & Tycko, R. (2000) Multiple quantum solid-state NMR indicates a parallel, not antiparallel, organization of β-sheets in Alzheimer's β-amyloid fibrils. *Proc. Natl. Acad. Sci. U. S. A.*, **97**, 13045–13050.

Arora, P., Oas, T.G., & Myers, J.K. (2004) Fast and faster: a designed variant of the B-domain of protein A folds in 3 μsec. *Protein Sci.*, **13**, 847–853.

Aurora, R., Creamer, T.P., Srinivasan, R., & Rose, G.D. (1997) Local Interactions in Protein Folding: Lessons from the α-Helix. *J. Biol. Chem.*, **272**, 1413–1416.

Austen, B.M., Paleologou, K.E., Ali, S.A.E., Qureshi, M.M., Allsop, D., & El-Agnaf, O.M. (2008) Designing Peptide Inhibitors for Oligomerization and Toxicity of Alzheimer's β-Amyloid Peptide. *Biochemistry*, **47**, 1984–1992.

Azia, A. & Levy, Y. (2009) Nonnative electrostatic interactions can modulate protein folding: molecular dynamics with a grain of salt. *J. Mol. Biol.*, **393**, 527–542.

Bai, Y. (2003) Hidden intermediates and levinthal paradox in the folding of small proteins. *Biochem. Biophys. Res. Commun.*, **305**, 785–788.

Balbach, J.J., Petkova, A.T., Oyler, N.A., Antzutkin, O.N., Gordon, D.J., Meredith, S.C., & Tycko, R. (2002) Supramolecular Structure in Full-Length Alzheimer's β-Amyloid Fibrils : Evidence for a Parallel β-Sheet Organization from Solid-State Nuclear Magnetic Resonance. *Biophys. J.*, **83**, 1205–1216.

Baldwin, R.L. & Rose, G.D. (1999a) Is protein folding hierarchic? I. Local structure and peptide folding. *Trends Biochem. Sci.*, **24**, 26–33.

Baldwin, R.L. & Rose, G.D. (1999b) Is protein folding hierarchic? II. Folding intermediates and transition states. *Trends Biochem. Sci.*, **24**, 77–83.

Bang, D., Gribenko, A. V, Tereshko, V., Kossiakoff, A.A., Kent, S.B., & Makhatadze, G.I. (2006) Dissecting the energetics of protein alpha-helix C-cap termination through chemical protein synthesis. *Nat. Chem. Biol.*, **2**, 139–143.

Barua, B. (2005) Design and study of Trp-cage miniproteins. Ph.D. Thesis, University of Washington, Seattle.

Barua, B. & Andersen, N.H. (2002) Determinants of miniprotein stability: can anything replace a buried H-bonded Trp sidechain? *Lett. Pept. Sci.*, **8**, 221–226.

Barua, B., Lin, J.C., Williams, D. V, Kummler, P., Neidigh, J.W., & Andersen, N.H. (2008) The Trp-cage: optimizing the stability of a globular miniprotein. *Protein Eng Des Sel*, **21**, 171–185.

Bax, A. & Davis, D.G. (1985) MLEV-17-Based Two-Dimensional Homonuclear Magnetization Transfer Spectroscopy. *J. Magn. Reson.*, **65**, 355–360.

Beasley, J.R. & Hecht, M.H. (1997) Protein design: the choice of de novo sequences. *J. Biol. Chem.*, **272**, 2031–2034.

Benzinger, T.L., Gregory, D.M., Burkoth, T.S., MIller-Auer, H., Lynn, D.G., Botto, R.E., & Meredith, S.C. (1998) Propagating structure of Alzheimer's β-amyloid (10-35) is a parallel β- 139 sheet with residues in exact register. *Proc. Natl. Acad. Sci. U. S. A.*, **95**, 13407–13412.

Bieschke, J., Russ, J., Friedrich, R.P., Ehrnhoefer, D.E., Wobst, H., Neugebauer, K., & Wanker, E.E. (2010) EGCG remodels mature alpha-synuclein and amyloid-beta fibrils and reduces cellular toxicity. *Proc. Natl. Acad. Sci. U. S. A.*, **107**, 7710–7715.

Bisaglia, M., Tessari, I., Pinato, L., Bellanda, M., Giraudo, S., Fasano, M., Bergantino, E., Bubacco, L., & Mammi, S. (2005) A Topological Model of the Interaction between R-Synuclein and Sodium Dodecyl. *Biochemistry*, **44**, 329–339.

Bisaglia, M., Trolio, A., Bellanda, M., Bergantino, E., Bubacco, L., & Mammi, S. (2006) Structure and topology of the non-amyloid-beta component fragment of human alpha-synuclein bound to micelles: implications for the aggregation process. *Protein Sci.*, **15**, 1408–1416.

Bodles, A.M., El-Agnaf, O.M., Greer, B., Guthrie, D.J., & Irvine, G.B. (2004) Inhibition of fibril formation and toxicity of a fragment of alpha-synuclein by an N-methylated peptide analogue. *Neurosci. Lett.*, **359**, 89–93.

Bodner, C.R., Maltsev, A.S., Dobson, C.M., & Bax, A. (2010) Differential phospholipid binding of alpha-synuclein variants implicated in Parkinson's disease revealed by solution NMR spectroscopy. *Biochemistry*, **49**, 862–871.

Brünger, A.T. (2007) Version 1.2 of the Crystallography and NMR system. *Nat. Protoc.*, **2**, 2728–2733.

Brünger, A.T., Adams, P.D., Clore, G.M., DeLano, W.L., Gros, P., Grosse-Kunstieve, R.W., Jiang, J., Kuszweski, J., Nilges, M., Pannu, N., Read, R., Rice, L., Simonson, T., & Warren, G. (1998) Crystallography & NMR System: A New Software Suite for Macromolecular Structure Determination. *Acta Crystallogr., Sect. D: Biol. Crystallogr.*, **54**, 905–921.

Bunagan, M.R., Yang, X., Saven, J.G., & Gai, F. (2006) Ultrafast folding of a computationally designed Trp-cage mutant: Trp2-cage. *J. Phys. Chem. B*, **110**, 3759–3763.

Camarero, J., Fushman, D., Sato, S., Giriat, I., Cowburn, D., Raleigh, D.P., & Muir, T.W. (2001) Rescuing a destabilized protein fold through backbone cyclization. *J. Mol. Biol.*, **308**, 1045–1062.

Camarero, J., Pavel, J., & Muir, T.W. (1998) Chemical Synthesis of a Circular Protein Domain: Evidence for Folding-Assisted Cyclization. *Angew. Chem. Int. Ed.*, **37**, 347–349.

Cerny, J., Vondrasek, J., & Hobza, P. (2009) Loss of dispersion energy changes the stability and folding/unfolding equilibrium of the Trp-cage protein. *J. Phys. Chem. B*, **113**, 5657–5660.

Chang, E.S.-H., Liao, T.-Y., Lim, T.-S., Fann, W., & Chen, R.P.-Y. (2009) A new amyloid-like beta-aggregate with amyloid characteristics, except fibril morphology. *J. Mol. Biol.*, **385**, 1257–1265.

Chatterjee, C. & Gerig, J.T. (2006) Interactions of hexafluoro-2-propanol with the Trp-cage peptide. *Biochemistry*, **45**, 14665–14674.

Chatterjee, C. & Gerig, J.T. (2007) Interactions of Trifluroethanol with the Trp-Cage Peptide. *Biopolymers*, **87**, 115–123.

Chiti, F. & Dobson, C.M. (2006) Protein misfolding, functional amyloid, and human disease. *Annu. Rev. Biochem.*, **75**, 333–366.

Chiti, F. & Dobson, C.M. (2009) Amyloid formation by globular proteins under native conditions. *Nat. Chem. Biol.*, **5**, 15–22.

Cho, J.-H. & Raleigh, D.P. (2005) Mutational analysis demonstrates that specific electrostatic interactions can play a key role in the denatured state ensemble of proteins. *J. Mol. Biol.*, **353**, 174–185.

Chowdhury, F.A. & Raleigh, D.P. (2005) A comparative study of the α-subdomains of bovine and human α-lactalbumin reveals key differences that correlate with molten globule stability. *Protein Sci.*, **14**, 89–96.

Chowdhury, S., Lee, M.C., & Duan, Y. (2004) Characterizing the Rate-Limiting Step of Trp-Cage Folding by All-Atom Molecular Dynamics Simulations. *J. Phys. Chem. B*, **108**, 13855–13865.

Chowdhury, S., Lee, M.C., Xiong, G., & Duan, Y. (2003) Ab initio folding simulation of the Trp-cage mini-protein approaches NMR resolution. *J. Mol. Biol.*, **327**, 711–717.

Cochran, A.G., Skelton, N.J., & Starovasnik, M.A. (2001) Tryptophan zippers: Stable, monomeric ß-hairpins. *Proc. Natl. Acad. Sci. U. S. A.*, **98**, 5578–5583.

Conway, K.A., Harper, J.D., & Lansbury, P.T. (1998) Accelerated in vitro fibril formation by a mutant α-synuclein linked to early-onset Parkinson disease. *Nat. Med.*, **4**, 1318–1320.

Cooper, G.J., Willis, a C., Clark, A., Turner, R.C., Sim, R.B., & Reid, K.B. (1987) Purification and characterization of a peptide from amyloid-rich pancreases of type 2 diabetic patients. *Proc. Natl. Acad. Sci. U. S. A.*, **84**, 8628–8632.

Culik, R.M., Annavarapu, S., Nanda, V., & Gai, F. (2013) Using D-amino acids to delineate the mechanism of protein folding: Application to Trp-cage. *Chem. Phys.*, 1–4.

Culik, R.M., Serrano, A.L., Bunagan, M.R., & Gai, F. (2011) Achieving Secondary Structural Resolution in Kinetic Measurements of Protein Folding: A Case Study of the Folding Mechanism of Trp-cage. *Angew. Chem. Int. Ed.*, **123**, 11076–11079.

Daggett, V. & Fersht, A.R. (2003a) The present view of the mechanism of protein folding. *Nat. Rev. Mol. Biol.*, **4**, 497–502.

Daggett, V. & Fersht, A.R. (2003b) Is there a unifying mechanism for protein folding? *Trends Biochem. Sci.*, **28**, 18–25.

De Marco, A. (1977) pH Dependence of Internal References. *J. Magn. Reson.*, **26**, 527–528.

DeLano, W.L. (2002) The PyMOL Molecular Graphics System, Version 1.5.0.4 Schrödinger, LLC.

Dill, K.A. & Chan, H.S. (1997) From Levinthal to pathways to funnels. *Nat. Struct. Biol.*, **4**, 10–19.

Dill, K.A., Ozkan, S.B., Shell, M.S., & Weikl, T.R. (2008) The Protein Folding Problem. *Annu. Rev. Biophys.*, **37**, 289–316.

Ding, F., Buldyrev, S. V, & Dokholyan, N. V (2005) Folding Trp-cage to NMR resolution native structure using a coarse-grained protein model. *Biophys. J.*, **88**, 147–155.

Dobson, C.M. & Karplus, M. (1999) The fundamentals of protein folding: bringing together theory and experiment. *Curr. Opin. Struct. Biol.*, **9**, 92–101.

Dong, F. & Zhou, H.-X. (2002) Electrostatic contributions to T4 lysozyme stability: solvent-exposed charges versus semi-buried salt bridges. *Biophys. J.*, **83**, 1341–1347.

Du, H.-N., Li, H.-T., Zhang, F., Lin, X.-J., Shi, J.-H., Shi, Y.-H., Ji, L.-N., Hu, J., Lin, D.-H., & Hu, H.-Y. (2006) Acceleration of alpha-synuclein aggregation by homologous peptides. *FEBS Lett.*, **580**, 3657–3664.

Eaton, W.A., Mun, V., Thompson, P.A., Henry, E.R., & Hofrichter, J. (1998) Kinetics and dynamics of loops, α-helices, β-hairpins, and fast-folding proteins. *Acc. Chem. Res.*, **31**, 745–753.

Eaton, W.A., Muñoz, V., & Hagen, S. (2000) Fast Kinetics and Mechanisms in Protein Folding 1. *Annu. Rev. Biochem.*, **29**, 327–359.

Eaton, W.A., Muñoz, V., Thompson, P. a, Chan, C.K., & Hofrichter, J. (1997) Submillisecond kinetics of protein folding. *Curr. Opin. Struct. Biol.*, **7**, 10–14.

Edison, A.S., Abildgaard, F., Westler, W.M., Mooberry, E.S., & Markley, J.L. (1994) Practical introduction to theory and implementation of multinuclear, multidimensional nuclear magnetic resonance experiments. *Meth. Enzymol.*, **239**, 3–79.

Ehrnhoefer, D.E., Bieschke, J., Boeddrich, A., Herbst, M., Masino, L., Lurz, R., Engemann, S., Pastore, A., & Wanker, E.E. (2008) EGCG redirects amyloidogenic polypeptides into unstructured, off-pathway oligomers. *Nat. Struct. Biol.*, **15**, 558–566.

Eidenschink, L., Kier, B.L., Huggins, K.N., & Andersen, N.H. (2009) Very short peptides with stable folds: building on the interrelationship of Trp/Trp, Trp/cation, and Trp/backbone-amide interaction geometries. *Proteins*, **75**, 308–322.

El-Agnaf, O.M., Paleologou, K.E., Greer, B., Abogrein, A.M., King, J.E., Salem, S.A., Fullwood, N.J., Benson, F.E., Hewitt, R., Ford, K.J., Martin, F.L., Harriott, P., Cookson, M.R., & Allsop, D. (2004) A strategy for designing inhibitors of alpha-

synuclein aggregation and toxicity as a novel treatment for Parkinson's disease and related disorders. *FASEB J*, **18**, 1315–1317.

Eliezer, D., Kutluay, E., Bussell, R.J., & Browne, G. (2001) Conformational properties of alpha-synuclein in its free and lipid-associated states. *J. Mol. Biol.*, **307**, 1061–1073.

Eriksen, J.L., Sagi, S.A., Smith, T.E., Weggen, S., Das, P., Mclendon, D.C., Ozols, V. V, Jessing, K.W., Zavitz, K.H., Koo, E.H., & Golde, T.E. (2003) NSAIDs and enantiomers of flurbiprofen target γ-secretase and lower Aβ42 in vivo. *J. Clin. Invest.*, **112**, 440–449.

Espinosa, J.F. & Gellman, S.H. (2000) A designed B-hairpin containing a natural hydrophobic cluster. *Angew. Chem. Int. Ed.*, **11**, 2330–2333.

Etienne, M.A., Aucoin, J.P., Fu, Y., McCarley, R.L., & Hammer, R.P. (2006) Stoichiometric inhibition of amyloid beta-protein aggregation with peptides containing alternating alpha,alpha-disubstituted amino acids. *J. Am. Chem. Soc.*, **128**, 3522–3523.

Fan, Y., Limprasert, P., Murray, I.V.J., Smith, A.C., Lee, V.M.-Y., Trojanowski, J.Q., Sopher, B.L., & La Spada, A.R. (2006) Beta-synuclein modulates alpha-synuclein neurotoxicity by reducing alpha-synuclein protein expression. *Hum. Mol. Gen.*, **15**, 3002–3011.

Ferguson, N. & Fersht, A.R. (2003) Early events in protein folding. *Curr. Opin. Struct. Biol.*, **13**, 75–81.

Fesinmeyer, R.M. (2005) Chemical Shifts Define the Structure and Folding Thermodynamics of Polypeptides. Ph.D. Thesis, University of Washington, Seattle.

Fesinmeyer, R.M., Hudson, F.M., & Andersen, N.H. (2004) Enhanced hairpin stability through loop design: the case of the protein G B1 domain hairpin. *J. Am. Chem. Soc.*, **126**, 7238–7243.

Fesinmeyer, R.M., Hudson, F.M., Olsen, K.A., White, G.W., Euser, A., & Andersen, N.H. (2005) Chemical shifts provide fold populations and register of beta hairpins and beta sheets. *J. Biomol. NMR*, **33**, 213–231.

Fink, A.L. (2006) The Aggregation and Fibrillation of α-Synuclein. *Acc. Chem. Res.*, **39**, 628–634.

Fitzpatrick, A.W.P., Debelouchina, G.T., Bayro, M.J., Clare, D.K., & Caporini, M.A. (2013) Atomic structure and hierarchical assembly of a cross-β amyloid fibril. *Proc. Natl. Acad. Sci. U. S. A.*, **5590**, 5468–5473.

Gazit, E. (2005) Mechanisms of amyloid fibril self-assembly and inhibition. Model short peptides as a key research tool. *FEBS J.*, **272**, 5971–5978.

Giasson, B.I., Murray, I. V, Trojanowski, J.Q., & Lee, V.M. (2001) A hydrophobic stretch of 12 amino acid residues in the middle of alpha-synuclein is essential for filament assembly. *J. Biol. Chem.*, **276**, 2380–2386.

Gilead, S. & Gazit, E. (2004) Inhibition of Amyloid Fibril Formation by Peptide Analogues Modified with α-Aminoisobutyric Acid. *Angew. Chem. Int. Ed.*, **116**, 4133–4136.

Gnanakaran, S. (2003) Peptide folding simulations. *Curr. Opin. Struct. Biol.*, **13**, 168–174.

Goddard, T.D. & Kneller, D.G. (2006) Sparky 3.

Goedert, M. (2001) Alpha-synuclein and neurodegenerative diseases. *Nat. Rev. Neurosci.*, **2**, 492–501.

Gordon, D.J., Tappe, R., & Meredith, S.C. (2002) Design and characterization of a membrane permeable N-methyl amino acid-containing peptide that inhibits Abeta1-40 fibrillogenesis. *J. Pept. Res.*, **60**, 37–55.

Gunther, H. (1992) *NMR Spectroscopy*. John Wiley & Sons Ltd., Chichester, UK.

Haass, C. & Selkoe, D.J. (2007) Soluble protein oligomers in neurodegeneration: lessons from the Alzheimer's amyloid beta-peptide. *Nat. Rev. Mol. Biol.*, **8**, 101–112.

Haataja, L., Gurlo, T., Huang, C.J., & Butler, P.C. (2008) Islet amyloid in type 2 diabetes, and the toxic oligomer hypothesis. *Endocr. Rev.*, **29**, 303–316.

Hałabis, A., Żmudzińska, W., Liwo, A., & Ołdziej, S. (2012) Conformational dynamics of the trp-cage miniprotein at its folding temperature. *J. Phys. Chem. B*, **116**, 6898–6907.

Hardy, J.A. & Higgins, G.A. (1992) Alzheimer's disease: The amyloid cascade hypothesis. *Science*, **256**, 184–185.

Head-Gordon, T. (2003) Minimalist models for protein folding and design. *Curr. Opin. Struct. Biol.*, **13**, 160–167.

Hellinga, H.W. (1997) Rational protein design: combining theory and experiment. *Proc. Natl. Acad. Sci. U. S. A.*, **94**, 10015–10017.

Horng, J.C., Moroz, V., Rigotti, D.J., Fairman, R., & Raleigh, D.P. (2002) Characterization of large peptide fragments derived from the N-terminal domain of the ribosomal protein L9: definition of the minimum folding motif and characterization of local electrostatic interactions. *Biochemistry*, **41**, 13360–13369.

Horovitz, A., Serrano, L., Avron, B., Bycroft, M., & Fersht, A.R. (1990) Strength and co-operativity of contributions of surface salt bridges to protein stability. *J. Mol. Biol.*, **216**, 1031–1044.

Hovmoller, S., Zhou, T., & Ohlson, T. (2002) Conformations of amino acids in proteins research papers. *Acta Crystallogr., Sect. D: Biol. Crystallogr.*, **58**, 768–776.

Hoyer, W., Antony, T., Cherny, D., Heim, G., Jovin, T.M., & Subramaniam, V. (2002) Dependence of α-Synuclein Aggregate Morphology on Solution Conditions. *J. Mol. Biol.*, **322**, 383–393.

Hoyer, W., Grönwall, C., Jonsson, A., Stahl, S., & Hard, T. (2008) Stabilization of a β-hairpin in monomeric Alzheimer's amyloid-β peptide inhibits amyloid formation. *Proc. Natl. Acad. Sci. U. S. A.*, **105**, 5099–5104.

Hu, Z., Tang, Y., Wang, H., Zhang, X., & Lei, M. (2008) Dynamics and cooperativity of Trp-cage folding. *Arch. Biochem. Biophys.*, **475**, 140–147.

Huang, C., Ren, G., Zhou, H., & Wang, C.C. (2005) A new method for purification of recombinant human alpha-synuclein in Escherichia coli. *PREP*, **42**, 173–177.

Huang, G.S. & Oas, G. (1995) Submillisecond folding of monomeric λ repressor. *Proc Natl Acad Sci U S A*, **92**, 6878–6882.

Hudaky, P., Straner, P., Farkas, V., Varadi, G., Toth, G., & Perczel, A. (2008) Cooperation between a salt bridge and the hydrophobic core triggers fold stabilization in a Trp-cage miniprotein. *Biochemistry*, **47**, 1007–1016.

Hudson, S.A., Ecroyd, H., Dehle, F.C., Musgrave, I.F., & Carver, J.A. (2009) (−)-Epigallocatechin-3-Gallate (EGCG) Maintains κ-Casein in Its Pre-Fibrillar State without Redirecting Its Aggregation Pathway. *J. Mol. Biol.*, **392**, 689–700.

Huggins, K.N. (2010) Designed Hairpin Peptides: Protein Folding Models and Inhibitors of Amyloid Fibril Formation. Ph.D. Thesis, University of Washington, Seattle.

Huggins, K.N., Bisaglia, M., Bubacco, L., Tatarek-Nossol, M., Kapurniotu, A., & Andersen, N.H. (2011) Designed hairpin peptides interfere with amyloidogenesis pathways: fibril formation and cytotoxicity inhibition, interception of the preamyloid state. *Biochemistry*, **50**, 8202–8212.

Hughes, R.M. & Waters, M.L. (2006a) Effects of lysine acetylation in a β-hairpin peptide: Comparison of an amide-π and a cation-π interaction. *J. Am. Chem. Soc.*, **128**, 13586–13591.

Hughes, R.M. & Waters, M.L. (2006b) Model systems for beta-hairpins and beta-sheets. *Curr. Opin. Struct. Biol.*, **16**, 514–524.

Huyghues-Despointes, B.M.P., Qu, X., Tsai, J., & Scholtz, J.M. (2006) Terminal Ion Pairs Stabilize the Second β-Hairpin of the B1 Domain of Protein G. *Proteins Struct. Funct. Bioinform*, **1017**, 1005–1017.

Hwang, T.L. & Shaka, A.J. (1995) Water Suppression That Works. Excitation Sculpting Using Arbitrary Wave-Forms and Pulsed-Field Gradients. *J. Magn. Reson., Ser A*, **112**, 275–279.

Iwai, H. & Plückthun, A. (1999) Circular beta-lactamase: stability enhancement by cyclizing the backbone. *FEBS Lett.*, **459**, 166–172.

Jao, C.C., Der-Sarkissian, A., Chen, J., & Langen, R. (2004) Structure of membrane-bound alpha-synuclein studied by site-directed spin labeling. *Proc. Natl. Acad. Sci. U. S. A.*, **101**, 8331–8336.

Jennings, P.A. & Wright, P.E. (1993) Formation of a molten globule intermediate early in the kinetic folding pathway of apomyoglobin. *Science*, **262**, 892–896.

Johnson, W.C. (1990) Protein secondary structure and circular dichroism: a practical guide. *Proteins: Struct., Funct., Genet.*, **7**, 205–215.

Juraszek, J. & Bolhuis, P.G. (2006) Sampling the multiple folding mechanisms of Trp-cage in explicit solvent. *Proc. Natl. Acad. Sci. U. S. A.*, **103**, 15859.

Juraszek, J. & Bolhuis, P.G. (2008) Rate constant and reaction coordinate of Trp-cage folding in explicit water. *Biophys. J.*, **95**, 4246–4257.

Kajava, A. V, Aebi, U., & Steven, A.C. (2005) The parallel superpleated beta-structure as a model for amyloid fibrils of human amylin. *J. Mol. Biol.*, **348**, 247–252.

Kannan, S. & Zacharias, M. (2009) Folding simulations of Trp-cage mini protein in explicit solvent using biasing potential replica-exchange molecular dynamics simulations. *Proteins*, **76**, 448–460.

Karplus, P.A. (1996) Experimentally observed conformation-dependent geometry and hidden strain in proteins. *Protein Sci.*, **5**, 1406–1420.

Karuppagounder, S.S., Pinto, J.T., Xu, H., Chen, H.-L., Beal, M.F., & Gibson, G.E. (2009) Dietary supplementation with resveratrol reduces plaque pathology in a transgenic model of Alzheimer's disease. *Neurochem. Int.*, **54**, 111–118.

Kier, B.L. & Andersen, N.H. (2008) Probing the lower size limit for protein-like fold stability: ten-residue microproteins with specific, rigid structures in water. *J. Am. Chem. Soc.*, **130**, 14675–14683.

Kim, J., Brych, S.R., Lee, J., Logan, T.M., & Blaber, M. (2003) Identification of a Key Structural Element for Protein Folding Within β-Hairpin Turns. *J. Mol. Biol.*, **328**, 951–961.

Kokkoni, N., Stott, K., Amijee, H., Mason, J.M., & Doig, A.J. (2006) N-Methylated peptide inhibitors of beta-amyloid aggregation and toxicity. Optimization of the inhibitor structure. *Biochemistry*, **45**, 9906–9918.

Kubelka, J., Hofrichter, J., & Eaton, W.A. (2004) The protein folding "speed limit". *Curr. Opin. Struct. Biol.*, **14**, 76–88.

Kuhlman, B., Boice, J.A., Fairman, R., & Raleigh, D.P. (1998) Structure and stability of the N-terminal domain of the ribosomal protein L9: evidence for rapid two-state folding. *Biochemistry*, **37**, 1025–1032.

Kukar, T.L., Ladd, T.B., Bann, M. a, Fraering, P.C., Narlawar, R., Maharvi, G.M., Healy, B., Chapman, R., Welzel, A.T., Price, R.W., Moore, B., Rangachari, V., Cusack, B., Eriksen, J.L., Jansen-West, K., Verbeeck, C., Yager, D., Eckman, C., Ye, W., Sagi, S., Cottrell, B.A., Torpey, J., Rosenberry, T.L., Fauq, A., Wolfe, M.S., Schmidt, B., Walsh, D.M., Koo, E.H., & Golde, T.E. (2008) Substrate-targeting gamma-secretase modulators. *Nature*, **453**, 925–929.

Lam, Y. & Kotowycz, G. (1977) Caution concerning the use of sodium 2,2-dimethyl-2-silapentane-5-sulfonate (DSS) as a reference for proton nmr chemical shift studies. *FEBS Lett.*, **78**, 181–183.

Lansbury, P.T. (1997) Inhibition of amyloid formation: a strategy to delat the onset of Alzheimer's disease. *Curr. Opin. Struct. Biol.*, **1**, 260–267.

Lee, S., Suh, S., & Kim, S. (2000) Protective effects of the green tea polyphenol (-)-epigallocatechin gallate against hippocampal neuronal damage after transient global ischemia in gerbils. *Neurosci. Lett.*, **287**, 191–194.

Levites, Y., Amit, T., Youdim, M.B.H., & Mandel, S. (2002) Involvement of protein kinase C activation and cell survival/ cell cycle genes in green tea polyphenol (-)-epigallocatechin 3-gallate neuroprotective action. *J. Biol. Chem.*, **277**, 30574–30580.

Levites, Y., Weinreb, O., Maor, G., Youdim, M.B.H., & Mandel, S. (2001) Green tea polyphenol (-)-epigallocatechin-3-gallate prevents N-methyl-4-phenyl-1,2,3,6-tetrahydropyridine-induced dopaminergic neurodegeneration. *J. Neurochem.*, **78**, 1073–1082.

Lin, J.C., Barua, B., & Andersen, N.H. (2004) The helical alanine controversy: an (Ala)6 insertion dramatically increases helicity. *J. Am. Chem. Soc.*, **126**, 13679–13684.

Linhananta, A., Boer, J., & MacKay, I. (2005) The equilibrium properties and folding kinetics of an all-atom Go model of the Trp-cage. *J. Chem. Phys.*, **122**, 114901.

Live, D.H., Davis, D.G., Agosta, W.C., & Cowburn, D. (1984) Long Range Hydrogen Bond Mediated Effects in Peptides: 15N NMR Study of Gramicidin S in Water and Organic Solvents. *J. Am. Chem. Soc.*, **106**, 1939–1941.

Lo, W.C., Lee, C.C., Lee, C.Y., & Lyu, P.C. (2009) CPDB: a database of circular permutation in proteins. *Nucleic Acids Res.*, **37**, D328–32.

Loladze, V. V, Ibarra-Molero, B., Sanchez-Ruiz, J.M., & Makhatadze, G.I. (1999) Engineering a thermostable protein via optimization of charge-charge interactions on the protein surface. *Biochemistry*, **38**, 16419–16423.

Lorenzo, A. & Yankner, B. (1994) β-Amyloid neurotoxicity requires fibril formation and is inhibited by Congo red. *Proc. Natl. Acad. Sci. U. S. A.*, **91**, 12243–12247.

Luca, S., Yau, W.-M., Leapman, R., & Tycko, R. (2007) Peptide conformation and supramolecular organization in amylin fibrils: constraints from solid-state NMR. *Biochemistry*, **46**, 13505–13522.

Ma, B., Elkayam, T., Wolfson, H., & Nussinov, R. (2003) Protein-protein interactions: structurally conserved residues distinguish between binding sites and exposed protein surfaces. *Proc. Natl. Acad. Sci. U. S. A.*, **100**, 5772–5777.

Madine, J., Doig, A.J., & Middleton, D.A. (2008) Design of an N-Methylated Peptide inhibitot of α-Synuclein Aggregation Guided by Solid_State NMR. *J. Am. Chem. Soc.*, **130**, 7873–7881.

Makhatadze, G.I., Loladze, V. V, Ermolenko, D.N., Chen, X., & Thomas, S.T. (2003) Contribution of surface salt bridges to protein stability: guidelines for protein engineering. *J. Mol. Biol.*, **327**, 1135–1148.

Marambaud, P., Zhao, H., & Davies, P. (2005) Resveratrol promotes clearance of Alzheimer's disease amyloid-beta peptides. *J. Biol. Chem.*, **280**, 37377–37382.

Marinelli, F., Pietrucci, F., Laio, A., & Piana, S. (2009) A kinetic model of trp-cage folding from multiple biased molecular dynamics simulations. *PLoS Comput. Biol.*, **5**, e1000452.

Matthews, B.W., Nicholson, H., & Becktel, W.J. (1987) Enhanced protein thermostability from site-directed mutations that decrease the entropy of unfolding. *Proc. Natl. Acad. Sci. U. S. A.*, **84**, 6663–6667.

McMillan, A.W., Kier, B.L., Shu, I., Byrne, A., Andersen, N.H., & Parson, W.W. (2013) Fluorescence of Tryptophan in Designed Hairpin and Trp-Cage Miniproteins: Measurements of Fluorescence Yields and Calculations by Quantum Mechanical Molecular Dynamics Simulations. *J. Phys. Chem. B*, **117**, 1790–1809.

Meier, J.J., Kayed, R., Lin, C.-Y., Gurlo, T., Haataja, L., Jayasinghe, S., Langen, R., Glabe, C.G., & Butler, P.C. (2006) Inhibition of human IAPP fibril formation does not prevent beta-cell death: evidence for distinct actions of oligomers and fibrils of human IAPP. *Am. J. Physiol. Endocrinol. Metab.*, **291**, E1317–24.

Millhauser, G.L. (1995) Views of Helical Peptides: A Proposal for the Position of 310-Helix along the Thermodynamic Folding Pathway. *Biochemistry*, **34**, 3873–3877.

Mok, K.H., Kuhn, L.T., Goez, M., Day, I.J., Lin, J.C., Andersen, N.H., & Hore, P.J. (2007) A pre-existing hydrophobic collapse in the unfolded state of an ultrafast folding protein. *Nature*, **447**, 106–109.

Munishkina, L.A., Phelan, C., Uversky, V.N., & Fink, A.L. (2003) Conformational Behavior and Aggregation of α-Synuclein in Organic Solvents : Modeling the Effects of Membranes. *Biochemistry*, **42**, 2720–2730.

Muñoz, V., Thompson, P.A., Hofrichter, J., & Eaton, W.A. (1997) Folding dynamics and mechanism of beta-hairpin formation. *Nature*, **390**, 196–199.

Myers, J.K. & Oas, T.G. (2001) Preorganized secondary structure as an important determinant of fast protein folding. *Nat. Struct. Biol.*, **8**, 552–558.

Myers, J.K. & Oas, T.G. (2002) Mechanism of Fast Protein Folding. *Annu. Rev. Biochem.*, **71**, 783–815.

Myers, J.K., Pace, C.N., & Scholtz, J.M. (1998) Trifluoroethanol effects on helix propensity and electrostatic interactions in the helical peptide from ribonuclease T1. *Protein Sci.*, **7**, 383–388.

Naduthambi, D. & Zondlo, N.J. (2006) Stereoelectronic tuning of the structure and stability of the trp cage miniprotein. *J. Am. Chem. Soc.*, **128**, 12430–12431.

Nagai, Y. (2000) Inhibition of Polyglutamine Protein Aggregation and Cell Death by Novel Peptides Identified by Phage Display Screening. *J. Biol. Chem.*, **275**, 10437–10442.

Nagai, Y., Inui, T., Popiel, H.A., Fujikake, N., Hasegawa, K., Urade, Y., Goto, Y., Naiki, H., & Toda, T. (2007) A toxic monomeric conformer of the polyglutamine protein. *Nat. Struct. Mol. Biol.*, **14**, 332–340.

Naganathan, A.N. (2012) Predictions from an Ising-like Statistical Mechanical Model on the Dynamic and Thermodynamic Effects of Protein Surface Electrostatics. *J. Chem. Theory Comput.*, **8**, 4646–4656.

Nanjo, F., Goto, K., Seto, R., Suzuki, M., Sakai, M., & Hara, Y. (1996) Scavenging effects of tea catechins and their derivatives on 1,1-diphenyl-2-picrylhydrazyl radical. *Free Radic. Biol. Med.*, **21**, 895–902.

Narhi, L., Wood, S.T., Steavenson, S., Jiang, Y., Wu, G.M., Anafi, D., Kaufman, S.A., Martin, F., Sitney, K., Denis, P., Louis, J., Wypych, J., Biere, A.L., & Citron, M. (1999) Both Familial Parkinson's Disease Mutations Accelerate alpha-Synuclein Aggregation. *J. Biol. Chem.*, **274**, 9843–9846.

Nauli, S., Kuhlman, B., & Baker, D. (2001) Computer-based redesign of a protein folding pathway. *Nat. Struct. Biol.*, **8**, 602–605.

Neidigh, J.W. (1999) Chemical shift tools in peptide folding and miniature protein design. Ph.D. Thesis, University of Washington, Seattle.

Neidigh, J.W., Fesinmeyer, R.M., & Andersen, N.H. (2002) Designing a 20-residue protein. *Nat. Struct. Biol.*, **9**, 425–430.

Neidigh, J.W., Fesinmeyer, R.M., Prickett, K.S., & Andersen, N.H. (2001) Exendin-4 and Glucagon-like-peptide-1: NMR Structural Comparisons in the Solution and Micelle-Associated States. *Biochemistry*, **40**, 13188–13200.

Nerelius, C., Sandegren, A., Sargsyan, H., Raunak, R., Leijonmarck, H., Chatterjee, U., Fisahn, A., & Imarisio, S. (2009) Alpha-helix targeting reduces amyloid-β peptide toxicity. *Proc. Natl. Acad. Sci. U. S. A.*, **106**, 9191–9196.

Neuman, R.C. & Gerig, J.T. (2008) Solvent interactions with the Trp-cage peptide in 35% ethanol-water. *Biopolymers*, **89**, 862–872.

Neuweiler, H., Doose, S., & Sauer, M. (2005) A microscopic view of miniprotein folding: enhanced folding efficiency through formation of an intermediate. *Proc. Natl. Acad. Sci. U. S. A.*, **102**, 16650–16655.

Nicholson, H., Söderlind, E., Tronrud, D.E., & Matthews, B.W. (1989) Contributions of left-handed helical residues to the structure and stability of bacteriophage T4 lysozyme. *J. Mol. Biol.*, **210**, 181–193.

Olsen, K.A., Fesinmeyer, R.M., Stewart, J.M., & Andersen, N.H. (2005) Hairpin folding rates reflect mutations within and remote from the turn region. *Proc. Natl. Acad. Sci. U. S. A.*, **102**, 15483–15487.

Onuchic, J.N. & Wolynes, P.G. (2004) Theory of protein folding. *Curr. Opin. Struct. Biol.*, **14**, 70–75.

Pace, C.N. & Scholtz, J.M. (1998) A helix propensity scale based on experimental studies of peptides and proteins. *Biophys. J.*, **75**, 422–427.

Padrick, S.B. & Miranker, A.D. (2002) Islet amyloid: phase partitioning and secondary nucleation are central to the mechanism of fibrillogenesis. *Biochemistry*, **41**, 4694–4703.

Pande, V.S., Grosberg AYu, Tanaka, T., & Rokhsar, D.S. (1998) Pathways for protein folding: is a new view needed? *Current opinion in structural biology*, **8**, 68–79.

Pandey, A.K., Naduthambi, D., Thomas, K.M., & Zondlo, N.J. (2013) Proline Editing: A General and Practical Approach to the Synthesis of Functionally and Structurally Diverse Peptides. Analysis of Steric versus Stereoelectronic Effects of 4-Substituted Prolines on Conformation within Peptides. *J. Am. Chem. Soc.*, **135**, 4333–4363.

Petkova, A.T., Ishii, Y., Balbach, J.J., Antzutkin, O.N., Leapman, R.D., Delaglio, F., & Tycko, R. (2002) A structural model for Alzheimer's β-amyloid fibrils based on experimental constraints from solid state NMR. *Proc. Natl. Acad. Sci. U. S. A.*, **99**, 16742–16747.

Piotto, M., Saudek, V., & Sklenar, V. (1992) Gradient-tailored excitation for single-quantum NMR spectroscopy of aqueous solutions. *J. Biomol. NMR*, **2**, 661–665.

Plaxco, K.W., Riddle, D.S., Grantcharova, V., & Baker, D. (1998) Simplified proteins: minimalist solutions to the "protein folding problem". *Curr*, **8**, 80–85.

Porat, Y., Mazor, Y., Efrat, S., & Gazit, E. (2004) Inhibition of Islet Amyloid Polypeptide Fibril Formation: A Potential Role for Heteroaromatic Interactions. *Biochemistry*, **43**, 14454–14462.

Ptitsyn, O.B., Pain, R.H., Semisotnov, G. V, Zerovnik, E., & Razgulyaev, O.I. (1990) Evidence for a molten globule state as a general intermediate in protein folding. *FEBS Lett.*, **262**, 20–24.

Qiu, L.L., Pabit, S.A., Roitberg, A.E., & Hagen, S.J. (2002) Smaller and faster: The 20-residue Trp-cage protein folds in 4 μs. *J. Am. Chem. Soc.*, **124**, 12952–12953.

Ramirez-Alvarado, M., Blanco, F.J., & Serrano, L. (2001) Elongation of the BH8 β-hairpin peptide : Electrostatic interactions in β-hairpin formation and stability. *Protein Sci.*, **10**, 1381–1392.

Reznichenko, L., Amit, T., Youdim, M.B.H., & Mandel, S. (2005) Green tea polyphenol (-)-epigallocatechin-3-gallate induces neurorescue of long-term serum-deprived PC12 cells and promotes neurite outgrowth. *J. Neurochem.*, **93**, 1157–1167.

Riemen, A.J. & Waters, M.L. (2009) Controlling peptide folding with repulsive interactions between phosphorylated amino acids and tryptophan. *J. Am. Chem. Soc.*, **131**, 14081–14087.

Ro, S., Lee, H.J., Ahn, I. a, Shin, D.K., Lee, K.B., Yoon, C.J., & Choi, Y.S. (2001) Torsion angle based design of peptidomimetics: a dipeptidic template adopting beta-I turn (Ac-Aib-AzGly--NH(2)). *Bioorg. Med. Chem.*, **9**, 1837–1841.

Roberts, B.E. & Shorter, J. (2008) Escaping amyloid fate. *Nature*, **15**, 544–546.

Robinson, J.A., Shankaramma, S.C., Jetter, P., Kienzl, U., Schwendener, R.A., Vrijbloed, J.W., & Obrecht, D. (2005) Properties and structure-activity studies of cyclic beta-hairpin peptidomimetics based on the cationic antimicrobial peptide protegrin I. *Bioorg. Med. Chem.*, **13**, 2055–2064.

Rochet, J.C. & Lansbury, P.T. (2000) Amyloid fibrillogenesis: themes and variations. *Curr. Opin. Struct. Biol.*, **10**, 60–68.

Rodriguez-Granillo, A., Annavarapu, S., Zhang, L., Koder, R.L., & Nanda, V. (2011) Computational design of thermostabilizing D-amino acid substitutions. *J. Am. Chem. Soc.*, **133**, 18750–18759.

Rovo, P., Farkas, V., Hegyi, O., Szolomajer-Csikos, O., Toth, G.K., & Perczel, A. (2011) Cooperativity network of Trp-cage miniproteins: probing salt-bridges. *J. Pept. Sci.*, **17**, 610–619.

Rovó, P., Stráner, P., Láng, A., Bartha, I., Huszár, K., Nyitray, L., & Perczel, A. (2013) Structural insights into the Trp-cage folding intermediate formation. *Chemistry*, **19**, 2628–2640.

Ruschak, A.M. & Miranker, A.D. (2007) Fiber-dependent amyloid formation as catalysis of an existing reaction pathway. *Proc. Natl. Acad. Sci. U. S. A.*, **104**, 12341–12346.

Sali, D., Bycroft, M., & Fersht, A.R. (1991) Surface electrostatic interactions contribute little of stability of barnase. *J. Mol. Biol.*, **220**, 779–788.

Sandstrom, J. (1982) *Dynamic NMR Spectroscopy*. Academic Press, New York.

Sato, T., Kienlen-Campard, P., Ahmed, M., Liu, W., Li, H., Elliott, J.I., Aimoto, S., Constantinescu, O.S.N., Octave, J.-N., & Smith, S.O. (2006) Inhibitors of amyloid toxicity based on β-sheet packing of Aβ 40 and Aβ 42. *Biochemistry*, **45**, 5503–5516.

Schneider, J.P. & DeGrado, W.F. (1998) The Design of Efficient α-Helical C-Capping Auxiliaries. *J. Am. Chem. Soc.*, **120**, 2764–2767.

Scholtz, J.M., Marqusee, S., Baldwin, R.L., York, E.J., Stewart, J.M., Santoro, M., & Bolen, D.W. (1991) Calorimetric determination of the enthalpy change for the α-helix to coil transition of an alanine peptide in water. *Proc. Natl. Acad. Sci. U. S. A.*, **88**, 2854–2858.

Scian, M., Lin, J.C., Le, I., Makhatadze, G.I., & Stenkamp, R.E. (2012) Crystal and NMR structures of a Trp-cage mini-protein benchmark for computational fold prediction. *Proc. Natl. Acad. Sci. U. S. A.*, **109**, 1–5.

Sciarretta, K.L., Gordon, D.J., & Meredith, S.C. (2006) Peptide-Based Inhibitors of Amyloid Assembley. *Meth. Enzymol.*, **413**, 273–312.

Searle, M.S. & Ciani, B. (2004) Design of beta-sheet systems for understanding the thermodynamics and kinetics of protein folding. *Curr. Opin. Struct. Biol.*, **14**, 458–464.

Shimizu, A., Ikeguchi, M., & Sugai, S. (1994) Appropriateness of DSS and TSP as internal references for 1H NMR studies of molten globule proteins in aqueous media. *J. Biomol. NMR*, **4**, 859–862.

Shu, I. (2011) Thermodynamics and Kinetics of Beta-Sheet Folding Models. Ph.D. Thesis, University of Washington, Seattle.

Simmerling, C., Strockbine, B., & Roitberg, A.E. (2002) All-atom structure prediction and folding simulations of a stable protein. *J. Am. Chem. Soc.*, **124**, 11258–11259.

Smith, T.J., Stains, C.I., Meyer, S.C., & Ghosh, I. (2006) Inhibition of beta-amyloid fibrillization by directed evolution of a beta-sheet presenting miniature protein. *J. Am. Chem. Soc.*, **128**, 14456–14457.

Snow, C.D., Zagrovic, B., & Pande, V.S. (2002) The Trp cage: folding kinetics and unfolded state topology via molecular dynamics simulations. *J. Am. Chem. Soc.*, **124**, 14548–14549.

Spector, S. & Raleigh, D.P. (1999) Submillisecond folding of the peripheral subunit-binding domain. *J. Mol. Biol.*, **293**, 763–768.

Stains, C.I., Mondal, K., & Ghosh, I. (2007) Molecules that target beta-amyloid. *ChemMedChem*, **2**, 1674–1692.

Stewart, J.M. (2009) The Use of 13C Carbonyl Labeled Residues to Develop and Refine Site-Specific NMR Secondary Structure Analysis Techniques. Ph.D. Thesis, University of Washington, Seattle.

Takahashi, T. & Mihara, H. (2008) Peptide and proteins mimetics inhibiting amyloid β-peptide aggregation. *Acc. Chem. Res.*, **41**, 1309–1318.

Thornton, J.M. & Sibanda, B.L. (1983) Amino and Carboxy-terminal Regions in Globular Proteins Department of Crystallography. *J. Mol. Biol.*, **167**, 443–460.

Tissot, A.C., Vuilleumier, S., & Fersht, A.R. (1996) Importance of two buried salt bridges in the stability and folding pathway of barnase. *Biochemistry*, **35**, 6786–6794.

Toniolo, C., Crisma, M., Formaggio, F., & Peggion, C. (2001) Control of Peptide Conformation by the Thorpe – Ingold Effect (Ca-Tetrasubstitution). *Biopolymers*, **60**, 396–419.

Trabi, M. & Craik, D.J. (2002) Circular proteins--no end in sight. *Trends Biochem. Sci.*, **27**, 132–138.

Tripathi, S., Makhatadze, G.I., & Garcia, A.E. (2013) Backtracking due to residual structure in the unfolded state changes the folding of the third fibronectin type III domain from tenascin-C. *J. Phys. Chem. B*, **117**, 800–810.

Uéda, K., Fukushima, H., Masliah, E., Xia, Y., Iwai, A., Yoshimoto, M., Otero, D. a, Kondo, J., Ihara, Y., & Saitoh, T. (1993) Molecular cloning of cDNA encoding an unrecognized component of amyloid in Alzheimer disease. *Proc. Natl. Acad. Sci. U. S. A.*, **90**, 11282–11286.

Ulmer, T.S. & Bax, A. (2005) Comparison of structure and dynamics of micelle-bound human alpha-synuclein and Parkinson disease variants. *J. Biol. Chem.*, **280**, 43179–43187.

Vilar, M., Chou, H.-T., Lührs, T., Maji, S.K., Riek-Loher, D., Verel, R., Manning, G., Stahlberg, H., & Riek, R. (2008) The fold of alpha-synuclein fibrils. *Proc. Natl. Acad. Sci. U. S. A.*, **105**, 8637–8642.

Vingtdeux, V., Giliberto, L., Zhao, H., Chandakkar, P., Wu, Q., Simon, J.E., Janle, E.M., Lobo, J., Ferruzzi, M.G., Davies, P., & Marambaud, P. (2010) AMP-

activated protein kinase signaling activation by resveratrol modulates amyloid-beta peptide metabolism. *J. Biol. Chem.*, **285**, 9100–9113.

Wafer, L.N., Streicher, W.W., & Makhatadze, G.I. (2010) Thermodynamics of the Trp-cage miniprotein unfolding in urea. *Proteins*, **78**, 1376–1381.

Waldburger, C.D., Schildbach, J.F., & Sauer, R.T. (1995) Are buried salt bridges important for protein stability and conformational specificity? *Nat. Struct. Biol.*, **2**, 122–128.

Wang, J. & Purisima, E.O. (1996) Analysis of Thermodynamic Determinants in Helix Propensities of Nonpolar Amino Acids through a Novel Free Energy Calculation. *J. Am. Chem. Soc.*, **118**, 995–1001.

Wang, M., Tang, Y., Sato, S., Vugmeyster, L., McKnight, C.J., & Raleigh, D.P. (2003) Dynamic NMR line-shape analysis demonstrates that the villin headpiece subdomain folds on the microsecond time scale. *J. Am. Chem. Soc.*, **125**, 6032–6033.

Werner, J.H., Dyer, R.B., Fesinmeyer, R.M., & Andersen, N.H. (2002) Dynamics of the Primary Processes of Protein Folding: Helix Nucleation. *J. Phys. Chem. B*, **106**, 487–494.

Williams, D. V, Barua, B., & Andersen, N.H. (2008) Hyperstable miniproteins: additive effects of D- and L-Ala mutations. *Org. Biomol. Chem.*, **6**, 4287–4289.

Williams, D. V, Byrne, A., Stewart, J.M., & Andersen, N.H. (2011) Concerning the Optimal Salt Bridge for Trp-cage Stabilization. *Biochemistry*, **50**, 1143–1152.

Wishart, D.S., Bigam, C.G., Yao, J., Abildgaard, F., Dyson, H.J., Oldfield, E., Markley, J.L., & Sykes, B.D. (1995) H-1, C-13 and N-15 Chemical-Shift Referencing in Biomolecular NMR. *J. Biomol. NMR*, **6**, 135–140.

Wishart, D.S., Sykes, B.D., & Richards, F.M. (1991) Relationship between nuclear magnetic resonance chemical shift and protein secondary structure. *J. Mol. Biol.*, **222**, 311–333.

Xu, W. & Mu, Y. (2008) Ab initio folding simulation of Trpcage by replica exchange with hybrid Hamiltonian. *Biophys. Chem.*, **137**, 116–125.

Yang, A. & Honig, B. (1995) Free Energy Determinants of Secondary Structure Formation : I. α-Helices. *J. Mol. Biol.*, **252**, 351–365.

Yang, J.T., Wu, C.S., & Martinez, H.M. (1986) Calculation of protein conformation from circular dichroism. *Meth. Enzymol.*, **130**, 208–269.

Yang, W., Dunlap, J.R., Andrews, R.B., & Wetzel, R. (2002) Aggregated polyglutamine peptides delivered to nuclei are toxic to mammalian cells. *Hum. Mol. Gen.*, **11**, 2905–2917.

Yang, W.Y. & Gruebele, M. (2003) Folding at the speed limit. *Nature*, **423**, 193–197.

Zhou, H.-X. (2003a) Effect of Backbone Cyclization on Protein Folding Stability: Chain Entropies of both the Unfolded and the Folded States are Restricted. *J. Mol. Biol.*, **332**, 257–264.

Zhou, R. (2003b) Trp-cage: folding free energy landscape in explicit water. *Proc. Natl. Acad. Sci. U. S. A.*, **100**, 13280–13285.

Appendix A

The Amino Acids

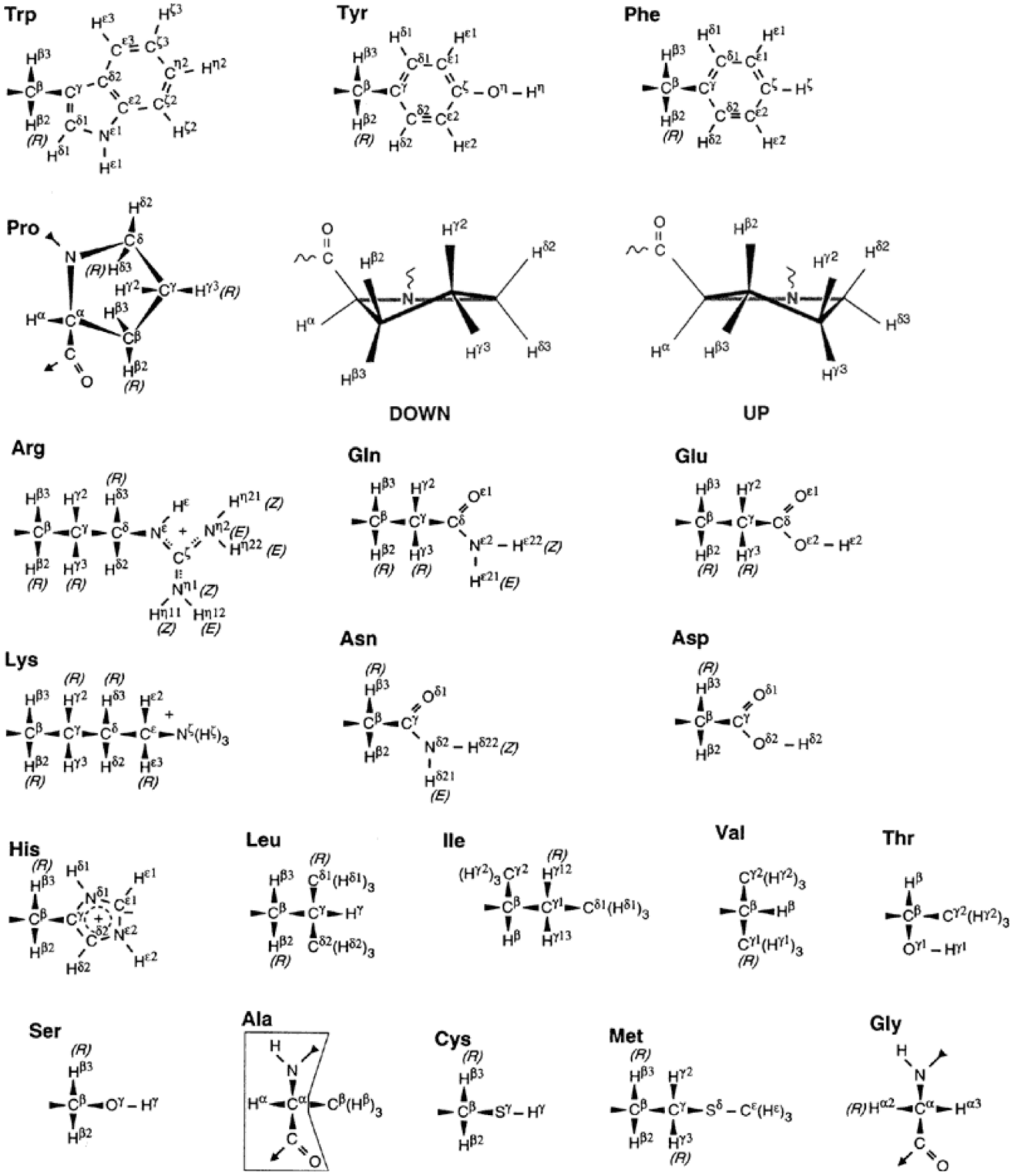

Appendix B: Chemical Shift Assignment Tables

Chemical shift assignments were collected in aqueous buffer (pH 7) at 280K unless otherwise specified. Isolated commas denote no data, horizontal lines denote not applicable.

TC10b D9R R16E

#	Res		Hα	Hβ	Hγ	Hδ	Hε	Hζ	Hη
1	Asp		4.369	3.293, 3.132	-----		-----	-----	-----
2	Ala	9.062	4.271	1.468	-----	-----	-----	-----	-----
3	Tyr	8.758	4.153	3.078,	-----	6.824	7.092	-----	
4	Ala	8.192	4.121	1.504	-----	-----	-----	-----	-----
5	Gln	8.032	4.083	2.481, 2.436	2.178, 2.138	-----	,	-----	-----
6	Trp	8.149	4.293	3.196, 3.516	-----	7.168	9.798, 7.161	7.298, 7.106	7.232
7	Leu	8.357	3.552	1.741, 1.429	1.532	0.927, 0.837	-----	-----	-----
8	Lys	7.950	4.075	1.928, 1.872	1.510, 1.439	1.679,	2.976,	7.607	-----
9	Arg	7.667	4.298	1.683, 1.928	, 1.838	3.181, 3.181	7.326	-----	,
10	Gly	7.812	3.641, 4.107	-----	-----	-----	-----	-----	-----
11	Gly		,	-----	-----	-----	-----	-----	-----
12	Pro	-----	4.559	2.030, 2.445	2.099, 2.099	3.725, 3.392	-----	-----	-----
13	Ser	8.069	4.448	3.913, 3.913		-----	-----	-----	-----
14	Ser	8.218	4.280	3.677, 3.912		-----	-----	-----	-----
15	Gly	8.100	3.870, 4.163	-----	-----	-----	-----	-----	-----
16	Asp	8.316	5.167	3.003, 2.752	-----		-----	-----	-----
17	Pro	-----	4.609	1.806, 2.198	2.000, 2.001	3.700, 3.864	-----	-----	-----
18	Pro	-----	3.315	1.546, 1.155	1.824, 1.820	3.584, 3.495	-----	-----	-----
19	Pro	-----	4.396	1.889, 2.254	1.914, 1.914	3.152, 3.323	-----	-----	-----
20	Ser	8.470	4.414	3.957, 3.829		-----	-----	-----	-----

TC10b D9R R16D

#	Res		Hα	Hβ	Hγ	Hδ	Hε	Hζ	Hη
1	Asp		4.263	3.162, 3.002	-----		-----	-----	-----
2	Ala		4.228	1.504	-----	-----	-----	-----	-----
3	Tyr	8.824	4.045	3.156, 3.156	-----	7.119	6.842	-----	
4	Ala	8.370	4.137	1.612	-----	-----	-----	-----	-----
5	Gln	8.091	4.057	2.577, 2.535	2.229, 2.169	-----	7.029^{21}, 7.664^{22}	-----	-----
6	Trp	8.171	4.121	3.134^{2}, 3.589^{3}	-----	7.102	9.627,	7.219, 6.995	7.065
7	Leu	8.495	3.332	1.872, 1.384	1.606	0.979, 0.815	-----	-----	-----
8	Lys	7.945	4.018	1.984, 1.935	1.567, 1.472	1.683,	2.975,		-----
9	Arg	7.475	4.326	1.912, 1.656	1.791,	3.279, 3.194	8.134	-----	,
10	Gly	7.570	3.509, 4.163	-----	-----	-----	-----	-----	-----
11	Gly	8.038	1.284^{2}, 2.932^{3}	-----	-----	-----	-----	-----	-----
12	Pro	-----	4.549	2.028^{2}, 2.490^{3}	2.090, 2.090	3.694^{2}, 3.123^{2}	-----	-----	-----
13	Ser	7.803	4.446	3.917, 3.917		-----	-----	-----	-----
14	Ser	8.125	4.233	3.844, 3.844		-----	-----	-----	-----
15	Gly	7.981	4.258, 3.832	-----	-----	-----	-----	-----	-----
16	Glu	8.154	4.804	2.149, 1.996	2.407, 2.345	-----		-----	-----
17	Pro	-----	4.679	2.022^{2}, 2.317^{3}	2.266, 2.266	3.728^{2}, 3.926^{3}	-----	-----	-----
18	Pro	-----	2.557	, 0.597^{3}	1.752, 1.375	3.525, 3.525	-----	-----	-----
19	Pro	-----	4.318	1.995^{2}, 2.225^{3}	1.943, 1.943	2.890^{2}, 3.030^{3}	-----	-----	-----
20	Ser	8.012	4.170	3.785, 3.785		-----	-----	-----	-----

TC13b A4G

#	Res		Hα	Hβ	Hγ	Hδ	Hε	Hζ	Hη
1	Asp		4.276	2.986^{2},3.208^{3}	-----		-----	-----	-----
2	Ala	9.066	4.285	1.498	-----	-----	-----	-----	-----
3	Tyr	9.084	4.045	3.099^{2}, 3.099^{3}	-----	7.095	6.824	-----	
4	Gly	8.704	4.142, 3.806	-----	-----	-----	-----	-----	-----
5	Gln	8.457	4.028	2.400, 2.400	2.213, 2.151	-----	7.074^{21},7.869^{22}	-----	-----
6	Trp	8.068	4.234	3.135^{2}, 3.585^{3}	-----	6.984	9.730, 7.003	7.183,7.128	7.220
7	Leu	8.530	3.388	1.906^{2}, 1.379^{3}	1.632	0.995^{1},0.875^{2}	-----	-----	-----
8	Ala	8.243	4.035	1.477	-----	-----	-----	-----	-----
9	Asp	7.914	4.551	2.736^{2}, 2.916^{3}	-----		-----	-----	-----
10	Gly	7.624	3.494^{2},4.163^{3}	-----	-----	-----	-----	-----	-----
11	Gly	8.525	0.655^{2},3.127^{3}	-----	-----	-----	-----	-----	-----
12	Pro	-----	4.617	2.031^{2}, 2.520^{3}	2.162^{2},2.162^{3}	3.800^{2},3.491^{3}	-----	-----	-----
13	Ala	7.486	4.331	1.390	-----	-----	-----	-----	-----
14	Ser	7.873	4.321	3.804^{2},3.804^{3}		-----	-----	-----	-----
15	Gly	7.987	3.781^{2},4.162^{3}	-----	-----	-----	-----	-----	-----
16	Arg	8.181	5.090	1.658^{2}, 1.924^{3}	1.816^{2}, 1.816^{3}	3.322, 3.223	7.755	-----	,
17	Pro	-----	4.772	1.772^{2}, 2.352^{3}	1.997^{2}, 1.997^{3}	3.681^{2}, 3.871^{3}	-----	-----	-----
18	Pro	-----	2.413	0.192^{2}, 1.301^{3}	1.717^{2}, 1.647^{3}	3.523^{2}, 3.523^{3}	-----	-----	-----
19	Pro	-----	4.344	1.805^{2}, 2.216^{3}	1.987^{2}, 1.987^{3}	2.951^{2}, 3.169^{3}	-----	-----	-----
20	Ser	8.110	4.237	3.846^{2}, 3.846^{3}		-----	-----	-----	-----

TC13b L7W

#	Res		Hα	Hβ	Hγ	Hδ	Hε	Hζ	Hη
1	Asp		4.292	2.982, 3.176	-----		-----	-----	-----
2	Ala		4.293	1.487	-----	-----	-----	-----	-----
3	Tyr	8.764	4.111	3.251, 3.170	-----	7.198	6.822	-----	
4	Ala	8.395	4.393	1.633	-----	-----	-----	-----	-----
5	Gln	8.247	4.044	2.424, 2.422	2.237, 2.147	-----	7.072, 7.831	-----	-----
6	Trp	8.154	4.240	3.140, 3.495	-----	6.912	9.628, 6.712	7.074, 6.620	7.053
7	Trp	8.565	3.742	3.286, 3.171	-----	7.092	9.982, 7.505	7.659, 7.177	7.335
8	Ala	8.521	4.116	1.546	-----	-----	-----	-----	-----
9	Asp	7.815	4.568	2.731, 2.906	-----		-----	-----	-----
10	Gly	7.638	3.444, 4.118	-----	-----	-----	-----	-----	-----
11	Gly		0.224, 2.475	-----	-----	-----	-----	-----	-----
12	Pro	-----	4.484	2.003, 2.475	2.143, 2.142	3.600, 3.098	-----	-----	-----
13	Ala	7.362	4.318	1.358	-----	-----	-----	-----	-----
14	Ser	8.127	4.065	3.398, 3.805		-----	-----	-----	-----
15	Gly	7.842	3.777, 4.252	-----	-----	-----	-----	-----	-----
16	Arg	8.128	5.067	1.612, 1.881	1.775, 1.776	3.283, 3.203	7.686	-----	, , ,
17	Pro	-----	4.721	1.750, 2.328	1.972, 1.973	3.651, 3.847	-----	-----	-----
18	Pro	-----	2.346	1.229, 0.177	1.587, 1.671	3.463, 3.465	-----	-----	-----
19	Pro	-----	4.268	1.878, 2.146	1.668, 1.668	2.692, 2.973	-----	-----	-----
20	Ser	7.914	4.157	3.787, 3.784		-----	-----	-----	-----

TC13b P18W

#	Res		Hα	Hβ	Hγ	Hδ	Hε	Hζ	Hη
1	Asp		4.300	2.995, 3.185	-----		-----	-----	-----
2	Ala	8.605	4.314	1.594	-----	-----	-----	-----	-----
3	Tyr	8.691	3.841	2.946, 2.945	-----	5.974	6.515	-----	
4	Ala	8.260	3.932	1.512	-----	-----	-----	-----	-----
5	Gln	8.079	3.964	2.181,	2.421,	-----	,	-----	-----
6	Trp	8.050	4.218	3.253, 3.292	-----	7.155	10.084, 7.327, 7.023		7.206
7	Leu	8.305	3.304	,		0.704, 0.588	-----	-----	-----
8	Ala	8.136	4.017	1.458	-----	-----	-----	-----	-----
9	Asp	7.904	4.562	2.729, 2.907	-----		-----	-----	-----
10	Gly	7.611	3.503, 4.139	-----	-----	-----	-----	-----	-----
11	Gly	8.127	0.944, 1.699	-----	-----	-----	-----	-----	-----
12	Pro	-----	4.539	, 2.518	2.138, 2.033	3.737, 3.365	-----	-----	-----
13	Ala	7.540	4.330	1.398	-----	-----	-----	-----	-----
14	Ser	7.925	4.315	3.804, 3.804		-----	-----	-----	-----
15	Gly	7.700	3.760, 4.142	-----	-----	-----	-----	-----	-----
16	Arg			,	,	,		-----	, , ,
17	Pro	-----		,	,	,	-----	-----	-----
18	Trp			,	-----	6.714	9.901,	,	
19	Pro	-----		,	,	,	-----	-----	-----
20	Ser			,		-----	-----	-----	-----

TC13b P18W ***pH 2.5***

#	Res		Hα	Hβ	Hγ	Hδ	Hε	Hζ	Hη
1	Asp		4.398	3.188, 3.379	-----		-----	-----	-----
2	Ala	9.086	4.366	1.627	-----	-----	-----	-----	-----
3	Tyr	8.793	3.655	2.765, 2.764	-----	6.400	6.594	-----	
4	Ala	8.122	3.918	1.481	-----	-----	-----	-----	-----
5	Gln	7.875	4.050	2.193, 2.161	2.473, 2.419	-----	,	-----	-----
6	Trp	8.101	4.272	3.268, 3.441	-----	7.274	10.107, 7.057	, 7.213	7.407
7	Leu	8.454	3.413	, 1.362	1.592	0.797, 0.745	-----	-----	-----
8	Ala	7.956	4.112	1.446	-----	-----	-----	-----	-----
9	Asp	7.747	4.758	2.928, 3.074	-----		-----	-----	-----
10	Gly	7.707	3.555, 4.136	-----	-----	-----	-----	-----	-----
11	Gly	8.084	, 2.567	-----	-----	-----	-----	-----	-----
12	Pro	-----	4.398	2.050, 2.431	2.050, 1.976	3.550, 3.014	-----	-----	-----
13	Ala	7.672	4.308	1.389	-----	-----	-----	-----	-----
14	Ser	8.101	4.242	3.822, 3.971		-----	-----	-----	-----
15	Gly	7.771	3.595, 4.112	-----	-----	-----	-----	-----	-----
16	Arg	8.028	4.827	1.825, 1.924	1.661, 1.660	3.254, 3.252	7.372	-----	, , ,
17	Pro	-----	4.588	1.784, 2.253	1.983, 1.983	3.631, 3.827	-----	-----	-----
18	Trp	8.218	3.960	2.550, 2.059	-----	6.896	9.909, 6.931	7.414, 7.072	7.258
19	Pro	-----	4.251	1.729, 2.034	1.636, 1.636	2.562, 3.177	-----	-----	-----
20	Ser	7.971	4.255	3.863, 3.863		-----	-----	-----	-----

TC13b P18W ***pH 2.5 Isomer***

#	Res		Hα	Hβ	Hγ	Hδ	Hε	Hζ	Hη
1	Asp			,	-----		-----	-----	-----
2	Ala	9.103	4.432	1.731	-----	-----	-----	-----	-----
3	Tyr		3.274	, 2.604	-----	6.083	6.551	-----	
4	Ala				-----	-----	-----	-----	-----
5	Gln	7.770	4.042	2.217, 2.165	2.468, 2.421	-----	,	-----	-----
6	Trp	8.037	4.231	3.260,	-----		, 6.934	, 7.004	7.139
7	Leu	8.404	3.334	1.532, 1.206	1.259	0.749, 0.653	-----	-----	-----
8	Ala	8.017	4.076	1.436	-----	-----	-----	-----	-----
9	Asp	7.720	4.731	2.928, 3.088	-----		-----	-----	-----
10	Gly	7.658	3.863, 4.191	-----	-----	-----	-----	-----	-----
11	Gly	8.103	, 2.713	-----	-----	-----	-----	-----	-----
12	Pro	-----	4.488	2.079, 2.476	2.079,	3.638, 3.197	-----	-----	-----
13	Ala	7.614	4.317	1.394	-----	-----	-----	-----	-----
14	Ser	8.115	4.227	3.828, 3.965		-----	-----	-----	-----
15	Gly	7.989	3.843, 4.246	-----	-----	-----	-----	-----	-----
16	Arg	8.089	4.887	1.711, 1.999	1.897,	3.302,	7.455	-----	, , ,
17	Pro	-----	4.694	1.861, 2.239	1.947, 1.947	3.714, 3.830	-----	-----	-----
18	Trp	8.131		, 2.035	-----	6.765	9.980,	7.470, 6.973	7.179
19	Pro	-----	4.251	1.725, 2.040	1.633, 1.626	2.561, 3.182	-----	-----	-----
20	Ser			,		-----	-----	-----	-----

TC13b P19W

#	Res		Hα	Hβ	Hγ	Hδ	Hε	Hζ	Hη
1	Asp		4.254	2.962, 3.100	-----		-----	-----	-----
2	Ala		4.259	1.463	-----	-----	-----	-----	-----
3	Tyr	8.448	4.192	3.035, 2.974	-----	6.922	6.763	-----	
4	Ala	8.196	4.032	1.507	-----	-----	-----	-----	-----
5	Gln	8.167	4.000	2.142, 2.095	2.406, 2.406	-----	7.022, 7.843	-----	-----
6	Trp	8.151	4.316	3.230, 3.523	-----	7.097	10.003, 7.194	7.290, 7.111	7.204
7	Leu	8.348	3.521	1.705, 1.377	1.463	0.837, 0.809	-----	-----	-----
8	Ala	8.082	4.043	1.450	-----	-----	-----	-----	-----
9	Asp	7.972	4.572	2.702, 2.808	-----		-----	-----	-----
10	Gly	7.699	3.592, 4.083	-----	-----	-----	-----	-----	-----
11	Gly	8.246	1.894, 3.126	-----	-----	-----	-----	-----	-----
12	Pro	-----	4.497	2.028, 2.404	2.073,	3.646, 3.336	-----	-----	-----
13	Ala	7.949	4.272	1.397	-----	-----	-----	-----	-----
14	Ser	8.218	4.251	3.903, 3.706		-----	-----	-----	-----
15	Gly	7.532	3.690, 4.131	-----	-----	-----	-----	-----	-----
16	Arg	8.065	4.614	1.515, 1.740	1.640,	3.131,	7.332	-----	, , ,
17	Pro	-----	4.365	1.170, 1.764	1.791,	3.469, 3.708	-----	-----	-----
18	Pro	-----	3.581	1.537, 1.512	1.677, 1.677	3.210, 3.317	-----	-----	-----
19	Trp	7.145	4.557	3.147, 3.147	-----	7.076	10.159, 7.445	7.402, 7.049	7.162
20	Ser			,		-----	-----	-----	-----

TC13b P12W P17A

#	Res		Hα	Hβ	Hγ	Hδ	Hε	Hζ	Hη
1	Asp		4.290	2.978, 3.180	-----		-----	-----	-----
2	Ala	9.055	4.258	1.490	-----	-----	-----	-----	-----
3	Tyr	8.851	3.955	3.099, 3.099	-----	7.040	6.772	-----	
4	Ala	8.311	4.090	1.575	-----	-----	-----	-----	-----
5	Gln	8.119	3.956	2.194, 2.127	2.389,	-----	7.051, 7.828	-----	-----
6	Trp	8.020	4.130	3.054, 3.445	-----	6.766	9.411, 6.800	5.768, 6.851	6.031
7	Leu	8.374	3.274	1.817, 1.345	1.552	0.959, 0.835	-----	-----	-----
8	Ala	8.231	4.018	1.465	-----	-----	-----	-----	-----
9	Asp	7.858	4.526	2.691, 2.892	-----		-----	-----	-----
10	Gly	7.543	4.159, 3.459	-----	-----	-----	-----	-----	-----
11	Gly	8.317	0.274, 2.984	-----	-----	-----	-----	-----	-----
12	Trp	9.014	4.645	3.576, 3.173	-----	7.598	10.554, 7.918	7.619, 7.244	7.333
13	Ala	7.862	4.420	1.461	-----	-----	-----	-----	-----
14	Ser	7.989	4.124	3.461, 3.860	4.993	-----	-----	-----	-----
15	Gly	7.993	4.370, 3.844	-----	-----	-----	-----	-----	-----
16	Arg	8.119	4.861	1.825, 1.523	1.745,	3.255, 3.164	7.644	-----	, , ,
17	Ala	8.552	3.928	1.322	-----	-----	-----	-----	-----
18	Pro	-----	2.163	1.074, -0.493	1.538, 1.165	3.254, 2.389	-----	-----	-----
19	Pro	-----	4.297	1.970, 2.166	1.804, 1.736	2.870, 3.150	-----	-----	-----
20	Ser	7.949	4.145	3.774, 3.777		-----	-----	-----	-----

TC13b P12W P18A

#	Res		Hα	Hβ	Hγ	Hδ	Hε	Hζ	Hη
1	Asp		4.251	2.962, 3.146	-----		-----	-----	-----
2	Ala		4.249	1.495	-----	-----	-----	-----	-----
3	Tyr	8.856	4.008	3.107, 3.106	-----	7.075	6.796	-----	
4	Ala	8.349	4.086	1.567	-----	-----	-----	-----	-----
5	Gln	8.130	3.969	2.124, 2.191	2.396,	-----	7.050, 7.826	-----	-----
6	Trp	8.102	4.167	3.048, 3.454	-----	6.821	9.486, 6.855	6.230, 6.835	6.120
7	Leu	8.448	3.290	1.788, 1.357	1.543	0.935, 0.817	-----	-----	-----
8	Ala	8.172	4.024	1.467	-----	-----	-----	-----	-----
9	Asp	7.861	4.539	2.701, 2.900	-----		-----	-----	-----
10	Gly	7.534	3.450, 4.140	-----	-----	-----	-----	-----	-----
11	Gly	8.324	0.480, 2.981	-----	-----	-----	-----	-----	-----
12	Trp	8.797	4.624	3.270, 3.541	-----	7.551	10.509, 7.901	7.634, 7.278	7.359
13	Ala	7.755	4.299	1.339	-----	-----	-----	-----	-----
14	Ser	7.970	4.102	3.844, 3.440		-----	-----	-----	-----
15	Gly	7.938	3.802, 4.309	-----	-----	-----	-----	-----	-----
16	Arg	8.155	5.045	1.785, 1.880	1.591,	3.293, 3.198	7.687	-----	, , ,
17	Pro	-----	4.413	2.019, 2.339	1.932, 1.786	3.639, 3.836	-----	-----	-----
18	Ala	7.178	1.850	0.239	-----	-----	-----	-----	-----
19	Pro	-----	4.298	1.927, 2.182	1.738, 1.738	2.716, 2.984	-----	-----	-----
20	Ser	7.943	4.165	3.781, 3.781		-----	-----	-----	-----

TC13b P12W P17A P18A

#	Res		Hα	Hβ	Hγ	Hδ	Hε	Hζ	Hη
1	Asp			,	-----		-----	-----	-----
2	Ala	9.048	4.258	1.492	-----	-----	-----	-----	-----
3	Tyr	8.825	4.030	3.102,3.100	-----	7.063	6.800	-----	
4	Ala	8.330	4.082	1.562	-----	-----	-----	-----	-----
5	Gln	8.134	3.975	2.190,2.119	2.387,	-----	,	-----	-----
6	Trp	8.095	4.184	3.066,3.473	-----	6.834	9.411, 6.866	5.847,6.291	6.231
7	Leu	8.408	3.312	1.775,1.351	1.527	0.923,0.807	-----	-----	-----
8	Ala	8.175	4.025	1.457	-----	-----	-----	-----	-----
9	Asp	7.883	4.539	2.697,2.888	-----		-----	-----	-----
10	Gly	7.543	4.132,3.455	-----	-----	-----	-----	-----	-----
11	Gly	8.305	0.596,2.985	-----	-----	-----	-----	-----	-----
12	Trp	8.774	4.631	3.504,3.259	-----	7.544	10.486,7.861	7.621,7.263	7.345
13	Ala	7.763	4.299	1.327	-----	-----	-----	-----	-----
14	Ser	7.961	4.116	3.767,3.825		-----	-----	-----	-----
15	Gly	8.091	4.230,3.839	-----	-----	-----	-----	-----	-----
16	Arg	8.114	4.789	1.842,1.561	1.777,	3.254,3.183	7.637	-----	, , 6.430,6.850
17	Ala	8.671	4.132	1.343	-----	-----	-----	-----	-----
18	Ala	7.237	2.019	0.236	-----	-----	-----	-----	-----
19	Pro	-----	4.308	1.938, 2.195	1.762, 1.761	2.796, 3.085	-----	-----	-----
20	Ser	7.958	4.167	3.764, 3.764		-----	-----	-----	-----

TC16b A4G

#	Res		Hα	Hβ	Hγ	Hδ	Hε	Hζ	Hη
1	Asp		4.283	2.994^{2},3.218^{3}	-----		-----	-----	-----
2	Ala	9.075	4.277	1.511	-----	-----	-----	-----	-----
3	Tyr	9.102	4.033	3.102^{2},3.102^{3}	-----	7.094	6.831	-----	
4	Gly	8.706	4.146, 3.810	-----	-----	-----	-----	-----	-----
5	Gln	8.462	4.021	2.412, 2.157	2.216, 2.157	-----	7.082^{21},7.912^{22}	-----	-----
6	Trp	8.063	4.200	3.125^{2}, 3.592^{3}	-----	6.957	9.711, 6.992	7.144,7.117	7.231
7	Leu	8.531	3.370	1.929^{2}, 1.370^{3}	1.650	1.006^{1},0.896^{2}	-----	-----	-----
8	Ala	8.197	4.016	1.485	-----	-----	-----	-----	-----
9	Asp	7.989	4.485	2.756^{2}, 2.864^{3}	-----		-----	-----	-----
10	dAla	7.442	4.314	1.258	-----	-----	-----	-----	-----
11	Gly	8.637	0.504^{2},3.205^{3}	-----	-----	-----	-----	-----	-----
12	Pro	-----	4.620	2.033^{2}, 2.546^{3}	2.220^{2}, 2.220^{3}	3.796^{2}, 3.607^{3}	-----	-----	-----
13	Ala	7.294	4.254	1.417	-----	-----	-----	-----	-----
14	Ser	8.231	4.026	3.870^{2}, 3.425^{3}	4.619	-----	-----	-----	-----
15	dAla	7.259	4.405	1.488	-----	-----	-----	-----	-----
16	Arg	8.165	5.086	1.929^{2}, 1.628^{3}	1.816^{2}, 1.816^{3}	3.331, 3.220	7.805	-----	, , ,
17	Pro	-----	4.781	1.771^{2}, 2.347^{3}	1.996^{2}, 1.996^{3}	3.686^{2}, 3.851^{3}	-----	-----	-----
18	Pro	-----	2.345	1.284^{2}, 0.117^{3}	1.704^{2}, 1.636^{3}	3.511^{2}, 3.511^{3}	-----	-----	-----
19	Pro	-----	4.349	1.815^{2}, 2.214^{3}	1.994^{2}, 1.994^{3}	2.931^{2}, 3.169^{3}	-----	-----	-----
20	Ser	7.972	4.160	3.779^{2}, 3.779^{3}		-----	-----	-----	-----

TC16b A8G

#	Res		Hα	Hβ	Hγ	Hδ	Hε	Hζ	Hη
1	Asp		4.299	2.984^{2}, 3.183^{3}	-----		-----	-----	-----
2	Ala	9.084	4.285	1.516	-----	-----	-----	-----	-----
3	Tyr	8.877	4.051	3.137^{2}, 3.137^{3}	-----	7.110	6.835	-----	
4	Ala	8.349	4.135	1.589	-----	-----	-----	-----	-----
5	Gln	8.140	4.033	2.456, 2.206	2.405,	-----	6.953, 7.796	-----	-----
6	Trp	8.121	4.205	3.168^{2}, 3.534^{3}	-----	6.971	9.699, 7.000	7.139, 7.005	7.237
7	Leu	8.649	3.374	1.855^{2}, 1.380^{3}	1.613	0.975^{1}, 0.889^{2}	-----	-----	-----
8	Gly	8.383	3.901, 3.791	-----	-----	-----	-----	-----	-----
9	Asp	7.735	4.619	2.704^{2}, 2.877^{3}	-----		-----	-----	-----
10	dAla	7.425	4.320	1.272	-----	-----	-----	-----	-----
11	Gly	8.489	0.575^{2}, 3.195^{3}	-----	-----	-----	-----	-----	-----
12	Pro	-----	4.612	2.041^{2}, 2.538^{3}	2.215^{2}, 2.215^{3}	3.801^{2}, 3.593^{3}	-----	-----	-----
13	Ala	7.305	4.245	1.411	-----	-----	-----	-----	-----
14	Ser	8.214	4.042	3.865^{2}, 3.439^{3}	4.662	-----	-----	-----	-----
15	dAla	7.282	4.399	1.484	-----	-----	-----	-----	-----
16	Arg	8.153	5.064	1.917^{2}, 1.641^{3}	1.818^{2}, 1.818^{3}	3.323, 3.221	7.764	-----	, , ,
17	Pro	-----	4.765	1.770^{2}, 2.346^{3}	1.994^{2}, 1.994^{3}	3.679^{2}, 3.852^{3}	-----	-----	-----
18	Pro	-----	2.363	1.296^{2}, 0.198^{3}	1.713^{2}, 1.644^{3}	3.506^{2}, 3.506^{3}	-----	-----	-----
19	Pro	-----	4.335	1.800^{2}, 2.207^{3}	1.986^{2}, 1.839^{3}	2.925^{2}, 3.142^{3}	-----	-----	-----
20	Ser	7.955	4.158	3.778^{2}, 3.778^{3}		-----	-----	-----	-----

TC16b A8G P18A

#	Res		Hα	Hβ	Hγ	Hδ	Hε	Hζ	Hη
1	Asp		4.262	2.967, 3.143	-----		-----	-----	-----
2	Ala		4.274	1.510	-----	-----	-----	-----	-----
3	Tyr	8.874	4.067	3.137, 3.136	-----	7.114	6.838	-----	
4	Ala	8.364	4.122	1.581	-----	-----	-----	-----	-----
5	Gln	8.150	4.031	2.401, 2.450	2.199,	-----	6.945, 7.789	-----	-----
6	Trp	8.138	4.208	3.140, 3.540	-----	6.941	9.738, 7.116	7.235, 7.115	7.003
7	Leu	8.664	3.389	1.833, 1.383	1.598	0.962, 0.888	-----	-----	-----
8	Gly	8.353	3.901, 3.792	-----	-----	-----	-----	-----	-----
9	Asp	7.732	4.627	2.891, 2.701	-----		-----	-----	-----
10	dAla	7.433	4.319	1.277	-----	-----	-----	-----	-----
11	Gly	8.513	0.594, 3.194	-----	-----	-----	-----	-----	-----
12	Pro	-----	4.608	2.033, 2.542	2.220, 2.221	3.796, 3.597	-----	-----	-----
13	Ala	7.297	4.246	1.405	-----	-----	-----	-----	-----
14	Ser	8.233	4.036	3.872, 3.450		-----	-----	-----	-----
15	dAla	7.289	4.402	1.481	-----	-----	-----	-----	-----
16	Arg	8.162	5.058	1.917, 1.612	1.804, 1.804	3.324, 3.222	7.776	-----	, , ,
17	Pro	-----	4.503	1.755, 2.268	1.965, 1.964	3.661, 3.823	-----	-----	-----
18	Ala	8.305	1.979	0.309	-----	-----	-----	-----	-----
19	Pro	-----	4.325	1.799, 2.209	1.962, 1.962	2.839, 3.131	-----	-----	-----
20	Ser	7.934	4.163	3.770, 3.770		-----	-----	-----	-----

TC16b S14A P18A

#	Res		Hα	Hβ	Hγ	Hδ	Hε	Hζ	Hη
1	Asp		4.266	3.158, 2.970	-----		-----	-----	-----
2	Ala		4.275	1.515	-----	-----	-----	-----	-----
3	Tyr	8.877	4.055	3.126, 3.126	-----	7.108	6.814	-----	
4	Ala	8.352	4.102	1.580	-----	-----	-----	-----	-----
5	Gln	8.153	3.984	2.227, 2.168	2.417,	-----	7.906, 7.055	-----	-----
6	Trp	8.125	4.198	3.569, 3.112	-----	6.932	9.689, 7.028	7.281, 7.093	7.211
7	Leu	8.395	3.391	1.839, 1.381	1.587	0.955, 0.875	-----	-----	-----
8	Ala	8.164	4.014	1.475	-----	-----	-----	-----	-----
9	Asp	8.059	4.489	2.848, 2.711	-----		-----	-----	-----
10	dAla	7.409	4.292	1.278	-----	-----	-----	-----	-----
11	Gly	8.420	1.151, 3.081	-----	-----	-----	-----	-----	-----
12	Pro	-----	4.513	2.473,	2.084, 2.082	3.668, 3.242	-----	-----	-----
13	Ala	7.302	4.262	1.386	-----	-----	-----	-----	-----
14	Ala	8.183	4.106	1.242	-----	-----	-----	-----	-----
15	dAla	7.662	4.302	1.438	-----	-----	-----	-----	-----
16	Arg	7.651	4.874	1.882, 1.878	1.604, 1.609	3.254, 3.254	7.756	-----	, , ,
17	Pro	-----	4.482	2.268, 1.783	1.985,	3.821, 3.644	-----	-----	-----
18	Ala	8.353	2.194	0.319	-----	-----	-----	-----	-----
19	Pro	-----	4.341	2.221, 1.815	1.963,	3.202, 2.909	-----	-----	-----
20	Ser	7.974	4.171	3.777, 3.781		-----	-----	-----	-----

TC16b P12W S14A P18A

#	Res		Hα	Hβ	Hγ	Hδ	Hε	Hζ	Hη
1	Asp		4.255	2.966, 3.135	-----		-----	-----	-----
2	Ala		4.251	1.484	-----	-----	-----	-----	-----
3	Tyr	8.748	4.082	3.107, 3.107	-----	7.080	6.792	-----	
4	Ala	8.309	4.077	1.558	-----	-----	-----	-----	-----
5	Gln	8.135	3.981	2.146, 2.175	2.409,	-----	7.014, 7.878	-----	-----
6	Trp	8.101	4.206	3.106, 3.506	-----	6.916	9.599, 6.986	6.666, 6.915	6.553
7	Leu	8.394	3.423	1.769, 1.404	1.536	0.921, 0.854	-----	-----	-----
8	Ala	8.102	4.011	1.460	-----	-----	-----	-----	-----
9	Asp	8.031	4.486	2.670, 2.761	-----		-----	-----	-----
10	dAla	7.356	4.245	1.192	-----	-----	-----	-----	-----
11	Gly	8.133	1.317, 2.942	-----	-----	-----	-----	-----	-----
12	Trp	8.238	4.620	3.285, 3.393	-----	7.404	10.400, 7.726	7.569, 7.181	7.301
13	Ala	7.495	4.135	1.214	-----	-----	-----	-----	-----
14	Ala	7.760	4.173	1.273	-----	-----	-----	-----	-----
15	dAla	7.787	4.309	1.462	-----	-----	-----	-----	-----
16	Arg	7.720	4.818	1.879, 1.777	1.593, 1.579	3.204,	7.537	-----	, , ,
17	Pro	-----	4.295	1.982, 2.276	1.948, 1.796	3.625, 3.802	-----	-----	-----
18	Ala	7.710	2.461	0.447	-----	-----	-----	-----	-----
19	Pro	-----	4.322	1.924, 2.205	1.797, 1.797	2.925, 3.177	-----	-----	-----
20	Ser	7.969	4.181	3.790, 3.790		-----	-----	-----	-----

TC16b tr

#	Res		Hα	Hβ	Hγ	Hδ	Hε	Hζ	Hη
2	Ala	8.724	4.218	1.487	-----	-----	-----	-----	-----
3	Tyr	9.186	4.046	3.084, 3.084	-----	7.063	6.814	-----	
4	Ala	8.537	4.110	1.525	-----	-----	-----	-----	-----
5	Gln	8.110	3.993	2.192, 2.125	2.375, 2.376	-----	7.068, 7.905	-----	-----
6	Trp	8.067	4.184	3.101, 3.550	-----	6.952	9.719, 6.932	7.135, 7.137	7.223
7	Leu	8.440	3.370	1.893, 1.356	1.635	1.005, 0.899	-----	-----	-----
8	Ala	8.148	4.020	1.485	-----	-----	-----	-----	-----
9	Asp	8.013	4.473	2.746, 2.863	-----		-----	-----	-----
10	dAla	7.420	4.311	1.257	-----	-----	-----	-----	-----
11	Gly	8.623	3.198, 0.478	-----	-----	-----	-----	-----	-----
12	Pro	-----	4.615	2.039, 2.540	2.220, 2.220	3.805, 3.610	-----	-----	-----
13	Ala	7.286	4.244	1.412	-----	-----	-----	-----	-----
14	Ser	8.222	4.025	3.417, 3.867	4.591	-----	-----	-----	-----
15	dAla	7.251	4.400	1.485	-----	-----	-----	-----	-----
16	Arg	8.154	5.083	1.924, 1.633	1.813,	3.333, 3.218	7.797	-----	, , ,
17	Pro	-----	4.771	1.762, 2.343	2.001, 2.001	3.686, 3.857	-----	-----	-----
18	Pro	-----	2.324	1.245, 0.070	1.644, 1.706	3.507,	-----	-----	-----
19	Pro	-----	4.368	1.939, 2.232	1.820,	2.898, 3.194	-----	-----	-----
20	Ser	8.354	4.283	3.807, 3.806		-----	-----	-----	-----

TC16b tr Q5A

#	Res		Hα	Hβ	Hγ	Hδ	Hε	Hζ	Hη
2	Ala	8.582	4.105	1.526	-----	-----	-----	-----	-----
3	Tyr	9.156	4.066	3.093, 3.088	-----	7.084	6.828	-----	
4	Ala	8.744	4.207	1.487	-----	-----	-----	-----	-----
5	Ala	8.199	4.051	1.497	-----	-----	-----	-----	-----
6	Trp	7.972	4.201	3.135, 3.556	-----	6.974	9.682, 6.946	7.159, 7.133	7.225
7	Leu	8.541	3.344	1.378, 1.880	1.632	1.002, 0.895	-----	-----	-----
8	Ala	8.117	4.192	1.492	-----	-----	-----	-----	-----
9	Asp	7.591	4.584	2.686, 2.828	-----		-----	-----	-----
10	dAla	7.409	4.316	1.262	-----	-----	-----	-----	-----
11	Gly	8.460	0.508, 3.164	-----	-----	-----	-----	-----	-----
12	Pro	-----	4.613	2.038, 2.540	2.218, 2.215	3.802, 3.591	-----	-----	-----
13	Ala	7.286	4.242	1.411	-----	-----	-----	-----	-----
14	Ser	8.200	4.048	3.869, 3.448		-----	-----	-----	-----
15	dAla	7.264	4.399	1.485	-----	-----	-----	-----	-----
16	Arg	8.160	5.062	1.638, 1.906	1.818, 1.825	3.335, 3.230	7.678	-----	, , ,
17	Pro	-----	4.763	1.770, 2.341	2.002, 2.001	3.690, 3.861	-----	-----	-----
18	Pro	-----	2.327	1.258, 0.126	1.689,	3.511, 3.516	-----	-----	-----
19	Pro	-----	4.360	1.927, 2.235	1.823,	2.896, 3.155	-----	-----	-----
20	Ser	8.366	4.285	3.811,		-----	-----	-----	-----

TC16b tr D9N

#	Res		Hα	Hβ	Hγ	Hδ	Hε	Hζ	Hη
2	Ala	8.689	4.191	1.478	-----	-----	-----	-----	-----
3	Tyr	9.136	4.047	3.091, 3.091	-----	6.814	7.075	-----	
4	Ala	8.561	4.122	1.535	-----	-----	-----	-----	-----
5	Gln	8.109	4.113	2.379, 2.423	2.167, 2.167	-----	7.084, 7.536	-----	-----
6	Trp	8.137	4.205	3.160, 3.566	-----	7.048	9.617, 6.964	7.184, 7.107	7.231
7	Leu	8.597	3.306	1.798, 1.455	1.596	0.972, 0.903	-----	-----	-----
8	Ala	8.196	4.054	1.480	-----	-----	-----	-----	-----
9	Asn	7.699	4.659	2.982, 2.790	-----	7.101, 7.579	-----	-----	-----
10	dAla	7.406	4.372	1.265	-----	-----	-----	-----	-----
11	Gly	8.257	3.062, 0.735	-----	-----	-----	-----	-----	-----
12	Pro	-----	4.617	2.042, 2.542	2.195, 2.196	3.760, 3.473	-----	-----	-----
13	Ala	7.369	4.228	1.408	-----	-----	-----	-----	-----
14	Ser	8.097	4.193	3.572, 3.900		-----	-----	-----	-----
15	dAla	7.383	4.406	1.499	-----	-----	-----	-----	-----
16	Arg	7.929	4.898	1.976, 1.754	1.704, 1.704	3.265,	7.385	-----	, , ,
17	Pro	-----	4.611	1.761, 2.183	1.991, 1.992	3.662, 3.849	-----	-----	-----
18	Pro	-----	2.544	1.315, 0.354	1.645, 1.705	3.464,	-----	-----	-----
19	Pro	-----	4.353	1.903, 2.246	1.832, 1.834	2.940, 3.188	-----	-----	-----
20	Ser	8.368	4.284	3.806, 3.806		-----	-----	-----	-----

TC16b tr R16Nva

#	Res		Hα	Hβ	Hγ	Hδ	Hε	Hζ	Hη
2	Ala	8.682	4.202	1.472	-----	-----	-----	-----	-----
3	Tyr	9.076	4.058	3.083, 3.082	-----	7.066	6.811	-----	
4	Ala	8.507	4.109	1.520	-----	-----	-----	-----	-----
5	Gln	8.099	3.995	2.408,	2.174,	-----	7.010, 7.963	-----	-----
6	Trp	8.106	4.292	3.161, 3.520	-----	7.120	9.555, 6.957	7.192, 6.977	7.079
7	Leu	8.462	3.308	1.815, 1.412	1.602	0.973, 0.888	-----	-----	-----
8	Ala	8.102	4.011	1.482	-----	-----	-----	-----	-----
9	Asp	8.037	4.513	2.724, 2.786	-----		-----	-----	-----
10	dAla	7.375	4.375	1.255	-----	-----	-----	-----	-----
11	Gly	8.421	0.831, 3.054	-----	-----	-----	-----	-----	-----
12	Pro	-----	4.600	2.036, 2.527	2.177, 2.178	3.731, 3.412	-----	-----	-----
13	Ala	7.373	4.220	2.816	-----	-----	-----	-----	-----
14	Ser	8.077	4.180	3.913, 3.568		-----	-----	-----	-----
15	dAla	7.352	4.417	1.488	-----	-----	-----	-----	-----
16	Xaa	8.038	4.822,	1.860, 1.763	1.462, 1.395	0.974,	,	,	,
17	Pro	-----	4.571	1.746, 2.130	1.986, 1.985	3.689, 3.846	-----	-----	-----
18	Pro	-----	2.596	1.325, 0.439	1.725, 1.671	3.469,	-----	-----	-----
19	Pro	-----	4.351	1.879, 2.251	1.844, 1.843	2.925, 3.192	-----	-----	-----
20	Ser	8.393	4.280	3.803, 3.803		-----	-----	-----	-----

TC16b tr R16Cit

#	Res		Hα	Hβ	Hγ	Hδ	Hε	Hζ	Hη
2	Ala	8.693	4.214	1.486	-----	-----	-----	-----	-----
3	Tyr	9.095	4.067	3.086, 3.086	-----	7.074	6.819	-----	
4	Ala	8.507	4.111	1.526	-----	-----	-----	-----	-----
5	Gln	8.095	4.000	2.169, 2.169	2.396, 2.395	-----	7.020, 7.958	-----	-----
6	Trp	8.100	4.284	3.154, 3.518	-----	7.077	9.595, 6.965	, 7.092	
7	Leu	8.463	3.336	1.849, 1.386	1.612	0.981, 0.890	-----	-----	-----
8	Ala	8.097	4.018	1.488	-----	-----	-----	-----	-----
9	Asp	8.054	4.494	2.760, 2.814	-----		-----	-----	-----
10	dAla	7.394	4.349	1.260	-----	-----	-----	-----	-----
11	Gly	8.512	3.102, 0.710	-----	-----	-----	-----	-----	-----
12	Pro	-----	4.603	2.049, 2.540	2.195, 2.196	3.760, 3.491	-----	-----	-----
13	Ala	7.350	4.234	1.417	-----	-----	-----	-----	-----
14	Ser	8.139	4.119	3.516, 3.937		-----	-----	-----	-----
15	dAla	7.309	4.415	1.492	-----	-----	-----	-----	-----
16	Arg	8.154	4.900	1.869, 1.867	1.574, 1.573	3.267, 3.127	6.470	-----	, , ,
17	Pro	-----	4.654	1.769, 2.215	1.998, 1.997	3.689, 3.836	-----	-----	-----
18	Pro	-----	2.471	1.290, 0.333	1.668, 1.720	3.482,	-----	-----	-----
19	Pro	-----	4.354	1.874, 2.270	1.846, 1.846	2.909, 3.183	-----	-----	-----
20	Ser	8.395	4.282	3.809, 3.809		-----	-----	-----	-----

TC16b tr Q5A D9N

#	Res		Hα	Hβ	Hγ	Hδ	Hε	Hζ	Hη
2	Ala	8.741	4.188	1.480	-----	-----	-----	-----	-----
3	Tyr	9.134	4.054	3.097, 3.097	-----	7.078	6.818	-----	
4	Ala	8.596	4.109	1.524	-----	-----	-----	-----	-----
5	Ala	8.148	4.208	1.487	-----	-----	-----	-----	-----
6	Trp	8.070	4.226	3.165, 3.569	-----	7.059	9.594, 6.976	7.207, 7.106	7.235
7	Leu	8.620	3.290	1.792, 1.461	1.591	0.973, 0.912	-----	-----	-----
8	Ala	8.233	4.067	1.484	-----	-----	-----	-----	-----
9	Asn	7.548	4.714	2.935, 2.727	-----	7.015, 7.586	-----	-----	-----
10	dAla	7.352	4.364	1.266	-----	-----	-----	-----	-----
11	Gly	8.188	0.776, 3.033	-----	-----	-----	-----	-----	-----
12	Pro	-----	4.617	2.058, 2.533	2.196, 2.059	3.750, 3.448	-----	-----	-----
13	Ala	7.373	4.223	1.412	-----	-----	-----	-----	-----
14	Ser	8.076	4.196	3.896, 3.593		-----	-----	-----	-----
15	dAla	7.393	4.402	1.502	-----	-----	-----	-----	-----
16	Arg	7.939	4.881	1.705, 1.975	1.778, 1.777	3.263, 3.263	7.374	-----	, , ,
17	Pro	-----	4.614	1.774, 2.194	2.002, 2.002	3.661, 3.849	-----	-----	-----
18	Pro	-----	2.525	1.330, 0.379	1.670, 1.717	3.467, 3.467	-----	-----	-----
19	Pro	-----	4.344	1.902, 2.252	1.833, 1.833	2.930, 3.158	-----	-----	-----
20	Ser	8.373	4.282	3.806, 3.806		-----	-----	-----	-----

TC16b tr Q5A R16Nva

#	Res		Hα	Hβ	Hγ	Hδ	Hε	Hζ	Hη
2	Ala	8.708	4.190	1.471	-----	-----	-----	-----	-----
3	Tyr	9.061	4.079	3.086, 3.086	-----	7.086	6.820	-----	
4	Ala	8.553	4.099	1.515	-----	-----	-----	-----	-----
5	Ala	8.119	4.186	1.504	-----	-----	-----	-----	-----
6	Trp	8.024	4.292	3.184^{2}, 3.524^{3}	-----	7.129	9.579, 6.996	7.202, 7.080	7.201
7	Leu	8.559	3.302	1.797, 1.438	1.587	0.967, 0.891	-----	-----	-----
8	Ala	8.151	4.051	1.494	-----	-----	-----	-----	-----
9	Asp	7.614	4.624	2.664^{2}, 2.775^{3}	-----		-----	-----	-----
10	dAla	7.362	4.360	1.261	-----	-----	-----	-----	-----
11	Gly	8.276	0.897^{2}, 3.038^{3}	-----	-----	-----	-----	-----	-----
12	Pro	-----	4.592	2.037^{2}, 2.525^{3}	2.175, 2.175	3.725^{2}, 3.412^{3}	-----	-----	-----
13	Ala	7.389	4.219	1.407	-----	-----	-----	-----	-----
14	Ser	8.087	4.185	3.925, 3.581		-----	-----	-----	-----
15	dAla	7.373	4.417	1.494	-----	-----	-----	-----	-----
16	Xaa	8.051	4.817,	1.860, 1.765	1.453, 1.396	0.979,	,	,	,
17	Pro	-----	4.579	1.760^{2}, 2.151^{3}	1.991, 1.992	3.689^{2}, 3.849^{3}	-----	-----	-----
18	Pro	-----	2.610	1.336^{2}, 0.510^{3}	1.718, 1.718	3.476, 3.477	-----	-----	-----
19	Pro	-----	4.346	1.883^{2}, 2.253^{3}	1.846, 1.846	2.925^{2}, 3.172^{3}	-----	-----	-----
20	Ser	8.401	4.285	3.808, 3.809		-----	-----	-----	-----

TC16b tr Q5A D9N R16Nva

#	Res		Hα	Hβ	Hγ	Hδ	Hε	Hζ	Hη
2	Ala	8.734	4.193	1.482	-----	-----	-----	-----	-----
3	Tyr	9.123	4.052	3.093, 3.092	-----	7.081	6.815	-----	
4	Ala	8.588	4.105	1.525	-----	-----	-----	-----	-----
5	Ala	8.141	4.200	1.485	-----	-----	-----	-----	-----
6	Trp	8.081	4.238	3.174[2], 3.560[3]	-----	7.081	9.597, 6.970	7.202, 7.093	7.092
7	Leu	8.635	3.271	1.475, 1.776	1.586	0.965, 0.912	-----	-----	-----
8	Ala	8.241	4.058	1.480	-----	-----	-----	-----	-----
9	Asn	7.550	4.700	2.928, 2.739	-----	6.979, 7.579	-----	-----	-----
10	dAla	7.351	4.383	1.259	-----	-----	-----	-----	-----
11	Gly	8.178	0.762[2], 3.045[3]	-----	-----	-----	-----	-----	-----
12	Pro	-----	4.625	2.051[2], 2.544[3]	2.199, 2.199	3.757[2], 3.452[3]	-----	-----	-----
13	Ala	7.363	4.213	1.409	-----	-----	-----	-----	-----
14	Ser	8.047	4.209	3.898, 3.598		-----	-----	-----	-----
15	dAla	7.345	4.410	1.502	-----	-----	-----	-----	-----
16	Xaa	7.901	4.830,	1.871, 1.730	1.457, 1.392	0.970,	,	,	,
17	Pro	-----	4.570	1.750[2], 2.132[3]	1.989, 1.989	3.692[2], 3.851[3]	-----	-----	-----
18	Pro	-----	2.548	1.326[2], 0.428[3]	1.692, 1.742	3.472, 3.472	-----	-----	-----
19	Pro	-----	4.344	1.881[2], 2.253[3]	1.831, 1.832	2.912[2], 3.156[3]	-----	-----	-----
20	Ser	8.383	4.281	3.804, 3.803		-----	-----	-----	-----

TC16b Y3F D9L

#	Res		Hα	Hβ	Hγ	Hδ	Hε	Hζ	Hη
1	Asp		4.269	2.995, 3.176	-----		-----	-----	-----
2	Ala		4.245	1.511	-----	-----	-----	-----	-----
3	Phe	8.850	4.114	3.236, 3.236	-----	7.260	7.411	7.516	-----
4	Ala	8.386	4.125	1.616	-----	-----	-----	-----	-----
5	Gln	8.134	4.130	2.239, 2.161	2.569, 2.435	-----	7.004, 7.573	-----	-----
6	Trp	8.104	4.188	3.176, 3.491	-----	7.054	9.573, 6.951	7.163, 7.113	7.221
7	Leu	8.601	3.303	1.394, 1.799	1.547	0.946, 0.850	-----	-----	-----
8	Ala	8.056	4.086	1.498	-----	-----	-----	-----	-----
9	Leu	7.385	4.229	, 1.829	1.615	0.901, 0.866	-----	-----	-----
10	dAla	7.452	4.355	1.257	-----	-----	-----	-----	-----
11	Gly	8.177	0.628, 3.098	-----	-----	-----	-----	-----	-----
12	Pro	-----	4.612	2.055, 2.547	2.209, 2.210	3.776, 3.526	-----	-----	-----
13	Ala	7.323	4.232	1.408	-----	-----	-----	-----	-----
14	Ser	8.099	4.115	3.476, 3.853		-----	-----	-----	-----
15	dAla	7.347	4.396	1.499	-----	-----	-----	-----	-----
16	Arg	8.053	4.881	1.683, 1.997	1.794, 1.796	3.233, 3.234	7.394	-----	, , ,
17	Pro	-----	4.697	1.781, 2.262	2.004, 2.004	3.662, 3.854	-----	-----	-----
18	Pro	-----	2.436	1.348, 0.424	1.681, 1.720	3.496,	-----	-----	-----
19	Pro	-----	4.306	1.926, 2.203	1.790, 1.790	2.905, 3.041	-----	-----	-----
20	Ser	7.969	4.165	3.779, 3.781		-----	-----	-----	-----

TC16b Y3F D9L R16I

#	Res		Hα	Hβ	Hγ	Hδ	Hε	Hζ	Hη
1	Asp		4.268	2.998, 3.182	-----		-----	-----	-----
2	Ala		4.236	1.509	-----	-----	-----	-----	-----
3	Phe	8.821	4.137	3.237, 3.239	-----	7.263	7.413	7.517	-----
4	Ala	8.372	4.134	1.618	-----	-----	-----	-----	-----
5	Gln	8.146	4.130	2.572, 2.453	2.232, 2.169	-----	6.997, 7.573	-----	-----
6	Trp	8.128	4.207	3.194, 3.503	-----	7.087	9.980, 7.103	7.184, 6.938	7.107
7	Leu	8.626	3.273	1.811, 1.380	1.545	0.947, 0.840	-----	-----	-----
8	Ala	7.997	4.082	1.498	-----	-----	-----	-----	-----
9	Leu	7.375	4.223	1.850, 1.527	1.621	0.918, 0.869	-----	-----	-----
10	dAla	7.420	4.388	1.247	-----	-----	-----	-----	-----
11	Gly	8.027	0.659, 3.097	-----	-----	-----	-----	-----	-----
12	Pro	-----	4.599	2.046, 2.559	2.221, 2.220	3.772, 3.492	-----	-----	-----
13	Ala	7.320	4.219	1.410	-----	-----	-----	-----	-----
14	Ser	7.975	4.096	3.776, 3.466		-----	-----	-----	-----
15	dAla	7.205	4.371	1.497	-----	-----	-----	-----	-----
16	Ile	8.101	4.626	2.016	1.157, , 0.925	0.910	-----	-----	-----
17	Pro	-----	4.678	1.736, 2.327	2.053, 1.992	3.730, 3.951	-----	-----	-----
18	Pro	-----	2.410	1.301, 0.306	1.698, 1.701	3.545, 3.547	-----	-----	-----
19	Pro	-----	4.311	1.919, 2.196	1.771, 1.771	2.814, 3.016	-----	-----	-----
20	Ser	7.973	4.163	3.775, 3.771		-----	-----	-----	-----

TC16b Y3F D9A R16Nva

#	Res		Hα	Hβ	Hγ	Hδ	Hε	Hζ	Hη
1	Asp		4.274	3.000, 3.188	-----		-----	-----	-----
2	Ala		4.234	1.509	-----	-----	-----	-----	-----
3	Phe	8.888	4.109	3.234, 3.231	-----	7.257	7.405	7.518	-----
4	Ala	8.399	4.133	1.626	-----	-----	-----	-----	-----
5	Gln	8.137	4.113	2.593, 2.462	2.252, 2.194	-----	7.627, 6.971	-----	-----
6	Trp	8.218	4.279	3.180, 3.505	-----	7.075	9.581, 6.935	7.167, 7.113	7.218
7	Leu	8.631	3.293	1.753, 1.429	1.533	0.945, 0.877	-----	-----	-----
8	Ala	8.173	4.063	1.478	-----	-----	-----	-----	-----
9	Ala	7.425	4.276	1.476	-----	-----	-----	-----	-----
10	dAla	7.362	4.359	1.253	-----	-----	-----	-----	-----
11	Gly	8.269	0.685, 3.085	-----	-----	-----	-----	-----	-----
12	Pro	-----	4.616	2.052, 2.551	2.210, 2.211	3.761, 3.491	-----	-----	-----
13	Ala	7.330	4.228	1.414	-----	-----	-----	-----	-----
14	Ser	8.087	4.138	3.507, 3.865		-----	-----	-----	-----
15	dAla	7.313	4.412	1.498	-----	-----	-----	-----	-----
16	Xaa	8.041	4.824,	1.872, 1.754	1.439, 1.382	0.962,	,	,	,
17	Pro	-----	4.606	1.753, 2.152	1.992, 1.991	3.690, 3.843	-----	-----	-----
18	Pro	-----	2.543	1.359, 0.497	1.682, 1.739	, 3.470	-----	-----	-----
19	Pro	-----	4.321	1.922, 2.218	1.794, 1.794	2.912, 3.085	-----	-----	-----
20	Ser	7.981	4.166	3.776, 3.771		-----	-----	-----	-----

TC16b Y3F R16Cit

#	Res		Hα	Hβ	Hγ	Hδ	Hε	Hζ	Hη
1	Asp		4.284	2.994, 3.190	-----		-----	-----	-----
2	Ala	9.086	4.257	1.508	-----	-----	-----	-----	-----
3	Phe	8.834	4.108	3.213, 3.213	-----	7.241	7.390	7.498	-----
4	Ala	8.304	4.109	1.590	-----	-----	-----	-----	-----
5	Gln	8.180	3.979	2.431, 2.431	2.200, 2.177	-----	,	-----	-----
6	Trp	8.140	4.285	3.171, 3.488	-----	7.081	9.577, 7.102	7.164, 6.959	7.200
7	Leu	8.405	3.325	1.805, 1.376	1.545	0.939, 0.862	-----	-----	-----
8	Ala	8.148	4.015	1.478	-----	-----	-----	-----	-----
9	Asp	7.984	4.511	2.736, 2.810	-----		-----	-----	-----
10	dAla	7.386	4.344	1.258	-----	-----	-----	-----	-----
11	Gly	8.479	0.763, 3.076	-----	-----	-----	-----	-----	-----
12	Pro	-----	4.592	2.029, 2.524	2.185, 2.186	3.739, 3.453	-----	-----	-----
13	Ala	7.351	4.230	1.412	-----	-----	-----	-----	-----
14	Ser	8.129	4.122	3.523, 3.932		-----	-----	-----	-----
15	dAla	7.320	4.413	1.487	-----	-----	-----	-----	-----
16	Arg	8.144	4.885	1.862, 1.862	1.588, 1.588	3.262, 3.129	6.469	-----	, , ,
17	Pro	-----	4.646	1.770, 2.212	1.987, 1.988	3.682, 3.831	-----	-----	-----
18	Pro	-----	2.501	1.344, 0.409	1.646, 1.720	3.473,	-----	-----	-----
19	Pro	-----	4.325	1.930, 2.229	1.812, 1.810	2.931, 3.138	-----	-----	-----
20	Ser	7.992	4.166	3.774, 3.774		-----	-----	-----	-----

TC16b Y3F S14V

#	Res		Hα	Hβ	Hγ	Hδ	Hε	Hζ	Hη
1	Asp		4.260	2.961, 3.113	-----		-----	-----	-----
2	Ala	9.018	4.254	1.458	-----	-----	-----	-----	-----
3	Phe	8.678	4.193	3.184, 3.184	-----	7.229	7.356	7.438	-----
4	Ala	8.283	4.104	1.534	-----	-----	-----	-----	-----
5	Gln	8.209	4.002	2.146, 2.145	2.437, 2.394	-----	7.930, 7.009	-----	-----
6	Trp	8.116	4.356	3.196, 3.511	-----	7.141	9.544, 7.137	7.305, 7.061	7.202
7	Leu	8.253	3.478	1.695, 1.444		0.885, 0.821	-----	-----	-----
8	Ala	8.107	4.011	1.448	-----	-----	-----	-----	-----
9	Asp	8.132	4.479	2.714, 2.715	-----		-----	-----	-----
10	dAla	7.472	4.349	1.293	-----	-----	-----	-----	-----
11	Gly	8.245	1.915, 3.052	-----	-----	-----	-----	-----	-----
12	Pro	-----	4.511	2.001, 2.386	2.003, 2.001	3.522, 3.065	-----	-----	-----
13	Ala	7.611	4.192	1.377	-----	-----	-----	-----	-----
14	Val	7.946	4.119	2.121	, 0.903	-----	-----	-----	-----
15	dAla	7.892	4.426	1.433	-----	-----	-----	-----	-----
16	Arg	8.049	4.564	1.626, 1.848	1.695, 1.694	3.212, 3.216	7.325	-----	, , ,
17	Pro	-----	4.169	1.809,	1.894, 1.700	3.534, 3.722	-----	-----	-----
18	Pro	-----	3.725	1.680, 1.450	1.795, 1.795	3.371, 3.493	-----	-----	-----
19	Pro	-----	4.339	1.918, 2.219	1.891,	3.283, 3.434	-----	-----	-----
20	Ser	8.008	4.188	3.782,		-----	-----	-----	-----

TC16b Y3F S14Abu

#	Res		Hα	Hβ	Hγ	Hδ	Hε	Hζ	Hη
1	Asp		4.273	2.980, 3.157	-----		-----	-----	-----
2	Ala	9.063	4.271	1.494	-----	-----	-----	-----	-----
3	Phe	8.815	4.140	3.203, 3.203	-----	7.234	7.366	7.472	-----
4	Ala	8.335	4.106	1.570	-----	-----	-----	-----	-----
5	Gln	8.186	3.987	2.172, 2.172	2.426, 2.426	-----	7.964, 7.045	-----	-----
6	Trp	8.113	4.266	3.177, 3.532	-----	7.079	9.538, 7.046	7.267, 7.094	7.206
7	Leu	8.335	3.398	1.753, 1.416	1.512	0.919, 0.869	-----	-----	-----
8	Ala	8.155	3.999	1.463	-----	-----	-----	-----	-----
9	Asp	8.133	4.451	2.719, 2.718	-----		-----	-----	-----
10	dAla	7.403	4.345	1.268	-----	-----	-----	-----	-----
11	Gly	8.358	1.301, 3.102	-----	-----	-----	-----	-----	-----
12	Pro	-----	4.531	2.014, 2.453	2.087, 2.088	3.643, 3.278	-----	-----	-----
13	Ala	7.423	4.200	1.378	-----	-----	-----	-----	-----
14	Xaa	8.071	4.058,	1.726, 1.681	0.847,	,	,	,	,
15	dAla	7.760	4.375	1.440	-----	-----	-----	-----	-----
16	Arg	7.817	4.761	1.654, 1.878	1.786, 1.788	3.249, 3.250	7.531	-----	, , ,
17	Pro	-----	4.433	1.735, 2.039	1.950, 1.949	3.622, 3.795	-----	-----	-----
18	Pro	-----	3.110	1.498, 0.819	1.660, 1.748	3.470, 3.424	-----	-----	-----
19	Pro	-----	4.345	1.950, 2.219	1.854, 1.854	3.118, 3.318	-----	-----	-----
20	Ser	8.009	4.178	3.781, 3.781		-----	-----	-----	-----

CircMut GNAA

#	Res		Hα	Hβ	Hγ	Hδ	Hε	Hζ	Hη
1	Arg		4.441	1.827,	1.999, 1.717	3.259,	7.490	-----	, , ,
2	Pro	-----	4.670	1.753, 2.264	1.987, 1.989	3.558, 3.759	-----	-----	-----
3	Pro	-----	3.556	1.523, 1.186	1.842, 1.843	3.394, 3.553	-----	-----	-----
4	Pro	-----	4.423	1.908, 2.195	1.778, 1.908	3.076, 3.358	-----	-----	-----
5	Ser	8.331	4.221	3.756, 3.756		-----	-----	-----	-----
6	Gly	8.366	4.159, 3.893	-----	-----	-----	-----	-----	-----
7	Asn	8.547	4.560	2.869, 2.869	-----	7.818, 7.070	-----	-----	-----
8	Ala	8.786	4.261	1.475	-----	-----	-----	-----	-----
9	Ala	8.477	4.255	1.431	-----	-----	-----	-----	-----
10	Tyr	8.647	4.141	3.090, 3.136	-----	6.792	7.077	-----	
11	Ala	8.164	4.108	1.540	-----	-----	-----	-----	-----
12	Gln	8.011	4.016	2.149, 2.149	2.400, 2.400	-----	7.014, 7.924	-----	-----
13	Trp	8.133	4.309	3.166, 3.562	-----	7.134	9.989, 7.126	7.342, 7.082	7.225
14	Leu	8.444	3.536	1.710, 1.446	1.495	0.882, 0.858	-----	-----	-----
15	Ala	7.914	4.029	1.462	-----	-----	-----	-----	-----
16	Asp	8.042	4.516	2.686, 2.775	-----		-----	-----	-----
17	dAla	7.498	4.288	1.276	-----	-----	-----	-----	-----
18	Gly	8.159	1.942, 2.789	-----	-----	-----	-----	-----	-----
19	Pro	-----	4.524	, 2.380	2.051, 2.053	3.502, 3.190	-----	-----	-----
20	Ser	8.108	4.544	3.924, 3.925		-----	-----	-----	-----
21	Ser	7.891	4.182	3.715, 3.875		-----	-----	-----	-----

CircMut GGNAA

#	Res		Hα	Hβ	Hγ	Hδ	Hε	Hζ	Hη
1	Arg		4.358	1.694, 1.802	1.958,	3.227, 3.233	7.464	-----	, , ,
2	Pro	-----	4.729	1.806, 2.349	1.996, 1.995	3.545, 3.727	-----	-----	-----
3	Pro	-----	3.767	1.631, 1.499	1.875, 1.875	3.526, 3.661	-----	-----	-----
4	Pro	-----	4.403	1.941, 2.202	1.868, 1.868	3.185, 3.366	-----	-----	-----
5	Ser	8.475	4.348	3.854, 3.853		-----	-----	-----	-----
6	Gly	8.357	4.077, 3.938	-----	-----	-----	-----	-----	-----
7	Gly	8.371	4.064, 3.958	-----	-----	-----	-----	-----	-----
8	Asn	8.537	4.642	2.888, 2.886	-----	7.796, 7.066	-----	-----	-----
9	Ala	8.761	4.253	1.472	-----	-----	-----	-----	-----
10	Ala	8.316	4.273	1.442	-----	-----	-----	-----	-----
11	Tyr	8.185	4.208	3.111, 3.112	-----	6.809	7.056	-----	
12	Ala	8.291	4.092	1.508	-----	-----	-----	-----	-----
13	Gln	8.127	4.026	2.131, 2.131	2.389, 2.389	-----	7.003, 7.890	-----	-----
14	Trp	8.017	4.352	3.197, 3.516	-----	7.150	10.005, 7.176	7.332, 7.101	7.213
15	Leu	8.348	3.552	1.699, 1.411	1.497	0.876, 0.828	-----	-----	-----
16	Ala	7.992	4.031	1.451	-----	-----	-----	-----	-----
17	Asp	8.036	4.514	2.698, 2.770	-----		-----	-----	-----
18	dAla	7.554	4.287	1.276	-----	-----	-----	-----	-----
19	Gly	8.156	2.064, 2.925	-----	-----	-----	-----	-----	-----
20	Pro	-----	4.533	2.046, 2.367	2.045, 2.045	3.538, 3.230	-----	-----	-----
21	Ser	8.143	4.534	3.917, 3.918		-----	-----	-----	-----
22	Ser	7.907	4.183	3.721, 3.875		-----	-----	-----	-----

CircMut GGGGNAA

#	Res		Hα	Hβ	Hγ	Hδ	Hε	Hζ	Hη
1	Arg		4.460	1.726, 1.834	1.997,	3.245, 3.250	7.531	-----	, , ,
2	Pro	-----	4.762	1.800, 2.367	2.014, 2.013	3.586, 3.775	-----	-----	-----
3	Pro	-----	3.508	1.547, 1.176	1.834,	3.510, 3.649	-----	-----	-----
4	Pro	-----	4.379	1.910, 2.243	1.871, 1.871	3.160, 3.354	-----	-----	-----
5	Ser	8.530	4.331	3.871, 3.822		-----	-----	-----	-----
6	Gly	8.625	4.061, 3.885	-----	-----	-----	-----	-----	-----
7	Gly	8.364	3.939, 3.807	-----	-----	-----	-----	-----	-----
8	Gly	8.412	3.946, 3.772	-----	-----	-----	-----	-----	-----
9	Gly	8.357	3.976, 3.976	-----	-----	-----	-----	-----	-----
10	Asn	8.238	4.749	2.913, 2.915	-----	7.826, 7.058	-----	-----	-----
11	Ala	8.818	4.249	1.487	-----	-----	-----	-----	-----
12	Ala	8.377	4.303	1.460	-----	-----	-----	-----	-----
13	Tyr	8.263	4.184	3.109, 3.109	-----	6.809	7.047	-----	
14	Ala	8.284	4.109	1.518	-----	-----	-----	-----	-----
15	Gln	8.178	4.030	2.179, 2.121	2.390, 2.390	-----	7.011, 7.891	-----	-----
16	Trp	7.982	4.315	3.184, 3.514	-----	7.093	9.917, 7.096	7.304, 7.110	7.216
17	Leu	8.343	3.510	1.735, 1.405	1.528	0.909, 0.834	-----	-----	-----
18	Ala	8.025	4.027	1.458	-----	-----	-----	-----	-----
19	Asp	8.047	4.509	2.711, 2.798	-----		-----	-----	-----
20	dAla	7.542	4.285	1.269	-----	-----	-----	-----	-----
21	Gly	8.201	1.841, 2.977	-----	-----	-----	-----	-----	-----
22	Pro	-----	4.574	, 2.400	2.067, 2.065	3.593, 3.284	-----	-----	-----
23	Ser	8.064	4.546	3.919, 3.919		-----	-----	-----	-----
24	Ser	7.870	4.147	3.667, 3.879		-----	-----	-----	-----

CircMut PADA

#	Res		Hα	Hβ	Hγ	Hδ	Hε	Hζ	Hη
1	Arg		4.402	1.969, 1.717	1.761,	3.233,	7.368	-----	, , ,
2	Pro	-----	4.799	1.871, 2.414	2.030,	3.776, 3.586	-----	-----	-----
3	Pro	-----	3.790	, 1.819	2.120, 2.121	3.605,	-----	-----	-----
4	Pro	-----	4.498	1.888, 2.294	1.994, 1.993	3.517, 3.691	-----	-----	-----
5	Ser	8.835	4.745	4.063, 3.933		-----	-----	-----	-----
6	Pro	-----	4.380	1.930, 2.351	2.116, 1.999	3.908, 3.747	-----	-----	-----
7	Ala	8.371	4.210	1.415	-----	-----	-----	-----	-----
8	Asp	8.175	4.541	2.788, 2.688	-----		-----	-----	-----
9	Ala	8.326	4.215	1.465	-----	-----	-----	-----	-----
10	Tyr	8.409	4.290	3.027, 3.026	-----	6.787	7.006	-----	
11	Ala	8.112	4.036	1.514	-----	-----	-----	-----	-----
12	Gln	8.107	4.016	2.138,	2.399,	-----	6.957, 7.855	-----	-----
13	Trp	8.110	4.360	3.240, 3.516	-----	7.167	10.122, 7.252	7.367, 7.116	7.210
14	Leu	8.347	3.609	1.644, 1.402		, 0.800	-----	-----	-----
15	Ala	7.940	4.032	1.443	-----	-----	-----	-----	-----
16	Asp	8.019	4.534	2.682, 2.725	-----		-----	-----	-----
17	dAla	7.616	4.283	1.278	-----	-----	-----	-----	-----
18	Gly	8.033	2.412, 2.896	-----	-----	-----	-----	-----	-----
19	Pro	-----	4.468	, 2.320	2.029, 2.028	3.437, 3.184	-----	-----	-----
20	Ser	8.324	4.526	3.922, 3.921		-----	-----	-----	-----
21	Ser	8.000	4.252	3.804, 3.855		-----	-----	-----	-----

CircMut TADA

#	Res		Hα	Hβ	Hγ	Hδ	Hε	Hζ	Hη
1	Arg		4.457	2.008, 1.718	1.840,	3.262,	7.526	-----	, , ,
2	Pro	-----	4.762	1.784, 2.348	1.997,	3.765, 3.571	-----	-----	-----
3	Pro	-----	3.402	1.527, 1.196	1.888, 1.888	3.503, 3.653	-----	-----	-----
4	Pro	-----	4.461	, 2.312	1.877,	3.046, 3.311	-----	-----	-----
5	Ser	8.680	4.363	3.974, 3.832		-----	-----	-----	-----
6	Thr	7.625	4.501	4.403	, 1.241	-----	-----	-----	-----
7	Ala	8.718	4.186	1.477	-----	-----	-----	-----	-----
8	Asp	8.818	4.500	2.729, 2.729	-----		-----	-----	-----
9	Ala	8.024	4.324	1.464	-----	-----	-----	-----	-----
10	Tyr	8.706	4.120	3.079, 3.080	-----	6.785	7.060	-----	
11	Ala	8.282	4.111	1.580	-----	-----	-----	-----	-----
12	Gln	7.948	4.008	2.155,	2.417,	-----	7.028, 7.931	-----	-----
13	Trp	8.151	4.283	3.169, 3.575	-----	7.111	9.952, 7.091	7.327, 7.419	7.226
14	Leu	8.501	3.480	1.725, 1.440	1.500	0.878,	-----	-----	-----
15	Ala	7.910	4.021	1.468	-----	-----	-----	-----	-----
16	Asp	8.018	4.512	2.691, 2.786	-----		-----	-----	-----
17	dAla	7.452	4.285	1.262	-----	-----	-----	-----	-----
18	Gly	8.186	2.752, 1.730	-----	-----	-----	-----	-----	-----
19	Pro	-----	4.536	, 2.398	2.058, 2.059	3.511, 3.185	-----	-----	-----
20	Ser	8.082	4.552	3.926, 3.927		-----	-----	-----	-----
21	Ser	7.904	4.164	3.695, 3.875		-----	-----	-----	-----

CircMut TUDA

#	Res		Hα	Hβ	Hγ	Hδ	Hε	Hζ	Hη
1	Arg		4.440	1.714, 2.001	1.836, 1.837	3.251,	7.447	-----	, , ,
2	Pro	-----	4.786	1.807, 2.372	1.997,	3.562, 3.750	-----	-----	-----
3	Pro	-----	3.480	1.527, 1.240	1.884, 1.885	3.540, 3.684	-----	-----	-----
4	Pro	-----	4.434	, 2.268	1.862,	3.056, 3.255	-----	-----	-----
5	Ser	8.624	4.399	3.963, 3.839		-----	-----	-----	-----
6	Thr	7.670	4.348	4.328	, 1.242	-----	-----	-----	-----
7	Aib	8.779	-----	1.512, 1.464	-----	-----	-----	-----	-----
8	Asp	8.497	4.480	2.740, 2.693	-----		-----	-----	-----
9	Ala	7.995	4.360	1.504	-----	-----	-----	-----	-----
10	Tyr	8.497	4.131	3.028, 3.147	-----	7.010	6.793	-----	
11	Ala	8.242	4.079	1.592	-----	-----	-----	-----	-----
12	Gln	8.113	4.015	2.194, 2.135	2.430, 2.429	-----	7.018, 7.877	-----	-----
13	Trp	8.068	4.279	3.190, 3.571	-----	7.108	9.961, 7.120	7.329, 7.104	7.224
14	Leu	8.505	3.478	, 1.707	1.452	0.856,	-----	-----	-----
15	Ala	7.947	4.029	1.467	-----	-----	-----	-----	-----
16	Asp	7.978	4.537	2.724, 2.818	-----		-----	-----	-----
17	dAla	7.463	4.288	1.269	-----	-----	-----	-----	-----
18	Gly	8.148	1.762[2], 2.749[3]	-----	-----	-----	-----	-----	-----
19	Pro	-----	4.522	, 2.376	2.045,	3.492, 3.158	-----	-----	-----
20	Ser	8.063	4.555	3.927, 3.929		-----	-----	-----	-----
21	Ser	7.895	4.182	3.710, 3.877		-----	-----	-----	-----

CircMut GUDA

#	Res		Hα	Hβ	Hγ	Hδ	Hε	Hζ	Hη
1	Arg		4.490	2.041, 1.749	1.884,	3.287,	7.546	-----	, , ,
2	Pro	-----	4.786	1.786, 2.366	2.002, 2.003	3.776, 3.595	-----	-----	-----
3	Pro	-----	3.057	1.377, 0.736	1.780, 1.860	3.517, 3.605	-----	-----	-----
4	Pro	-----	4.486	1.736, 2.207	1.900, 1.900	2.898, 3.213	-----	-----	-----
5	Ser	8.413	4.329	3.803, 3.804		-----	-----	-----	-----
6	Gly	8.419	4.051, 3.804	-----	-----	-----	-----	-----	-----
7	Aib	8.703	-----	1.513, 1.476	-----	-----	-----	-----	-----
8	Asp	8.441	4.524	2.738, 2.661	-----		-----	-----	-----
9	Ala	8.254	4.258	1.451	-----	-----	-----	-----	-----
10	Tyr	8.943	4.111	3.116, 3.118	-----	6.796	7.083	-----	
11	Ala	8.022	4.108	1.632	-----	-----	-----	-----	-----
12	Gln	8.064	4.013	2.166,	2.426,	-----	7.013, 7.924	-----	-----
13	Trp	8.143	4.269	3.156, 3.622	-----	7.103	9.900, 7.115	7.342, 7.108	7.244
14	Leu	8.538	3.466	1.744, 1.445	1.494	0.880,	-----	-----	-----
15	Ala	7.919	4.027	1.479	-----	-----	-----	-----	-----
16	Asp	8.016	4.518	2.693, 2.796	-----		-----	-----	-----
17	dAla	7.407	4.293	1.267	-----	-----	-----	-----	-----
18	Gly	8.200	2.699, 1.647	-----	-----	-----	-----	-----	-----
19	Pro	-----	4.556	, 2.419	2.066, 2.067	3.535, 3.179	-----	-----	-----
20	Ser	7.990	4.563	3.931, 3.931		-----	-----	-----	-----
21	Ser	7.860	4.156	3.675, 3.880		-----	-----	-----	-----

CircMut DAAA

#	Res		Hα	Hβ	Hγ	Hδ	Hε	Hζ	Hη
1	Arg			,	,	,		-----	, , ,
2	Pro	-----	4.770	1.762, 2.373	1.946, 1.945	3.293, 3.631	-----	-----	-----
3	Pro	-----	3.431	, 1.135	1.878, 1.522	3.572, 3.638	-----	-----	-----
4	Pro	-----	4.139	1.785, 2.059	1.783, 1.783	3.078, 3.276	-----	-----	-----
5	Ser	8.063	4.170	3.882, 3.770		-----	-----	-----	-----
6	Asp	7.900	4.687	2.801, 2.662	-----		-----	-----	-----
7	Ala	8.537	4.099	1.506	-----	-----	-----	-----	-----
8	Ala	8.649	4.305	1.522	-----	-----	-----	-----	-----
9	Ala	8.241	4.332	1.531	-----	-----	-----	-----	-----
10	Tyr	9.103	4.056	3.095, 3.041	-----	6.782	7.067	-----	
11	Ala	8.258	4.124	1.588	-----	-----	-----	-----	-----
12	Gln	7.843	4.003	2.184, 2.184	2.431, 2.433	-----	7.027, 7.961	-----	-----
13	Trp	8.210	4.273	3.167, 3.592	-----	7.145	10.028, 7.059	7.338, 7.082	7.225
14	Leu	8.486	3.473	1.749, 1.426	1.505	0.887, 0.857	-----	-----	-----
15	Ala	7.894	4.022	1.478	-----	-----	-----	-----	-----
16	Asp	8.020	4.512	2.677, 2.781	-----		-----	-----	-----
17	dAla	7.404	4.282	1.265	-----	-----	-----	-----	-----
18	Gly	8.132	2.622, 1.711	-----	-----	-----	-----	-----	-----
19	Pro	-----	4.535	2.100, 2.395	2.076, 2.078	3.486, 3.172	-----	-----	-----
20	Ser	8.117	4.563	3.943, 3.943		-----	-----	-----	-----
21	Ser	7.885	4.182	3.715, 3.881		-----	-----	-----	-----

CircMut DUAA

#	Res		Hα	Hβ	Hγ	Hδ	Hε	Hζ	Hη
1	Arg		4.248	1.877, 1.520	1.792,	3.191,	7.439	-----	, , ,
2	Pro	-----	4.797	1.770, 2.400	1.964, 1.962	3.367, 3.665	-----	-----	-----
3	Pro	-----	3.190	1.450, 0.988	1.837, 1.836	3.566, 3.641	-----	-----	-----
4	Pro	-----	4.162	1.847, 2.103	1.803, 1.809	3.181, 2.982	-----	-----	-----
5	Ser	8.023	4.211	3.869, 3.764		-----	-----	-----	-----
6	Asp	7.873	4.564	2.793, 2.608	-----		-----	-----	-----
7	Aib	8.587	-----	,	-----	-----	-----	-----	-----
8	Ala	8.391	4.253	1.510	-----	-----	-----	-----	-----
9	Ala	8.253	4.400	1.546	-----	-----	-----	-----	-----
10	Tyr	8.823	4.067	3.147, 3.145	-----	6.793	7.038	-----	
11	Ala	8.251	4.115	1.604	-----	-----	-----	-----	-----
12	Gln	8.055	4.001	2.154, 2.213	2.432,	-----	7.038, 7.948	-----	-----
13	Trp	8.090	4.270	3.172, 3.599	-----	7.125	9.916, 7.099	7.324, 7.081	7.230
14	Leu	8.513	3.445	1.753, 1.428	1.514	0.879, 0.861	-----	-----	-----
15	Ala	7.949	4.021	1.480	-----	-----	-----	-----	-----
16	Asp	8.009	4.522	2.705, 2.817	-----		-----	-----	-----
17	dAla	7.396	4.284	1.265	-----	-----	-----	-----	-----
18	Gly	8.169	1.565, 2.651	-----	-----	-----	-----	-----	-----
19	Pro	-----	4.557	2.080, 2.416	2.082, 2.082	3.522, 3.189	-----	-----	-----
20	Ser	8.020	4.568	3.942, 3.940		-----	-----	-----	-----
21	Ser	7.847	4.164	3.676, 3.885		-----	-----	-----	-----

CircMut DAUA

#	Res		Hα	Hβ	Hγ	Hδ	Hε	Hζ	Hη
1	Arg		4.139	1.854, 1.446	1.744,	3.161,	7.372	-----	, , ,
2	Pro	-----	4.686	1.754, 2.288	1.950,	3.298, 3.618	-----	-----	-----
3	Pro	-----	3.582	1.570, 0.864	1.864, 1.866	3.476, 3.589	-----	-----	-----
4	Pro	-----	4.460	, 2.308	2.022,	3.302, 3.616	-----	-----	-----
5	Ser	8.428	4.537	3.953, 3.953		-----	-----	-----	-----
6	Asp	7.966	4.733	2.833, 2.730	-----		-----	-----	-----
7	Ala	8.385	4.039	1.486	-----	-----	-----	-----	-----
8	Aib	8.747	-----	, 1.548	-----	-----	-----	-----	-----
9	Ala	7.803	4.297	1.522	-----	-----	-----	-----	-----
10	Tyr	8.893	4.067	3.115, 3.112	-----	7.052	6.783	-----	
11	Ala	8.347	4.134	1.611	-----	-----	-----	-----	-----
12	Gln	7.773	4.056	2.191,	2.446,	-----	7.062, 7.735	-----	-----
13	Trp	8.217	4.257	3.184, 3.554	-----	7.151	10.074, 7.099	7.337, 7.131	7.222
14	Leu	8.487	3.477	1.725, 1.453	1.509	0.893, 0.868	-----	-----	-----
15	Ala	7.960	4.043	1.478	-----	-----	-----	-----	-----
16	Asp	7.909	4.593	2.805, 2.922	-----		-----	-----	-----
17	dAla	7.452	4.274	1.276	-----	-----	-----	-----	-----
18	Gly	8.064	2.649, 1.757	-----	-----	-----	-----	-----	-----
19	Pro	-----	4.523	, 2.387	2.070, 2.074	3.458, 3.159	-----	-----	-----
20	Ser	8.145	4.561	3.945, 3.948		-----	-----	-----	-----
21	Ser	7.915	4.225	3.738, 3.896		-----	-----	-----	-----

CircMut DAAU

#	Res	Hα	Hβ	Hγ	Hδ	Hε	Hζ	Hη
1	Arg	4.335	1.919, 1.653	1.731,	3.182,	7.278	-----	, , ,
2	Pro	-----	4.743	1.827, 2.367	1.994, 1.993	3.507, 3.715	-----	-----	-----
3	Pro	-----	4.471	1.989, 1.823	2.141, 2.140	3.581, 3.754	-----	-----	-----
4	Pro	-----	4.341	, 2.222	1.924,	3.481, 3.629	-----	-----	-----
5	Ser	8.365	4.238	3.892, 3.760		-----	-----	-----	-----
6	Asp	8.260	4.587	2.689, 2.687	-----		-----	-----	-----
7	Ala				-----	-----	-----	-----	-----
8	Ala				-----	-----	-----	-----	-----
9	Aib		-----	,	-----	-----	-----	-----	-----
10	Tyr	7.892	4.353	3.045, 3.045	-----	7.109	6.827	-----	
11	Ala	7.969	4.149	1.244	-----	-----	-----	-----	-----
12	Gln	8.173	4.202	2.011, 1.901	, 2.140	-----	,	-----	-----
13	Trp	8.232	4.544	3.216, 3.316	-----	7.201	10.127, 7.203	7.464,	
14	Leu	8.017	4.243	1.467,	1.414	0.857, 0.807	-----	-----	-----
15	Ala				-----	-----	-----	-----	-----
16	Asp	8.205	4.561	2.604, 2.668	-----		-----	-----	-----
17	dAla		4.278	1.300	-----	-----	-----	-----	-----
18	Gly		,	-----	-----	-----	-----	-----	-----
19	Pro	-----	4.451	, 2.276	1.991,	3.733, 3.590	-----	-----	-----
20	Ser	8.468	4.467	3.905, 3.906		-----	-----	-----	-----
21	Ser	8.034	4.254	3.861, 3.862		-----	-----	-----	-----

CircMut DAAL

#	Res		Hα	Hβ	Hγ	Hδ	Hε	Hζ	Hη
1	Arg		4.402	1.978, 1.661	1.857,	3.257,	7.544	-----	, , ,
2	Pro	-----	4.805	1.774, 2.373	1.981, 1.982	3.494, 3.728	-----	-----	-----
3	Pro	-----	2.954	1.370, 0.791	1.761, 1.835	3.616, 3.530	-----	-----	-----
4	Pro	-----	4.278	1.850, 2.223	1.801, 1.801	2.907, 3.168	-----	-----	-----
5	Ser	8.310	4.199	3.889, 3.792		-----	-----	-----	-----
6	Asp	7.948	4.640	2.766, 2.662	-----		-----	-----	-----
7	Ala	8.548	4.106	1.488	-----	-----	-----	-----	-----
8	Ala	8.567	4.328	1.512	-----	-----	-----	-----	-----
9	Leu	8.225	4.392	1.841, 1.640	1.749	1.008, 0.898	-----	-----	-----
10	Tyr	8.735	4.056	3.103, 3.103	-----	7.070	6.799	-----	
11	Ala	8.476	4.126	1.580	-----	-----	-----	-----	-----
12	Gln	7.998	4.006	2.200, 2.118	2.442,	-----	,	-----	-----
13	Trp	8.065	4.277	3.148, 3.601	-----	7.105	9.817, 7.175	7.318, 7.081	7.234
14	Leu	8.514	3.421	1.502,	1.444	0.905, 0.881	-----	-----	-----
15	Ala	7.924	4.025	1.476	-----	-----	-----	-----	-----
16	Asp	7.999	4.522	2.706, 2.825	-----		-----	-----	-----
17	dAla	7.389	4.287	1.258	-----	-----	-----	-----	-----
18	Gly	8.201	1.470, 2.703	-----	-----	-----	-----	-----	-----
19	Pro	-----	4.579	, 2.425	2.070, 2.070	3.556, 3.199	-----	-----	-----
20	Ser	7.923	4.575	3.924, 3.923		-----	-----	-----	-----
21	Ser	7.823	4.135	3.638, 3.887		-----	-----	-----	-----

CircMut DGUDA

#	Res		Hα	Hβ	Hγ	Hδ	Hε	Hζ	Hη
1	Arg		4.501	2.073, 1.894	2.016, 1.751	3.290,	7.537	-----	, , ,
2	Pro	-----	4.782	1.791, 2.358	1.996, 1.993	3.597, 3.767	-----	-----	-----
3	Pro	-----	2.994	1.396, 0.725	1.761, 1.857	3.515, 3.580	-----	-----	-----
4	Pro	-----	4.442	1.726, 2.172	1.892, 1.891	2.913, 3.204	-----	-----	-----
5	Asp	8.309	4.498	2.593, 2.548	-----		-----	-----	-----
6	Gly	8.245	4.086, 3.775	-----	-----	-----	-----	-----	-----
7	Aib	8.658	-----	,	-----	-----	-----	-----	-----
8	Asp	8.461	4.531	2.744, 2.663	-----		-----	-----	-----
9	Ala	8.262	4.262	1.450	-----	-----	-----	-----	-----
10	Tyr	8.890	4.094	3.131, 3.132	-----	7.068	6.809	-----	
11	Ala	8.050	4.125	1.637	-----	-----	-----	-----	-----
12	Gln	8.068	4.022	2.192, 2.159	2.418,	-----	7.020, 7.900	-----	-----
13	Trp	8.130	4.262	3.142, 3.615	-----	7.095	9.837, 7.238	7.344, 7.110	7.233
14	Leu	8.554	3.442	1.440, 1.742	1.507	0.892, 0.869	-----	-----	-----
15	Ala	7.918	4.034	1.477	-----	-----	-----	-----	-----
16	Asp	7.997	4.528	2.702, 2.817	-----		-----	-----	-----
17	dAla	7.396	4.296	1.264	-----	-----	-----	-----	-----
18	Gly	8.208	1.576, 2.716	-----	-----	-----	-----	-----	-----
19	Pro	-----	4.566	2.056, 2.423	2.056, 2.055	3.541, 3.155	-----	-----	-----
20	Ser	7.926	4.570	3.929, 3.926		-----	-----	-----	-----
21	Ser	7.840	4.154	3.665, 3.888		-----	-----	-----	-----

CircMut GAUDA

#	Res		Hα	Hβ	Hγ	Hδ	Hε	Hζ	Hη
1	Arg		4.252	1.887, 1.768	1.888, 1.589	3.198,	7.382	-----	, , ,
2	Pro	-----	4.749	1.786, 2.358	1.953, 1.953	3.425, 3.649	-----	-----	-----
3	Pro	-----	3.715	1.595, 1.595	1.876, 1.876	3.514, 3.665	-----	-----	-----
4	Pro	-----	4.214	1.871, 2.159	1.873, 1.872	3.200, 3.387	-----	-----	-----
5	Gly	8.364	3.935, 3.771	-----	-----	-----	-----	-----	-----
6	Ala	7.933	4.342	1.430	-----	-----	-----	-----	-----
7	Aib	8.615	-----	, 1.393	-----	-----	-----	-----	-----
8	Asp	8.541	4.513	2.749, 2.749	-----		-----	-----	-----
9	Ala	7.945	4.363	1.525	-----	-----	-----	-----	-----
10	Tyr	8.500	4.175	3.108, 3.108	-----	7.017	6.806	-----	
11	Ala	8.253	4.081	1.566	-----	-----	-----	-----	-----
12	Gln	8.165	4.020	2.178, 2.136	2.416,	-----	7.013, 7.888	-----	-----
13	Trp	8.042	4.314	3.204, 3.569	-----	7.157	10.031, 7.175	7.348, 7.109	7.225
14	Leu	8.455	3.527	1.422, 1.703	1.489	0.851,	-----	-----	-----
15	Ala	7.976	4.037	1.462	-----	-----	-----	-----	-----
16	Asp	7.995	4.543	2.709, 2.792	-----		-----	-----	-----
17	dAla	7.509	4.293	1.278	-----	-----	-----	-----	-----
18	Gly	8.125	1.960, 2.765	-----	-----	-----	-----	-----	-----
19	Pro	-----	4.523	2.061, 2.369	2.060, 2.060	3.487, 3.186	-----	-----	-----
20	Ser	8.158	4.557	3.936, 3.938		-----	-----	-----	-----
21	Ser	7.913	4.207	3.742, 3.885		-----	-----	-----	-----

CircMut GGDA S20A

#	Res		Hα	Hβ	Hγ	Hδ	Hε	Hζ	Hη
1	Arg		4.455	1.982, 1.698	1.828,	3.257,	7.465	-----	, , ,
2	Pro	-----	4.612	1.740, 2.205	1.987, 1.987	3.541, 3.748	-----	-----	-----
3	Pro	-----	3.545	1.512, 1.177	1.846, 1.849	3.394, 3.547	-----	-----	-----
4	Pro	-----	4.402	1.885, 2.258	,	3.075, 3.400	-----	-----	-----
5	Ser	8.426	4.163	3.778, 3.778		-----	-----	-----	-----
6	Gly	8.114	4.120, 3.872	-----	-----	-----	-----	-----	-----
7	Gly	8.513	4.044, 4.044	-----	-----	-----	-----	-----	-----
8	Asp	8.772	4.539	2.737, 2.697	-----		-----	-----	-----
9	Ala	8.654	4.264	1.469	-----	-----	-----	-----	-----
10	Tyr	8.326	4.148	3.045, 3.045	-----	7.090	6.807	-----	
11	Ala	8.054	4.102	1.566	-----	-----	-----	-----	-----
12	Gln	8.156	4.019	2.158, 2.117	2.411, 2.411	-----	6.988, 7.869	-----	-----
13	Trp	8.070	4.296	3.239, 3.547	-----	7.120	10.047, 7.087	7.332, 7.089	7.222
14	Leu	8.429	3.529	, 1.719		0.882, 0.861	-----	-----	-----
15	Ala	7.939	4.031	1.462	-----	-----	-----	-----	-----
16	Asp	7.994	4.527	2.707, 2.793	-----		-----	-----	-----
17	dAla	7.481	4.289	1.277	-----	-----	-----	-----	-----
18	Gly	8.173	1.837, 2.759	-----	-----	-----	-----	-----	-----
19	Pro	-----	4.495	2.064, 2.370	2.063, 2.063	3.511, 3.269	-----	-----	-----
20	Ala	8.008	4.433	1.413	-----	-----	-----	-----	-----
21	Ser	7.860	4.148	3.688, 3.866		-----	-----	-----	-----

CircMut GGDA S21A

#	Res		Hα	Hβ	Hγ	Hδ	Hε	Hζ	Hη
1	Arg		4.409	1.961, 1.694	1.782, 1.784	3.234,	7.342	-----	, , ,
2	Pro	-----	4.551	1.746, 2.151	1.982,	3.526, 3.741	-----	-----	-----
3	Pro	-----	3.976	, 1.626	1.867,	3.563, 3.360	-----	-----	-----
4	Pro	-----	4.355	1.845, 2.247	1.906, 1.905	3.457, 3.212	-----	-----	-----
5	Ser	8.417	4.178	3.799, 3.746		-----	-----	-----	-----
6	Gly	8.224	4.097, 3.903	-----	-----	-----	-----	-----	-----
7	Gly	8.464	4.059,	-----	-----	-----	-----	-----	-----
8	Asp	8.743	4.589	2.784, 2.784	-----		-----	-----	-----
9	Ala	8.070	4.053	1.548	-----	-----	-----	-----	-----
10	Tyr	8.313	4.151	3.006, 3.007	-----	7.020	6.807	-----	
11	Ala	8.631	4.240	1.486	-----	-----	-----	-----	-----
12	Gln	8.197	4.044	2.142, 2.145	2.438, 2.438	-----	7.014, 7.677	-----	-----
13	Trp	8.090	4.260	3.222, 3.532	-----	7.138	10.124, 7.182	7.358, 7.102	7.223
14	Leu	8.458	3.537	, 1.647	1.428	0.834, 0.832	-----	-----	-----
15	Ala	7.973	4.047	1.453	-----	-----	-----	-----	-----
16	Asp	7.912	4.597	2.793, 2.892	-----		-----	-----	-----
17	dAla	7.518	4.283	1.278	-----	-----	-----	-----	-----
18	Gly	7.991	2.130, 2.740	-----	-----	-----	-----	-----	-----
19	Pro	-----	4.462	, 2.335	2.020, 2.021	3.410, 3.119	-----	-----	-----
20	Ser	8.159	4.478	3.909, 3.909		-----	-----	-----	-----
21	Ala	7.877	4.141	1.317	-----	-----	-----	-----	-----

CircMut DUAA S20A

#	Res		Hα	Hβ	Hγ	Hδ	Hε	Hζ	Hη
1	Arg		4.244	1.867, 1.519	1.789,	3.194,	7.464	-----	, , ,
2	Pro	-----	4.806	1.771, 2.402	1.965, 1.969	3.373, 3.670	-----	-----	-----
3	Pro	-----	3.156	1.439, 0.954	1.823, 1.854	3.559, 3.639	-----	-----	-----
4	Pro	-----	4.172	1.801, 2.096	1.856, 1.846	2.985, 3.195	-----	-----	-----
5	Ser	8.028	4.217	3.875, 3.763		-----	-----	-----	-----
6	Asp	7.876	4.566	2.795, 2.611	-----		-----	-----	-----
7	Aib	8.596	-----	,	-----	-----	-----	-----	-----
8	Ala	8.394	4.256	1.511	-----	-----	-----	-----	-----
9	Ala	8.258	4.409	1.546	-----	-----	-----	-----	-----
10	Tyr	8.819	4.076	3.150, 3.151	-----	7.053	6.790	-----	
11	Ala	8.260	4.119	1.604	-----	-----	-----	-----	-----
12	Gln	8.058	4.000	2.149, 2.216	2.429, 2.432	-----	7.046, 7.962	-----	-----
13	Trp	8.087	4.266	3.165, 3.607	-----	7.102	9.948, 7.096	7.315, 7.221	7.229
14	Leu	8.505	3.465	1.765, 1.414	1.512	0.887, 0.869	-----	-----	-----
15	Ala	7.960	4.024	1.483	-----	-----	-----	-----	-----
16	Asp	8.019	4.516	2.700, 2.821	-----		-----	-----	-----
17	dAla	7.402	4.300	1.269	-----	-----	-----	-----	-----
18	Gly	8.229	1.520, 2.639	-----	-----	-----	-----	-----	-----
19	Pro	-----	4.535	2.088, 2.401	2.089, 2.090	3.547, 3.276	-----	-----	-----
20	Ala	7.897	4.464	1.416	-----	-----	-----	-----	-----
21	Ser	7.814	4.123	3.643, 3.880		-----	-----	-----	-----

CircMut DUAA P19W S20A

#	Res		Hα	Hβ	Hγ	Hδ	Hε	Hζ	Hη
1	Arg		4.509	1.979, 1.821	1.936, 1.645	3.173,	7.421	-----	, , ,
2	Pro	-----	4.006	1.724, 2.422	2.101, 2.007	3.526, 3.811	-----	-----	-----
3	Pro	-----	2.262	1.115, -0.073	1.454, 1.646	3.237, 2.548	-----	-----	-----
4	Pro	-----	4.336	1.956, 2.164	1.794, 1.735	2.711, 3.054	-----	-----	-----
5	Ser	8.229	4.189	3.837, 3.764		-----	-----	-----	-----
6	Asp	7.852	4.511	2.716, 2.618	-----		-----	-----	-----
7	Aib	8.769	-----	,	-----	-----	-----	-----	-----
8	Ala	8.338	4.239	1.500	-----	-----	-----	-----	-----
9	Ala	8.272	4.474	1.542	-----	-----	-----	-----	-----
10	Tyr	8.545	3.931	3.183, 3.119	-----	7.011	6.754	-----	
11	Ala	8.417	4.125	1.585	-----	-----	-----	-----	-----
12	Gln	8.164	3.955	2.181, 2.100	2.407,	-----	8.027, 7.048	-----	-----
13	Trp	7.964	4.120	2.997, 3.515	-----	6.752	9.214, 6.817	6.093, 6.876	6.530
14	Leu	8.458	3.245	1.725, 1.433	1.512	0.940, 0.880	-----	-----	-----
15	Ala	7.924	3.991	1.466	-----	-----	-----	-----	-----
16	Asp	8.099	4.454	2.711, 2.801	-----		-----	-----	-----
17	dAla	7.290	4.328	1.225	-----	-----	-----	-----	-----
18	Gly	8.187	2.807, 0.645	-----	-----	-----	-----	-----	-----
19	Trp	8.767	4.627	3.517, 3.166	-----	7.571	10.534, 7.849	7.584, 7.243	7.345
20	Ala	7.851	4.498	1.406	-----	-----	-----	-----	-----
21	Ser	7.580	4.047	3.469, 3.861		-----	-----	-----	-----

CircMut DUAA P3A S20A

1	Arg		4.210	1.855, 1.455	1.770,	3.188, 3.157	7.466	-----	, , ,
2	Pro	-----	4.520	1.769, 2.295	1.933, 1.891	3.215, 3.605	-----	-----	-----
3	Ala	8.515	3.030	0.736	-----	-----	-----	-----	-----
4	Pro	-----	4.024	, 2.059	1.803, 1.782	3.055, 3.287	-----	-----	-----
5	Ser	7.901	4.231	3.904, 3.754		-----	-----	-----	-----
6	Asp	7.939	4.582	2.846, 2.660	-----		-----	-----	-----
7	Aib	8.448	-----	,	-----	-----	-----	-----	-----
8	Ala	8.415	4.258	1.509	-----	-----	-----	-----	-----
9	Ala	8.252	4.380	1.541	-----	-----	-----	-----	-----
10	Tyr	8.862	4.082	3.141, 3.143	-----	7.021	6.804	-----	
11	Ala	8.216	4.117	1.606	-----	-----	-----	-----	-----
12	Gln	8.040	4.001	2.224, 2.150	2.433, 2.426	-----	7.043, 7.960	-----	-----
13	Trp	8.078	4.277	3.160, 3.591	-----	7.094	9.990, 7.088	7.329, 7.077	7.223
14	Leu	8.498	3.463	1.761, 1.405	1.505	0.880, 0.848	-----	-----	-----
15	Ala	7.937	4.025	1.480	-----	-----	-----	-----	-----
16	Asp	8.008	4.518	2.700, 2.821	-----		-----	-----	-----
17	dAla	7.398	4.300	1.268	-----	-----	-----	-----	-----
18	Gly	8.227	1.555, 2.624	-----	-----	-----	-----	-----	-----
19	Pro	-----	4.529	, 2.400	2.080, 2.080	3.533, 3.257	-----	-----	-----
20	Ala	7.917	4.462	1.415	-----	-----	-----	-----	-----
21	Ser	7.828	4.133	3.663, 3.889		-----	-----	-----	-----

CircMut New Cut 1

#	Res		Hα	Hβ	Hγ	Hδ	Hε	Hζ	Hη
1	Gly		,	-----	-----	-----	-----	-----	-----
2	Pro	-----	4.513	, 2.322	2.001,2.002	3.593,3.540	-----	-----	-----
3	Ser	8.724	4.470	3.915,3.848		-----	-----	-----	-----
4	Ser	8.465	4.433	3.912,3.912		-----	-----	-----	-----
5	dAla	8.421	4.368	1.421	-----	-----	-----	-----	-----
6	Arg	8.331	4.611	1.830,1.627	1.704,	3.190,	7.241	-----	,,6.534,6.958
7	Pro	-----	4.335	, 1.961	1.749,1.748	3.543,3.763	-----	-----	-----
8	Pro	-----	4.354	1.861,2.253	1.932,1.932	3.391,3.616	-----	-----	-----
9	Pro	-----	4.249	, 1.882	1.736,	3.374,3.578	-----	-----	-----
10	Ser	8.422	4.195	3.813, 3.749		-----	-----	-----	-----
11	Gly	8.292	4.076, 3.911	-----	-----	-----	-----	-----	-----
12	Gly	8.422	4.061, 4.061	-----	-----	-----	-----	-----	-----
13	Asp	8.661	4.568	2.731,2.693	-----		-----	-----	-----
14	Ala	8.578	4.244	1.437	-----	-----	-----	-----	-----
15	Tyr	8.246	4.250	3.047,3.055	-----	6.817	7.090	-----	
16	Ala	8.056	4.069	1.487	-----	-----	-----	-----	-----
17	Gln	8.216	4.070	2.106,	2.412,2.367	-----	6.970, 7.742	-----	-----
18	Trp	8.063	4.322	3.237,3.435	-----	7.230	10.102, 7.492	7.493, 7.104	7.245
19	Leu	8.394	3.677	1.555,	1.433	0.863,	-----	-----	-----
20	Ala	7.748	4.070	1.408	-----	-----	-----	-----	-----
21	Asp	8.027	4.542	2.670, 2.671	-----		-----	-----	-----
22	Gly	7.902	3.812, 3.637	-----	-----	-----	-----	-----	-----

CircMut New Cut 2

#	Res		Hα	Hβ	Hγ	Hδ	Hε	Hζ	Hη
1	Pro	-----	4.445	2.044,2.457	2.092,2.092	3.377,3.417	-----	-----	-----
2	Ser	8.913	4.544	3.821,3.879		-----	-----	-----	-----
3	Ser	8.712	4.480	3.908,3.909		-----	-----	-----	-----
4	dAla	8.460	4.377	1.417	-----	-----	-----	-----	-----
5	Arg	8.402	4.588	1.810,1.624	1.686,	3.192,	7.241	-----	,6.517,6.959
6	Pro	-----	4.226	, 1.935	1.711,1.710	3.754,3.524	-----	-----	-----
7	Pro	-----	4.359	1.887,1.740	1.984,1.983	3.283,3.522	-----	-----	-----
8	Pro	-----	4.326	1.852,2.253	1.938,1.938	3.398,3.617	-----	-----	-----
9	Ser	8.389	4.143	3.787,3.709		-----	-----	-----	-----
10	Gly	8.285	4.083,3.903	-----	-----	-----	-----	-----	-----
11	Gly	7.825	3.987,3.682	-----	-----	-----	-----	-----	-----
12	Asp	8.696	4.578	2.733,2.733	-----		-----	-----	-----
13	Ala	8.599	4.213	1.476	-----	-----	-----	-----	-----
14	Tyr	8.306	4.210	3.038,3.061	-----	6.817	7.061	-----	
15	Ala	8.087	4.053	1.546	-----	-----	-----	-----	-----
16	Gln	8.300	4.096	, 2.130	2.399,2.471	-----	6.988, 7.599	-----	-----
17	Trp	8.091	4.258	3.508, 3.251	-----	7.196	10.097, 7.169	7.446, 7.068	7.209
18	Leu	8.489	3.554	1.597,	1.424	0.838,	-----	-----	-----
19	Ala	7.878	4.093	1.427	-----	-----	-----	-----	-----
20	Asn	7.849	4.708	2.875, 2.727	-----	7.029, 7.667	-----	-----	-----
21	Gly	7.887	3.977, 3.691	-----	-----	-----	-----	-----	-----
22	Gly	7.898	2.904, 2.994	-----	-----	-----	-----	-----	-----

CircMut New Cut 2 P1W ***300 K***

#	Res	Hα	Hβ	Hγ	Hδ	Hε	Hζ	Hη
1	Trp		,	-----	7.280	10.158, 7.571	7.477, 7.128	7.223
2	Ser	8.494	4.368 , 3.815		-----	-----	-----	-----
3	Ser	8.275	4.422 , 3.757		-----	-----	-----	-----
4	dAla	8.316	4.377 1.403	-----	-----	-----	-----	-----
5	Arg	8.060	4.245 1.690,	1.495,	3.048,	7.052	-----	, , ,
6	Pro	-----	4.399 1.690, 2.083	1.831,	3.556, 3.253	-----	-----	-----
7	Pro	-----	4.314 , 2.159	,	3.435, 3.570	-----	-----	-----
8	Pro	-----	4.068 1.776, 2.010	1.829,	3.327, 3.407	-----	-----	-----
9	Ser	7.885	4.255 3.917, 3.786		-----	-----	-----	-----
10	Gly		, -----	-----	-----	-----	-----	-----
11	Gly		, -----	-----	-----	-----	-----	-----
12	Asp	7.901	4.637 2.705, 2.833	-----		-----	-----	-----
13	Ala	7.968	4.248 1.419	-----	-----	-----	-----	-----
14	Tyr	8.362	4.242 3.091, 3.019	-----	7.041	6.792	-----	
15	Ala	7.923	4.097 1.446	-----	-----	-----	-----	-----
16	Gln	7.893	4.140 2.077,	2.376, 2.312	-----	,	-----	-----
17	Trp	7.991	4.411 3.205, 3.396	-----	7.187	10.050, 7.332	7.424, 7.082	6.998
18	Leu	8.276	3.855 1.555,	1.449	0.814,	-----	-----	-----
19	Ala	7.510	4.330 1.427	-----	-----	-----	-----	-----
20	Asn	7.938	4.626 2.814, 2.576	-----	,	-----	-----	-----
21	Gly		, -----	-----	-----	-----	-----	-----
22	Gly		, -----	-----	-----	-----	-----	-----

CircMut TADA a17q

#	Res		Hα	Hβ	Hγ	Hδ	Hε	Hζ	Hη
1	Arg		4.452	2.014, 1.713	1.833,	3.264,	7.517	-----	, , ,
2	Pro	-----	4.769	1.788, 2.351	2.006,	3.768, 3.570	-----	-----	-----
3	Pro	-----	3.427	1.545, 1.197	1.892, 1.892	3.498, 3.660	-----	-----	-----
4	Pro	-----	4.471	, 2.315	1.896,	3.056, 3.329	-----	-----	-----
5	Ser	8.648	4.366	3.971, 3.841		-----	-----	-----	-----
6	Thr	7.622	4.504	4.407	, 1.243	-----	-----	-----	-----
7	Ala	8.704	4.197	1.484	-----	-----	-----	-----	-----
8	Asp	8.799	4.506	2.733, 2.733	-----		-----	-----	-----
9	Ala	8.008	4.332	1.470	-----	-----	-----	-----	-----
10	Tyr	8.692	4.142	3.093, 3.093	-----	6.795	7.080	-----	
11	Ala	8.277	4.119	1.585	-----	-----	-----	-----	-----
12	Gln	7.938	4.019	2.156,	2.428,	-----	7.008, 7.925	-----	-----
13	Trp	8.155	4.289	3.181, 3.571	-----	7.115	9.939, 7.084	7.331, 7.099	7.229
14	Leu	8.515	3.465	1.741, 1.435	1.505	0.897, 0.866	-----	-----	-----
15	Ala	7.889	4.046	1.477	-----	-----	-----	-----	-----
16	Asp	8.098	4.531	2.718, 2.764	-----		-----	-----	-----
17	dGln	7.499	4.198	2.151,	2.225,	-----	6.821, 7.471	-----	-----
18	Gly	8.226	2.897, 1.763	-----	-----	-----	-----	-----	-----
19	Pro	-----	4.556	, 2.406	2.081, 2.081	3.563, 3.261	-----	-----	-----
20	Ser	8.105	4.530	3.920, 3.920		-----	-----	-----	-----
21	Ser	7.886	4.163	3.685, 3.879		-----	-----	-----	-----

CircMut GUDA a17r

#	Res		Hα	Hβ	Hγ	Hδ	Hε	Hζ	Hη
1	Arg		4.495	2.045, 1.735	1.888,	3.286,	7.550	-----	, , ,
2	Pro	-----	4.782	1.792, 2.369	1.998, 1.998	3.595, 3.771	-----	-----	-----
3	Pro	-----	3.043	1.368, 0.697	1.777, 1.858	3.592, 3.520	-----	-----	-----
4	Pro	-----	4.492	1.744, 2.219	1.914, 1.914	3.235, 2.913	-----	-----	-----
5	Ser	8.404	4.334	3.803, 3.805		-----	-----	-----	-----
6	Gly	8.410	4.050, 3.803	-----	-----	-----	-----	-----	-----
7	Aib	8.701	-----	, 1.513	-----	-----	-----	-----	-----
8	Asp	8.435	4.529	2.742, 2.661	-----		-----	-----	-----
9	Ala	8.255	4.253	1.455	-----	-----	-----	-----	-----
10	Tyr	8.947	4.114	3.119, 3.123	-----	7.084	6.798	-----	
11	Ala	8.020	4.105	1.636	-----	-----	-----	-----	-----
12	Gln	8.057	4.012	2.183, 2.143	2.428,	-----	6.997, 7.916	-----	-----
13	Trp	8.153	4.256	3.143, 3.619	-----	7.095	9.886, 7.095	7.332, 7.093	7.236
14	Leu	8.556	3.418	1.753, 1.420	1.489	0.875, 0.869	-----	-----	-----
15	Ala	7.896	4.020	1.478	-----	-----	-----	-----	-----
16	Asp	8.054	4.521	2.719, 2.795	-----		-----	-----	-----
17	dArg	7.396	4.222	1.847, 1.468	1.539, 1.539	3.060,	7.131	-----	, , ,
18	Gly	8.264	1.565, 2.810	-----	-----	-----	-----	-----	-----
19	Pro	-----	4.590	, 2.431	2.081, 2.081	3.584, 3.261	-----	-----	-----
20	Ser	7.982	4.550	3.912, 3.913		-----	-----	-----	-----
21	Ser	7.842	4.144	3.643, 3.871		-----	-----	-----	-----

CircMut TADA +d

#	Res		Hα	Hβ	Hγ	Hδ	Hε	Hζ	Hη
1	Arg		4.515	1.974, 1.703	1.769,	3.214,		-----	, , ,
2	Pro	-----	4.785	1.763, 2.367	1.997, 1.996	3.581, 3.786	-----	-----	-----
3	Pro	-----	2.976	1.420, 0.782	1.838, 1.880	3.511, 3.609	-----	-----	-----
4	Pro	-----	4.516	1.896, 2.314	2.072,	2.912, 3.228	-----	-----	-----
5	Ser	8.628	4.370	3.954, 3.827		-----	-----	-----	-----
6	Thr	7.396	4.580	4.430	, 1.241	-----	-----	-----	-----
7	Ala	8.760	4.173	1.495	-----	-----	-----	-----	-----
8	Asp	8.287	4.473	2.739, 2.539	-----		-----	-----	-----
9	Ala	7.878	4.369	1.463	-----	-----	-----	-----	-----
10	Tyr	8.804	4.073	3.091, 3.091	-----	7.089	6.797	-----	
11	Ala	8.300	4.150	1.604	-----	-----	-----	-----	-----
12	Gln	7.864	4.014	2.202, 2.146	2.418,	-----	7.024, 7.903	-----	-----
13	Trp	8.164	4.246	3.122, 3.583	-----	7.075	9.912, 7.004	7.287, 7.082	7.231
14	Leu	8.520	3.425	1.791, 1.424	1.562	0.947, 0.875	-----	-----	-----
15	Ala	7.894	4.030	1.481	-----	-----	-----	-----	-----
16	Asp	7.983	4.526	2.708, 2.849	-----		-----	-----	-----
17	dAla	7.396	4.278	1.250	-----	-----	-----	-----	-----
18	Gly	8.277	1.283, 2.811	-----	-----	-----	-----	-----	-----
19	Pro	-----	4.587	, 2.437	2.065, 2.064	3.570, 3.219	-----	-----	-----
20	Ser	7.897	4.590	3.915, 3.915		-----	-----	-----	-----
21	Ser	8.017	4.277	3.651, 3.858		-----	-----	-----	-----
22	dAsp	8.917	4.495	2.721, 2.721	-----		-----	-----	-----

cp-WW2 ***298 K***

#	Res		Hα	Hβ	Hγ	Hδ	Hε	Hζ	Hη
-2	dPro	-----	4.759	2.307, 1.898	2.135, 2.002	3.859, 3.529	-----	-----	-----
-1	Pro	-----	4.538	2.242, 2.104	, 1.918	3.977, 3.741	-----	-----	-----
1	Lys	7.778	4.465	1.867,	1.439, 1.367	1.697,	2.984,		-----
2	Lys	8.423	5.110	1.699,	1.396, 1.299	1.579,	2.899,		-----
3	Leu	9.060	4.779	1.622, 1.502		, 0.872	-----	-----	-----
4	Thr	8.604	5.420	4.008	, 1.214	-----	-----	-----	-----
5	Val	9.420	4.921	2.091	0.942, 0.888	-----	-----	-----	-----
6	Trp	8.643	4.674	2.705, 1.781	-----	6.772	9.991, 5.181	7.187, 6.424	6.901
7	Ile	8.353	4.188	1.733	, , 0.604		-----	-----	-----
8	dPro	-----	4.452	2.225, 2.099	1.938, 1.811	2.793, 3.343	-----	-----	-----
9	Gly		3.679, 3.056	-----	-----	-----	-----	-----	-----
10	Lys	7.412	4.372	1.704,	,	1.620,	,		-----
11	Trp	8.519	5.438	3.150, 3.086	-----	7.536	10.158, 7.190	7.242, 7.513	7.162
12	Ile	9.507	4.811	1.888	, , 0.857		-----	-----	-----
13	Thr	8.533	5.342	3.947	, 1.133	-----	-----	-----	-----
14	Val	9.333	4.550	2.086	, 0.896	-----	-----	-----	-----
15	Ser	8.595	5.259	3.860, 3.749		-----	-----	-----	-----
16	Ile	8.821	4.580	1.813	1.433, 1.093, 0.875	0.808	-----	-----	-----

Appendix C: Distance Constraints for NMR Structure Ensembles

# Denotes shift-coincident methyl or germinal methylene protons
* Denotes stereotopically ambiguous methylene protons

C1. NOE Constraint List for [D9R,R16E]-TC10b

Intraresidue (i, i) constraints

	d	d-	d+	δ values
assign (residue 1 and name ha) (residue 1 and name hb1)	2.92	0.56	0.70	4.28 3.15
assign (residue 1 and name ha) (residue 1 and name hb2)	3.04	0.57	0.47	4.27 2.98
assign (residue 3 and name hb#) (residue 3 and name ha)	2.76	0.36	0.42	3.14 4.05
assign (residue 3 and name ha) (residue 3 and name hn)	2.97	0.37	0.46	4.04 8.85
assign (residue 3 and name ha) (residue 3 and name hd#)	3.29	0.41	0.95	4.05 7.12
assign (residue 3 and name hd#) (residue 3 and name hn)	4.27	0.47	1.17	7.12 8.85
assign (residue 3 and name hb#) (residue 3 and name he#)	4.34	0.51	1.19	3.14 6.84
assign (residue 3 and name hb2) (residue 3 and name hn)	2.40	0.15	0.20	
assign (residue 4 and name ha) (residue 4 and name hn)	2.94	0.37	0.45	4.15 8.38
assign (residue 5 and name hb2) (residue 5 and name hn)	2.86	0.36	0.69	2.24 8.10
assign (residue 5 and name hb1) (residue 5 and name hn)	2.99	0.37	0.66	2.19 8.10
assign (residue 5 and name hg2) (residue 5 and name hn)	3.10	0.88	0.73	2.54 8.10
assign (residue 5 and name ha) (residue 5 and name hn)	2.94	0.36	0.45	4.06 8.10
assign (residue 5 and name hg1) (residue 5 and name hn)	3.10	0.38	0.48	2.58 8.10
assign (residue 5 and name ha) (residue 5 and name hg1)	3.69	0.43	0.61	4.07 2.57
assign (residue 5 and name ha) (residue 5 and name hg2)	3.95	0.46	0.68	4.07 2.54
assign (residue 6 and name hb2) (residue 6 and name hd1)	2.51	0.33	0.58	3.13 7.10
assign (residue 6 and name hb1) (residue 6 and name hn)	2.56	0.33	0.39	3.59 8.18
assign (residue 6 and name hb2) (residue 6 and name hn)	2.68	0.34	0.41	3.14 8.18
assign (residue 6 and name ha) (residue 6 and name hd1)	2.83	0.35	0.63	4.12 7.10
assign (residue 6 and name hb1) (residue 6 and name he3)	2.82	0.36	0.45	3.59 6.99
assign (residue 6 and name ha) (residue 6 and name hn)	3.01	0.37	0.47	4.12 8.18
assign (residue 6 and name hb1) (residue 6 and name hd1)	3.27	0.39	0.72	3.59 7.10
assign (residue 6 and name hb1) (residue 6 and name hz3)	3.98	0.45	0.96	3.58 7.07
assign (residue 6 and name ha) (residue 6 and name he3)	3.99	0.46	0.89	4.12 6.99
assign (residue 7 and name hg) (residue 7 and name hb1)	2.60	0.33	0.40	1.61 1.36
assign (residue 7 and name hb2) (residue 7 and name hn)	2.73	0.48	0.42	1.88 8.51
assign (residue 7 and name hg) (residue 7 and name hn)	2.76	0.35	0.42	1.61 8.51
assign (residue 7 and name ha) (residue 7 and name hn)	3.00	0.37	0.46	3.33 8.51
assign (residue 7 and name ha) (residue 7 and name hb1)	2.78	0.36	0.29	3.33 1.38
assign (residue 7 and name ha) (residue 7 and name hd2#)	2.76	0.35	0.42	3.33 0.82
assign (residue 7 and name hb1) (residue 7 and name hn)	3.31	0.40	0.53	1.39 8.51
assign (residue 7 and name hb2) (residue 7 and name hd1#)	3.34	0.44	0.55	1.88 0.98
assign (residue 7 and name hb1) (residue 7 and name hd2#)	3.35	0.4	0.53	1.39 0.82
assign (residue 7 and name ha) (residue 7 and name hb2)	3.64	0.63	0.60	3.34 1.89
assign (residue 7 and name ha) (residue 7 and name hg)	3.52	0.63	0.61	3.33 1.61
assign (residue 7 and name hb1) (residue 7 and name hd1#)	3.25	0.40	0.53	1.39 0.98
assign (residue 7 and name hb2) (residue 7 and name hd2#)	4.32	0.51	0.70	1.87 0.82
assign (residue 7 and name hd1#) (residue 7 and name hn)	4.59	0.54	0.76	0.98 8.51
assign (residue 7 and name hd2#) (residue 7 and name hn)	4.64	0.54	0.77	0.82 8.51

assign (residue 7 and name ha) (residue 7 and name hd1#) 4.67 0.55 0.78 3.33 0.98
assign (residue 8 and name hb2) (residue 8 and name hn) 2.66 0.34 0.41 1.92 7.95
assign (residue 8 and name ha) (residue 8 and name hn) 2.85 0.36 0.44 4.04 7.94
assign (residue 8 and name hb1) (residue 8 and name hn) 2.88 0.36 0.44 1.97 7.95
assign (residue 8 and name ha) (residue 8 and name hb2) 3.23 0.69 0.51 4.03 1.94
assign (residue 8 and name ha) (residue 8 and name hb1) 3.32 0.4 0.53 4.03 2.00
assign (residue 8 and name hg#) (residue 8 and name hn) 3.75 0.44 0.63 1.56 7.95
assign (residue 8 and name hd2) (residue 8 and name hn) 4.4 0.50 0.81 1.70 7.95
assign (residue 9 and name ha) (residue 9 and name hb1) 2.64 0.34 0.40 4.33 1.92
assign (residue 9 and name hb1) (residue 9 and name hn) 2.75 0.35 0.42 1.92 7.48
assign (residue 9 and name hg1) (residue 9 and name hn) 2.75 0.35 0.67 1.92 7.47
assign (residue 9 and name ha) (residue 9 and name hn) 2.89 0.36 0.44 4.33 7.48
assign (residue 9 and name hg2) (residue 9 and name hn) 3.27 0.69 0.52 1.80 7.47
assign (residue 9 and name hb2) (residue 9 and name hn) 3.37 0.40 0.54 1.66 7.47
assign (residue 9 and name hd1) (residue 9 and name hh**) 3.48 1.00 0.56 3.29 7.03
assign (residue 9 and name hd2) (residue 9 and name hh**) 3.65 1.00 0.70 3.20 7.01
assign (residue 9 and name ca) (residue 9 and name cd) 4 0.50 0.50
assign (residue 9 and name cb) (residue 9 and name ne) 4 0.50 0.50
assign (residue 10 and name ha2) (residue 10 and name hn) 2.50 0.20 0.25 3.52 7.58
assign (residue 10 and name ha1) (residue 10 and name hn) 3.20 0.25 0.25 4.18 7.57
assign (residue 11 and name ha2) (residue 11 and name hn) 2.53 0.35 0.22 1.26 8.04
assign (residue 11 and name ha1) (residue 11 and name hn) 3.08 0.28 0.48 2.92 8.04
assign (residue 12 and name ha) (residue 12 and name hb1) 2.60 0.39 0.50 4.56 2.49
assign (residue 12 and name ha) (residue 12 and name hb2) 3.20 0.31 0.55 4.56 2.09
assign (residue 12 and name hd1) (residue 12 and name hb1) 4.00 0.20 0.30 3.13 2.03
assign (residue 12 and name hd2) (residue 12 and name hb2) 3.00 0.20 0.30 3.13 2.03
assign (residue 12 and name ha) (residue 12 and name hd1) 4.25 0.48 0.77 4.56 3.15
assign (residue 13 and name hb#) (residue 13 and name hn) 3.06 0.38 0.47 3.93 7.81
assign (residue 13 and name ha) (residue 13 and name hn) 3.33 0.40 0.53 4.45 7.82
assign (residue 14 and name hb2) (residue 14 and name ha) 2.59 0.33 0.39 3.96 4.29
assign (residue 14 and name ha) (residue 14 and name hb1) 2.71 0.34 0.41 4.29 3.58
assign (residue 14 and name hb1) (residue 14 and name hn) 2.9 0.36 0.45 3.59 8.15
assign (residue 14 and name ha) (residue 14 and name hn) 2.93 0.36 0.45 4.29 8.16
assign (residue 14 and name hb2) (residue 14 and name hn) 3.33 0.40 0.53 3.96 8.16
assign (residue 15 and name ha2) (residue 15 and name hn) 2.52 0.34 0.40 3.84 7.98
assign (residue 15 and name ha1) (residue 15 and name hn) 3.23 0.61 0.55 4.29 7.99
assign (residue 16 and name ha) (residue 16 and name hn) 2.86 0.36 0.44 4.82 8.15
assign (residue 16 and name hb1) (residue 16 and name hn) 2.99 0.37 0.71 2.00 8.16
assign (residue 16 and name hb2) (residue 16 and name hn) 3.33 0.40 0.78 2.15 8.16
assign (residue 16 and name hg2) (residue 16 and name hn) 3.92 0.45 0.67 2.34 8.16
assign (residue 16 and name hg1) (residue 16 and name hn) 4.2 0.48 0.75 2.42 8.16
assign (residue 17 and name ha) (residue 17 and name hb1) 2.69 0.34 0.41 4.69 2.26
assign (residue 17 and name ha) (residue 17 and name hb2) 3.20 0.41 0.57 4.69 1.82
assign (residue 17 and name ha) (residue 17 and name hg#) 4.04 0.47 0.67 4.69 2.02
assign (residue 18 and name hb1) (residue 18 and name ha) 2.30 0.20 0.20
assign (residue 18 and name ha) (residue 18 and name hb2) 2.80 0.25 0.25
assign (residue 18 and name hd2) (residue 18 and name hb2) 4.00 0.25 0.65
assign (residue 18 and name hb1) (residue 18 and name hd1) 3.00 0.43 0.43
assign (residue 18 and name hb1) (residue 18 and name hg2) 3.04 0.65 0.67
assign (residue 19 and name ha) (residue 19 and name hb*) 2.89 0.36 0.44 4.33 2.23
assign (residue 20 and name hb#) (residue 20 and name hn) 3.67 0.44 0.59 3.80 8.03

i , i+1

assign (residue 2 and name ha) (residue 3 and name hn) 3.49 0.41 0.57 4.24 8.85
assign (residue 2 and name hb#) (residue 3 and name hn) 3.84 0.47 0.60 1.51 8.85
assign (residue 3 and name hb1) (residue 4 and name hn) 2.99 0.38 0.46 3.15 8.38
assign (residue 3 and name ha) (residue 4 and name hn) 3.52 0.42 0.57 4.05 8.38
assign (residue 3 and name hd2) (residue 4 and name hn) 4.11 0.48 1.13 7.12 8.39
assign (residue 4 and name hn) (residue 3 and name hn) 2.83 0.35 0.43 8.39 8.85
assign (residue 4 and name ha) (residue 5 and name hn) 3.40 0.41 0.55 4.15 8.10
assign (residue 4 and name hb#) (residue 5 and name hn) 3.67 0.46 0.57 1.62 8.10
assign (residue 5 and name hn) (residue 4 and name hn) 2.77 0.35 0.42 8.11 8.38
assign (residue 5 and name hn) (residue 6 and name hn) 2.44 0.32 0.37 8.11 8.17
assign (residue 5 and name ha) (residue 6 and name hn) 3.24 0.39 0.51 4.07 8.18
assign (residue 5 and name hb2) (residue 6 and name hn) 3.25 0.39 0.71 2.24 8.18
assign (residue 5 and name hb1) (residue 6 and name hn) 3.4 0.61 0.55 2.19 8.18
assign (residue 6 and name hn) (residue 7 and name hn) 2.74 0.35 0.42 8.19 8.51
assign (residue 6 and name hb1) (residue 7 and name hn) 2.91 0.36 0.45 3.59 8.51
assign (residue 6 and name he3) (residue 7 and name hn) 3.20 0.39 0.70 7.00 8.51
assign (residue 6 and name ha) (residue 7 and name hn) 3.26 0.39 0.52 4.12 8.51
assign (residue 6 and name hb2) (residue 7 and name hn) 3.62 0.43 0.60 3.13 8.51
assign (residue 7 and name hg) (residue 6 and name he3) 3.03 0.37 0.67 1.61 6.99
assign (residue 7 and name ha) (residue 6 and name he3) 3.6 0.42 0.79 3.33 6.99
assign (residue 7 and name hg) (residue 6 and name hz3) 3.7 0.43 0.81 1.61 7.07
assign (residue 7 and name hd2#) (residue 6 and name hz3) 3.71 0.46 0.82 0.82 7.07
assign (residue 7 and name hd2#) (residue 6 and name he3) 3.88 0.47 0.86 0.81 6.99
assign (residue 7 and name hb2) (residue 6 and name he3) 4.27 0.48 0.97 1.89 6.99
assign (residue 7 and name hd1#) (residue 6 and name he3) 4.99 0.57 1.11 0.98 6.99
assign (residue 7 and name hd1#) (residue 6 and name hz3) 5.23 0.60 1.18 0.98 7.07
assign (residue 7 and name hb2) (residue 8 and name hn) 2.88 0.36 0.44 1.88 7.95
assign (residue 7 and name ha) (residue 8 and name hn) 3.43 0.41 0.55 3.33 7.95
assign (residue 7 and name hb1) (residue 8 and name hn) 3.45 0.41 0.56 1.38 7.95
assign (residue 7 and name hg) (residue 8 and name hn) 4.04 0.46 0.70 1.61 7.95
assign (residue 8 and name hn) (residue 7 and name hn) 2.83 0.35 0.43 7.96 8.51
assign (residue 8 and name ha) (residue 9 and name hn) 3.56 0.42 0.58 4.03 7.48
assign (residue 8 and name hb1) (residue 9 and name hn) 3.76 0.44 0.63 1.99 7.48
assign (residue 9 and name hn) (residue 8 and name hn) 2.8 0.35 0.43 7.49 7.95
assign (residue 9 and name hn) (residue 10 and name hn) 2.84 0.36 0.44 7.48 7.57
assign (residue 9 and name ha) (residue 10 and name hn) 3.56 0.42 0.58 4.33 7.57
assign (residue 9 and name hb1) (residue 10 and name hn) 3.84 0.45 0.65 1.91 7.57
assign (residue 9 and name hg2) (residue 10 and name hn) 4.47 0.5 0.84 1.82 7.56
assign (residue 10 and name hn) (residue 11 and name hn) 2.49 0.33 0.25 7.58 8.04
assign (residue 10 and name ha2) (residue 11 and name hn) 3.66 0.43 0.61 3.51 8.04
assign (residue 12 and name hd1) (residue 11 and name ha1) 2.31 0.17 0.27 3.13 2.90
assign (residue 12 and name hd2) (residue 11 and name ha1) 2.61 0.37 0.47 3.71 2.91
assign (residue 12 and name hd1) (residue 11 and name ha2) 3.50 0.37 0.43 3.12 1.26
assign (residue 12 and name hd2) (residue 11 and name ha2) 4.30 0.40 0.82 3.71 1.25
assign (residue 12 and name ha) (residue 13 and name hn) 3.64 0.43 0.60 4.56 7.81
assign (residue 12 and name hd2) (residue 13 and name hn) 3.61 0.63 0.62 3.69 7.81
assign (residue 12 and name hb2) (residue 13 and name hn) 3.75 0.44 0.63 2.02 7.81
assign (residue 12 and name hg2) (residue 13 and name hn) 4.14 0.48 0.70 2.08 7.81
assign (residue 13 and name hn) (residue 14 and name hn) 2.89 0.56 0.44 7.82 8.16

assign (residue 13 and name ha) (residue 14 and name hn) 2.95 0.37 0.46 4.45 8.16
assign (residue 13 and name hb#) (residue 14 and name hn) 3.70 0.44 0.60 3.92 8.16
assign (residue 14 and name ha) (residue 15 and name hn) 3.43 0.41 0.55 4.29 7.99
assign (residue 14 and name hb2) (residue 15 and name hn) 4.31 0.49 0.79 3.96 7.99
assign (residue 14 and name hb1) (residue 15 and name hn) 4.69 0.52 0.91 3.59 7.98
assign (residue 15 and name hn) (residue 14 and name hn) 2.63 0.34 0.40 8.01 8.15
assign (residue 15 and name ha1) (residue 16 and name hn) 2.93 0.36 0.55 4.29 8.16
assign (residue 15 and name ha2) (residue 16 and name hn) 3.58 0.62 0.59 3.85 8.15
assign (residue 16 and name ha) (residue 17 and name hd1) 2.48 0.32 0.38 4.82 3.92
assign (residue 16 and name ha) (residue 17 and name hd2) 2.71 0.64 0.41 4.82 3.72
assign (residue 16 and name hb2) (residue 17 and name hd2) 3.75 0.44 0.88 2.15 3.73
assign (residue 16 and name hg1) (residue 17 and name hd2) 4.01 0.46 0.70 2.41 3.73
assign (residue 17 and name hd2) (residue 16 and name hb1) 3.19 0.39 0.75 3.74 1.99
assign (residue 17 and name hd2) (residue 16 and name hb2) 4.00 0.50 0.90
assign (residue 17 and name ha) (residue 18 and name hd#) 2.78 0.56 0.42 4.69 3.52
assign (residue 17 and name hb2) (residue 18 and name hd2) 3.29 0.41 0.51
assign (residue 18 and name hd1) (residue 17 and name hb1) 4.28 0.49 0.74 3.53 2.25
assign (residue 19 and name hd1) (residue 18 and name ha) 2.63 0.34 0.41 3.03 2.54
assign (residue 19 and name hd2) (residue 18 and name ha) 2.85 0.56 0.44 2.89 2.54
assign (residue 19 and name hd2) (residue 18 and name hb2) 3.74 0.44 0.63 2.89 1.37
assign (residue 19 and name hd2) (residue 18 and name hb1) 4.16 0.47 0.74 2.89 0.57
assign (residue 19 and name hd1) (residue 18 and name hb1) 4.41 0.50 0.82 3.02 0.56
assign (residue 19 and name ha) (residue 20 and name hn) 2.47 0.32 0.38 4.33 8.04

i, i+2

assign (residue 10 and name hn) (residue 8 and name hn) 3.63 0.43 0.60 7.57 7.95
assign (residue 12 and name ha) (residue 14 and name hn) 3.77 0.44 0.63 4.56 8.16
assign (residue 13 and name ha) (residue 15 and name hn) 4.19 0.48 0.75 4.45 7.99
assign (residue 8 and name ha) (residue 10 and name hn) 4.27 0.48 0.77 4.02 7.57
assign (residue 9 and name hn) (residue 11 and name hn) 3.95 0.46 0.68 7.48 8.04
assign (residue 11 and name hn) (residue 9 and name hg1) 2.82 0.50 0.85

i, i+3

assign (residue 14 and name hb1) (residue 11 and name hn) 4.04 0.46 0.70 3.59 8.04
assign (residue 1 and name hb2) (residue 4 and name hn) 4.2 0.48 1.00 3.00 8.38
assign (residue 2 and name ha) (residue 5 and name hn) 3.48 0.41 0.56 4.24 8.10
assign (residue 2 and name ha) (residue 5 and name hb1) 3.94 0.45 0.68 4.24 2.19
assign (residue 2 and name ha) (residue 5 and name hb2) 3.76 0.44 0.83 4.24 2.24
assign (residue 2 and name ha) (residue 5 and name hg1) 3.99 0.46 0.94 4.23 2.56
assign (residue 3 and name ha) (residue 6 and name hb2) 2.58 0.33 0.39 4.05 3.14
assign (residue 3 and name ha) (residue 6 and name hb1) 2.9 0.36 0.45 4.05 3.58
assign (residue 3 and name ha) (residue 6 and name hn) 3.14 0.38 0.49 4.05 8.18
assign (residue 3 and name he2) (residue 6 and name hz3) 3.46 0.42 1.20 6.86 7.06
assign (residue 4 and name ha) (residue 7 and name hn) 3.19 0.39 0.50 4.15 8.51
assign (residue 4 and name ha) (residue 7 and name hd1#) 3.83 0.47 0.60 4.15 0.98
assign (residue 5 and name ha) (residue 8 and name hn) 3.20 0.39 0.50 4.06 7.95
assign (residue 5 and name ha) (residue 8 and name hb2) 3.55 0.42 0.58 4.07 1.92
assign (residue 5 and name ha) (residue 8 and name hb1) 3.69 0.43 0.61 4.06 1.99
assign (residue 6 and name ha) (residue 9 and name hh**) 4.53 0.48 0.76 4.13 7.03
assign (residue 7 and name ha) (residue 10 and name hn) 4.27 0.48 0.77 3.33 7.57
assign (residue 7 and name o) (residue 10 and name hn) 3.20 0.20 2.00

assign (residue 7 and name hb2) (residue 4 and name ha) 3.14 0.38 0.49 1.88 4.14
assign (residue 7 and name hb1) (residue 4 and name ha) 3.93 0.45 0.67 1.39 4.14
assign (residue 9 and name hd2) (residue 6 and name hd1) 3.44 0.41 0.75 3.20 7.10
assign (residue 9 and name he) (residue 6 and name he1) 3.59 0.42 0.59 8.17 9.63
assign (residue 9 and name hg2) (residue 6 and name hd1) 3.76 0.44 0.83 1.80 7.10
assign (residue 4 and name ha) (residue 7 and name hb2) 3.39 0.41 0.54 4.14 1.88
assign (residue 9 and name hg*) (residue 6 and name hd1) 3.62 0.43 0.85
assign (residue 9 and name hd*) (residue 6 and name hd1) 3.00 0.37 0.46

i, i+4

assign (residue 11 and name ha2) (residue 7 and name ha) 3.51 0.42 0.57 1.26 3.33
assign (residue 11 and name ha1) (residue 7 and name ha) 3.82 0.44 0.65 2.92 3.32
assign (residue 11 and name ha1) (residue 7 and name hd2#) 4.54 0.53 0.75 2.94 0.81
assign (residue 2 and name ha) (residue 6 and name hn) 3.49 0.41 0.56 4.24 8.18
assign (residue 3 and name ha) (residue 7 and name hn) 3.82 0.44 0.65 4.04 8.51
assign (residue 4 and name ha) (residue 8 and name hn) 3.79 0.44 0.64 4.14 7.95
assign (residue 5 and name hb1) (residue 9 and name hh**) 4.47 0.50 1.09 2.18 7.02
assign (residue 7 and name ha) (residue 11 and name hn) 2.76 0.56 0.65 3.33 8.04
assign (residue 7 and name hd1#) (residue 3 and name he2) 4.04 0.50 1.17 0.98 6.85
assign (residue 7 and name hg) (residue 3 and name hd2) 4.07 0.48 1.12 1.62 7.12
assign (residue 7 and name hg) (residue 3 and name he2) 4.17 0.49 1.14 1.61 6.85
assign (residue 7 and name hd2#) (residue 3 and name he2) 4.46 0.54 1.25 0.82 6.85
assign (residue 7 and name hd1#) (residue 3 and name hd2) 4.54 0.55 1.27 0.98 7.12
assign (residue 7 and name hd2#) (residue 3 and name hd2) 5.49 0.63 1.50 0.82 7.12

i, i+n (n > 4)

assign (residue 3 and name ha) (residue 19 and name hg2) 3.38 0.52 0.55 4.04 1.81
assign (residue 3 and name ha) (residue 19 and name hd2) 3.67 0.43 0.61 4.04 2.88
assign (residue 3 and name ha) (residue 19 and name hb2) 4.00 0.46 0.6 4.04 2.88
assign (residue 9 and name hd1) (residue 14 and name hb*) 2.50 0.20 2.00
assign (residue 9 and name hd2) (residue 14 and name hb*) 2.50 0.20 2.00
assign (residue 9 and name he) (residue 16 and name oe#) 2.00 0.10 0.30
assign (residue 11 and name ha2) (residue 6 and name hz2) 3.72 0.43 0.82 1.26 7.22
assign (residue 11 and name ha1) (residue 6 and name hz2) 3.87 0.45 0.86 2.93 7.22
assign (residue 11 and name ha2) (residue 6 and name he3) 4.24 0.48 0.96 1.26 6.99
assign (residue 11 and name ha1) (residue 6 and name hz3) 4.51 0.51 1.05 2.93 7.07
assign (residue 12 and name ha) (residue 6 and name hz2) 2.84 0.33 0.34 4.56 7.22
assign (residue 12 and name hd1) (residue 6 and name hh2) 3.03 0.35 0.38 3.13 7.22
assign (residue 12 and name hd1) (residue 6 and name hz2) 3.03 0.35 0.38 3.12 7.22
assign (residue 12 and name hg1) (residue 6 and name hh2) 3.00 0.20 0.20 2.09 7.22
assign (residue 12 and name hd1) (residue 6 and name hz3) 3.8 0.42 0.53 3.13 7.07
assign (residue 12 and name hb1) (residue 6 and name hz2) 4.01 0.44 0.58 2.50 7.22
assign (residue 12 and name hg1) (residue 6 and name hz2) 3.00 0.25 0.20 2.02 7.22
assign (residue 16 and name hb1) (residue 6 and name hd1) 3.09 0.38 0.93 2.00 7.10
assign (residue 16 and name hb1) (residue 6 and name he1) 3.19 0.39 1.15 2.00 9.63
assign (residue 16 and name hb2) (residue 6 and name he1) 3.26 0.39 1.57 2.15 9.62
assign (residue 16 and name hb2) (residue 6 and name hd1) 3.37 0.40 0.99 2.15 7.10
assign (residue 16 and name hg1) (residue 6 and name hd1) 3.99 0.46 0.69 2.42 7.10
assign (residue 16 and name ha) (residue 6 and name he1) 3.74 0.44 0.82 4.80 9.62
assign (residue 17 and name ha) (residue 6 and name hz2) 3.63 0.43 0.80 4.69 7.22
assign (residue 17 and name ha) (residue 6 and name he1) 3.85 0.45 0.85 4.69 9.63

assign (residue 18 and name hb2) (residue 3 and name hd1) 4.08 0.48 1.12 1.38 7.12
assign (residue 18 and name hb1) (residue 3 and name he1) 4.17 0.49 1.14 0.58 6.85
assign (residue 18 and name hd1) (residue 6 and name hz2) 3.18 0.36 0.40 3.55 7.22
assign (residue 18 and name hg1) (residue 6 and name hh2) 3.74 0.42 0.52 1.75 7.22
assign (residue 18 and name ha) (residue 6 and name hd1) 3.76 0.42 0.52 2.54 7.10
assign (residue 18 and name hb1) (residue 6 and name hz2) 3.78 0.42 0.53 0.57 7.22
assign (residue 18 and name ha) (residue 6 and name he1) 3.80 0.42 0.53 2.54 9.62
assign (residue 18 and name ha) (residue 6 and name hh2) 3.85 0.42 0.54 2.54 7.22
assign (residue 18 and name hb2) (residue 6 and name hz2) 4.26 0.46 0.65 1.37 7.22
assign (residue 18 and name hb1) (residue 6 and name he3) 4.62 0.49 0.75 0.58 6.99
assign (residue 19 and name hb*) (residue 2 and name hb#) 4.34 0.52 0.70 2.23 1.51
assign (residue 19 and name hd2) (residue 3 and name hd1) 3.62 0.44 1.01 2.89 7.12
assign (residue 19 and name hg2) (residue 3 and name hd1) 3.83 0.45 0.84 1.81 7.12
assign (residue 19 and name hd2) (residue 3 and name he1) 4.68 0.53 1.27 2.89 6.84
assign (residue 19 and name hg#) (residue 3 and name hn) 4.46 0.51 0.79 1.80 8.85
assign (residue 19 and name hd1) (residue 6 and name hd1) 3.18 0.39 0.70 3.04 7.10
assign (residue 19 and name hd2) (residue 6 and name hd1) 3.76 0.44 0.83 2.89 7.10
assign (residue 19 and name hd2) (residue 6 and name hz2) 4.13 0.47 1.03 2.89 7.22
assign (residue 19 and name hd2) (residue 6 and name he3) 4.27 0.48 0.97 2.89 6.99
Constraints employed only during the initial phases of the restrained dynamics
assign (residue 16 and name oe#) (residue 9 and name he) 2.00 0.10 0.30
assign (residue 16 and name hg*) (residue 9 and name hh11) 3.50 0.20 2.00
assign (residue 16 and name hg*) (residue 9 and name hh21) 3.50 0.20 2.00
assign (residue 16 and name hb*) (residue 9 and name hh11) 3.50 0.20 2.00
assign (residue 16 and name hb*) (residue 9 and name hh21) 3.50 0.20 2.00
assign (residue 16 and name hg*) (residue 9 and name hh11) 3.50 0.20 2.00
assign (residue 16 and name hg*) (residue 9 and name he) 2.75 0.20 2.00
assign (residue 16 and name hg*) (residue 9 and name hh11) 3.50 0.20 2.00
assign (residue 16 and name hb2) (residue 9 and name hd1) 3.50 0.20 2.00
assign (residue 16 and name hb2) (residue 9 and name hd2) 3.50 0.20 2.00
assign (residue 16 and name hg*) (residue 9 and name hh12) 3.50 0.20 2.00
assign (residue 16 and name hg*) (residue 9 and name hh22) 3.50 0.20 2.00
assign (residue 16 and name hb*) (residue 9 and name hh12) 3.50 0.20 2.50
assign (residue 16 and name hb*) (residue 9 and name hh22) 3.50 0.20 2.25
assign (residue 16 and name hg*) (residue 9 and name hh12) 3.50 0.20 2.00
assign (residue 16 and name hg*) (residue 9 and name hh12) 3.50 0.20 2.00
assign (residue 16 and name hb*) (residue 9 and name he) 3.20 0.20 2.00

C2. Minimum Set of Common TC10b NOE Constraints

i, i	d	d-	d+
assign (residue 11 and name ha2) (residue 11 and name hn)	2.20	0.20	0.25
i, i+1			
assign (residue 3 and name hn) (residue 4 and name hn)	2.80	0.35	0.35
assign (residue 3 and name ha) (residue 4 and name hn)	3.50	0.40	0.50
assign (residue 4 and name hn) (residue 5 and name hn)	2.80	0.35	0.25
assign (residue 4 and name ha) (residue 5 and name hn)	3.50	0.50	0.50
assign (residue 5 and name hn) (residue 6 and name hn)	2.80	0.35	0.35
assign (residue 5 and name ha) (residue 6 and name hn)	3.50	0.50	0.50

assign (residue 6 and name hn) (residue 7 and name hn) 2.80 0.35 0.35
assign (residue 6 and name ha) (residue 7 and name hn) 3.50 0.50 0.50
assign (residue 6 and name he3) (residue 7 and name hg) 2.50 0.40 0.50
assign (residue 6 and name hz3) (residue 7 and name hd2#) 2.50 0.50 0.70
assign (residue 6 and name hz3) (residue 7 and name hg) 4.00 0.70 1.00
assign (residue 7 and name hn) (residue 8 and name hn) 2.80 0.35 0.35
assign (residue 7 and name ha) (residue 8 and name hn) 3.50 0.50 0.50
assign (residue 8 and name ha) (residue 9 and name hn) 3.50 0.50 0.50
assign (residue 9 and name hn) (residue 10 and name hn) 2.80 0.35 0.35
assign (residue 10 and name hn) (residue 11 and name hn) 2.30 0.30 0.30
assign (residue 11 and name ha1) (residue 12 and name hd1) 2.50 0.50 0.50
assign (residue 11 and name ha1) (residue 12 and name hd2) 2.30 0.30 0.40
assign (residue 12 and name hg2) (residue 13 and name hn) 3.10 0.20 0.20
assign (residue 12 and name hg2) (residue 13 and name hn) 3.00 0.20 0.20
assign (residue 14 and name ha) (residue 15 and name hn) 3.50 0.60 0.50
assign (residue 14 and name hn) (residue 15 and name hn) 2.70 0.30 0.25
assign (residue 17 and name hb1) (residue 18 and name hd2) 3.00 0.50 0.60

i, i+2

assign (residue 5 and name hn) (residue 7 and name hn) 4.00 0.60 1.00
assign (residue 8 and name ha) (residue 10 and name hn) 3.80 0.60 0.60
assign (residue 9 and name hn) (residue 11 and name hn) 4.00 0.50 0.70
assign (residue 12 and name ha) (residue 14 and name hn) 4.00 0.60 0.60
assign (residue 13 and name hn) (residue 14 and name hn) 2.70 0.30 0.25
assign (residue 13 and name ha) (residue 15 and name hn) 3.80 0.50 0.70
assign (residue 13 and name ha) (residue 15 and name hn) 3.50 0.50 0.50

i, i+3

assign (residue 2 and name ha) (residue 5 and name hb*) 3.50 0.50 0.70
assign (residue 3 and name ha) (residue 6 and name hn) 3.50 0.50 0.50
assign (residue 3 and name ha) (residue 6 and name hb1) 2.80 0.50 0.50
assign (residue 4 and name ha) (residue 7 and name hn) 3.30 0.50 0.50
assign (residue 4 and name ha) (residue 7 and name hb2) 3.30 0.50 0.50
assign (residue 5 and name ha) (residue 8 and name hn) 3.30 0.50 0.50
assign (residue 5 and name ha) (residue 8 and name hb*) 3.20 0.50 0.50
assign (residue 6 and name hz3) (residue 3 and name he2) 3.00 0.35 0.35
assign (residue 6 and name ha) (residue 9 and name hn) 3.50 0.50 0.50
assign (residue 6 and name ha) (residue 9 and name hb*) 3.50 0.60 0.80
assign (residue 7 and name ha) (residue 10 and name hn) 4.00 0.50 1.00

i, i+4

assign (residue 3 and name he2) (residue 7 and name hd1#) 3.00 0.50 0.50
assign (residue 3 and name he2) (residue 7 and name hd1#) 3.00 0.50 0.70

i, i+n (n > 4)

assign (residue 3 and name he1) (residue 18 and name hb2) 3.40 0.40 0.30
assign (residue 3 and name ha) (residue 19 and name hg*) 3.00 0.60 0.30
assign (residue 3 and name ha) (residue 19 and name hd2) 3.00 0.40 0.40
assign (residue 3 and name hd1) (residue 19 and name hd2) 3.00 0.60 0.50
assign (residue 6 and name hz2) (residue 11 and name ha2) 3.80 0.40 0.50
assign (residue 6 and name hh2) (residue 11 and name ha2) 3.80 0.40 0.50

assign (residue 6 and name he3) (residue 11 and name ha2) 3.80 0.40 0.50
assign (residue 6 and name hz2) (residue 11 and name ha1) 4.00 0.60 0.60
assign (residue 6 and name hz2) (residue 12 and name ha) 2.50 0.40 0.60
assign (residue 6 and name hh2) (residue 12 and name hd1) 2.60 0.40 0.60
assign (residue 6 and name hz2) (residue 12 and name hd1) 3.20 0.40 0.50
assign (residue 6 and name hz2) (residue 12 and name hg1) 3.10 0.40 0.50
assign (residue 6 and name hh2) (residue 12 and name hg1) 2.80 0.60 0.50
assign (residue 6 and name he1) (residue 17 and name ha) 3.80 0.60 0.60
assign (residue 6 and name hz2) (residue 17 and name ha) 4.00 0.60 0.60
assign (residue 6 and name hz2) (residue 18 and name hd1) 2.80 0.50 0.50
assign (residue 6 and name hh2) (residue 18 and name hd1) 3.80 0.60 0.50
assign (residue 6 and name he2) (residue 18 and name ha) 3.60 0.50 0.60
assign (residue 6 and name hz2) (residue 18 and name hb1) 3.50 0.50 0.60
assign (residue 6 and name he3) (residue 18 and name hb1) 3.80 0.50 0.60
assign (residue 6 and name hh2) (residue 18 and name hb1) 3.80 0.50 0.60
assign (residue 6 and name hd1) (residue 18 and name ha) 3.30 0.40 0.40
assign (residue 6 and name hh2) (residue 18 and name hg1) 4.00 0.70 1.00
assign (residue 6 and name hz2) (residue 18 and name hg1) 4.00 0.70 1.00
assign (residue 6 and name hd1) (residue 18 and name ha1) 3.50 0.50 0.50
assign (residue 6 and name he3) (residue 18 and name hb1) 3.80 0.50 0.60
assign (residue 6 and name hd1) (residue 19 and name hd2) 3.60 0.60 0.70
assign (residue 6 and name he3) (residue 19 and name hd2) 4.00 0.60 0.70
assign (residue 7 and name ha) (residue 11 and name hn) 2.50 0.50 0.50
assign (residue 7 and name ha) (residue 11 and name ha1) 4.00 0.60 0.70
assign (residue 7 and name ha) (residue 11 and name ha2) 3.50 0.60 0.50
assign (residue 7 and name hd2#) (residue 11 and name ha1) 4.00 0.60 0.80
assign (residue 16 and name o) (residue 6 and name he1) 2.00 0.35 0.35
assign (residue 14 and name hb*) (residue 9 and name hb*) 3.50 0.40 0.40

The bold constraint immediately above is the sidechain/sidechain constraint inserted with the aim of tightening up the loop region, which results in improving the 3-19 backbone RMSD to 0.58 ± 0.19 Å. This NOE interaction is only observed in WT TC10b, [D9E]- and [D9R,R16E]-TC10b. The indole ring H-bonding constraint reflects the common chemical shift of He1, which is 0.55±0.04 ppm upfield of the random coil value for all mutants examined.

C3. NOE Constraint List for TC16b tr R16Nva

i, i

d d- d+ δ values
assign (residue 10 and name ha2) (residue 10 and name hn) 2.48 0.27 0.23 0.75 8.31
assign (residue 10 and name ha1) (residue 10 and name hn) 3.11 0.47 0.37 3.07 8.30
assign (residue 11 and name ha) (residue 11 and name hb1) 2.30 0.21 0.21 4.62 2.54
assign (residue 11 and name ha) (residue 11 and name hb2) 3.60 0.62 0.54 4.62 2.04
assign (residue 11 and name hd2) (residue 11 and name hb2) 3.60 0.63 0.74
assign (residue 12 and name ha) (residue 12 and name hn) 2.64 0.32 0.26 4.23 7.35
assign (residue 12 and name hb#) (residue 12 and name hn) 2.84 0.28 0.26 1.42 7.35
assign (residue 13 and name hb1) (residue 13 and name hn) 2.41 0.40 0.32 3.57 8.09

assign (residue 13 and name ha) (residue 13 and name hn) 3.04 0.45 0.36 4.17 8.10
assign (residue 13 and name hb2) (residue 13 and name hn) 3.42 0.73 0.68 3.91 8.09
assign (residue 14 and name ha) (residue 14 and name hn) 2.66 0.42 0.33 4.43 7.33
assign (residue 14 and name hb#) (residue 14 and name hn) 3.02 0.34 0.29 1.5 7.33
assign (residue 15 and name hb2) (residue 15 and name hn) 3.04 0.45 0.35 1.77 8.07
assign (residue 15 and name ha) (residue 15 and name hn) 3.04 0.45 0.35 4.83 8.07
assign (residue 15 and name hg*) (residue 15 and name hn) 4.06 0.77 0.75 1.42 8.07
assign (residue 15 and name hb1) (residue 15 and name hn) 2.85 0.37 0.30 1.87 8.07
assign (residue 15 and name hg*) (residue 15 and name hn) 4.27 0.83 0.87 1.47 8.07
assign (residue 17 and name ha) (residue 17 and name hb1) 2.3 0.21 0.21 2.56 0.44
assign (residue 17 and name ha) (residue 17 and name hb2) 3 0.43 0.34 2.56 1.33
assign (residue 18 and name ha) (residue 18 and name hb1) 2.52 0.37 0.30 4.35 2.25
assign (residue 18 and name hd1) (residue 18 and name hg#) 2.78 0.43 0.34 3.17 1.84
assign (residue 18 and name hd2) (residue 18 and name hg#) 2.54 0.29 0.25 2.91 1.84
assign (residue 18 and name ha) (residue 18 and name hg#) 3.59 0.62 0.53 4.35 1.84
assign (residue 18 and name ha) (residue 18 and name hb2) 2.89 0.62 0.53
assign (residue 19 and name ha) (residue 19 and name hn) 3.50 0.59 0.50 4.28 8.40
assign (residue 19 and name ha) (residue 19 and name h1) 3.81 0.69 0.62
assign (residue 19 and name hb1) (residue 19 and name hn) 4.03 0.76 0.73 3.82 8.38
assign (residue 1 and name ha) (residue 1 and name hn) 2.51 0.37 0.46 4.20 8.68
assign (residue 1 and name hb#) (residue 1 and name hn) 3.09 0.69 0.97 1.48 8.68
assign (residue 2 and name he#) (residue 2 and name hd#) 2.2 0.26 1.02 6.83 7.09
assign (residue 2 and name hb#) (residue 2 and name hn) 2.54 0.29 0.25 3.10 9.11
assign (residue 2 and name hb#) (residue 2 and name hn) 2.54 0.29 0.25 3.10 9.11
assign (residue 2 and name hb#) (residue 2 and name hd#) 2.33 0.2 0.62 3.10 7.07
assign (residue 2 and name ha) (residue 2 and name hd#) 3.23 0.48 0.8 4.06 7.08
assign (residue 2 and name ha) (residue 2 and name hn) 3.29 0.53 0.43 4.07 9.11
assign (residue 3 and name hb#) (residue 3 and name hn) 2.80 0.27 0.25 1.54 8.54
assign (residue 3 and name ha) (residue 3 and name hn) 2.98 0.43 0.34 4.12 8.54
assign (residue 4 and name hb#) (residue 4 and name hn) 2.63 0.42 0.41 2.17 8.10
assign (residue 4 and name ha) (residue 4 and name hn) 2.94 0.41 0.33 4.09 8.10
assign (residue 4 and name hb#) (residue 4 and name he#) 3.93 0.73 0.68
assign (residue 4 and name hg#) (residue 4 and name hn) 4.37 0.87 0.94 2.39 8.10
assign (residue 5 and name hd1) (residue 5 and name he1) 2.31 0.22 0.61 7.11 9.59
assign (residue 5 and name hb1) (residue 5 and name hn) 2.65 0.37 0.38 3.54 8.12
assign (residue 5 and name hb2) (residue 5 and name hd1) 2.55 0.29 0.45 3.16 7.09
assign (residue 5 and name hb2) (residue 5 and name hn) 2.6 0.31 0.26 3.17 8.12
assign (residue 5 and name ha) (residue 5 and name hb2) 2.54 0.38 0.31 4.23 3.16
assign (residue 5 and name hz2) (residue 5 and name he1) 2.86 0.39 0.71 7.20 9.60
assign (residue 5 and name hb1) (residue 5 and name he3) 2.90 0.50 0.52 3.54 6.95
assign (residue 5 and name ha) (residue 5 and name hn) 2.93 0.41 0.33 4.23 8.12
assign (residue 5 and name ha) (residue 5 and name hd1) 2.94 0.41 0.53 4.22 7.09
assign (residue 5 and name hb1) (residue 5 and name hd1) 3.28 0.62 0.73 3.54 7.09
assign (residue 5 and name hb2) (residue 5 and name he3) 4.1 0.78 0.97 3.16 6.95
assign (residue 6 and name hb2) (residue 6 and name hn) 2.71 0.34 0.28 1.81 8.58
assign (residue 6 and name hg) (residue 6 and name hn) 2.83 0.38 0.30 1.60 8.58
assign (residue 6 and name ha) (residue 6 and name hn) 2.96 0.42 0.33 3.32 8.58
assign (residue 6 and name hb1) (residue 6 and name hn) 3.21 0.50 0.40 1.44 8.58
assign (residue 6 and name ha) (residue 6 and name hb1) 2.50 0.30 0.30 3.31 1.43
assign (residue 6 and name ha) (residue 6 and name hb2) 3.44 0.57 0.48 3.31 1.81
assign (residue 6 and name ha) (residue 6 and name hd1#) 4.08 0.67 0.56 3.31 0.97

assign (residue 6 and name hd2#) (residue 6 and name hn) 4.90 0.93 0.91 0.90 8.58
assign (residue 6 and name hd1#) (residue 6 and name hn) 5.06 0.98 1.01 0.98 8.58
assign (residue 7 and name ha) (residue 7 and name hn) 2.87 0.39 0.31 4.07 8.19
assign (residue 7 and name hb#) (residue 7 and name hn) 2.75 0.29 0.27 1.48 8.19
assign (residue 8 and name hb2) (residue 8 and name hn) 2.86 0.39 0.31 2.99 7.79
assign (residue 8 and name ha) (residue 8 and name hb2) 2.73 0.44 0.35 4.63 2.99
assign (residue 8 and name ha) (residue 8 and name hn) 3.11 0.47 0.37 4.63 7.79
assign (residue 8 and name ha) (residue 8 and name hb1) 2.85 0.48 0.38 4.63 3.11
assign (residue 8 and name hb1) (residue 8 and name hn) 3.31 0.22 0.46 3.08 7.79
assign (residue 9 and name ha) (residue 9 and name hb#) 2.75 0.31 0.38 4.38 1.26
assign (residue 9 and name hb#) (residue 9 and name hn) 3.12 0.49 0.39 1.27 7.41
assign (residue 9 and name ha) (residue 9 and name hn) 3.23 0.67 0.59 4.37 7.41

i, i + 1

assign (residue 11 and name hd1) (residue 10 and name ha1) 2.50 0.50 0.22 3.45 3.07
assign (residue 11 and name hd2) (residue 10 and name ha1) 2.38 0.25 0.21 3.75 3.07
assign (residue 11 and name hd1) (residue 10 and name ha2) 2.80 0.50 0.50 3.46 0.75
assign (residue 11 and name hd2) (residue 10 and name ha2) 4.25 0.83 0.86
assign (residue 11 and name hd2) (residue 10 and name hn) 5.25 1.00 1.00
assign (residue 11 and name hd1) (residue 10 and name hn) 4.69 0.97 1.19
assign (residue 11 and name hd2) (residue 12 and name hn) 3.01 0.35 0.25
assign (residue 11 and name hb1) (residue 12 and name hn) 4.34 0.86 1.12
assign (residue 11 and name ha) (residue 12 and name hn) 3.65 0.64 0.56 4.62 7.35
assign (residue 11 and name hb2) (residue 12 and name hn) 3.69 0.65 0.57 2.04 7.35
assign (residue 11 and name hg2) (residue 12 and name hn) 3.71 0.56 0.54 2.20 7.36
assign (residue 11 and name hd1) (residue 12 and name hn) 4.17 0.80 0.81 3.45 7.35
assign (residue 12 and name hn) (residue 13 and name hn) 2.60 0.21 0.21 7.35 8.09
assign (residue 12 and name ha) (residue 13 and name hb1) 4.65 0.81 1.22 4.23 3.57
assign (residue 12 and name hb#) (residue 13 and name hn) 3.87 0.61 0.49 1.42 8.09
assign (residue 12 and name ha) (residue 13 and name hn) 3.96 0.74 0.70 4.22 8.10
assign (residue 13 and name ha) (residue 14 and name hn) 3.94 0.73 0.69 4.16 7.33
assign (residue 13 and name hb2) (residue 14 and name hn) 4.69 0.97 1.19
assign (residue 14 and name hn) (residue 13 and name hn) 2.54 0.29 0.25 7.33 8.09
assign (residue 14 and name hn) (residue 15 and name hn) 2.58 0.30 0.25 7.34 8.07
assign (residue 14 and name ha) (residue 15 and name hn) 3.24 0.45 0.36 4.43 8.07
assign (residue 15 and name ha) (residue 16 and name hd1) 2.51 0.28 0.24 4.84 3.85
assign (residue 15 and name ha) (residue 16 and name hd2) 2.70 0.48 0.49 4.84 3.69
assign (residue 16 and name hd1) (residue 15 and name hb*) 4.32 0.86 1.12
assign (residue 16 and name hd1) (residue 15 and name hb*) 4.11 0.78 0.77
assign (residue 16 and name hd2) (residue 15 and name hb*) 3.74 0.67 0.59 3.70 1.88
assign (residue 16 and name hd2) (residue 15 and name hb*) 3.93 0.73 0.68 3.70 1.76
assign (residue 16 and name hb1) (residue 17 and name hd2) 3.16 0.68 0.77 2.12 3.47
assign (residue 18 and name hd1) (residue 17 and name ha) 2.31 0.35 0.24 3.17 2.56
assign (residue 18 and name hd2) (residue 17 and name ha) 2.58 0.38 0.30 2.92 2.56
assign (residue 18 and name hd2) (residue 17 and name hb1) 4.05 0.71 0.94
assign (residue 18 and name hd2) (residue 17 and name hb2) 3.80 0.69 0.62
assign (residue 18 and name ha) (residue 19 and name hn) 2.40 0.24 0.22 4.35 8.38
assign (residue 18 and name hb2) (residue 19 and name hn) 3.61 0.63 0.74
assign (residue 18 and name hb1) (residue 19 and name hn) 4.28 0.84 0.88 2.26 8.38
assign (residue 1 and name hn) (residue 2 and name hn) 2.92 0.41 0.88 8.70 9.11
assign (residue 1 and name ha) (residue 2 and name hn) 3.74 0.67 0.59 4.19 9.11

assign (residue 1 and name hb#) (residue 2 and name hn) 3.08 0.46 0.36 1.48 9.11
assign (residue 2 and name hb#) (residue 3 and name hn) 2.68 0.33 0.27 3.10 8.54
assign (residue 2 and name ha) (residue 3 and name hn) 3.89 0.72 0.66 4.06 8.54
assign (residue 3 and name ha) (residue 2 and name hd2) 3.17 0.49 0.59
assign (residue 3 and name hb#) (residue 2 and name hd2) 4.3 0.40 0.60
assign (residue 3 and name hn) (residue 2 and name hn) 2.83 0.45 0.30 8.56 9.12
assign (residue 3 and name ha) (residue 4 and name hn) 3.40 0.56 0.46 4.12 8.10
assign (residue 3 and name hb#) (residue 4 and name hn) 3.60 0.52 0.41 1.54 8.10
assign (residue 4 and name hn) (residue 3 and name hn) 2.81 0.37 0.30 8.11 8.54
assign (residue 4 and name hn) (residue 5 and name hn) 2.62 0.41 0.53 8.10 8.12
assign (residue 4 and name hb#) (residue 5 and name hn) 2.85 0.39 0.31 2.17 8.12
assign (residue 4 and name ha) (residue 5 and name hn) 3.35 0.44 0.44 4.09 8.12
assign (residue 5 and name hn) (residue 6 and name hn) 2.67 0.33 0.27 8.13 8.58
assign (residue 5 and name hb1) (residue 6 and name hn) 2.89 0.4 0.32 3.54 8.58
assign (residue 5 and name he3) (residue 6 and name hn) 3.07 0.45 0.56 6.96 8.58
assign (residue 5 and name hb2) (residue 6 and name hn) 3.81 0.69 0.62 3.16 8.58
assign (residue 5 and name ha) (residue 6 and name hn) 3.5 0.40 0.60 4.21 8.58
assign (residue 6 and name hg) (residue 5 and name he3) 2.72 0.50 0.48 1.60 6.95
assign (residue 6 and name hd2#) (residue 5 and name hz3) 3.00 0.55 0.68 0.90 7.09
assign (residue 6 and name hd1#) (residue 5 and name hz3) 3.92 0.62 0.74 0.98 7.08
assign (residue 6 and name hg) (residue 5 and name hz3) 4.00 0.75 0.91 1.59 7.09
assign (residue 6 and name hd2#) (residue 5 and name he3) 3.54 0.60 0.71
assign (residue 6 and name hd2#) (residue 5 and name hh2) 4.69 0.97 1.19
assign (residue 6 and name hb2) (residue 5 and name he3) 4.06 0.77 0.95 1.82 6.96
assign (residue 6 and name hb2) (residue 5 and name hn) 4.45 0.89 1.00 1.82 8.12
assign (residue 6 and name ha) (residue 5 and name he3) 4.53 0.92 1.26 3.33 6.95
assign (residue 6 and name hd1#) (residue 5 and name he3) 5.18 1.02 1.33 0.97 6.95
assign (residue 6 and name hb2) (residue 7 and name hn) 3.14 0.48 0.38 1.81 8.19
assign (residue 6 and name hb1) (residue 7 and name hn) 3.34 0.54 0.44 1.44 8.19
assign (residue 6 and name ha) (residue 7 and name hn) 3.61 0.61 0.63 3.31 8.19
assign (residue 6 and name hg) (residue 7 and name hn) 4.29 0.84 0.89 1.60 8.19
assign (residue 7 and name hn) (residue 6 and name hn) 2.67 0.33 0.27 8.20 8.58
assign (residue 7 and name hb#) (residue 8 and name hn) 3.79 0.58 0.46 1.48 7.79
assign (residue 7 and name ha) (residue 8 and name hn) 3.74 0.64 0.69 4.07 7.79
assign (residue 8 and name hn) (residue 7 and name hn) 3.06 0.45 0.36 7.80 8.19
assign (residue 8 and name hb1) (residue 9 and name hn) 4.60 0.92 1.17
assign (residue 8 and name hb2) (residue 9 and name hn) 4.29 0.97 1.19
assign (residue 8 and name ha) (residue 9 and name hn) 4.01 0.88 0.97 4.63 7.41
assign (residue 9 and name hn) (residue 10 and name hn) 2.43 0.25 0.23 7.42 8.31
assign (residue 9 and name ha) (residue 10 and name hn) 3.81 0.69 0.63 4.38 8.31
assign (residue 9 and name hb#) (residue 10 and name hn) 4.69 0.86 0.8 1.27 8.31
assign (residue 9 and name hn) (residue 8 and name hn) 2.83 0.38 0.30 7.42 7.79

i, i + 2

assign (residue 10 and name ha1) (residue 12 and name hn) 4.30 0.83 1.07
assign (residue 10 and name hn) (residue 8 and name hn) 3.86 0.87 0.95 8.32 7.79
assign (residue 11 and name ha) (residue 13 and name hn) 4.20 0.81 0.83 4.62 8.09
assign (residue 12 and name ha) (residue 14 and name hn) 3.56 0.58 0.48 4.23 7.33
assign (residue 13 and name hb2) (residue 15 and name hn) 3.80 0.50 0.60
assign (residue 7 and name ha) (residue 9 and name hn) 3.91 0.78 0.77 4.07 7.41
assign (residue 8 and name hb2) (residue 10 and name hn) 3.76 0.65 0.61

assign (residue 13 and name og) (residue 15 and name hn) 3.10 0.25 0.25

i, i + 3

assign (residue 13 and name hb1) (residue 10 and name hn) 4.25 0.83 0.86
assign (residue 1 and name ha) (residue 4 and name hb*) 3.29 0.40 1.02 4.19 2.16
assign (residue 1 and name ha) (residue 4 and name hn) 3.55 0.49 0.53
assign (residue 1 and name ha) (residue 4 and name hg*) 4.45 0.89 1.00 4.19 2.39
assign (residue 2 and name he2) (residue 5 and name hz3) 3.30 0.51 1.03 6.84 6.94
assign (residue 2 and name ha) (residue 5 and name hb2) 2.92 0.41 0.32
assign (residue 2 and name ha) (residue 5 and name hb1) 2.64 0.40 0.60 4.06 3.54
assign (residue 2 and name ha) (residue 5 and name hn) 3.52 0.60 0.51 4.06 8.12
assign (residue 2 and name ha) (residue 5 and name he3) 4.28 0.84 1.08 4.06 6.95
assign (residue 2 and name ha) (residue 6 and name hn) 4.02 0.76 0.73 4.07 8.58
assign (residue 3 and name ha) (residue 6 and name hn) 3.48 0.59 0.49 4.12 8.58
assign (residue 3 and name ha) (residue 6 and name hb2) 3.58 0.68 0.61 4.12 1.81
assign (residue 3 and name ha) (residue 6 and name hd1#) 3.85 0.6 0.48 4.12 0.98
assign (residue 3 and name hb#) (residue 6 and name hn) 4.85 0.92 0.89 1.54 8.58
assign (residue 4 and name ha) (residue 7 and name hn) 3.13 0.48 0.38 4.09 8.19
assign (residue 5 and name ha) (residue 8 and name hb2) 3.60 0.45 0.51 4.23 3.10
assign (residue 5 and name hb1) (residue 2 and name hd1) 3.96 0.72 1.06
assign (residue 5 and name ha) (residue 8 and name hn) 3.75 0.73 0.66 4.23 7.79
assign (residue 6 and name ha) (residue 9 and name hn) 3.85 0.70 0.64
assign (residue 7 and name hb3) (residue 4 and name hn) 4.65 0.79 0.70 1.48 8.10
assign (residue 9 and name ha) (residue 12 and name hb#) 3.93 0.63 0.51 4.38 1.42
assign (residue 9 and name ha) (residue 12 and name hn) 3.92 0.72 0.67
assign (residue 13 and name og) (residue 10 and name o) 2.85 0.20 0.20

i, i + 4

assign (residue 6 and name ha) (residue 10 and name hn) 2.92 0.41 0.33 3.32 8.31
assign (residue 6 and name ha) (residue 10 and name ha1) 3.66 0.71 0.65 3.31 3.05
assign (residue 6 and name ha) (residue 10 and name ha2) 3.12 0.41 0.33 3.31 0.75
assign (residue 6 and name hd1#) (residue 2 and name he2) 3.07 0.55 0.94 0.98 6.82
assign (residue 6 and name hd1#) (residue 2 and name hd2) 3.80 0.50 0.60
assign (residue 6 and name hg) (residue 2 and name hd2) 3.95 0.86 1.05
assign (residue 6 and name hg) (residue 2 and name he2) 3.67 0.62 0.94
assign (residue 6 and name hd2#) (residue 2 and name he2) 3.88 0.58 1.17
assign (residue 9 and name ha) (residue 13 and name hb1) 3.10 0.40 0.90
assign (residue 9 and name ha) (residue 13 and name hn) 3.82 0.69 0.63

i, i+n (n > 4)

assign (residue 10 and name ha2) (residue 5 and name hz2) 3.59 0.49 0.56 0.75 7.18
assign (residue 10 and name ha2) (residue 5 and name hz3) 4.03 0.76 0.93
assign (residue 10 and name ha2) (residue 5 and name he1) 3.86 0.71 0.65
assign (residue 10 and name ha2) (residue 5 and name he3) 3.82 0.59 0.63
assign (residue 10 and name ha2) (residue 5 and name hh2) 4.05 0.75 0.95 0.74 7.22
assign (residue 10 and name ha1) (residue 5 and name hh2) 4.34 0.86 1.12
assign (residue 10 and name ha1) (residue 5 and name hz2) 3.87 0.65 0.76
assign (residue 11 and name hd1) (residue 5 and name hz2) 3.03 0.44 0.55 3.45 7.21
assign (residue 11 and name ha) (residue 5 and name hh2) 4.05 0.73 0.89
assign (residue 11 and name hd1) (residue 5 and name hz3) 4.59 0.90 0.85

assign (residue 11 and name hd1) (residue 5 and name he1) 4.70 0.92 1.17
assign (residue 11 and name hd1) (residue 5 and name he3) 5.25 1.00 1.00
assign (residue 11 and name hb1) (residue 5 and name hh2) 4.60 0.92 1.17
assign (residue 11 and name ha) (residue 5 and name hz2) 2.62 0.47 0.58 4.62 7.19
assign (residue 11 and name hd1) (residue 5 and name hh2) 2.53 0.49 0.60 3.45 7.22
assign (residue 11 and name hg1) (residue 5 and name hz2) 3.38 0.55 0.65 2.19 7.19
assign (residue 11 and name hg1) (residue 5 and name hh2) 2.88 0.58 0.69 2.19 7.22
assign (residue 11 and name hb1) (residue 5 and name hz2) 4.00 0.75 0.91 2.54 7.18
assign (residue 11 and name hd2) (residue 5 and name hz3) 5.25 1.00 1.00
assign (residue 11 and name hd2) (residue 5 and name hh2) 4.19 0.81 1.02 3.76 7.21
assign (residue 13 and name hb2) (residue 8 and name hb2) 4.00 0.60 0.60
assign (residue 13 and name hb2) (residue 8 and name hb1) 4.40 0.60 0.60
assign (residue 15 and name hb2) (residue 5 and name hd1) 3.17 0.49 0.59 1.77 7.09
assign (residue 15 and name hb2) (residue 5 and name he1) 3.32 0.54 0.64 1.77 9.59
assign (residue 15 and name hb1) (residue 5 and name he1) 3.95 0.83 0.86
assign (residue 15 and name hn) (residue 5 and name he1) 3.88 0.71 0.86 8.09 9.60
assign (residue 15 and name ha) (residue 5 and name he1) 4.25 0.83 1.06 4.83 9.59
assign (residue 16 and name ha) (residue 5 and name hz2) 4.23 0.72 0.95 4.59 7.19
assign (residue 16 and name ha) (residue 5 and name he1) 4.04 0.79 0.95 4.59 9.59
assign (residue 17 and name hb2) (residue 2 and name he1) 3.31 0.54 0.48 1.31 6.82
assign (residue 17 and name hb1) (residue 2 and name he1) 3.99 0.82 1.23 0.45 6.81
assign (residue 17 and name hb1) (residue 2 and name hd1) 4.69 0.97 1.19
assign (residue 17 and name hb1) (residue 5 and name hh2) 4.32 0.86 1.12
assign (residue 17 and name hb2) (residue 2 and name hd1) 3.92 0.72 0.67
assign (residue 17 and name hd1) (residue 5 and name hh2) 4.09 0.78 0.97
assign (residue 17 and name hd1) (residue 5 and name hz2) 2.75 0.58 0.41 3.48 7.18
assign (residue 17 and name hd1) (residue 5 and name hh2) 3.49 0.59 0.69 3.48 7.22
assign (residue 17 and name ha) (residue 5 and name hd1) 3.61 0.63 0.74 2.55 7.09
assign (residue 17 and name ha) (residue 5 and name he1) 3.65 0.64 0.76 2.56 9.59
assign (residue 17 and name hd1) (residue 5 and name hd1) 4.08 0.71 0.81 3.47 7.10
assign (residue 17 and name ha) (residue 5 and name hz2) 4.08 0.78 0.96 2.56 7.19
assign (residue 17 and name hg1) (residue 5 and name hz2) 4.21 0.85 1.10 1.68 7.18
assign (residue 17 and name ha) (residue 5 and name hh2) 4.33 0.85 1.11 2.55 7.21
assign (residue 17 and name hg1) (residue 5 and name hh2) 3.8 0.65 0.94
assign (residue 17 and name hb1) (residue 5 and name hz2) 3.70 0.61 0.83 0.44 7.19
assign (residue 18 and name hd1) (residue 2 and name hd1) 4.45 0.51 0.52 3.17 7.08
assign (residue 18 and name hd2) (residue 2 and name hd1) 3.14 0.71 0.66 2.91 7.09
assign (residue 18 and name hg#) (residue 2 and name hd1) 4.04 0.74 1.10 1.82 7.07
assign (residue 18 and name hg#) (residue 2 and name hn) 4.39 0.87 0.96 1.83 9.11
assign (residue 18 and name hd2) (residue 2 and name he1) 4.60 0.92 1.43 2.91 6.82
assign (residue 18 and name hd1) (residue 5 and name he1) 5.25 1.00 1.00
assign (residue 18 and name hd2) (residue 5 and name he3) 3.91 0.62 0.64
assign (residue 18 and name hd2) (residue 5 and name hn) 5.05 0.98 1 .00
assign (residue 18 and name hd2) (residue 5 and name hd1) 3.74 0.66 0.79 2.92 7.10
assign (residue 2 and name ha) (residue 18 and name hg*) 2.80 0.53 0.43 4.06 1.84
assign (residue 2 and name ha) (residue 18 and name hd2) 3.00 0.50 0.50 4.07 2.92
assign (residue 5 and name he3) (residue 17 and name hb1) 3.80 0.50 0.60
assign (residue 5 and name he3) (residue 17 and name hb1) 3.80 0.50 0.60

C4. NOE Constraint List for CircMut DUAA P19W S20A

i, i

	d	d-	d+	δ values	
assign (residue 10 and name he#) (residue 10 and name hd#)	1.96	0.06	1.02	6.76	7.01
assign (residue 10 and name hb2) (residue 10 and name hd#)	2.48	0.25	0.65	3.11	7.00
assign (residue 10 and name hb2) (residue 10 and name hn)	2.56	0.29	0.25	3.12	8.54
assign (residue 10 and name hb1) (residue 10 and name hn)	2.70	0.34	0.28	3.19	8.54
assign (residue 10 and name hb1) (residue 10 and name hd#)	2.71	0.32	0.69	3.18	7.00
assign (residue 10 and name ha) (residue 10 and name hb1)	2.98	0.43	0.34	3.94	3.20
assign (residue 10 and name ha) (residue 10 and name hb2)	2.71	0.37	0.32	3.94	3.13
assign (residue 10 and name ha) (residue 10 and name hd1)	3.12	0.45	0.78	3.94	7.00
assign (residue 10 and name ha) (residue 10 and name hn)	3.18	0.49	0.39	3.94	8.54
assign (residue 11 and name ha) (residue 11 and name hb#)	2.53	0.18	0.22	4.14	1.60
assign (residue 11 and name hb#) (residue 11 and name hn)	2.86	0.29	0.26	1.59	8.41
assign (residue 11 and name ha) (residue 11 and name hn)	2.87	0.39	0.31	4.13	8.41
assign (residue 12 and name hg#) (residue 12 and name hb2)	2.46	0.20	0.20	2.40	2.18
assign (residue 12 and name hg#) (residue 12 and name he#)	2.39	0.21	0.35	2.41	8.01
assign (residue 12 and name ha) (residue 12 and name hb1)	2.78	0.25	0.22	3.96	2.10
assign (residue 12 and name ha) (residue 12 and name hn)	2.64	0.26	0.23	3.96	8.15
assign (residue 12 and name hb2) (residue 12 and name hn)	2.52	0.28	0.24	2.19	8.15
assign (residue 12 and name hb1) (residue 12 and name hn)	2.62	0.31	0.26	2.10	8.15
assign (residue 12 and name ha) (residue 12 and name hb2)	2.71	0.34	0.28	3.97	2.19
assign (residue 12 and name ha) (residue 12 and name hg#)	2.84	0.38	0.31	3.96	2.40
assign (residue 12 and name ha) (residue 12 and name he#)	3.54	0.60	0.51	3.96	8.01
assign (residue 12 and name hg3) (residue 12 and name hn)	3.78	0.68	0.61	2.40	8.15
assign (residue 13 and name hz3) (residue 13 and name he3)	2.20	0.20	0.54	6.88	6.82
assign (residue 13 and name hb1) (residue 13 and name hn)	2.33	0.22	0.21	3.52	7.96
assign (residue 13 and name hh2) (residue 13 and name hz3)	2.41	0.25	0.62	6.54	6.88
assign (residue 13 and name hb2) (residue 13 and name hn)	2.50	0.27	0.24	3.00	7.96
assign (residue 13 and name hz2) (residue 13 and name hh2)	2.50	0.27	0.64	6.10	6.53
assign (residue 13 and name hd1) (residue 13 and name he1)	2.60	0.31	0.66	6.76	9.21
assign (residue 13 and name ha) (residue 13 and name hn)	2.65	0.32	0.27	4.12	7.95
assign (residue 13 and name hb2) (residue 13 and name hd1)	2.66	0.32	0.47	3.00	6.75
assign (residue 13 and name hb1) (residue 13 and name he3)	2.78	0.36	0.49	3.52	6.81
assign (residue 13 and name ha) (residue 13 and name hb2)	2.82	0.38	0.30	4.12	3.00
assign (residue 13 and name ha) (residue 13 and name hd1)	2.92	0.41	0.53	4.12	6.75
assign (residue 13 and name ha) (residue 13 and name hb1)	3.04	0.45	0.36	4.14	3.54
assign (residue 13 and name hz2) (residue 13 and name he1)	3.11	0.47	0.77	6.10	9.21
assign (residue 13 and name hb2) (residue 13 and name he3)	3.73	0.66	0.79	3.00	6.81
assign (residue 13 and name hb1) (residue 13 and name hd1)	3.81	0.69	0.82	3.52	6.75
assign (residue 14 and name hb2) (residue 14 and name hn)	2.64	0.25	0.23	1.73	8.45
assign (residue 14 and name hg) (residue 14 and name hn)	2.55	0.29	0.25	1.52	8.45
assign (residue 14 and name ha) (residue 14 and name hn)	2.69	0.33	0.27	3.25	8.45
assign (residue 14 and name ha) (residue 14 and name hb1)	2.51	0.34	0.28	3.25	1.44
assign (residue 14 and name hb1) (residue 14 and name hn)	3.31	0.37	0.3	1.44	8.45
assign (residue 14 and name ha) (residue 14 and name hb2)	3.08	0.39	0.31	3.24	1.71
assign (residue 14 and name ha) (residue 14 and name hd2#)	2.74	0.37	0.31	3.25	0.88

```
assign (residue 14 and name ha ) (residue 14 and name hg ) 3.39  0.62 0.53       3.25    1.51
assign (residue 14 and name hb2 ) (residue 14 and name hd2# ) 3.72 0.56 0.45    1.73    0.88
assign (residue 14 and name ha ) (residue 14 and name hd1# ) 4.09 0.58 0.67     3.25    0.93
assign (residue 14 and name hd2# ) (residue 14 and name hn ) 3.54 0.62 0.74     0.88    8.45
assign (residue 14 and name hd1# ) (residue 14 and name hn ) 3.49 0.54 0.76     0.94    8.45
assign (residue 15 and name ha ) (residue 15 and name hb# ) 2.28 0.09 0.28      3.98    1.45
assign (residue 15 and name hb# ) (residue 15 and name hn ) 2.57 0.20 0.22      1.46    7.92
assign (residue 15 and name ha ) (residue 15 and name hn ) 2.66 0.33 0.27       3.98    7.91
assign (residue 16 and name hb2 ) (residue 16 and name hn ) 2.52 0.28 0.24      2.71    8.09
assign (residue 16 and name ha ) (residue 16 and name hb1 ) 2.93 0.41 0.33      4.46    2.79
assign (residue 16 and name hb1 ) (residue 16 and name hn ) 3.28 0.52 0.42      2.80    8.09
assign (residue 16 and name ha ) (residue  16 and name hn  ) 3.35 0.54 0.45     4.45    8.08
assign (residue 16 and name ha ) (residue  16 and name hb2 ) 3.03  0.56 0.49    4.46    2.72
assign (residue 17 and name ha ) (residue 17 and name hb# ) 2.36 0.16 0.27      4.34    1.22
assign (residue 17 and name ha ) (residue 17 and name hn ) 2.71 0.28 0.24       4.33    7.28
assign (residue 17 and name hb# ) (residue 17  and name hn ) 3.02 0.34 0.29     1.22    7.28
assign (residue 18 and name ha1 ) (residue 18 and name hn ) 2.85 0.35 0.29      0.66    8.19
assign (residue 18 and name ha2 ) (residue 18 and name hn ) 2.33 0.30 0.29      2.81    8.18
assign (residue 19 and name hh2 ) (residue 19 and name hz2 ) 2.19 0.18 0.59     7.35    7.58
assign (residue 19 and name hd1 ) (residue 19 and name he1 ) 2.3 0.21 0.61      7.57    10.52
assign (residue 19 and name hz3 ) (residue 19 and name he3 ) 2.43 0.25 0.63     7.23    7.83
assign (residue 19 and name ha ) (residue 19 and name he3 ) 2.70 0.30 0.45      4.64    7.84
assign (residue 19 and name hb2 ) (residue 19 and name he3 ) 4.10 0.76 0.81     3.51    7.84
assign (residue 19 and name hb1 ) (residue 19 and name hd1 ) 3.21 0.37 0.50     3.17    7.56
assign (residue 19 and name hb1 ) (residue 19 and name hn ) 3.62 0.41 0.33      3.17    8.75
assign (residue 19 and name ha ) (residue 19 and name hb1 ) 2.60 0.27 0.31      4.65    3.19
assign (residue 19 and name ha ) (residue 19 and name hn ) 2.54 0.48 0.38       4.64    8.75
assign (residue 19 and name hb1 ) (residue 19 and name he3 ) 3.19 0.49 0.60     3.17    7.84
assign (residue 19 and name ha ) (residue 19 and name hb2 ) 3.27 0.52 0.42      4.63    3.51
assign (residue 19 and name hd1 ) (residue 19 and name hn ) 3.46 0.58 0.68      7.57    8.75
assign (residue 19 and name hb2 ) (residue 19 and name hd1 ) 2.69 0.59 0.69     3.52    7.56
assign (residue 19 and name hb2 ) (residue 19 and name hn ) 2.72 0.43 0.48      3.52    8.75
assign (residue 19 and name ha ) (residue 19 and name hd1 ) 4.23 0.82 1.05      4.64    7.56
assign (residue 1 and name hd# ) (residue 1 and name he ) 2.41 0.25 0.22        3.18    7.42
assign (residue 1 and name ha ) (residue 1 and name hb2 ) 2.75 0.45 0.36        4.51    1.93
assign (residue 1 and name ha ) (residue 1 and name hb1 ) 2.7 0.50 0.40         4.51    1.96
assign (residue 1 and name hg2 ) (residue 1 and name he ) 3.51 0.60 0.50        1.65    7.41
assign (residue 1 and name hg1 ) (residue 1 and name he ) 3.56 0.61 0.52        1.82    7.41
assign (residue 1 and name hb2 ) (residue 1 and name he ) 3.95 0.73 0.69        1.93    7.41
assign (residue 1 and name ha ) (residue 1 and name hg* ) 3.99 0.75 0.71        4.51    1.63
assign (residue 1 and name ha ) (residue 1 and name  hg* ) 4.25 0.83 0.86       4.51    1.81
assign (residue 20 and name ha ) (residue 20 and name hb# ) 2.36 0.13 0.19      4.48    1.40
assign (residue 20 and name ha ) (residue 20 and name hn ) 2.69 0.27 0.39       4.49    7.85
assign (residue 20 and name hb# ) (residue 20 and name hn ) 2.82 0.27 0.26      1.40    7.84
assign (residue 21 and name ha ) (residue 21 and name hb1 ) 2.40 0.24 0.22      4.05    3.87
assign (residue 21 and name ha ) (residue 21 and name hb2 ) 2.73 0.35 0.28      4.05    3.46
assign (residue 21 and name ha ) (residue 21 and name hn ) 2.85 0.38 0.31       4.06    7.58
assign (residue 21 and name hb2 ) (residue 21 and name hn ) 3.11 0.47 0.37      3.48    7.57
assign (residue 21 and name hb1 ) (residue 21 and name hn ) 3.19 0.65 0.57      3.87    7.57
assign (residue 2 and name hd1 ) (residue 2 and name hg2 ) 3.01  0.44 0.35      3.82    2.11
assign (residue 2 and name hd1 ) (residue 2 and name hg1  ) 2.77 0.49 0.39      3.82    2.01
```

assign (residue 2 and name ha) (residue 2 and name hb2) 3.26 0.51 0.42 4.01 1.70
assign (residue 2 and name hd2) (residue 2 and name hg1) 3.31 0.53 0.43 3.52 2.02
assign (residue 2 and name hd2) (residue 2 and name hb2) 3.76 0.67 0.60 3.53 1.72
assign (residue 2 and name hd1) (residue 2 and name hb1) 4.10 1.00 1.29 3.81 2.41
assign (residue 2 and name ha) (residue 3 and name hd1) 2.51 0.31 0.26 4.01 3.24
assign (residue 2 and name ha) (residue 3 and name hd2) 2.73 0.41 0.33 4.01 2.55
assign (residue 3 and name hd2) (residue 3 and name hg2) 2.67 0.46 0.37 2.54 1.45
assign (residue 3 and name hd1) (residue 3 and name hg1) 2.33 0.27 0.38 3.24 1.66
assign (residue 3 and name hd2) (residue 3 and name hg1) 3.02 0.33 0.44 2.56 1.66
assign (residue 3 and name ha) (residue 3 and name hb2) 2.93 0.26 0.39 2.27 1.11
assign (residue 3 and name ha) (residue 3 and name hb1) 2.30 0.47 0.40 2.26 -0.09
assign (residue 3 and name hg2) (residue 3 and name hb1) 3.01 0.39 0.43 1.42 -0.08
assign (residue 3 and name hg1) (residue 3 and name hb1) 2.28 0.32 0.47 1.66 -0.05
assign (residue 4 and name ha) (residue 4 and name hb1) 2.59 0.30 0.25 4.34 2.15
assign (residue 4 and name hd1) (residue 4 and name hg1) 2.58 0.40 0.32 3.06 1.78
assign (residue 4 and name hd2) (residue 4 and name hg2) 2.48 0.49 0.39 2.72 1.73
assign (residue 4 and name hd2) (residue 4 and name hg1) 3.33 0.54 0.44 2.71 1.79
assign (residue 4 and name ha) (residue 4 and name hb2) 3.10 0.56 0.46 4.34 1.95
assign (residue 4 and name hd1) (residue 4 and name hg2) 3.41 0.56 0.47 3.04 1.71
assign (residue 4 and name hd1) (residue 4 and name hb1) 3.57 0.61 0.52 3.06 2.15
assign (residue 4 and name hd2) (residue 4 and name hb2) 4.00 0.75 0.71 2.71 1.95
assign (residue 4 and name hd2) (residue 4 and name hb1) 4.18 0.81 0.82 2.71 2.15
assign (residue 5 and name ha) (residue 5 and name hb1) 2.60 0.31 0.26 4.20 3.76
assign (residue 5 and name ha) (residue 5 and name hb2) 2.85 0.32 0.37 4.19 3.83
assign (residue 5 and name ha) (residue 5 and name hn) 2.69 0.33 0.27 4.19 8.21
assign (residue 5 and name hb1) (residue 5 and name hn) 2.73 0.51 0.41 3.77 8.22
assign (residue 5 and name hb2) (residue 5 and name hn) 3.21 0.53 0.43 3.84 8.22
assign (residue 6 and name ha) (residue 6 and name hn) 2.88 0.38 0.33 4.51 7.85
assign (residue 6 and name hb2) (residue 6 and name hn) 2.69 0.34 0.28 2.62 7.84
assign (residue 6 and name hb1) (residue 6 and name hn) 2.72 0.35 0.28 2.72 7.84
assign (residue 6 and name ha) (residue 6 and name hb2) 2.77 0.36 0.29 4.51 2.62
assign (residue 6 and name ha) (residue 6 and name hb1) 2.55 0.23 0.21 4.52 2.71
assign (residue 8 and name ha) (residue 8 and name hb#) 2.56 0.26 0.37 4.24 1.50
assign (residue 8 and name ha) (residue 8 and name hn) 2.67 0.33 0.32 4.24 8.33
assign (residue 8 and name hb#) (residue 8 and name hn) 2.40 0.14 0.20 1.50 8.33
assign (residue 9 and name ha) (residue 9 and name hb#) 2.48 0.16 0.21 4.47 1.54
assign (residue 9 and name ha) (residue 9 and name hn) 2.62 0.31 0.26 4.47 8.26
assign (residue 9 and name hb#) (residue 9 and name hn) 2.74 0.25 0.24 1.54 8.26

i, i+1

assign (residue 10 and name hn) (residue 11 and name hn) 2.68 0.27 0.24 8.53 8.40
assign (residue 10 and name hb1) (residue 11 and name hn) 2.96 0.42 0.33 3.19 8.41
assign (residue 10 and name hb2) (residue 11 and name hn) 3.80 0.69 0.62 3.12 8.40
assign (residue 10 and name ha) (residue 11 and name hn) 3.76 0.69 0.64 3.94 8.41
assign (residue 11 and name hn) (residue 10 and name hd#) 3.65 0.62 0.94 8.43 7.00
assign (residue 11 and name ha) (residue 10 and name hd#) 4.06 0.75 1.11 4.13 7.00
assign (residue 11 and name hb#) (residue 12 and name hn) 3.12 0.37 0.31 1.59 8.15
assign (residue 11 and name ha) (residue 12 and name hn) 3.55 0.61 0.51 4.13 8.15
assign (residue 12 and name hn) (residue 11 and name hn) 2.89 0.40 0.32 8.16 8.41
assign (residue 12 and name hb1) (residue 13 and name hn) 2.89 0.40 0.32 2.10 7.96
assign (residue 12 and name hb2) (residue 13 and name hn) 3.26 0.52 0.42 2.19 7.96

assign (residue 13 and name hn) (residue 12 and name hn) 2.47 0.27 0.23	7.97	8.15
assign (residue 13 and name hb1) (residue 14 and name hn) 2.65 0.32 0.27	3.52	8.45
assign (residue 13 and name hn) (residue 14 and name hn) 2.67 0.33 0.27	7.97	8.45
assign (residue 13 and name he3) (residue 14 and name hn) 2.90 0.40 0.52	6.82	8.45
assign (residue 13 and name hb2) (residue 14 and name hn) 3.61 0.63 0.54	3.00	8.45
assign (residue 14 and name hg) (residue 13 and name he3) 2.72 0.41 0.52	1.51	6.81
assign (residue 14 and name ha) (residue 13 and name he3) 3.37 0.55 0.65	3.25	6.81
assign (residue 14 and name hb2) (residue 13 and name he3) 3.62 0.63 0.74	1.73	6.81
assign (residue 14 and name hd2#) (residue 13 and name he3) 3.64 0.53 0.66	0.88	6.81
assign (residue 14 and name hd2#) (residue 13 and name hz3) 2.72 0.56 0.68	0.88	6.87
assign (residue 14 and name hg) (residue 13 and name hz3) 3.87 0.71 0.85	1.52	6.87
assign (residue 14 and name ha) (residue 13 and name hz3) 3.93 0.73 0.88	3.25	6.87
assign (residue 14 and name hb1) (residue 13 and name he3) 4.14 0.79 0.99	1.44	6.81
assign (residue 14 and name hd1#) (residue 13 and name hz3) 4.32 0.75 0.88	0.94	6.87
assign (residue 14 and name hd1#) (residue 13 and name he3) 4.62 0.84 1.01	0.94	6.81
assign (residue 14 and name hb1) (residue 15 and name hn) 3.21 0.41 0.46	1.44	7.92
assign (residue 14 and name hb2) (residue 15 and name hn) 2.82 0.37 0.30	1.73	7.92
assign (residue 14 and name ha) (residue 15 and name hn) 3.52 0.60 0.50	3.25	7.92
assign (residue 15 and name hn) (residue 14 and name hn) 2.64 0.32 0.27	7.93	8.45
assign (residue 15 and name hb#) (residue 16 and name hn) 3.28 0.42 0.34	1.47	8.09
assign (residue 15 and name ha) (residue 16 and name hn) 3.63 0.63 0.55	3.98	8.09
assign (residue 15 and name hn) (residue 16 and name hn) 2.80 0.35 0.35		
assign (residue 16 and name ha) (residue 17 and name hn) 3.83 0.70 0.63	4.46	7.28
assign (residue 16 and name hb1) (residue 17 and name hn) 3.99 0.75 0.71	2.80	7.31
assign (residue 16 and name hb2) (residue 17 and name hn) 4.42 0.88 0.98	2.72	7.28
assign (residue 17 and name hn) (residue 16 and name hn) 2.91 0.37 0.30	7.29	8.09
assign (residue 17 and name hn) (residue 18 and name hn) 2.46 0.13 0.22	7.29	8.18
assign (residue 17 and name ha) (residue 18 and name hn) 3.59 0.62 0.53	4.34	8.18
assign (residue 17 and name hb#) (residue 18 and name hn) 4.26 0.73 0.62	1.22	8.18
assign (residue 18 and name ha2) (residue 17 and name hn) 4.25 0.83 0.86	2.81	7.28
assign (residue 18 and name ha2) (residue 19 and name hn) 3.10 0.57 0.38	2.81	8.75
assign (residue 18 and name ha1) (residue 19 and name hn) 2.60 0.38 0.51	0.65	8.75
assign (residue 19 and name ha) (residue 18 and name ha2) 4.07 0.77 0.76	4.63	2.81
assign (residue 19 and name ha) (residue 20 and name hn) 3.10 0.39 0.45	4.63	7.84
assign (residue 1 and name ha) (residue 2 and name hd1) 2.35 0.35 0.25	4.51	3.81
assign (residue 1 and name ha) (residue 2 and name hd2) 2.86 0.39 0.31	4.51	3.52
assign (residue 1 and name hb1) (residue 2 and name hd2) 3.89 0.40 0.42	1.97	3.52
assign (residue 1 and name hb2) (residue 2 and name hd2) 3.00 0.53 0.43	1.93	3.52
assign (residue 20 and name hn) (residue 19 and name hn) 2.82 0.27 0.26		
assign (residue 20 and name ha) (residue 21 and name hn) 3.39 0.56 0.46	4.49	7.57
assign (residue 20 and name hb#) (residue 21 and name hn) 4.50 0.81 0.72	1.40	7.57
assign (residue 3 and name hd1) (residue 2 and name hb1) 3.43 0.57 0.47	3.24	2.42
assign (residue 4 and name hd1) (residue 3 and name ha) 2.35 0.22 0.33	3.05	2.26
assign (residue 4 and name hd2) (residue 3 and name ha) 2.65 0.48 0.38	2.71	2.27
assign (residue 4 and name hd2) (residue 3 and name hb2) 3.80 0.69 0.62	2.71	1.11
assign (residue 4 and name hd2) (residue 3 and name hb1) 4.03 0.76 0.73	2.72	-0.07
assign (residue 4 and name hd1) (residue 3 and name hb2) 4.13 0.79 0.79	3.05	1.12
assign (residue 4 and name ha) (residue 5 and name hn) 2.25 0.20 0.05	4.34	8.22
assign (residue 4 and name hb2) (residue 5 and name hn) 3.68 0.65 0.57	1.95	8.22
assign (residue 4 and name hb1) (residue 5 and name hn) 4.39 0.87 0.95	2.15	8.22
assign (residue 5 and name ha) (residue 6 and name hn) 3.45 0.57 0.48	4.19	7.85

assign (residue 5 and name hb1) (residue 6 and name hn) 4.05 0.77 0.74 3.77 7.84
assign (residue 5 and name hb2) (residue 6 and name hn) 4.17 0.80 0.81 3.85 7.84
assign (residue 6 and name hn) (residue 5 and name hn) 2.68 0.46 0.39 7.85 8.22
assign (residue 6 and name ha) (residue 7 and name hn) 2.68 0.51 0.48 4.51 8.76
assign (residue 6 and name hn) (residue 7 and name hn) 4.35 0.46 0.40 7.86 8.75
assign (residue 8 and name hn) (residue 7 and name hn) 2.59 0.52 0.62 8.34 8.76
assign (residue 8 and name hn) (residue 9 and name hn) 2.54 0.19 0.40 8.33 8.26
assign (residue 8 and name hb#) (residue 9 and name hn) 3.32 0.43 0.35 1.50 8.27
assign (residue 9 and name hn) (residue 10 and name hn) 2.47 0.32 0.27 8.27 8.54
assign (residue 9 and name hb#) (residue 10 and name hn) 3.55 0.50 0.40 1.53 8.53
assign (residue 9 and name ha) (residue 10 and name hn) 3.48 0.61 0.57 4.48 8.54

i, i+2

assign (residue 14 and name ha) (residue 16 and name hn) 4.05 0.76 0.74 3.25 8.09
assign (residue 15 and name ha) (residue 17 and name hn) 3.93 0.73 0.68 3.98 7.28
assign (residue 16 and name hb2) (residue 18 and name hn) 4.04 0.76 0.74 2.71 8.18
assign (residue 4 and name hb2) (residue 6 and name hn) 3.05 0.45 0.36 1.95 7.84
assign (residue 3 and name hb1) (residue 5 and name hn) 4.50 0.50 2.50
assign (residue 3 and name hb2) (residue 5 and name hn) 4.50 0.50 1.50

i, i+3

assign (residue 10 and name ha) (residue 13 and name hb1) 3.07 0.42 0.34 3.94 3.52
assign (residue 10 and name ha) (residue 13 and name hn) 3.21 0.50 0.40 3.94 7.95
assign (residue 10 and name ha) (residue 13 and name he3) 3.77 0.68 0.80 3.94 6.81
assign (residue 10 and name ha) (residue 13 and name hb2) 3.48 0.68 0.61 3.93 3.00
assign (residue 10 and name ha) (residue 14 and name hn) 3.93 0.73 0.68 3.94 8.45
assign (residue 11 and name ha) (residue 14 and name hn) 3.24 0.45 0.35 4.13 8.45
assign (residue 11 and name ha) (residue 14 and name hb2) 3.72 0.50 0.40 4.13 1.73
assign (residue 11 and name ha) (residue 14 and name hd1#) 3.59 0.52 0.41 4.13 0.94
assign (residue 11 and name hb#) (residue 14 and name hn) 4.86 0.82 0.74 1.59 8.45
assign (residue 12 and name ha) (residue 15 and name hb#) 2.61 0.18 0.31 3.96 1.46
assign (residue 12 and name ha) (residue 15 and name hn) 3.05 0.45 0.36 3.96 7.92
assign (residue 13 and name ha) (residue 16 and name hb2) 3.17 0.49 0.39 4.12 2.71
assign (residue 13 and name ha) (residue 16 and name hb1) 3.64 0.64 0.55 4.12 2.80
assign (residue 13 and name ha) (residue 16 and name hn) 3.91 0.72 0.67 4.12 8.09
assign (residue 14 and name hg) (residue 11 and name hn) 4.59 0.70 0.69 1.51 8.40
assign (residue 14 and name ha) (residue 17 and name hn) 3.65 0.64 0.55 3.25 7.28
assign (residue 15 and name hb#) (residue 12 and name he#) 3.88 0.61 0.49 1.46 7.04
assign (residue 15 and name hb#) (residue 12 and name hn) 4.63 0.85 0.78 1.47 8.16
assign (residue 21 and name hb2) (residue 18 and name ha2) 3.53 0.54 0.44 3.86 2.81
assign (residue 21 and name hb*) (residue 18 and name hn) 3.66 0.64 0.56 3.47 8.18
assign (residue 21 and name hb1) (residue 18 and name ha2) 4.02 0.76 0.73 3.46 2.80
assign (residue 6 and name hb1) (residue 9 and name hb#) 4.21 0.40 0.33 2.72 1.54
assign (residue 6 and name hb*) (residue 9 and name hb#) 4.51 0.40 0.33
assign (residue 9 and name ha) (residue 12 and name hn) 3.44 0.57 0.48 4.48 8.15
assign (residue 9 and name ha) (residue 12 and name hb*) 3.81 0.69 0.62 4.47 2.10
assign (residue 9 and name ha) (residue 12 and name hb*) 4.17 0.80 0.81 4.47 2.18
assign (residue 9 and name hb#) (residue 12 and name hn) 5.22 1.03 1.11 1.53 8.15
assign (residue 9 and name hb#) (residue 6 and name hn) 5.52 1.13 1.33 1.53 7.84

i, i+4

assign (residue 12 and name ha) (residue 16 and name hn) 3.85 0.70 0.64	3.96	8.09
assign (residue 14 and name hd1#) (residue 10 and name he2) 3.24 0.40 0.57	0.94	6.75
assign (residue 14 and name hd2#) (residue 10 and name he2) 3.39 0.45 0.60	0.87	6.75
assign (residue 14 and name hg) (residue 10 and name he2) 3.57 0.61 0.72	1.52	6.75
assign (residue 14 and name hg) (residue 10 and name hd2) 3.84 0.70 0.64	1.51	7.00
assign (residue 14 and name hd1#) (residue 10 and name hd2) 4.23 0.72 0.61	0.94	7.00
assign (residue 14 and name hd2#) (residue 10 and name hd2) 4.79 0.90 0.86	0.87	7.00
assign (residue 14 and name ha) (residue 18 and name hn) 2.98 0.43 0.34	3.25	8.18
assign (residue 14 and name ha) (residue 18 and name ha2) 3.69 0.65 0.57	3.24	2.81
assign (residue 14 and name ha) (residue 18 and name ha1) 4.23 0.82 0.85	3.25	0.65
assign (residue 6 and name o) (residue 10 and name hn) 2.25 0.25 0.25		
assign (residue 7 and name o) (residue 11 and name hn) 2.25 0.25 0.25		
assign (residue 8 and name o) (residue 12 and name hn) 2.25 0.25 0.25		

i, i+n (n > 4)

assign (residue 10 and name ha) (residue 4 and name hg1) 3.05 0.51 0.42	3.94	1.78
assign (residue 10 and name ha) (residue 4 and name hg2) 2.35 0.23 0.22		
assign (residue 10 and name ha) (residue 4 and name hd2) 2.78 0.55 0.45	3.94	2.71
assign (residue 13 and name hh2) (residue 19 and name hd1) 3.62 0.63 0.94	6.53	7.56
assign (residue 13 and name hz2) (residue 19 and name hd1) 3.69 0.65 0.97	6.10	7.56
assign (residue 13 and name hz2) (residue 19 and name he3) 4.20 0.81 1.23	6.10	7.83
assign (residue 13 and name hh2) (residue 19 and name hn) 4.46 0.89 1.20	6.53	8.73
assign (residue 13 and name hd1) (residue 1 and name he) 3.63 0.63 0.75	6.76	7.40
assign (residue 13 and name hb2) (residue 4 and name hg1) 3.45 0.58 0.48	3.00	1.78
assign (residue 18 and name ha1) (residue 13 and name hz3) 4.07 0.77 0.96	0.66	6.87
assign (residue 19 and name ha) (residue 13 and name hz2) 3.87 0.71 0.85	4.63	6.09
assign (residue 19 and name ha) (residue 13 and name he1) 4.29 0.84 1.09	4.63	9.21
assign (residue 1 and name hg2) (residue 13 and name hd1) 2.74 0.35 0.49	1.65	6.75
assign (residue 1 and name hg1) (residue 13 and name hd1) 2.95 0.42 0.53	1.82	6.75
assign (residue 1 and name hd#) (residue 13 and name hd1) 3.20 0.50 0.60	3.17	6.75
assign (residue 1 and name hg2) (residue 13 and name he1) 3.37 0.55 0.65	1.65	9.21
assign (residue 1 and name hb*) (residue 13 and name hd1) 3.78 0.68 0.81	1.97	6.75
assign (residue 1 and name hg1) (residue 13 and name he1) 3.96 0.74 0.90	1.81	9.21
assign (residue 1 and name hb*) (residue 13 and name hd1) 4.03 0.76 0.93	1.93	6.75
assign (residue 2 and name ha) (residue 13 and name hz2) 3.33 0.53 0.68	4.03	6.10
assign (residue 2 and name ha) (residue 19 and name hz3) 2.99 0.42 0.53	4.01	7.24
assign (residue 2 and name ha) (residue 19 and name he3) 3.90 0.72 0.86	4.00	7.83
assign (residue 2 and name hb1) (residue 19 and name hz3) 3.40 0.52 0.66	2.42	7.23
assign (residue 2 and name hb1) (residue 19 and name hh2) 2.28 0.35 0.31	2.42	7.34
assign (residue 3 and name hb2) (residue 10 and name he1) 3.17 0.49 0.59	1.12	6.75
assign (residue 3 and name hb1) (residue 10 and name he1) 3.50 0.59 0.70	-0.08	6.75
assign (residue 3 and name hb2) (residue 10 and name hd1) 3.50 0.59 0.70	1.12	7.00
assign (residue 3 and name hb1) (residue 10 and name hd1) 4.53 0.92 1.26	-0.09	7.00
assign (residue 3 and name hd2) (residue 13 and name hz2) 3.14 0.48 0.58	2.55	6.09
assign (residue 3 and name ha) (residue 13 and name he1) 3.83 0.70 0.83	2.27	9.21
assign (residue 3 and name ha) (residue 13 and name hd1) 3.90 0.72 0.87	2.27	6.75
assign (residue 3 and name hd2) (residue 13 and name hh2) 4.27 0.84 1.08	2.53	6.52
assign (residue 3 and name hb1) (residue 13 and name hz3) 4.32 0.85 1.11	-0.09	6.87
assign (residue 3 and name hb1) (residue 13 and name hz2) 4.42 0.88 1.18	-0.08	6.09
assign (residue 3 and name hb1) (residue 13 and name he3) 4.69 0.97 1.38	-0.09	6.80

assign (residue 3 and name hd1) (residue 19 and name hh2) 3.72 0.66 0.79 3.23 7.34
assign (residue 3 and name hd1) (residue 19 and name hz3) 3.91 0.72 0.87 3.23 7.24
assign (residue 4 and name hd2) (residue 10 and name hd1) 3.08 0.39 0.49 2.71 7.01
assign (residue 4 and name hg2) (residue 10 and name hd1) 3.50 0.65 0.57 1.73 7.01
assign (residue 4 and name hg2) (residue 10 and name hn) 3.28 0.54 0.41 1.71 8.54
assign (residue 4 and name hb2) (residue 10 and name hn) 4.12 0.79 0.78 1.94 8.54
assign (residue 4 and name hg1) (residue 10 and name hn) 4.22 0.82 0.84 1.79 8.54
assign (residue 4 and name hg2) (residue 10 and name he1) 5.22 0.82 0.84
assign (residue 4 and name hd1) (residue 13 and name hd1) 3.01 0.44 0.55 3.05 6.75
assign (residue 1 and name o) (residue 13 and name he1) 2.25 0.25 0.25
assign (residue 9 and name hb#) (residue 4 and name hd2) 4.35 0.50 0.60
assign (residue 9 and name hb#) (residue 4 and name hb2) 3.50 0.50 0.50
assign (residue 9 and name hb#) (residue 4 and name hg1) 2.90 0.40 0.40

Vita

Aimee Byrne

Education

Doctor of Philosophy, Chemistry, 2013
University of Washington
Seattle, WA

Masters of Science, Chemistry, 2010
University of Washington
Seattle, WA

Bachelor of Science, Chemistry and Pharmacology, 2007
University College Dublin
Dublin, Ireland

Publications

Byrne, A; Kier, BL; Williams, DV; Scian, M; Andersen, NH. Circular Permutation of the Trp-cage Folding Motif. *RSC Advances,* 2013, In press.

Williams, DV; Byrne, A; Stewart JM; Andersen NH. Concerning the Optimal Salt Bridge for Trp-cage Stabilization. *Biochemistry* 2011, 50, 1143-1152.

McMillan, AW; Kier, BL; Shu, I; Byrne, A; Andersen, NH; Parson, WW. Fluorescence of Tryptophan in Designed Hairpin and Trp-cage Miniproteins: Measurements of Fluorescence Yields and Calculations by Quantum Mechanical Molecular Dynamics Simulations. *Journal of Physical Chemistry B.* 2013 6,1790-809.

Byrne, A; Bisaglia, M; Bubacco, L; Andersen, NH. Probing Alpha-Synuclein Molecular Binding Sites and their Effects on Aggregation by NMR Spectroscopy. *32nd European Peptide Symposium* 2012.

Kier, BL; Byrne, A; Scian, M; Anderson, JM; Andersen NH. Folding Landscape Exploration by Circular Permutation and Capping b-Structures. *32nd European Peptide Symposium* 2012.